SIMIAN IMMUNODEFICIENCY VIRUS (SIV) PRODUCTION FROM RHESUS MACAQUE CD4$^+$ T LYMPHOCYTES *IN VITRO:* INSIGHTS INTO THE HOST FACTORS CONTROLLING THE RATE OF PROGRESSION TO AIDS *IN VIVO.*

by

Amy Lynn Hartman

B.A. Washington and Jefferson College, Washington, PA, 1998

Submitted to the Graduate Faculty of the

School of Medicine, Department of Molecular Genetics and Biochemistry in partial fulfillment

of the requirements for the degree of

Doctor of Philosophy

University of Pittsburgh

2003

UNIVERSITY OF PITTSBURGH

SCHOOL OF MEDICINE

This dissertation was presented

by

___Amy Lynn Hartman___

It was defended on

___May 16th, 2003___

and approved by

Simon Barratt-Boyes, D.V.M., Ph.D.
Assistant Professor, Department of Infectious Diseases and Microbiology

JoAnne L. Flynn, Ph.D.
Associate Professor, Department of Molecular Genetics and Biochemsitry

Todd A. Reinhart, Sc.D.
Assistant Professor, Department of Infectious Diseases and Microbiology

Albert D. Donnenberg, Ph.D.
Professor, Department of Medicine

Michael Murphey-Corb, Ph.D.
Dissertation Director
Professor, Department of Molecular Genetics and Biochemistry

SIMIAN IMMUNODEFICIENCY VIRUS (SIV) PRODUCTION FROM RHESUS MACAQUE CD4$^+$ T LYMPHOCYTES *IN VITRO:* INSIGHTS INTO THE HOST FACTORS CONTROLLING THE RATE OF PROGRESSION TO AIDS *IN VIVO.*

Amy L. Hartman, Ph.D.

University of Pittsburgh, 2003

The interplay between the host and virus that controls the rate of disease progression in HIV-1- and SIV-infected individuals is highly complex. Host factor(s) play a major role in this process, however, because in the SIV-infected rhesus macaque (*Macaca mulatta*), differences in disease progression and survival exist among individuals even though identical virus stocks, doses, and routes of inoculation are used for infection. We have developed a simplified *in vitro* SIV replication assay that significantly correlates with disease progression and length of survival after infection *in vivo.* The amount of virus produced from primary CD4$^+$ T cells obtained from uninfected monkeys and infected *in vitro* correlated significantly with the rate of disease progression and survival after inoculation of the animal. The goal of this dissertation was to conduct a detailed molecular and immunological analysis to determine: 1) why differential *in vitro* SIV virus production occurs, 2) what the relationship is between virus production *in vitro* and disease progression.

Analysis of the events during virus infection of CD4$^+$ T cells *in vitro* revealed that low SIV production was associated with: 1) a decreased efficiency of the early steps of reverse transcription, which appeared to affect virus dissemination within the culture, and 2) a decreased susceptibility to mitogen-induced apoptosis both in the presence and absence of virus infection.

Together, these data suggest that multiple, cooperative factors mediated by the host cell may influence virus production and the rate of virus spread *in vitro*.

Subsequently, the impact of these events on infection and disease progression *in vivo* in these same animals was examined in detail. After intra-rectal infection with SIV, the four high producer animals exhibited characteristics of rapidly progressing animals (higher viral loads during the set-point, faster decline in memory $CD4^+$ T cells, weaker virus-specific immune responses), while the low producers, in contrast, appeared to be slow progressors. Interestingly, the number of infected cells in the peripheral blood and the timing of their emergence, rather than the peak viral load, was an accurate indicator of the eventual set point.

The apparent slower disease progression in the low producer monkeys could potentially be a direct result of slower viral replication during the very first few rounds of infection, as suggested by our *in vitro* data. The finding that incredibly early events during *in vivo* infection may play a dominant role in determining the extent of viral replication in the blood, and hence disease progression, underscores the studies of others who have shown that a better clinical prognosis can be achieved the earlier that antiretroviral treatment is initiated after infection. The studies presented here enable not only the identification of novel host factors that may influence disease outcome, but also provide a potential framework for the design of new therapeutic agents that target specific host factors exerting their influence very early after infection.

PREFACE

This work would not have been possible without the immeasurable support from many people in my life – namely my parents, Richard and Lorry, who have given tirelessly of their time, effort, and money to ensure that I am here today. Their sacrifices for my life and my education are beyond expressing in words. I appreciate that they have supported me through everything that I have wanted to do, and have never questioned my decisions. I would like to thank my entire family as well as my friends, all of whom have served as an anchor to keep me grounded throughout this long journey.

Undoubtedly, the completion of this work would not have been possible without the endless patience and love from my husband, Matt. When asked by a number of people during my time here if my decision to attend the University of Pittsburgh for graduate school was a good one, my reply is yes, because I would not have met my husband if I had chosen another school. I am incredibly grateful to have had his support throughout this process. His ability to make me laugh at myself, especially during the ups-and-downs of graduate school, has been an immense relief. I am also grateful for his sacrifices that are allowing me to pursue my career beyond graduate school. I can not imagine a more wonderful person to spend my life with.

I am indebted to my advisor, Mickey Corb, for instilling in me a passion for discovering the unknown. I truly appreciate all the time, effort, and patience she took in training me during my years here. She has guided me in a way that still allowed for the development of my own independent thought, which will be an incredible tool for me in the future. Additionally, this

work would not have been possible without the dedication of my thesis committee members. I would like to thank them for taking the time and interest to serve on my committee.

I also appreciate all of the past and present members of the Corb Lab, who have provided me with incredible support, both professionally and personally. I am thankful for having been able to work with all of them. Rachel Taber has been both a wonderful colleague and friend to me these past several years. Graduate school is much easier to get through if there is someone to laugh with. I have also enjoyed getting to know Premi Rajakumar personally and working with her professionally. Her advice and mentorship has given me a great role model for women in science. I am also indebted to Dawn McClemens-McBride, who has the difficult job of keeping everyone happy. She has been both patient and flexible, and I really appreciate everything she has done to make my work go more smoothly. Finally, it has been an incredible pleasure to work with Pat Dowling, who always has a good story to tell.

In conclusion, I dedicate this dissertation to my Grandfather, Pat Thomassey. Although he is not here to see the completion of my work, I have no doubt that he is shaking his head in amused disbelief that I have finally become the 'bug-catcher' he always predicted.

"Education is not the filling of a pail, but the lighting of a fire." -William Butler Yeats

TABLE OF CONTENTS

LIST OF TABLES

LIST OF FIGURES

CHAPTER 1

INTRODUCTION

1.1. The global impact of the AIDS epidemic.

Like a scene from the movie 'Outbreak' gone bad, the AIDS epidemic has spread unabated in most of the world for the past 20 years, killing more than 3 million people in 2002 alone (203), and it is showing no signs of slowing down. According to the Joint United Nations Program on HIV/AIDS (UNAIDS) and the World Health Organization (WHO), 42 million people worldwide are currently infected with Human Immunodeficiency Virus (HIV)-1, the virus that causes AIDS (see http://www.unaids.org). Seventy-one percent of these people live in Sub-Saharan Africa, a region where the infection is spreading mainly through heterosexual contact (203). Astoundingly, the adult HIV prevalence in the Sub-Saharan region has exceeded 30% in several countries including Botswana (38.8%), Lesotho (31%), Swaziland (33.4%) and Zimbabwe (33.7%) (203). Many people in this region have no access to running water, let alone drugs to treat the infection. Coupled with a lack of proper preventative education on how the virus is spread, the social traditions of the region often confound many control measures. Southeast Asian countries are also victims of the rapidly spreading epidemic, with 6 million people currently infected (203). Even in the United States, where approximately 1 million people are infected, the epidemic continues to spread, especially among minority groups (29). In addition to the enormity of the AIDS epidemic itself, HIV has caused a resurgence in many other diseases, such as tuberculosis, leshmaniasis, and cryptosporidiasis. The already weak infrastructure of many third world countries is being devastated by AIDS.

Unfortunately, mortality of humans infected with HIV is nearly 100 %; that is, very few people infected with the virus are known to have cleared the infection. There is currently no licensed effective vaccine to prevent infection, nor are there any drug treatments that will eliminate the infection. Current antiretroviral drug regimens prolong patients' lives, but

ultimately, nearly all HIV-1-infected people succumb to AIDS. While many advances have been made, the HIV/AIDS epidemic remains one of the greatest threats to the human species in the 21st Century. Frequent underestimation of the severity of the epidemic stems from the fact that HIV-1-infected humans often live several years after infection; therefore, the threat may not feel immediate. However, continued study of the biological agent that causes AIDS is and will continue to be a main contributing factor in the design of new drugs and vaccines. Successful preventative measures, treatments that eliminate the infection, and prophylactic vaccines are the only hope to slow the exploding epidemic.

1.2. Retroviruses and Retroviral Infections.

1.2.1. Retroviruses.

Since the discovery of the first Retrovirus in 1904, the family *Retroviridae* has been shown to contain some of the most diverse and well-studied viruses to date (196). The hallmark feature of retroviruses is the presence of an enzyme, reverse transcriptase, which converts single-stranded RNA to double stranded DNA (8, 197, 198). The discovery of this enzyme in 1970 revolutionized the field of molecular biology, enabling the conversion of mRNA to cDNA for use in a wide range of applications (196). Other distinguishing features of retroviruses include: 1) the ability to stably integrate into the host cell genome, potentially resulting in oncogenesis, and 2) the ability to mutate rapidly and therefore exist as a quasispecies (33). The diseases caused by retroviruses are as diverse as the viruses themselves and include immunodeficiencies, malignancies, neurological disorders, and wasting diseases (33, 196).

The *Retroviridae* family consists of seven genera: *Lentivirus*, *Spumavirus*, Mammalian type B, Mammalian type C, Mammalian type D, Avian type C, and HTLV/BLV-like viruses (33, 196). The Mammalian type B, Mammalian type C, Avian type C, and HTLV/BLV-like viruses cause malignancies such as sarcomas, lymphomas, and leukemias. Lentiviruses cause immunodeficiencies and neurological diseases, while spumaviruses have not been associated with any disease to date and are thought to be benign.

The genome of retroviruses consists of two copies of a single stranded RNA molecule approximately 7 to 10 kb in length, with a uniform structural gene order of *gag-pro-pol-env* that encode for the structural, protease, polymerase, and envelope proteins, respectively (Figure 1) (33). The genome is flanked on both ends by a long terminal repeat (LTR) composed of a repeat sequence (R) and two unique regions, one on the 5' end (U_5) and the other on the 3' end (U_3).

Retroviral virions are approximately 100 nm in diameter and contain a roughly conical nucleocapsid surrounded by a host cell-derived envelope.

1.2.2. Lentiviruses.

The Lentivirus genus has been the most intensely studied group of retroviruses over the last 20 years due to the emergence of the AIDS epidemic. This genus includes, among others, the Human immunodeficiency viruses -1 and -2 (HIV-1, HIV-2), and their closely-related counterpart, Simian immunodeficiency virus (SIV). Unlike simple retroviruses which encode only the structural proteins, Lentiviruses have a much more complex genome. They contain a number of accessory and regulatory proteins that play various roles, including control and regulation of transcription, inhibition of the host's immune response, and viral assembly (Figure 1).

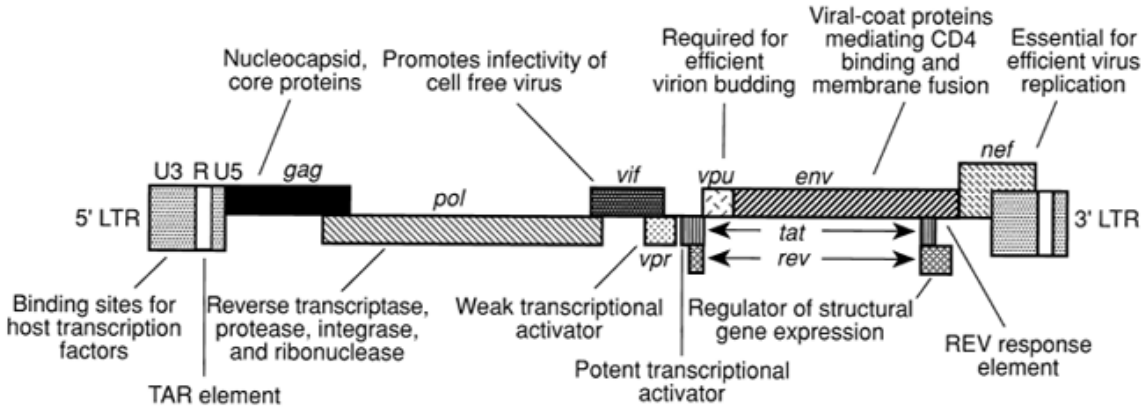

Figure 1. The genomic organization of HIV-1.

Typical elements of a lentiviral genome are shown. Accessory and regulatory proteins are also shown with descriptions of some of their known functions. (Reproduced with permission from Cohen et al. (34) © 1999 Lippincott Williams and Wilkins).

1.2.3. Disease course of HIV-1 infection in humans.

The clinical course of HIV-1 infection in humans can be divided into three stages (Figure 2) (153). The first stage, termed primary infection, encompasses the first 9 – 10 weeks after infection and is characterized by a large burst in viral replication and dissemination throughout the body. The peak of viral replication occurs approximately 3 – 6 weeks post-infection (p.i.) and can result in an acute HIV syndrome, which includes symptoms such as fever, pharyngitis, lymphadenopathy, headache, myalgia, lethargy, anorexia, nausea, and vomiting (31, 40, 58). During the peak of viral replication, $CD4^+$ T cell numbers can decline dramatically.

Clinical latency, the second stage of infection, ensues when the host immune response rapidly contains, but does not eliminate, viral replication. The number of virus particles in the blood decline and level off to a 'set-point'. The level at which the virus plateaus during the set-point is a prognostic indicator and predicts how long the infected individual will survive (130). Individuals with lower set-points will survive for longer periods than those with higher set-points. Indeed, the variation in set point levels between individuals can vary as much as 4 logs (130). Concomitant with the decrease in viral loads after the acute phase, the number of $CD4^+$ T cells rebounds. However, $CD4^+$ T cell numbers continue to slowly decline during this period. The second stage is defined as clinical latency because there are generally no outward symptoms. However, it is not a period of viral latency, because viral replication can still be detected in most individuals.

The final stage is AIDS-defining illness. Eventually, the number of $CD4^+$ T cells becomes low enough such that viral replication can not be effectively curtailed. Consequently, constitutional symptoms (cachexia, lymphadenopathy, fever, diarrhea) and opportunistic diseases (candidiasis, listeriosis, *P. carinii* pneumonia, *Mycobacterium* spp., toxoplasmosis,

cryptosporidiosis, Kaposi's sarcoma, Burkitt's lymphoma, among others) ensue, eventually leading to death of the patient (58). At death, viral loads in the plasma are generally high, while $CD4^+$ T cell counts are low.

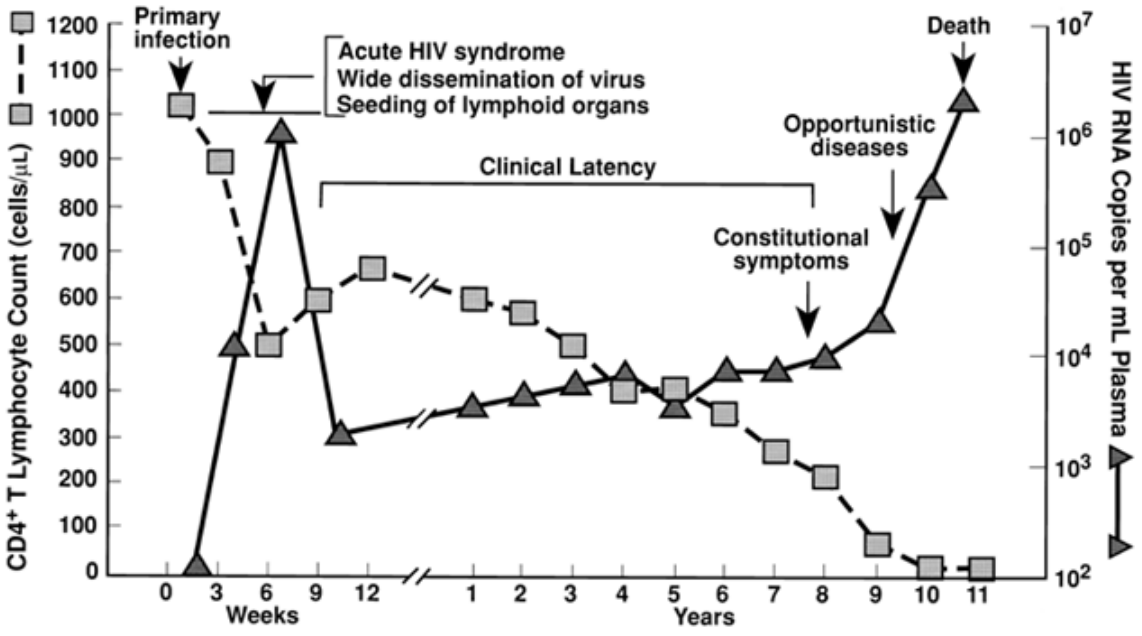

Figure 2. The typical clinical course of an HIV-1-infected individual.

During primary HIV-1 infection, a burst of plasma viremia occurs in concert with a transient decline in the $CD4^+$ T-cells. Partial immune control over viral replication ensues, resulting in a variable period of clinical latency. As the $CD4^+$ T-cell count declines, the risk of developing constitutional symptoms and opportunistic diseases increases. (Reproduced with permission from Cohen et al. (34) © 1999 Lippincott Williams and Wilkins).

1.2.4. The replication cycle of HIV-1.

The lentiviral replication cycle takes approximately 28 – 32 hours to complete (91) and can be divided into early and late phases (Figure 3). The early phase begins with attachment of the virus to the host cell. HIV-1 initiates infection with the binding of gp120, the viral surface glycoprotein, to the CD4 molecule on T cells and macrophages. This binding leads to a conformational change in the gp120 molecule, thereby allowing binding to a co-receptor (CCR5, CXCR4) and fusion of the viral envelope with the host cell membrane (33). Subsequently, the viral nucleocapsid is released into the cytoplasm, and partial uncoating occurs, along with a rearrangement of viral proteins, to allow initiation of reverse transcription. A host-cell-derived $tRNA^{lys}$ molecule acts as a primer for initiation of reverse transcription by binding to the primer binding site (PBS) downstream of the 5' long terminal repeat (LTR) (33). Synthesis of double-stranded DNA with identical LTRs at either end of the genome is completed using a complex series of strand transfers (Figure 4). Generally, linear viral DNA can be detected within infected cells as early as 4 hours post-infection (91).

After reverse transcription, the viral DNA, complexed with the capsid (CA), integrase (IN), reverse transcriptase (RT), and nucleocapsid (NC) proteins, is translocated into the nucleus, where it can be stably integrated into the host cell genome (33). The integration process is critical because integrated proviral genomes are required for efficient RNA transcription (192, 217). This completes the initial phase of the virus life cycle.

The late phase of the virus life cycle begins with viral RNA transcription, the regulation of which is very complex and involves both viral and cellular elements. The U3 region of the LTR contains a TATA box for transcription initiation by host RNA polymerase II, as well as numerous binding sites for transcription factors, including Sp1, NF-κB, AP-1, NFAT-1, USF-1,

Ets-1, and LEF (33). Transcription initiation begins at the U_3-R border, which forms the 5' end of all transcripts. Transcription initiation and elongation are both enhanced by the regulatory protein, Tat.

RNA transcription generates full-length RNA molecules that are polyadenylated at the 3' end and capped at the 5' end. Around 12 – 16 hours p.i., spliced RNA species can be detected within infected cells (91). Generally not until around 24 hours p.i. can full-length genomic RNA and unspliced mRNA be detected. Therefore, while DNA expression is rapid following infection, RNA expression follows a temporal pattern, with spliced species being made first followed by unspliced mRNA and genomic RNA.

The structural proteins of HIV-1 are synthesized as precursor polyproteins that are subsequently cleaved into individual proteins by the viral protease (33). Structural gene expression and active release of viral particles occurs at 28 – 32 hours p.i. (91). The Gag and Gag-Pol polyproteins assemble near the cell membrane where genomic RNA is encapsidated to form immature nucleocapsids. The nucleocapsid then interacts with Env proteins within the host cell membrane, and the virus buds from the cell surface. After budding, cleavage of the polyproteins into individual proteins by the viral protease results in a mature viral particle (33).

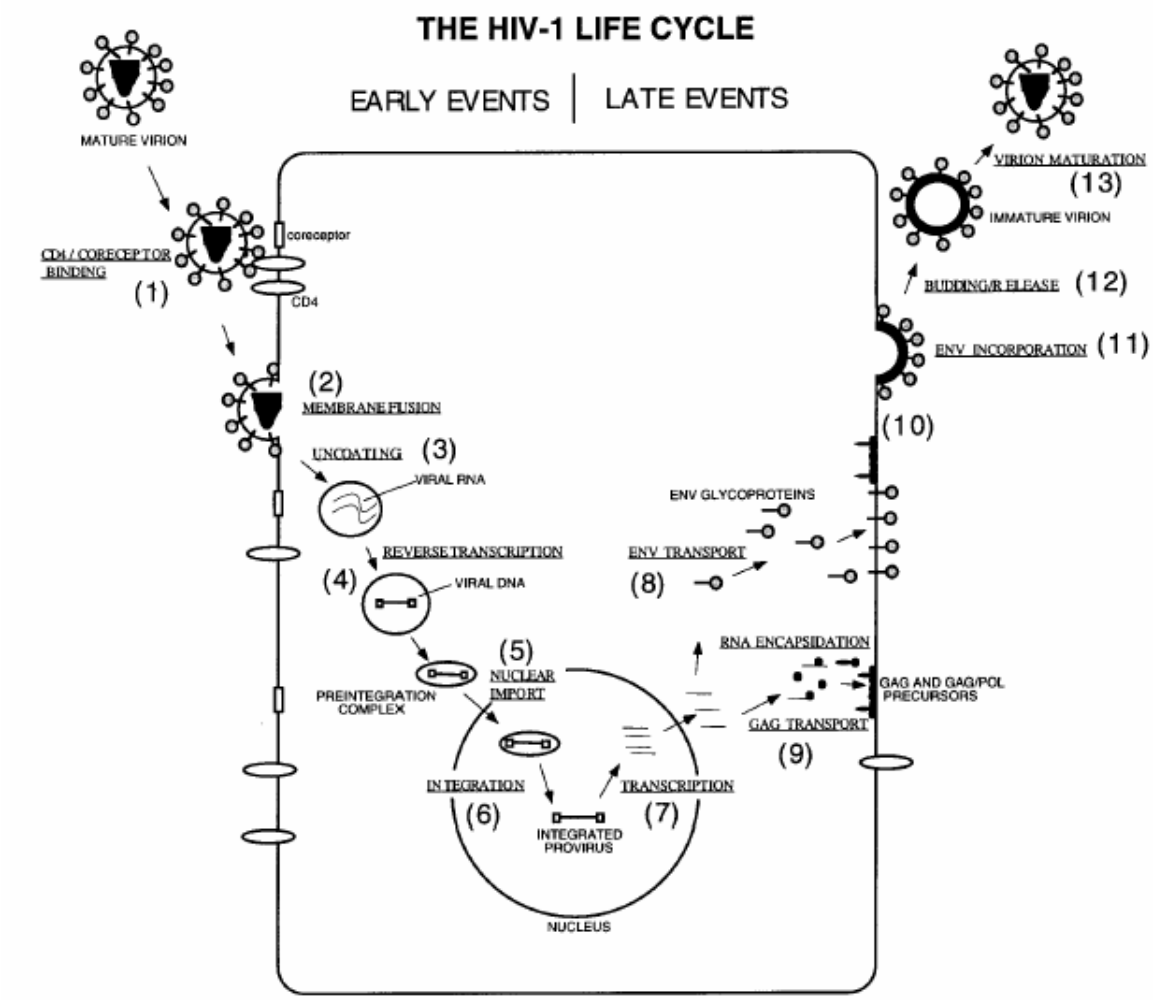

Figure 3. The life cycle of HIV-1.

(Reproduced with permission from Freed, E.O. (63) © 1998 Elsevier)

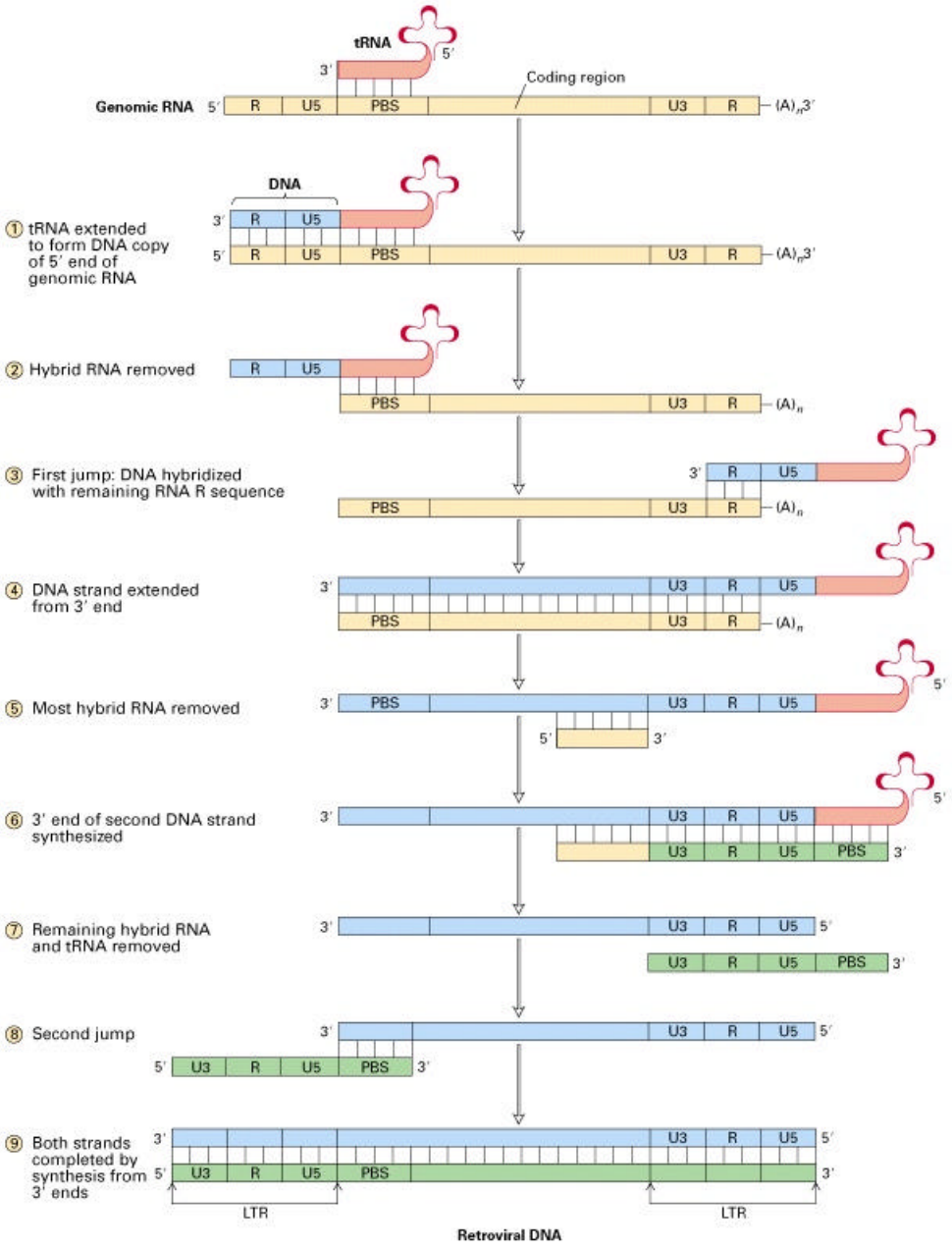

Figure 4. Detailed description of the reverse transcription process.

(Reproduced with permission from Lodish, et al. (116) © W.H. Freeman & Co.)

1.3. SIV-infected rhesus macaques as a model for HIV-1-infection in humans.

1.3.1. Natural Hosts of SIV infection

SIV is an endogenous retrovirus found in many primate species in Africa, including African green monkeys, mangabeys, mandrills, Sykes monkeys, and chimpanzees (65, 143, 206). In these 'natural' hosts, the virus causes no disease despite high levels of virus replication. Inadvertent transmission of SIV from a natural host (e.g. African monkeys) to a susceptible host (e.g. Asian macaques) via contact in primate centers has resulted in persistent, lethal infections that are very similar to AIDS in humans. Asian macaques are now routinely used to study the pathogenesis of simian AIDS. The species most commonly used are the rhesus macaque (*Macaca mulatta*), the cynomologus macaque (*M. fascicularis*), and the pigtailed macaque (*M. nemestrina*).

1.3.2. Discovery and Isolation of SIV strains.

Not long after isolation and discovery of HIV-1 as the virus that causes AIDS in humans, another retrovirus, initially named STLV-III, was isolated from captive Asian macaques (41, 143). Later renamed Simian Immunodeficiency Virus (SIV), it causes a fatal AIDS-like disease in a variety of macaque species (93, 102, 107, 143). SIV is genetically the most closely related lentivirus to HIV; it is 50 % and 75 % homologous to HIV-1 and HIV-2, respectively, at the nucleic acid level (66). Despite the sequence divergence, SIV and HIV have some serological cross-reactivity.

In susceptible hosts, the immune deficiency induced by SIV in rhesus macaques resembles HIV-induced AIDS. The main difference is that SIV induces disease within months to

years after infection, which is a shorter time span than HIV, making *in vivo* laboratory experiments more manageable. Because the virus and the disease it causes closely mimics HIV-1 in humans, the SIV-infected macaque has served as the main animal model for the study of the pathogenesis of HIV-1 (107). However, this model does have disadvantages, which include: 1) the cost of the animals, housing, and veterinary care may prohibit extensive studies; 2) the availability of various monkey species may be inadequate, and 3) primate-specific reagents may be limited.

There have been numerous strains of SIV isolated from different primate species (65). In 1985, Daniel and colleagues (41) isolated a strain of SIV from immunodeficient rhesus monkeys housed at the New England Regional Primate Center. Co-culture of PBMC from these animals led to isolation of the SIV_{mac} strain, of which numerous molecular infectious clones have been generated (i.e., mac239) and used extensively in AIDS-related studies (145). Shortly thereafter, the closely related SIV_{mne} strain was isolated from a sick pigtailed macaque at the University of Washington (12).

There have also been several strains of SIV isolated from healthy African monkey species at primate centers in the United States (65). Murphey-Corb and colleagues at the Tulane Regional Primate Center isolated STLV-III/Delta (later renamed SIV_{Delta}) from PBMC of a healthy sooty mangabey that was seropositive for HIV-1 antibodies (143). When inoculated into rhesus monkeys, the SIV_{Delta} isolate induced a lethal AIDS-like disease (10).

1.4. Immune responses to lentiviral infections.

In both HIV-1-infected humans and SIV-infected macaques, the decrease in plasma viremia after the acute phase of infection (Figure 2) can be attributed to both cellular and

humoral immune responses (18, 31, 86, 98, 105, 176, 178, 179). While neither arm of the adaptive immune response appears to be able to completely eliminate the infection, considerable control of the infection, at least temporarily, is possible.

Antibodies to the capsid protein (p24) of HIV-1 are readily detectable after only a few weeks of infection (178). Control of plasma viremia is associated with neutralizing antibodies, most of which recognize the V3 loop of the HIV-1 Env protein, thereby preventing interaction of Env with the co-receptor during fusion of the virus with the cell (172). Other neutralizing epitopes exist within gp41 and the CD4-binding regions of gp120 (36). Neutralizing antibodies are thought to play a major role in controlling SIV viremia in rhesus macaques (25).

Cell-mediated immune responses, particularly virus-specific, MHC class I-restricted $CD8^+$ cytotoxic T lymphocytes (CTL), are also critical in controlling the initial viremia and establishing the viral set point (18, 98, 109, 213). Antigens from intracellular pathogens, such as viruses, are presented within MHC class I molecules on infected cells. $CD8^+$ CTL are subsequently able to recognize and lyse the infected cell. During the clinically latent phase, CTL have been found to be directed at both structural and accessory proteins (78). The important role for CTL is emphasized by the finding that a loss of virus-specific CTL activity coincides with disease progression (18, 78). In addition to direct lysis of infected cells, $CD8^+$ T cells also inhibit both HIV-1 and SIV replication by secretion of a $CD8^+$ T cell antiviral factor (CAF) that can modulate viral gene transcription in a non-cytolytic manner (204).

1.5. Disease progression rates in SIV-infected monkeys.

It is estimated that 20% of HIV-infected people not on drug therapy will progress to AIDS within 5 years (termed rapid progressors), while 12% will remain free of disease for nearly 20 years (slow progressors) (112, 139, 140). Although the dose and strains responsible for human HIV-1 infections are highly variable, some studies have shown that a difference in survival period persisted even though an identical route of infection and strain of virus could be documented (115, 152). A considerable variation in the length of survival has also been noted in SIV-infected rhesus monkeys. The average time until death of an SIV-infected macaque is 1-2 years depending upon the strain of SIV used (46, 93). However, a wide range of survival is observed in animals infected by the same strain of virus, with some animals dying within months while others live for many years (22, 27, 108, 112, 113, 134, 149, 152, 219). This plieotropy is particularly striking because, in most SIV studies, the same route and dose of a cryopreserved inoculum are used to infect the animals.

Similar to HIV-1 infected humans (78), SIV-infected macaques have been classified into three groups based on survival time after infection: fast progressors, typical (intermediate) progressors, and slow progressors (Figure 5) (49, 93, 108, 153, 219). Most SIV-infected macaques exhibit a typical disease progression course that is similar to HIV-1-infected humans (Figure 5B). After the acute phase of infection, SIV-specific antibody and $CD8^+$ CTL responses develop, which coincide with the stabilization of the viral loads to a set-point (18, 98). Seroconversion generally occurs 6 – 8 weeks post-infection (108). Typically progressing animals experience a period of clinical latency that lasts 1-2 years, until the rise of virus titers and emergence of simian AIDS.

On one end of the clinical spectrum are the SIV-infected rapid progressors. These animals have persistent high-level viremia and are termed 'non-responders' because little or no virus-specific immune responses are usually detected (Figure 5A) (49, 57, 134, 219). The acute phase and clinical syndrome can be extended in comparison with typical progressors, and the clinically latent phase is very short or non-existent (153). Rapid progressors are often unable to control the initial burst of viremia, which results in uncontrolled viral replication until the time of death of the animal. Survival of these animals is approximately two to six months after infection.

At the opposite end of the clinical spectrum are the slowly progressing animals. Slow progressors become persistently infected with SIV (as determined by the ability to detect viral sequences by PCR), but virus is often difficult to culture from peripheral blood (Figure 5C). Virus-specific humoral and cellular immune responses are strong, and $CD4^+$ T cell counts can remain relatively normal (45). The immune response in these animals is able to control the initial burst of viremia and lowers the set-point to a level that is 1-4 logs lower than intermediate and rapid progressors (113). These animals remain asymptomatic for long periods of time and can survive for 5 or more years.

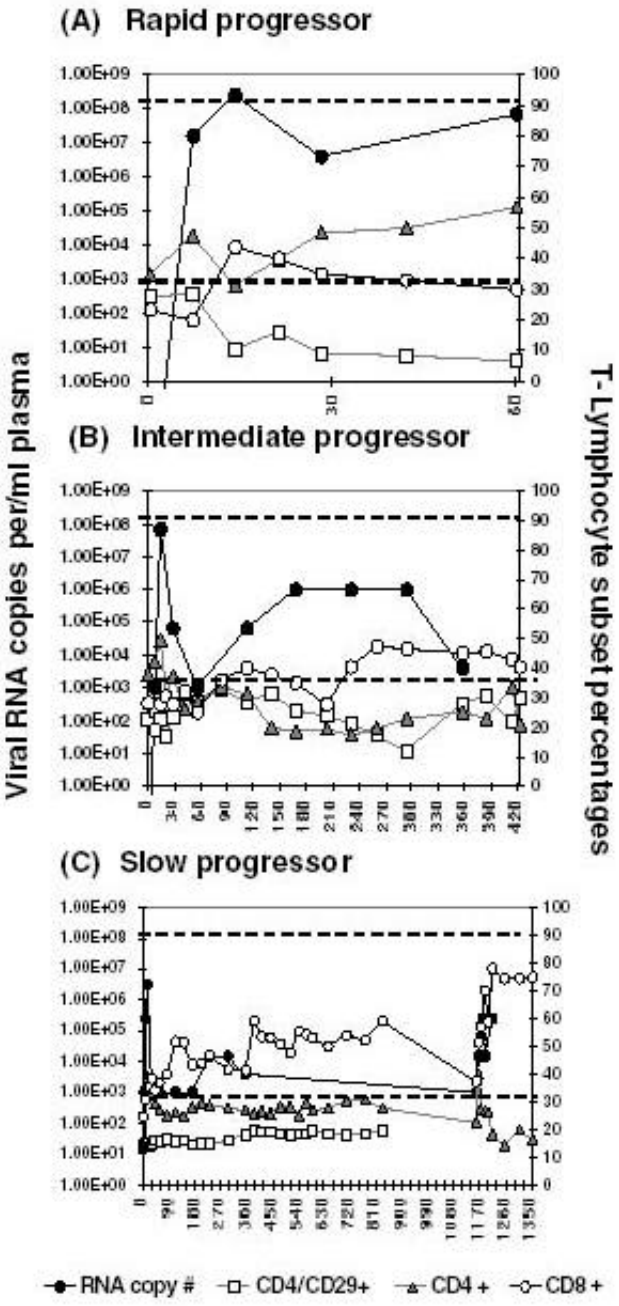

Figure 5. Typical disease progression profiles of SIV-infected Indian rhesus macaques.

Examples of (A) a rapid progressor, (B) a typical (intermediate) progressor, and (C) a slow progressor. Not the differences in the scales of the x-axes. (reproduced with permission from Trichel, A.M. et al. (201) (c) 2002 Blackwell Publishing, Ltd.).

1.6. The influence of host factors on disease progression rates.

Clearly, the genetic makeup of the host has a profound impact on the clinical outcome of the disease because variation in survival time occurs after infection with identical doses of SIV. Indeed, susceptibility to some human infectious diseases has been associated with a single genetic polymorphism (16, 126). For example, genetic polymorphisms associated with proteins of erythrocytes have been shown to affect disease susceptibility, progression, and outcome of *Plasmodium* infection and the disease malaria (61).

Infection with HIV-1 triggers a complex and chronic disease, and while a number of host factors have been postulated to influence the variation in both HIV-1- and SIV-induced disease progression rates (148), no single gene has been the key. The susceptibility to infection and disease progression is clearly multifactorial. Some of the human genes known to be associated with HIV-1 infection, disease progression, and clinical outcome are listed in Table 1, and include MHC haplotype and chemokine or chemokine receptor polymorphisms (2, 17, 133, 171, 182). In addition to these factors, both HIV-1 and SIV are known to interact with cellular factors at almost every step of the viral life cycle (193). While extensive studies on the effects of a number of genetic polymorphisms on disease progression have been conducted, no consensus has yet been reached as to exactly what the most important factors are in determining survival time after infection. O'Brien and colleagues (148) used population association analysis to study the influence of several known genetic factors on AIDS pathogenesis. They have shown that this type of modeling is feasible for analyzing polygenic and multifactorial diseases such as AIDS to determine the relative contribution of a number of genes to a particular outcome.

Table 1. Identified genes that affect HIV-1 infection, progression to AIDS, and AIDS outcome

Allele	Mode	Effect	Time
1. *CCR5 delta 32*	Recessive	Prevent infection	—
CCR5 delta 32	Dominant	Prevent lymphoma	Late
CCR5 delta 32	Dominant	Delay AIDS	Overall
2. *CCR5 P1*	Recessive	Accelerate AIDS	Early
3. *CCR2 641*	Dominant	Delay AIDS	Overall
4. *SDF1 3′A*	Recessive	Delay AIDS	Early
5. *HLA A, B, C,* "Homozygosity"	Co-dominant	Accelerate AIDS	Overall
6. *HLA B*35*	Co-dominant	Accelerate AIDS	Overall
7. *HLA C*04*	Co-dominant	Accelerate AIDS	Overall
8. *IL10 5′A*	Dominant	Limit Infection	—
IL10 5′A	Dominant	Accelerate AIDS	Late

Reprinted with permission from O'Brien et al. (148).

1.6.1. Co-receptor polymorphisms and HIV/SIV-induced disease.

One of the most well-studied host genes influencing infection and disease progression in HIV-1-infected humans is a 32-base pair deletion (Δ32-CCR5) within the CCR5 gene (42, 114, 174), which results in a truncated protein that is not expressed on the cell surface. Individuals homozygous for this mutation are resistant to infection with HIV-1, while heterozygotes have a slower disease progression rate (42, 82, 131, 135, 174). Since the discovery of this mutation, widespread searches have revealed several other mutations within the CCR5 coding region, as well as in the genes for CXCR4 and CCR2, two other co-receptors for HIV (35, 188). However, none have been shown to have as dramatic of an effect on infection or disease progression as has the Δ32-CCR5 mutation. Several minor polymorphisms have been identified in the CCR5 genes of some primate species (100, 101, 156). To date, none have been found to alter CCR5 expression and consequently SIV infection.

1.6.2. Influence of the MHC on disease progression.

The most polymorphic human genes are that of the major histocompatibility complex, or MHC, which present foreign antigens to either $CD4^+$ (class II) or $CD8^+$ (class I) T cells for induction of humoral and cellular immunity against invading pathogens, respectively. The human versions of the MHC are known as the human leukocyte antigens, or HLA. The equivalent of these genes in the rhesus macaque have been partially characterized and are known as Mamu (17, 207). An individual's particular HLA genotype determines which epitopes are presented to the immune system and in theory how aggressively the immune system responds to the invading virus. Presentation of a conserved epitope may lead to slower disease progression,

while presentation of a variable epitope may quickly lead to escape mutants and rapid onset of disease.

Certain MHC alleles have been associated with either rapid or slow disease progression in both humans and monkeys (2, 17, 28, 119). Despite numerous published studies, there has been no consensus on a single MHC locus and its relationship to disease progression *in vivo.* However, homozygosity at one or more loci has been shown to be associated with rapid progression, most likely because this limits the breadth of peptides that can be presented (175, 221). While the MHC is a promising candidate as the factor responsible for controlling disease progression, a distinct possibility is that genes that are closely linked to the HLA could be determining resistance or susceptibility to infection, and not the HLA itself. In addition, the small population sizes studied may make the interpretation of results problematic (147), suggesting that caution be applied when interpreting studies on MHC involvement in disease progression. Due to the variation in reports and no agreement on a single HLA locus, MHC alleles alone are most likely not the primary factor controlling disease progression rates.

1.6.3. Cytokine polymorphisms and disease progression.

Cytokines are soluble, secreted proteins of the immune system that affect the behavior of other immune cells by binding to their respective receptors (85). Genetic polymorphisms within the coding region and/or promotor region of certain cytokine genes have been associated with altered secretion levels (3, 54, 165, 187), and some have been shown to have effects on allograft rejection (4, 5, 53, 202). With regard to HIV-1 infection, polymorphisms in the promotor region of the IL-10 gene have been linked to increased susceptibility to infection and more rapid disease progression (182). Conversely, a polymorphism within the promotor region of TNF-α was

found to have no effect on susceptibility to HIV-1 infection or disease progression (21, 96) The role of these cytokine polymorphisms and others in AIDS pathogenesis are still under investigation.

1.7. The role of host genes in the susceptibility of cells to infection with HIV/SIV.

1.7.1. Endogenous retroviral sequences.

The idea that host cell factors can influence susceptibility to retroviral infection and disease is not new. Continuous exposure to retroviral infections throughout evolution has led to the development of host genes that limit retroviral replication. Early work done during the late 1960's and 1970's by Frank Lilly and colleagues identified host genes that prevented disease in murine leukemia virus (MuLV)-infected mice (160). One gene, identified as *Fv1*, was found to be an endogenous retroviral *gag* sequence (15). *Fv1* is expressed at very low levels in non-permissive cell lines and restricts MuLV-infection by interacting with the capsid (CA) protein of the incoming virion, specifically at amino acid 110 (15, 99). *Fv1* is thought to block viral replication after reverse transcription but before integration, possibly by inhibiting nuclear translocation of the pre-integration complex (68). Interestingly, *Fv1* is a dominant-negative mutant; that is, very few *Fv1* molecules can confer resistance to an incoming virion that contains ~1500 CA molecules (68). Though the restriction is not absolute, it can reduce virus replication by 50- to 1,000-fold (73). In addition, titration of the virus on non-permissive cells showed second-order (two-hit) kinetics, rather than the expected first order kinetics, leading investigators to believe that the incoming Gag protein is able to saturate the block caused by *Fv1* (68). Therefore, a high enough dose of virus can titer out the *Fv1*, allowing the remaining live virus to infect the cell.

While mammalian cells lack a direct homologue of *Fv1*, they do have a gene, *Ref1*, that functions in a similar manner to restrict MuLV-infection of mammalian cells (199). *Ref1* blocks incoming virions by interacting with amino acid 110 of the *gag* gene; however, unlike *Fv1*, *Ref1* appears to act after viral entry but before reverse transcription (199). *Ref1* may accomplish this by destabilizing the incoming viral core, resulting in its elimination. Indeed, it has been postulated that the efficiency of the destabilization of the core may lead to the accumulation of more or less reverse-transcribed genomes in the infected cell (199).

An *Fv1*-like restriction of HIV-1 infection has been reported (210). This type of restriction is thought to be responsible for the finding that HIV-1 is unable to productively infect monkeys or monkey cells *in vitro* (110, 137). In this case, entry of HIV-1 into monkey cells is not inhibited; rather, a block generally occurs before completion of reverse transcription (30, 80). Towers and colleagues (15, 199, 200) have shown that resistance of monkey cells to infection with HIV-1 is due to *Ref1*, and, similarly to *Fv1*, this activity is both dominant and saturable at high virus concentrations (38).

Intraspecies variation in expression of *Ref1*-like factors may influence the permissivity of cells for HIV and/or SIV infection and consequently disease progression. Expression of very few copies of *Fv1* are required for the restriction of MuLV replication (68). It is feasible, then, that variation among individuals within a species in the expression level of *Ref1*-like elements could affect the permissivity of the cells to infection. Indeed, variation in the ability of human cells to support HIV-1 replication (190, 210), as well as monkey cells to support SIV replication (69, 151, 180) exists. While a mechanism for the resistance of human cells to infection with HIV-1 has not yet been identified, studies with SIV-infected monkey cells have shown that virus replication is restricted after viral entry and during the early steps of reverse transcription (75,

156), which is indeed the point at which *Ref1* functions. The potential role of *Ref1*-like proteins in the susceptibility of cells to HIV-1 and SIV infection, as well as their role in disease progression in the infected individual, remains to be explored. However, since such small amounts of these proteins are required for restriction of viral replication, they pose unique opportunities for the development of novel HIV therapies.

1.7.2. CEM15.

Recently, an endogenous cellular protein, CEM15, has been identified that inhibits HIV-1 infection at the level of reverse transcription and prevents infection of the cell (181). Its discovery came from studies investigating the function of the viral Vif protein, whose activities proved elusive for many years. The viral infectivity factor, or Vif protein, is one of the accessory genes found within most lentiviruses. A functional Vif protein is required for pathogenic SIV infection *in vivo* (43), as well as for HIV-1 and SIV infection of primary cells and some cell lines (60, 186, 194). In non-permissive cell lines, replication of Vif-deleted viruses is blocked at a very early stage of reverse transcription (70), possibly due to instability of viral nucleoprotein complexes (184) or modulation of virion nucleic acid components (44). However, in certain cell lines, Vif is dispensable for replication. This dichotomy in the ability of Vif-negative viruses to replicate in different cell lines ultimately led to the discovery of the gene responsible. Two groups showed that non-permissive cell lines contained an endogenous inhibitor of HIV replication that is overcome by the Vif protein (120, 185). Identification of the gene responsible came from Michael Malim's group (181) who used a complementary DNA subtraction method to isolate CEM15. Based on homology with other known proteins, it was determined that CEM15 is closely related to the mRNA-editing cytosine deaminases. From this, the authors

postulated that CEM15 most likely interacts with viral RNA, and Vif itself is known to bind RNA (44). The mechanism by which CEM15 inhibits viral replication is under investigation.

Generally, the viral accessory protein, Vif, inhibits the activity of CEM15, rendering the cell susceptible to infection; in the absence of Vif, CEM15-expressing cells are non-permissive for viral infection (120, 181). It is possible that the varying susceptibility of cells to infection with HIV (190, 210) or SIV (69, 180) may be due to intraspecies variation in the expression of CEM15. For example, one could speculate that in cells in which polymorphisms exist that lead to high levels of CEM15 expression, Vif would not be able to be overcome all of the CEM15, rendering the cells less permissive for infection. Alternatively, polymorphisms in CEM15 may exist that affect the ability of Vif to bind and inhibit its function, leading to a less permissive cell. While a non-human primate homologue to CEM15 has yet to be identified, this gene poses yet another additional cellular gene that can specifically inhibit retroviral replication. Indeed, studies of SIV-infected of monkey cells have revealed individual variation in susceptibility of the cells to infection that resides at the level of reverse transcription (75, 156), which is the point at which CEM15 exerts its effects.

1.7.3. Interferon (IFN)-α/β.

One of the earliest host cell antiviral mechanisms discovered was that of the Type I Interferon system, or IFN-α/β (215). The antiviral activity of interferons was found to be due to the induction of several enzymes (RNase L, Mx proteins, PKR, and 2'-5' OAS) that disrupt viral replication at many levels, including RNA transcription, mRNA stability, and translation (205). Studies of the molecular effects of interferons on lentivirus replication have revealed that HIV-1 replication is blocked at a late stage of virus replication, resulting in altered protein processing,

while SIV replication is inhibited at the level of reverse transcription (97). The causes behind the two different mechanisms have not been identified. Despite the clear ability to block retroviral replication *in vitro*, several studies have suggested that higher IFN-α expression in lymphoid tissues and sera is not associated with better control of either HIV-1 or SIV replication *in vivo* (1, 62, 90, 163). Clearly, interferons have the potential to influence virus infection, replication, and even disease progression. However, the interplay between the *in vitro* observations and *in vivo* events has never been examined in molecular detail. The development of *in vitro* systems (69, 180) to study host factors and their role in the early events during acute infection *in vivo* (74) will facilitate identification of the exact role of Type I interferons in susceptibility to infection as well as disease progression.

1.7.4. Other virus-cell interactions that may influence susceptibility to infection.

Cellular genes may affect virus replication at any step in which the virus interacts with the cells; indeed, viral and cellular proteins interact at virtually every step of the viral life cycle (193). Therefore, the number of potential genes is great, some of which include proteins of the nuclear import/export pathway, signaling molecules, cell cycle regulation proteins, proteins of the endocytosis/exocytosis pathway, subunits of the proteasome, and proteins of the non-homologous DNA end joining (NHEJ) pathway (24, 84, 111, 177, 189, 193).

While many genes have been implicated to play a role in determining host susceptibility to infection and disease progression, it is clear that further work in this area is vital. Now that techniques are available to study gene and protein expression on a global level, the identification of new genes is feasible. The ability to generate polygenic and multifactorial gene associations

(148) is the key to understanding the interplay between the numerous factors that determine the fate of an infected individual.

1.8. The role of cellular activation and apoptosis in HIV-1/SIV replication.

1.8.1. T-cell activation.

The successful activation of a T cell requires the recognition of a foreign peptide bound to an MHC molecule on the surface of an antigen presenting cell as well as the binding of a co-stimulatory molecule. The signaling component entails not only the γ, δ, ε, and ζ chains of the TCR itself, but also CD4 or CD8, CD45, and the co-stimulatory molecule CD28 (128). The initial signaling cascade involves the activation of the kinases Fyn, Lck, and ZAP-70. A diagram of the downstream signaling cascade from the TCR is shown in Figure 14. Numerous signaling pathways are initiated from the TCR, the end result of which is the activation of the transcription factors NF-AT, NF-κB, and AP-1, among others. These transcription factors bind to promoters for genes encoding proteins required for cellular growth, proliferation, differentiation, apoptosis, as well as cytokines. The activated T cell expands clonally and differentiates into an effector T cell that can then contribute to the removal of the invading pathogen that it recognizes.

1.8.2. HIV/SIV replication and T cell activation.

Many viruses have manipulated cell division to enable their own replication; for instance, dividing cells often contain the appropriate enzymes or other proteins required for viral replication. Indeed, replication of HIV-1 and SIV in primary peripheral blood cells requires that the cells be activated with a mitogen either prior to or shortly after infection (218). Both HIV-1

and SIV are able to enter resting cells and begin reverse transcription at the same rate as activated cells (216); however, replication thereafter is incomplete or proceeds very slowly (162). Cellular factors existing in activated, but not resting, T cells are required for completion of reverse transcription, efficient translocation of the pre-integration complex to the nucleus, and integration (161, 162). One reason for this may be that activated cells have a greater pool of dNTPs available for DNA synthesis, which proceeds faster as a result (162). The exact mechanism by which host cell proteins augment reverse transcription, nuclear translocation, and integration are not well understood.

What is well understood is that an activated cell is required for efficient viral RNA transcription from the viral LTR. Activated NF-AT, NF-κB, and AP-1, in addition to binding cellular promoters, also bind to the enhancer region within the U3 viral LTR and stimulate viral transcription (117). These transcription factors, along with the cellular RNA polymerase II and binding of the transcription factor SP1 to the core promotor element within the LTR, are required for initiation of RNA transcription. Thus, HIV-1- and SIV-infected cells are dependent on activation of the cells for efficient transcription and hence progeny virus production.

1.8.3. Apoptosis.

Just as cellular proliferation and activation are regulated in a highly controlled manner, so is programmed cell death, or apoptosis. Apoptosis is the main mechanism by which clonally expanded T cells in the periphery are eliminated. Cells can receive both extracellular (TNFR/Fas) or intracellular (DNA damage, hypoxia) signals that lead to apoptosis (173). Both of these pathways involve the activation of initiatior caspases, or cysteine proteases, which subsequently activate effector caspases that in turn degrade intracellular proteins (173).

Extracellular signals typically activate the initiator caspase-8, while intracellular signals activate caspase-9. The two pathways converge upon activation of caspase-3, one of the main effector enzymes. The end result of both pathways is the degradation of cellular and nuclear proteins, as well as the breakdown of chromosomal DNA. The affected cell is then engulfed and removed by phagocytic cells, leading to little or no inflammation as compared to necrotic cell death.

1.8.4. HIV-1/SIV replication and apoptosis.

Viruses are also efficient at manipulating the cell death program for their own benefit; in fact, apoptosis can be advantageous or disadvantageous to viruses, depending upon the situation (77). For some viruses, survival is dependent upon a live cell for use of the cellular machinery. Alternatively, apoptosis can benefit virus replication because engulfment of apoptotic bodies by phagocytic cells can be a means for virus dissemination under the radar of the immune system. One recent study using adenovirus showed that while apoptosis during DNA synthesis is detrimental to the virus, apoptosis during assembly promoted dissemination of the virus (132). With regards to HIV-1 pathogenesis, apoptosis is thought to be the primary mechanism by which both $CD4^+$ and $CD8^+$ T cells are eliminated during HIV-1-infection of humans. The majority of these cells are not directly infected with the virus, implying that bystander cell apoptosis is significant (7).

The mechanism(s) by which HIV-1 and SIV cause apoptosis of infected and bystander cells is not well understood, but both viruses are known to encode pro- and anti-apoptotic genes. The Tat, gp160, Vpr, and Nef proteins have all been shown to have pro-apoptotic activities, while Tat, Vpr, and p24 proteins have anti-apoptotic properties (77). Hence, viral proteins like Tat and Vpr can provide dual functions depending on the situation. This duality is thought to

regulate different stages of virus infection. For instance, the Vpr protein protects cells from apoptosis in HIV-1-infected cultures during the first 4 days of infection (37). Subsequently, from 8 – 14 days post-infection, Vpr enhances apoptosis by increasing caspase-8 activity (155). Clearly, the regulation of apoptosis by lentiviruses is complex and mediated by a number of viral proteins. A better understanding of the mechanism by which viral proteins manipulate apoptosis will give more insight into the contribution of apoptotic cell death to the induction of virus-induced disease progression during infection *in vivo.*

1.8.5. The interplay between T-cell activation, apoptosis, and retroviral replication.

Undeniably, cellular activation and apoptosis are intimately linked. The signaling pathway initiated from both the TCR and death receptors (TNFR, Fas) can lead to either proliferation or death of the cell, depending on the particular intracellular environment at the time (23, 128, 158). For instance, binding of FasL to Fas generally initiates apoptosis by activation of caspase-8 (23). However, FLIP, a protein that is homologous to caspase-8 but has a non-functional caspase domain, can divert the signaling pathway away from cell death and towards activation of ERK and NF-κB, which lead to proliferation and differentiation.

The link between T-cell activation and apoptosis is controlled by a number of redox and metabolic switches (158). Controlled levels of reactive oxygen species (ROS), the byproduct of oxidative phosphorylation within the mitochondria, are essential for the regulation of signal transduction. Shifting of the redox equilibrium toward oxidation enhances cellular activation by stimulating the activation of NF-kB and SP-1 transcription factors. However, disruption of the membrane potential of the mitochondria is the point of no return in apoptosis signaling. In general, high levels of oxidative stress promote a favorable environment for apoptosis (158).

The interplay between T-cell activation, apoptosis, and viral replication is not yet completely understood. However, cross-talk between the three events has been shown with respect to the redox control of intracellular signaling. Glutathione (GSH) is a necessary cellular antioxidant that reduces harmful reactive oxygen species (ROS) that are known to induce apoptosis (158). Intriguingly, high levels of GSH are known to block HIV-1 reverse transcription (88). Also, high levels of glutathione peroxidase (GPx), another essential antioxidant, inhibit NF-kB activation, thereby inhibiting viral transcription from the LTR (122). Therefore, maintaining cells at a reduced state serves to limit retroviral replication as well as apoptosis.

HIV-1-infected patients have been shown to have reduced levels of both GSH and GPx (48, 191), and the levels of reduction correlate with the stage of disease. Without appropriate levels of both antioxidants, cells are under oxidative stress, which is a prime inducer of apoptosis. The high level of apoptosis seen in HIV-1-infected humans at end-stage AIDS may be due to dysregulation of the redox system. Indeed, many of the disease manifestations in AIDS patients, such as loss of $CD4^+$ T cells by apoptosis, opportunistic infections, lymphoproliferative diseases, disruption of energy metabolism, and generalized wasting can be attributed to: 1) depletion of intracellular antioxidants, such as GSH, 2) increased reactive oxygen species (ROS) production, and 3) changes in mitochondrial transmembrane potential (157). Therefore, the findings that AIDS patients have high viral replication as well as high levels of apoptosis may be at least partially due to excessive oxidative stress. A greater understanding of the interplay between these events is key to discerning the role of the redox system in controlling viral replication as well as disease progression.

CHAPTER 2

SPECIFIC AIMS

The rate of disease progression and length of survival of humans infected with HIV-1 (115, 140, 152) and rhesus macaques infected with its simian relative, SIV (46, 93, 219), varies significantly among individuals. For macaques, differences in survival persist even though an identical route, strain, and dose of virus are used for infection, suggesting that innate host factor(s) play a dominant role in disease progression (108, 112, 134, 219). Since detailed, informative analysis of the host factors influencing disease progression is hampered by the complexity and expense of the required studies in both humans and monkeys, we (141, 180) and others (69, 156) have developed a simplified *in vitro* assay that significantly correlates with disease progression after infection *in vivo*. Primary $CD4^+$ T lymphocytes infected *in vitro* that support little virus production (low producers) predict slow disease progression, whereas cells that produce large amounts of virus (high producers) predict rapid disease progression. The goal of this dissertation was to conduct a detailed molecular and immunological analysis of why differential *in vitro* virus production occurs and how it relates to disease progression and survival. The studies presented here are based on the following central hypothesis: **The amount of virus produced from $CD4^+$ T cells infected *in vitro* is controlled by a host factor(s); this host factor(s) not only affects virus production *in vitro*, but also has a dramatic effect on virus dissemination and disease progression within infected animals.**

The specific aims of this thesis are:

Aim 1: Determine the usefulness of classification of animals based on differential virus production *in vitro* as a predictor of disease progression and survival *in vivo*. The primary objective of the first aim was to statistically analyze the relationship between the amount of virus produced after *in vitro* infection of an uninfected animal's PBMC and survival after intravenous infection of that same animal. A retrospective study of 59 rhesus macaques was conducted to determine whether classification of animals as high, intermediate, or low producers of virus based on infection of the cells *in vitro* correlates with disease progression (as measured by T-cell counts and antigenemia) and survival. Indeed, classification of animals based on this simple *in vitro* assay was highly predictive of survival and is therefore useful in highlighting host factors involved in disease progression.

Aim 2: Characterize the growth properties of SIV on $CD4^+$ T cells from high and low virus producer animals. The properties of rhesus macaque primary cells infected *in vitro* can play a significant role in shedding light onto the cause of differential virus production. Extensive analysis of both the virus and the cells in culture was conducted to determine basic properties of the *in vitro* assay which may be crucial to understanding this phenomenon. These studies revealed that differential virus production was associated with the response of the cells to mitogen stimulation. In both the presence and absence of viral infection, high virus production was associated with increased levels of caspase-3 mediated apoptosis and consequently decreased cell viability as compared to cells from low virus producers.

Aim 3: **Identify the step of the SIV life cycle that is impaired in cells from low producer animals.** Clearly, virus replication is inherently different within cells from high and low producer animals. Determining how the virus replication cycle differs between these two cell types is key to identifying host factors that are controlling this observation. Detailed, quantitative analysis of a number of steps in the viral life cycle was conducted to determine the exact point(s) at which high and low producer cells differ with respect to virus replication. The difference was found to be at the level of reverse transcription; all other steps of the life cycle appeared to be equivalent. The partial block at the level of reverse transcription within low producer $CD4^+$ T cells was concordant with a significant delay in spread of the virus throughout the culture.

Aim 4: Determine whether the results from the *in vitro* studies correlate with virological and immunological events after infection of the animals *in vivo*. We tested the biological relevance of our *in vitro* observations by infecting the same 8 animals that were intensively studied throughout this thesis. The efficiency of virus replication during the first few rounds of infection appeared to have a profound effect on both the virological and immunological events during acute infection. The low producer animals had a slower rate of virus dissemination and developed more effective immune responses as compared to their high producer counterparts, resulting in a lower viral set-point by 8 weeks post-infection. The rate of virus spread through the peripheral blood, as well as the number of infected cells, correlated with the viral load at the set-point in these animals.

CHAPTER 3

THE REPLICATIVE CAPACITY OF RHESUS MACAQUE PERIPHERAL BLOOD MONONUCLEAR CELLS FOR SIMIAN IMMUNODEFICIENCY VIRUS *IN VITRO* IS PREDICTIVE OF THE RATE OF PROGRESSION TO AIDS *IN VIVO*

This chapter was modified with permission from:

Amy L. Seman (Hartman), William F. Pewen, Lynn F. Fresh, Louis N. Martin, and Michael Murphey-Corb. 2000. The Replicative Capacity of Rhesus Macaque Peripheral Blood Mononuclear Cells for Simian Immunodeficiency Virus *In vitro* is Predictive of the Rate of Progression to AIDS *In vivo*.

Journal of General Virology. 81:2441-2449.

3.1. Introduction.

Simian immunodeficiency virus (SIV) causes a fatal AIDS-like disease in rhesus macaques (93, 102, 143). For this reason, the non-human primate serves as a useful animal model for the study of the pathogenesis of HIV-1 and AIDS in humans. The average time until death of an SIV-infected macaque is 1-2 years depending upon the strain of SIV used (46, 93). However, a wide range of survival is observed (22, 27, 108, 112, 113, 134, 149, 152, 219), with some animals dying within months while others live for many years. This plieotropy is particularly striking because, in most SIV studies, the same route and dose of a cryopreserved inoculum are used to infect the animals. A considerable variation in the length of survival has also been noted in HIV-1-infected humans (112, 140). It is estimated that 20% of HIV-1-infected people will progress to AIDS within 5 years, while 12% will remain free of disease for nearly 20 years (139). Although the dose and strain responsible for human HIV-1 infections are highly variable, some studies have shown that a difference in survival persisted even though an identical route and strain could be documented (115, 152).

Like that seen in HIV-1 infected humans (78), SIV-infected macaques have been classified into three groups: rapid progressors, typical progressors, and slow/nonprogressors (49, 93, 108, 219). SIV-infected rapid progressors have a persistent viremia with little or no virus-specific antibody response. Survival of these animals is approximately two to three months. Typical progressors have detectable viremia, but also have a strong antibody response and survive for 1-3 years. Slow/nonprogressors remain persistently infected because viral sequences can be detected by PCR, but virus is difficult to recover from peripheral blood. These animals can survive for 5 or more years.

We have determined that cultured peripheral blood mononuclear cells (PBMC) from different naïve animals vary widely in their ability to support viral replication *in vitro*. To determine whether a relationship exists between this phenomenon and the variable survival noted *in vivo* following experimental infection, data from a cohort of 59 control animals used over the last decade were evaluated. These data demonstrate that there is a statistical relationship between the ability of an animal's PBMC to produce virus *in vitro* and the rate of progression to disease and death following experimental infection. Furthermore, comparative evaluation of virus production in purified $CD4^+$ T cell cultures produced similar results, a finding that demonstrates that this phenotype is a property of the $CD4^+$ T cell itself.

3.2. Materials and Methods.

Cells and virus. 20-40 ml blood was collected via the femoral vein from individual rhesus macaques using acid citrate dextrose (ACD) as the anticoagulant. Peripheral blood mononuclear cells (PBMC) were isolated from whole blood by Ficoll-Paque (Pharmacia Biotech) density-gradient centrifugation. Cells were grown in modified RPMI 1640 supplemented with 15% fetal bovine serum, penicillin-streptomycin (100 U/ml; 100 U/ml), L-glutamine (2 mM), HEPES buffer solution (10 mM)(GibcoBRL), and recombinant human IL-2 (40 U/ml)(Hoffman-LaRoche). $SIV_{DeltaB670}$ stocks used in the *in vitro* assays were propagated on rhesus PHA blasts; *in vivo* infections employed stocks propagated on either rhesus or human PHA blasts as described (142). All virus stocks were cryopreserved in 1 ml aliquots in liquid nitrogen until needed.

Animal manipulations. Rhesus macaques (*Macaca mulatta*) of either sex were obtained from the Tulane Regional Primate Center breeding colony. Animals were infected by inoculation of one ml of 10-100 monkey infectious doses into the saphenous vein using a 23-gauge butterfly needle. Each injection was chased with 1-2 ml sterile saline to assure accurate delivery of the inoculum. Physical examinations were performed at biweekly intervals, and animals were provided full supportive care until they were deemed moribund by the attending veterinarian. Blood was drawn at these times for measurements of antigenemia and for quantification of T lymphocytes. Antigenemia was determined by ELISA according to the manufacturer's instructions (Coulter). Flow cytometric determination of lymphocyte subsets was performed as described (124). Complete necropsies were performed following humane sacrifice.

Analysis of virus replication *in vitro*. PBMC were obtained as described above. Cell pellets containing $1x10^7$ PBMC were infected by incubation with 1 ml of a cryopreserved stock of $SIV_{DeltaB670}$ containing 1,000- 100,000 tissue culture infectious doses for 1-2 hours at 37 °C. No difference in the hierarchy with respect to virus production was observed when inocula within this range of infectivity were used (data not shown). After infection, cells were washed twice in complete medium (RPMI 1640 supplemented with 15% FBS, L-glutamine, and penicillin-streptomycin at concentrations indicated above). Twenty-four hours after infection, 10 µg/ml of phytohemagglutinin (PHA) (Gibco BRL) was added. On day 4, the PHA was removed by washing the cells 3 times in complete medium. Cells were cultured in complete medium supplemented with human IL-2 (40 U/ml) for the entire experiment (21 days) and maintained at a concentration of $1x10^6$ cells/ml. On days 7, 10, 14, 18, and 21, 1 ml of supernatant was removed and stored at –70 °C until analysis. The amount of virus in culture supernatants was determined by measuring reverse transcriptase activity in cell culture supernatants as described below. Alternatively, virus production was measured using an SIV Core antigen ELISA (Coulter), as per the manufacturer's instructions. Measurement of reverse transcriptase activity or p27 antigen yielded similar results.

Measurement of reverse transcriptase activity. Cell-free culture fluid was collected in 1 ml aliquots and subjected to centrifugation at 12,000 x g for 45 minutes in a refrigerated microfuge. The supernatant was decanted, and the virus pellet was stored at –70 °C until needed. The pellet was thawed on ice and 50 µl of solubilization buffer (0.5% Triton X-100, 0.8 M NaCl, 0.5 mM PMSF, 20% glycerol and 50 mM Tris-HCl, pH 7.8) was added to lyse the pelleted virus

particles. The pellet was resuspended by vortexing, and the sample was retained on ice until incorporation into the assay. To each well of a 96 well flat-bottomed microtiter plate, 10 µl of the solubilized pellet was added to 90 µl of a solution containing 10 mM $MgCl_2$, 5 mM dithiothreitol, 83 µg/ml dATP, 5 µg/ml poly(r-A)p$(dT)_{12-18}$ (Pharmacia), 52 µCi/ml ^{3}H-TTP (New England Nuclear) and 52mM Tris HCl, pH 7.8. The plates were then incubated at 37 °C for 2 hours, and the reaction was stopped by the addition of 10 µl 25 mg/ml tRNA (Gibco BRL). To each well, 90 ul of cold 10% TCA $^+$ 0.02% $Na_4P_2O_7$ was then added and the reaction was allowed to sit for 30 min. Acid precipitable radiolabeled nucleotides were harvested using a Skatron plate washer and the resulting radioactivity counted using a scintillation counter.

Purification of CD4$^+$ T cells. $CD4^+$ T cells were purified from PBMC using MACS, a magnetic cell selection system (Miltenyi Biotec). After isolation from peripheral blood as described above, PBMC were washed two times in PBS and once in MACS buffer (PBS containing 5 mM EDTA (Sigma), 0.5% BSA (Sigma), and 10 mM HEPES (GibcoBrL)). Cells were incubated in 200 ul buffer and 50 ul $CD4^+$ microbeads per $4x10^7$ cells for 20 minutes at 4°C. For all experiments, cells were run over two MS^+ selection columns. Purity of selected cells was determined using flow cytometry and was >95% for all assays. Rhesus-reactive antibodies used for flow cytometry were: phycoerythrin-conjugated anti-CD4 clone MT477 (Pharmingen), fluorescein-conjugated anti-CD8 clone SK1 (Becton-Dickinson), and either phycoerythrin- or fluorescein-conjugated anti-CD3 clone SP34 (Pharmingen).

Statistics. Analysis of data utilized Microsoft Excel 97 for data entry and coding (Microsoft Corporation). Statistical analysis was performed using SPSS Version 9.0 (SPSS Inc.). A p value of < 0.05 was considered significant. Kaplan-Meier analysis was used to evaluate survival among groups. Statistical relationship of maximum RT and survival was analyzed by one-way ANOVA.

3.3. Results.

Classification of animals based on *in vitro* SIV production from PBMC. To determine the capacity of rhesus macaque peripheral blood mononuclear cells (PBMC) to replicate SIV *in vitro,* ficoll-paque purified PBMC were exposed to a cryopreserved stock of $SIV_{DeltaB670}$, and virus production was measured at biweekly intervals by analysis of reverse transcriptase activity (RT) in culture supernatants. Isolated PBMC were infected with SIV immediately following purification and prior to the addition of phytohemagglutinin (PHA) to ensure that the state of these cells would most closely approximate their condition *in vivo.* The outcome of infection of PBMC from 10 monkeys selected randomly from the Tulane Regional Primate Center breeding colony is shown in Figure 6. A wide range of virus production was observed, even though the input virus and the cell number were held constant. Cells from three monkeys (animals H779, H727, and H695) had maximum (peak) RT levels in culture supernatants greater than 400,000 cpm/ml. Four monkeys had peak RT values ranging between 80,000-105,000 cpm/ml, and 3 animals had RT values of less than 25,000 cpm/ml. The difference observed in these cultures was not due to a failure of the cells to become infected, because all cultures contained SIV sequences readily detectable by polymerase chain amplification (PCR) of PBMC DNA (data not shown). Based on these results, these animals were arbitrarily assigned to high, intermediate, and low producer groups, respectively.

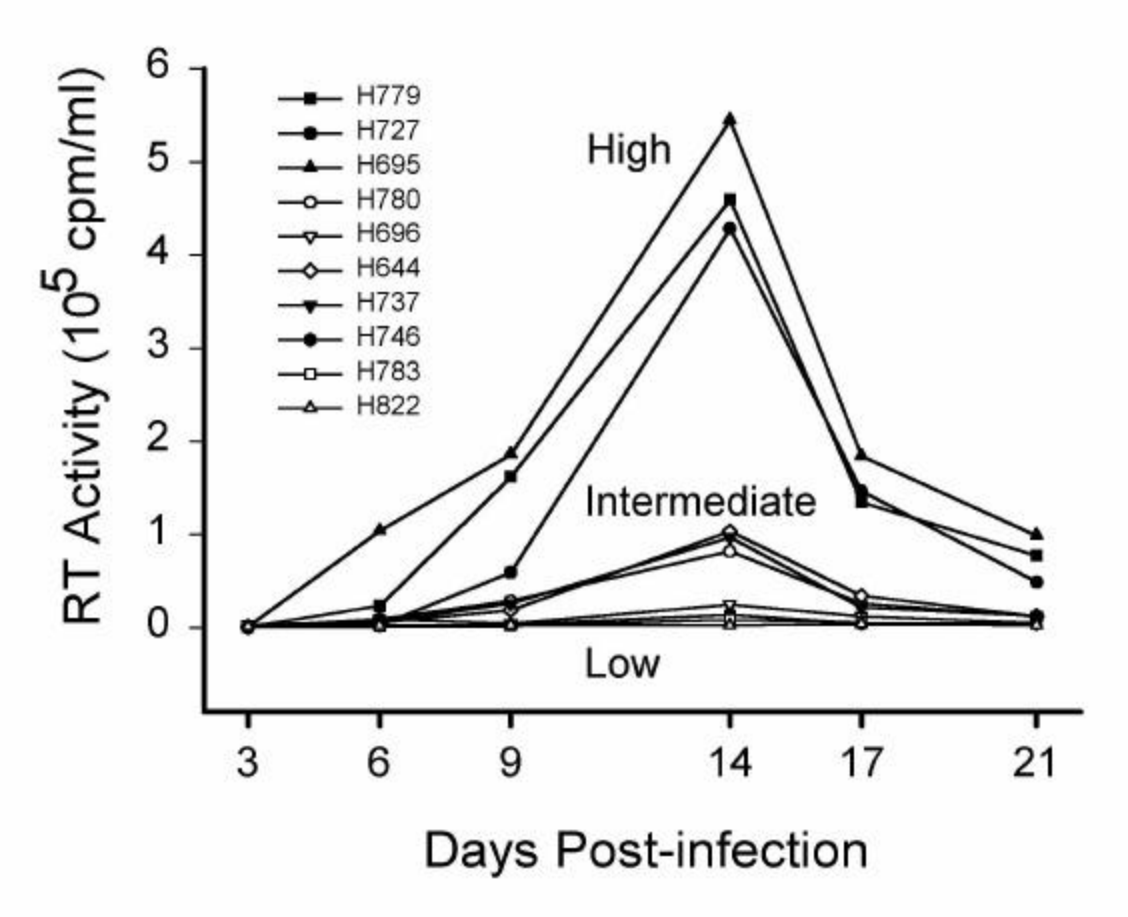

Figure 6. ***In vitro*** **replicative capacity of SIV in PBMC from randomly chosen rhesus monkeys.**

Ficoll-paque purified PBMC from each animal were infected with 1,000 $TCID_{50}$/million cells of a cryopreserved stock of $SIV_{DeltaB670}$, and virus production was analyzed by measuring reverse transcriptase activity in culture supernatants as described. Animals were classified as high, intermediate, or low producers of virus based on overall rank in the group. Animals classified as low producers have RT values below 10,000 cpm/ml, which is considered negative for this assay.

To determine whether the virus replication phenotypes observed among these 10 animals were consistent over time, *in vitro* infections of PBMC were repeated twice more over the course of a year. The results of representative animals from each of the subgroups (high, intermediate, low producers) are shown in Figure 7. In each case, the amount of virus produced was consistent over time for cells from a given animal. These data suggest that the viral replicative capacity of PBMC is a property of the animal itself, and that the differences in replication between animals were not due to variability in the assays.

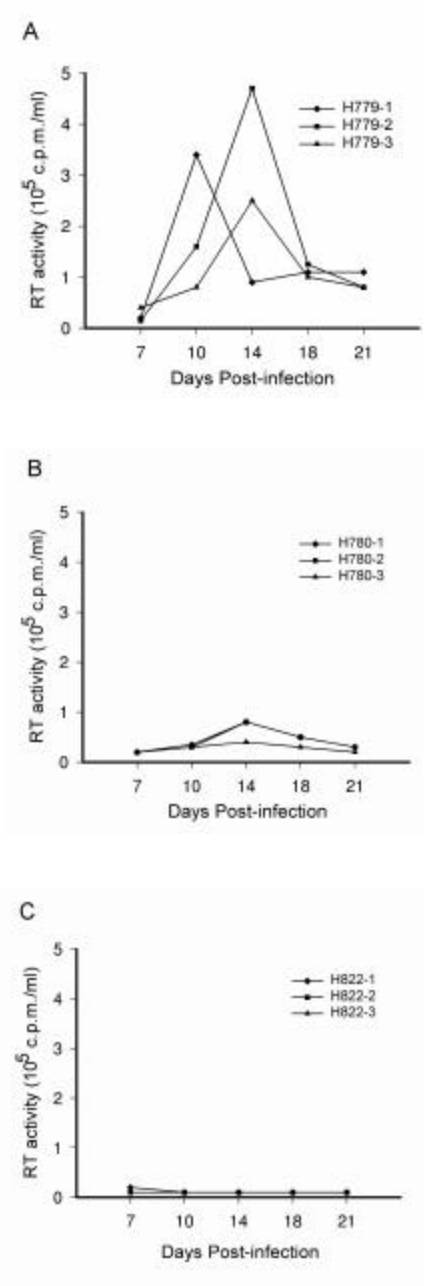

Figure 7. Reproducibility of the *in vitro* SIV producer phenotype.

All 10 animals shown in Figure 6 were assayed 3 times over a period of a year. Data from a representative animal from each group is depicted. Reverse transcriptase activity (in cpm/ml) was measured for all three trials. (A) Animal H779, a high producer. (B) Animal H780, an intermediate producer. (C) H822, a low producer.

***In vitro* classification is predictive of disease progression *in vivo*.** To determine whether our *in vitro* classification of animals as high, intermediate, or low producers correlated with the rate of disease progression *in vivo*, the 10 animals described in the previous section were inoculated intravenously with 10-100 monkey infectious doses of the same virus stock of $SIV_{DeltaB670}$ that had been used for the phenotyping *in vitro*. The rate of disease progression was determined by 1) quantifying SIV p27 antigenemia, 2) analyzing changes in T cell subsets in the peripheral blood, and 3) survival. SIV p27 antigenemia was used to determine the virus burden in these animals because adequately preserved plasma samples for quantifying of plasma RNA were not available. The relationship between the amount and persistence of antigenemia to disease progression and survival, however, has been well documented (57, 123-125, 219). In our analysis of peripheral blood T cell subsets, we were particularly interested in determining whether a selective loss of the $CD4^+CD29^+$ memory subset of T lymphocytes in the peripheral blood had occurred, since we had previously shown that these changes were the most indicative of rapid disease progression (123-125). The amount of SIV p27 detected in the serum of the three groups is shown in Figure 8, panels A, B, and C, respectively. Persistent antigenemia was observed in all three high producer animals, a finding indicative of rapid disease progression and early death. The remaining animals showed declines in antigenemia by 3 weeks post-infection (p.i.). Two of three intermediate producers (monkeys H737 and H644), however, had recurrences of antigenemia that were detectable by 18 and 24 weeks p.i., respectively. In contrast, low producers had the lowest peak antigenemia, with recurrences detectable only after 28 weeks p.i.

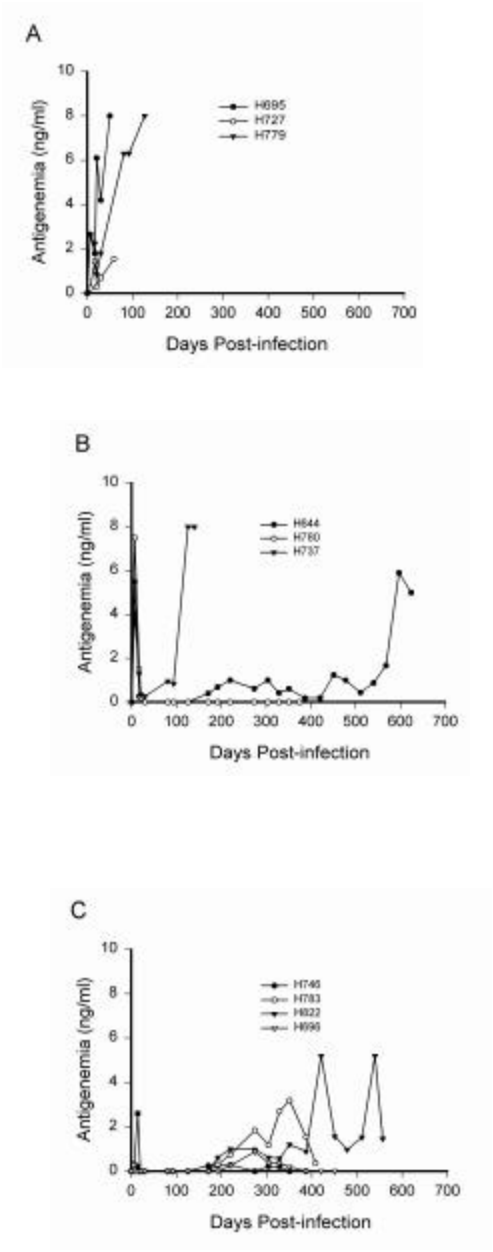

Figure 8. Relationship between post-infection SIV p27 antigenemia and monkeys with different *in vitro* replicative phenotypes.

All animals were infected intravenously with 10-100 monkey infectious doses of $SIV_{DeltaB670}$ as described. Antigenemia (ng/ml) in the blood was monitored serially by ELISA until sacrifice due to the onset of AIDS for (A) high producers, (B) intermediate producers, and (C) low producers.

The changes in the $CD4^+CD29^+$ memory T cell subset identified by flow cytometry in each animal (Figure 9) were consistent with the antigenemia observed. All three high producers had rapid selective declines in $CD4^+CD29^+$ T lymphocytes that coincided with persistent antigenemia. This decline was evident by the first month p.i., whereas a decline in this population was much more variable in intermediate and low producers and generally progressed at a much slower rate. The intermediate producer that had the earliest recurrence of antigenemia and earliest death in the group (monkey H737) also had a very rapid selective decrease in $CD4^+CD29^+$ cells. An increase in the $CD4^+CD29^+$ T cell population was also observed in some animals late in the infection. This finding is consistent with the observation of others (146) and likely reflects activation of these cells associated with the increases in virus burden that occur near death.

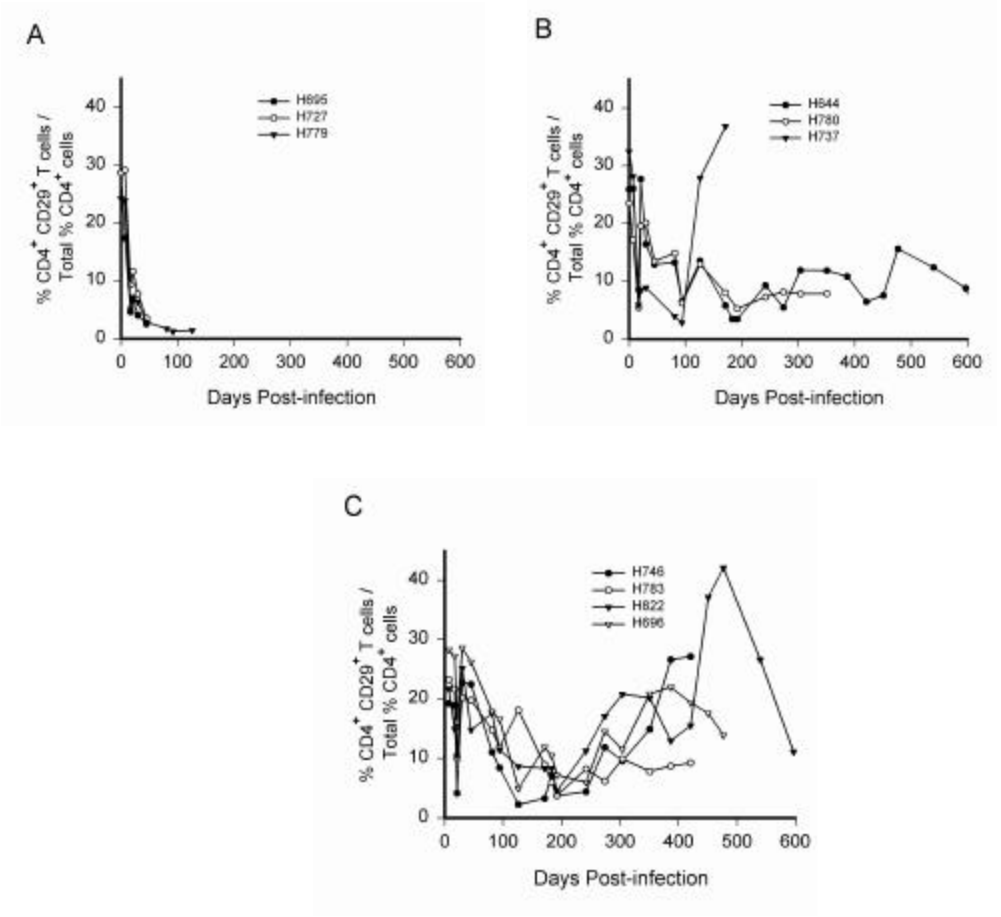

Figure 9. Relationship between changes in $CD4^+CD29^+$ T helper lymphocytes and monkeys with different *in vitro* replicative phenotypes.

At regular intervals after infection, the percentage of memory (% $CD4^+$ $CD29^+$/total % $CD4^+$) T cells in peripheral blood was evaluated by flow cytometry as described for (A) high producers, (B) intermediate producers, and (C) low producers.

Physical examinations were performed at biweekly intervals, and animals were provided full supportive care until they were deemed moribund by the attending veterinarian. Moribund animals were humanely sacrificed and given complete pathological examinations. As expected from the differences observed in viral replication, a wide range of survival was observed among the ten animals. Deaths occurred from 50 to 557 days p.i. with a median time of 381 days. The three high producers survived less than the median, while the four low producers survived beyond the median survival time. Survival of the intermediate producers was more variable. The patterns of clinical and pathological findings were also associated with the RT rank and rate of disease progression, with high producers developing a generalized rash soon after infection, showing little evidence of lymphadenopathy, and dying early with severe opportunistic infections. In contrast, low producers had more chronic disease progression characterized by lymphadenopathy, splenomegaly, chronic diarrhea, and wasting. Lymphoma occurred in one low producer, a finding associated with lengthened survival in macaques (72). Histopathological examination of tissues taken from these animals at necropsy confirmed the clinical profile of SAIDS in all cases.

Although the data from these 10 animals suggested a striking relationship between SIV production *in vitro* and rate of SIV-induced disease progression and time to death *in vivo,* larger numbers of animals were required to definitively establish this phenomenon. Since adequate cage space was available at the Tulane Primate Center, the majority of animals enrolled in SIV studies spanning a decade of research were provided supportive clinical care until they were moribund so that crucial data on survival in a large cohort of infected animals could be obtained. Furthermore, because we believed that the results of virus production *in vitro* were highly useful in the selection of animals for experimental groups, this analysis was performed on most of the

animals used during this time period. Fifty-nine animals were chosen for further analysis. This cohort was comprised of all animals infected with $SIV_{DeltaB670}$ that were 1) inoculated intravenously, 2) received no other effective therapeutic or vaccine, and 3) died of an AIDS-defining illness. However, different cryopreserved stocks (both human and monkey propagated) and different doses (10-10,000 animal infectious doses) were used over this time period. Maximum RT determined for each animal is graphically presented in Figure 10. The overall mean peak RT was 101,120 ± 118,764 cpm/ml. Animals were divided into 3 cohorts using natural breakpoints detected by direct visualization of the data. Each breakpoint is indicated by the vertical line in Figure 10 A. These cohorts consisted of 1) the upper 20th percentile: peak RT > 160,000 cpm/ml (mean = 298,119 ± 128,355 cpm/ml); 12 animals, 2) the lower 20th percentile: peak RT < 15,000 cpm/ml (mean = 7,838 ± 4,004 cpm/ml); 12 animals, and 3) the remaining animals falling into the median range: 160,000 > peak RT > 15,000 cpm/ml (mean = 66,548 ± 32,793 cpm/ml); 35 animals. The cause of death in these cohorts was consistent with their survival, with SIV-giant cell disease, pneumonia, and colitis most prevalent in rapid progressors, and lymphoma, lymphoproliferative disease, and amyloidosis being the predominant findings in slow progressors.

The overall mean survival for the 59 animals was 289 ± 151 days. Kaplan-Meier analysis of survival for the individual cohorts is shown in Figure 10B. Striking differences in survival were apparent in the three groups, with early mortality almost exclusively within animals in the highest peak RT group and long-term survivors associated with the lowest peak RT group. Some of the animals in the lowest peak RT group lived over 400 days post infection, which was over 100 days beyond the mean survival for the entire study group.

The statistical relationship between peak RT and survival of the 3 cohorts is shown in Figure 10 C. Mean survival differed markedly among the groups, with survival in high producers less than half that of low producers (168 ± 123 vs. 367 ± 106). This difference was highly significant by one-way ANOVA ($p = 0.002$). High producers also experienced reduced survival compared to that of the intermediate group (304 ± 152, $p = 0.013$). However, no significant difference in overall survival between intermediate and low producers was observed.

The phenotypic differences observed between high and low producers were not due to infection with other viruses commonly encountered in macaques (e.g., SRV, STLV-1, Herpes B) because differences in viral replicative capacity were observed in cells from monkeys that were PCR and/or antibody negative for these viruses (data not shown).

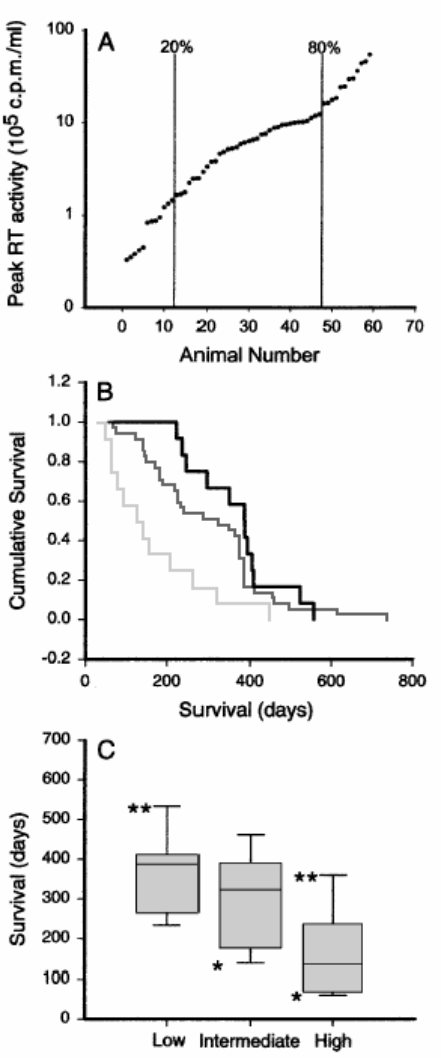

Figure 10. Correlation between *in vitro* virus production and survival in 59 rhesus macaques infected with $SIV_{DeltaB670}$.

(A) Distribution of peak RT values obtained from the *in vitro* assay among the cohort of 59 animals. Animals were stratified based on peak RT into upper 20th percentile (high producers), lower 20th percentile (low producers) and middle 60% (intermediate producers). (B) Kaplan-Meier analysis of survival within each group: Low producers (black line), Intermediate producers (dark gray line), High producers (light gray line). (C) Statistical relationship of peak RT and survival among the 3 groups. One-way ANOVA was performed on stratified groups defined in (A). Statistically significant differences are depicted by the asterisks. ** $p = 0.002$; * $p = 0.013$. For each group, the box encloses the median value line and the 25th and 75th percentile values. Lines extend to encompass the 10th and 90th percentiles.

The high/low producer phenotype is maintained in purified $CD4^+$ T cell populations. To determine the relative contribution of other cell types in PBMC to virus production during the kinetics assay, cultures of purified $CD4^+$ T cells and whole PBMC were run in parallel. $CD4^+$ T cells were purified using anti-$CD4^+$ antibodies coupled to magnetic beads according to the Miltenyi Biotec system. Flow cytometry was used to monitor the purity of the $CD4^+$ T cell cultures, and in all cases, purity was equal to or greater than 95% (data not shown). The results from these assays are shown in Figure 11. A comparison of virus production from whole PBMC cultures from high and low producer animals shows at least a log difference in the amount of virus produced, as measured by p27 antigen in the cell culture supernatants (Figure 11 A and B). When comparing virus production from purified $CD4^+$ T cell cultures (Figure 11 C and D), there is still a difference of at least a log in virus production (notice difference in y-axes). This confirms that the $CD4^+$ T cell itself is responsible for the differences in virus production *in vitro*.

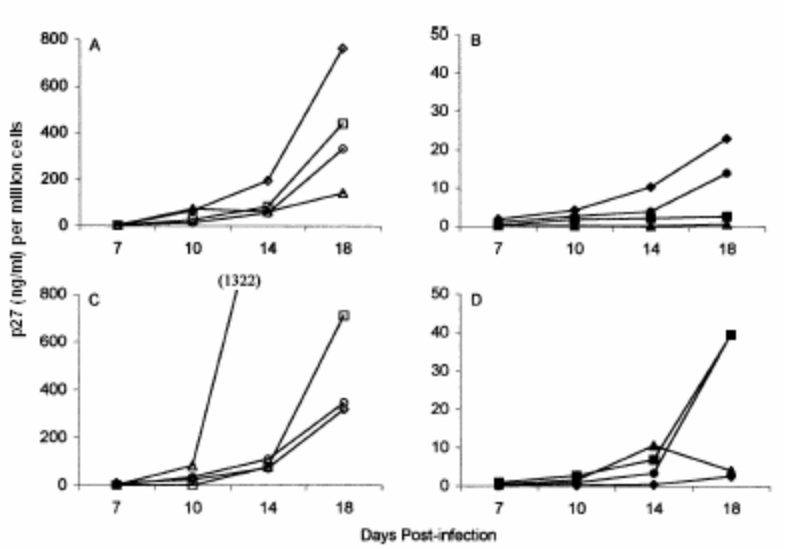

Figure 11. The phenotype of high/low virus production persists in both PBMC and CD4$^+$ T cell cultures.

Whole PBMC (A and B) or purified CD4$^+$ T cells (C and D) were infected with $SIV_{DeltaB670}$ in the standard viral growth kinetics assay. Virus production was measured by a p27 ELISA and is expressed as ng/ml p27 per million cells. The high producer animals are shown in (A) and (C) and the low producers are shown in (B) and (D). Notice the difference in y-axis scales between high and low producers.

3.4. Discussion.

In a survey of rhesus monkeys infected intravenously with the primary virulent isolate $SIV_{DeltaB670}$, we have shown that the viral replicative capacity of the naïve animal's PBMC following *in vitro* infection is highly predictive of disease progression and survival *in vivo* following experimental inoculation. Monkeys whose cells produce high amounts of SIV following an *in vitro* infection (high producers) are more likely to develop SAIDS sooner and die more quickly than those animals whose cells support little virus replication (low producers). As expected, these animals displayed a continuum of virus production and survival spanning high virus production/early death to low virus production/long-term survival. The relationship between the maximum reverse transcriptase activity produced in cell culture supernatants during a 21 day culture period and survival was highly significant when high producers were compared to intermediate and low producers ($p = 0.013$ and 0.002, respectively; ANOVA). The direct correlation between high *in vitro* replicative capacity and shortened survival that has persisted throughout these experiments is even more striking given that results obtained over a long time interval were compared, and multiple virus stocks propagated in both human and monkey PBMC were used during this time period. Furthermore, this property determines the fate of the animal once infected, with low producers progressing to AIDS more slowly and surviving longer than high producers. This relationship is particularly intriguing in view of the likelihood that *in vitro* control of virus does not involve virus-specific immunity.

These data support observations reported by Lifson *et al.* (113) in which plasma viral loads and survival in 8 macaques correlated with the amount of virus required to infect macaque PBMC *in vitro*. Taken together with our findings, the two studies clearly identify an innate

property of individual macaques that controls virus replication both *in vitro* and *in vivo*. Further insight into this phenomenon was gained by determining that the hierarchy associated with high and low producer phenotypes was retained in cultures of infected purified $CD4^+$ T lymphocytes. These findings indicate this phenotype is an intrinsic property of the $CD4^+$ T cell itself. Control of virus production could be at the level of viral entry (e.g., viral receptor(s)), or post-entry, with the differential production of either suppressor (in low producer) or enhancer (in high producer) proteins.

The intrinsic property of macaque PBMC to support the replication of SIV *in vitro* may be analogous to the differences in replicative capacity observed for human PBMC infected *in vitro* with HIV-1 (210). Together with the variable length of time from infection to death also observed in HIV^+ humans (22, 27, 112, 134, 139, 152), the data reported here may be highly relevant to the pathogenesis of HIV as well. The experimental system described in this report should enable the identification of the specific host gene(s) responsible for this phenomenon and as well as provide crucial information for the development of effective strategies for disease intervention.

The advantage of accurately predicting survival prior to selection of monkeys for SIV studies is obvious, particularly in experiments where both control and test groups are infected and more subtle parameters of efficacy are required. Since limited numbers of animals are often used in macaque trials due to the expense, optimal stratification of groups is crucial so that differences in delays in disease progression be appropriately identified. In this regard, it is important to note that *in vitro* determination of viral replicative capacity not only predicted overall survival in the animals reported here, but also correlated with other parameters such as

antigenemia and the rate of T cell decline (reported here) and plasma virus loads (113), which are all used to determine the rate of disease progression before death.

We have successfully used this simple, *in vitro* assay in the design of many therapeutic and vaccine trials performed on $SIV_{DeltaB670}$-infected macaques at the Tulane Primate Center. Stratification of groups prior to the initiation of the study using this assay has enhanced the interpretation of these studies. For example, in a therapeutic trial evaluating the efficacy of treatment with cyclosporin during the acute viremic episode (123), the parameters of survival, T cell changes, and antigenemia were used as indicators of efficacy. Stratification of the treatment and control groups with respect to maximum RT obtained form the *in vitro* assay permitted pair-wise analysis of efficacy. This analysis identified differences in persistence of antigenemia among the two groups that were statistically significant, even though the variability among the group as a whole precluded a significant outcome. The opposite effect can also occur. Differences in survival may be suggested when statistical analysis of small groups (n = 4 animals) of randomly chosen animals is performed, but when the group size is doubled, the difference may no longer be significant. The inclusion of analysis of the *in vitro* replicative capacity of monkeys used in experimental trials should permit an appropriate interpretation of the outcome of these studies.

3.5. Acknowledgements.

The statistical analyses for the studies presented within this chapter were conducted by Bill Pewen. In addition, Lynn Fresh performed the original viral growth kinetics assays and Louis Martin contributed data from the retrospective animal experiment.

CHAPTER 4

VIRAL AND CELLULAR GROWTH PROPERTIES OF RHESUS CD4$^+$ T CELLS INFECTED WITH SIV *IN VITRO.*

4.1. Introduction.

There is a clear and distinct association between the amount of virus produced from an uninfected animal's $CD4^+$ T lymphocytes after infection *in vitro* and survival of that animal after *in vivo* infection. Animals whose cells produced large amounts of virus (high producers) after infection *in vitro* succumbed to AIDS and died significantly more rapidly than animals whose cells produced small amounts of virus (low producers) (Chapter 3) (180). The mechanism(s) behind the differences in virus production *in vitro* and how these mechanism(s) relate to survival are not clear.

Rhesus macaques are an incredibly useful model for HIV-1-infection in humans because they are both genetically closely related to humans and succumb to an AIDS-like disease after infection with SIV (93). However, these advantages pose several limitations as well. Because of their out bred nature, genetic analyses and other studies are complicated. As is the case with human studies, determining the causes of rapid versus slow disease progression in SIV-infected monkeys is hampered by the complexity, cost, and ethics involved with *in vivo* studies.

Therefore, our simple *in vitro* assay that can effectively predict survival is a useful tool to help identify host factors that may contribute to disease progression and survival in infected monkeys. This *in vitro* assay can be used to tease out possible mechanisms for the differential virus production *in vitro* that can then be tested in an *in vivo* setting. While a large group of animals displays a wide range of *in vitro* virus production spanning from very low to very high amounts, we chose 8 animals at the opposite ends of the spectrum for further study so that differences between the two phenotypes would be readily visible. Four of these consistently exhibited high virus production when either their PBMC or $CD4^+$ cells were infected with

$SIV_{DeltaB670}$ (high producers), and four of these exhibited low virus production (low producers). The studies described in this chapter were directed at identifying basic viral and cellular growth properties *in vitro* as well as applications of our assay so that future studies designed to identify the mechanism are more focused. Our initial *in vitro* observations prompted numerous simple questions about the cultures themselves that needed to be addressed formally. Therefore, we developed several hypotheses to answer the important questions. These include:

Hypothesis 1: Virus secreted into the cell culture media from low producer cells is infectious. Retroviruses like HIV-1 and SIV often have a low specific infectivity of viral stocks, with an infectious to total particle ratio of up to 1:1000 (92). Since low producer cultures make very small amounts of virus, we identified whether the particles made are infectious or completely defective particles.

Hypothesis 2: $CD3^+$ lymphocytes, rather than B cells, NK cells, or monocytes, are the predominating cell population within SIV-infected PBMC cultures. Our previous data have shown that the high/low virus production phenotype occurred when either whole PBMC or purified $CD4^+$ T cell cultures were infected with SIV *in vitro* (Chapter 3) (180). Clearly, this phenotype is a property of the $CD4^+$ T cell itself and is not entirely due to the presence of other cells and/or factors secreted from other cells, such as chemokines or suppressor factors made by $CD8^+$ cells (9, 20, 32, 94). However, due to the limited numbers of purified $CD4^+$ T cells available, some of the experiments were conducted with whole PBMC cultures. We therefore wanted to better understand the dynamics of these cells in culture. Possibly, a cell population specifically susceptible or resistant to virus infection may be overgrowing either the high or low

producer cultures, respectively, thereby influencing virus replication. A detailed analysis of the evolution of T cells, B cells, monocytes, and NK cells within PBMC cultures was undertaken to answer this question.

Hypothesis 3: The high/low producer phenotype persists irrespective of the method used to activate the cells. Cellular activation is intimately linked to replication of both HIV-1 and SIV (162, 192, 216, 217), with the replication of both viruses being more efficient in activated T cells as compared to resting cells. It was important to determine whether our observations occur only when PHA, a glycoprotein that non-specifically activates cells through the TCR, is used to activate the cells. In addition, we began preliminary investigations of whether the proximal part of the TCR signaling cascade is playing a role in the differences in virus production observed.

Hypothesis 4: High producer cells secrete more virus into the cell culture supernatant because they are at a higher activation state than low producer cells. As stated above, SIV replicates more efficiently in activated T cells (162, 192, 216, 217). It was possible that high producer cells secreted more virus because they were getting activated to a higher degree than low producer cells as a result of identical activation stimuli. This critical question was addressed by evaluating activation marker expression, proliferation, and apoptosis after activation of the cells in the presence or absence of virus infection.

Hypothesis 5: The high/low phenotype is consistent with differential expression of a cytokine or chemokine known to influence viral replication. Initial studies focused on two cytokines in particular, IFN-γ and TNF-α, which are known to play key roles in both directly

influencing HIV-1/SIV replication and in the development of adaptive immune responses *in vivo* (34). Besides influencing virus replication, these cytokines are also known to affect cellular activation and apoptosis (34, 95, 103, 208, 212). Differential secretion of one of these cytokines may be a cause the virus producer phenotypes observed. ELISA and intracellular flow cytometry were used to analyze expression of these cytokines. Secondly, because numerous cytokines and chemokines are known to affect viral replication (164), we took a broader approach and used cDNA array hybridization to analyze the expression of a large number of genes simultaneously.

Hypothesis 6: The high/low phenotype occurs when molecular infectious clones of SIV are used in the *in vitro* kinetics assay. Goldstein and colleagues (69) have shown differential susceptibility of rhesus cells to infection with two strains of virus, $SIV_{smE543\text{-}3}$ (a molecular infectious clone) and SIV_{mac251} (a primary isolate). We determined the applicability and usefulness of our *in vitro* assay for monitoring the replication of a series of molecular infectious clones of SIV that use specific co-receptors for entry.

Hypothesis 7: The high/low producer phenotype is maintained in $CD4^+$ T cells transformed by *Herpesvirus saimiri*. Transformation of rhesus monkey $CD4^+$ T cells using *Herpesvirus saimiri* has been demonstrated to be a useful tool in HIV-1/SIV research (129). Because primary cells are limited in number and difficult to work with, we evaluated whether transformed $CD4^+$ T cell lines made from each animal maintained the high/low virus production phenotype. Establishment of cell lines that maintain their phenotypic properties would make more complicated assays feasible due to a greater number of available cells.

Whereas the end goal of these studies is to identify a mechanism behind differential virus production *in vitro* and the host factor(s) that is responsible, a focused analysis requires a knowledge and understanding of the basic properties and applications of the *in vitro* assay. The data presented in this chapter accomplish this by closely examining both the viral and cellular growth properties in culture.

4.2. Materials and Methods.

Analysis of virus replication *in vitro*. 20-40 ml blood was collected via the femoral vein from individual rhesus macaques using acid citrate dextrose (ACD) as the anticoagulant. Peripheral blood mononuclear cells (PBMC) were isolated from whole blood by Ficoll-Paque (Pharmacia Biotech) density-gradient centrifugation. Cells were grown in complete media consisting of: modified RPMI 1640 supplemented with 15% fetal bovine serum, penicillin-streptomycin (100 U/ml; 100 U/ml), L-glutamine (2 mM), HEPES buffer solution (10 mM), and recombinant human IL-2 (40 U/ml) (Hoffman-LaRoche).

Cell pellets containing 5 x 10^6 PBMC were infected by incubation with 0.5 ml of a 1:10 dilution of a cryopreserved stock of $SIV_{DeltaB670}$ containing 1,000 tissue culture infectious doses for 2 hours at 37 °C. After infection, cells were washed twice in complete medium and cultured overnight. Twenty-four hours after infection (day 1), the cells were stimulated with either: 1) 5 µg/ml of phytohemagglutinin (PHA) (Gibco BRL); 2) 5 ug/ml plate-bound anti-CD3 and anti-CD28 antibodies (Pharmingen; clones SP34 and CD28.2, respectively), or 3) 10 ng/ml Phorbol 12-myristate 13-acetate (PMA) and 200 ng/ml ionomycin (Sigma). On day 4, the cells were removed from the source of activation by washing the cells 3 times in complete medium. Cells were cultured in complete medium supplemented with human IL-2 (40 U/ml) for the entire experiment (21 days) and maintained at a concentration of 1 x 10^6 cells/ml. On days 7, 10, 14, 18, and 21, the cells were counted by trypan blue exclusion and 1 ml of supernatant was removed and stored at –70 °C. The amount of virus in culture supernatants was determined using an SIV Core antigen ELISA (Coulter), as per the manufacturer's instructions.

Flow Cytometry. A list of antibodies used throughout these studies is shown in Table 2. For cell surface staining, approximately 1 x 10^6 cells were added per tube (Falcon #35-3058) and washed once in FACS staining buffer (PBS containing 5 % FBS, 2 % Normal Human Serum, 2 % Goat Serum, and 0.1 % Sodium Azide). To each cell pellet, 5 ul of each antibody was added, and the tubes were incubated for 20 minutes on ice in the dark. After the incubation, the cells were washed once in staining buffer and resuspended in 500 ul of 1% paraformaldehyde in 1 X PBS.

Table 2. List of monoclonal antibodies.

Antibody	Source	Clone
CD3	Pharmingen	SP34
CD4	Pharmingen	M-T477
CD8	Immunotech	B9.11
CD14	Immunotech	RMO52
CD16	BD Pharmingen	3G8
CD20	Becton-Dickinson	Leu-16
CD25	Immunotech	B1.49.9
CD27	BD Pharmingen	M-T271
CD28	BD Pharmingen	CD28.2
CD29	Coulter	4B4
CD45	Pharmingen	TU116
CD45RA	Immunotech	2H4
CD56	Pharmingen	MY31
CD62L	Becton-Dickinson	Leu-8 (SK11)
CD69	Pharmingen	FN50
CD71	Becton-Dickinson	LO1.1
CD95	Pharmingen	DX2
CD154 (CD40L)	BD Pharmingen	TRAP1
CD195 (CCR5)	BD Pharmingen	2D7/CCR5
Ki-67	Coulter	MIB-1
human CCR5	R&D systems	CTC5
TNF-alpha	Pharmingen	Mab11
IFN-gamma	Pharmingen	4S.B3

Intracellular Flow Cytometry. Fresh PBMC from each animal were stimulated with anti-CD3/CD28 antibodies in the presence of 2 uM monensin (Pharmingen) for 5 hours at 37 °C. Subsequently, the cells were aliquoted into 5 ml FACS tubes. The cells were washed once with staining buffer by filling the tube and centrifuging at 1400 rpm for 10 min at 4 °C. After decanting the supernatant, 5 ul of each surface antibody was added, and the tubes were mixed and incubated for 30 minutes on ice in the dark. The cells were washed two times with 1 ml FACS buffer each, using centrifuge conditions above. After decanting the supernatant, 500 ul 1% paraformaldehyde (PFA) in 1 X PBS was added per tube, and the tubes were incubated for 20 minutes at room temperature. After the incubation, the tubes were centrifuged and decanted. They were then washed once more in FACS buffer, followed by one wash in permeabilization buffer (FACS buffer $^{+}$ 0.1 % Saponin). After decanting the supernatant, 5 ul of IFN-γ, TNF-α, or the control IgG antibody was added per tube. The tubes were mixed and incubated for 15 minutes at RT in the dark. Following this, the cells were washed once in permeabilization buffer and once in FACS buffer before being fixed by the addition of 500 ul 1 % PFA.

Measurement of cell proliferation. Freshly isolated PBMC were incubated in RPMI $^{+}$ 15% FBS (no IL-2) for 2 days at 37 °C to ensure the accuracy of the non-dividing negative control. Subsequently, the cells were washed twice in PBS, and the cell pellets were incubated with 1 ml of a 10 uM solution of carboxyfluorescein succinimidyl ester (CFSE; Molecular Probes) for 8 minutes at RT in the dark (CFSE is diluted fresh in PBS from a 10 mM stock solution in DMSO). Each tube was vortexed after addition of the substrate. An equal volume (1 ml) of FBS was added to stop the reaction. The cells were then washed 3 times in RPMI $^{+}$ 15% FBS (no IL-

2). Half of the cells were then cultured in RPMI $^{+}$ 15% FBS without IL-2 (to serve as a negative control). The other half were cultured in media containing IL-2 and stimulated with either PHA or anti-CD3/CD28 antibodies. Some cultures were infected with SIV as described above prior to labeling with CFSE and activation. Approximately 3 – 6 days after labeling, cells were removed from culture and stained with antibodies to cell surface antigens (CD4, CD8, etc.). They were analyzed on a flow cytometer (CoulterXLS) with CFSE fluorescence in the FL1 channel.

Measurement of apoptosis. To detect apoptosis using the fluorescent caspase-3 substrate PhiPhiLux (OncoImmunin), cells were first stained for cell surface molecules as previously described, but they were not fixed. The media was completely removed from each tube and 50 ul of 10 uM substrate was added. The tubes were mixed by flicking and incubated with cap off at 37 °C for 45 minutes to 1 hour. Then, 1 ml ice cold flow cytometry buffer was added and the tubes were centrifuged for 10 minutes at 1200 rpm. They were resuspended in 500 ul fresh buffer and analyzed on a flow cytometer within 1 hour.

cDNA Array Hybridization. Purified rhesus $CD4^{+}$ cells were isolated as described above. They were infected with SIV (m.o.i. = 0.01) for 2 hours at 37 °C. Twenty-four hours later, the cells were lysed in 1 ml trizol for RNA isolation. RNA samples from three low producers (M0898, M12797, M6498) were pooled, as were RNA samples from three high producers (M8697, M0198, M7699). The cytokine cDNA Expression Array (Cat. #GA001) and the cDNA Labeling and Hybridization Kit (Cat. #GAC10) were obtained from R&D Systems. Ribonuclease Inhibitor (RNasin) was obtained from Perkin Elmer, ^{33}P-deoxycytidine 5-triphosphate (dCTP) was obtained from ICN Radiochemicals, and Oligo$(dT)_{20-25}$ was obtained

from GibcoBRL. Total RNA was used for preparation of cDNA using oligo(dT). The manufacturer's instructions were followed for the entire protocol. Hybridization was overnight at 63.5 – 64.5 °C. The filters were exposed to a phosphorimager screen for 3 days, scanned, and analyzed using Imagene software in the Pitt Array Facility. Data were analyzed as described previously (168).

Generation of virus stocks. Rhesus high producer and human PBMC were stimulated with PHA for 3 days. On day 7, the cells were aliquoted and infected with a 1:10 dilution of the various stocks of virus for 2 hours at 37 °C. The virus was washed off, and the cells were cultured at a high cell density (~3 x 10^6 cells/ml). Every 3 days, the cells were counted. At each of these times, approximately 90 % of the old media was removed and replaced with fresh media to a concentration of 3 x 10^6 cells/ml. On days 7, 10, and 14 post-infection, the supernatant was frozen in cyrovials of 500 ul/each. The vials were snap-frozen in liquid nitrogen and then transferred and stored at -80 °C.

Titration of virus stocks. The virus stocks were titered by the method of Reed and Meunch (166). Human PHA blasts were aliquoted into a 48-well plate (5 x 10^5 cells / well). The cells were incubated with 100 ul of virus (10-fold dilutions), with 3 replicates at each dilution, and incubated for 2 hrs at 37 °C. The virus was washed off after adsorption, and the cells were cultured in 1 ml of complete media containing IL-2. Twice weekly, 0.5 ml of media was removed and replaced by 0.5 ml of fresh media. The supernatant was harvested at either day 14 or day 18 and tested for the presence of virus by p27 ELISA.

Transformation of rhesus CD4$^+$ cells. Stocks of *Herpesvirus saimiri* were generated by culture on owl monkey kidney (OMK) cells and frozen in 1 ml aliquots. Media for transformation of rhesus cells consisted of: RPMI 1640, penicillin-streptomycin (100 U/ml each), l-glutamine (2 mM), 20 % FBS, 1:260,000 dilution of β-mercaptoethanol, and IL-2 (40 U/ml). Freshly-isolated rhesus CD4$^+$ cells were seeded in 12-well plates (2 x 10^6 cells / well) and cultured overnight. The next day, ~1.5 ml was removed from each well, and 1 ml of *H. saimiri* stock was added for 2 hours at 37 °C. After the adsorption, 1 ml of fresh media was added. The plates were cultured for several weeks with ½ media changes twice weekly or when needed. Cultures that appeared to be growing were split when necessary. By 4 – 6 weeks, only transformed cell lines remained alive. These cells were grown into large stocks and viably frozen in 0.5 ml aliquots in culture media containing 10 % DMSO.

4.3. Results.

The unique and striking correlation between our simple *in vitro* assay and survival of SIV-infected rhesus monkeys called for a detailed analysis of the culture conditions to better understand the dynamics of both virus and cell replication. Throughout these studies, we used 8 animals representing the extreme ends of the spectrum with regard to virus production to facilitate comparison analyses.

Infectivity of virus secreted from low producer cells. Lentiviruses are notorious for having a low specific infectivity of viral stocks, often having an infectious to total particle ratio as low as 1:1000 (92). Since low producer cultures secreted very small amounts of virus (Figure 11), we sought to identify whether the particles made from these cells were infectious. For each animal, supernatant samples were harvested at various time points during the *in vitro* viral growth kinetics assay and tested for the presence of infectious virus by inoculation onto uninfected PHA-stimulated PBMC. A sample was considered positive if the day 18 supernatant sample from the inoculated well was positive for the viral p27 protein by ELISA. Supernatant samples were tested for infectivity on PBMC from one high producer animal (M7799, Table 3) and one low producer animal (M0898, data not shown). Supernatants from both high and low producer cultures were almost uniformly infectious on cells from the same or different phenotype of animal (Table 3). Therefore, the virus made in low producer cultures was infectious and did not consist entirely of defective particles.

Table 3. Infectivity of supernatant samples from high and low producer cultures.

		Day Post-infection[1]					
Producer status	**Animal #**	**4**	**7**	**10**	**14**	**18**	**21**
Low	M0898	+	+	+	+	+	+
Low	M12797	-	+	+	+	+	+
Low	M6498	-	+	+	+	+	+
Low	M6698	+/-	+	+	+	+	+
High	M8697	+	+	+	+	+	+
High	M0198	+	+	+	+	NA	NA
High	M7699	+	+	+	+	+	+
High	M7799	+	+	+	+	+	+

[1]Supernatant samples were harvested during the *in vitro* viral growth kinetics assay and tested for the presence of infectious virus by inoculation onto PHA-stimulated PBMC from high producer animal M7799. A sample was considered positive if the day 18 supernatant sample from the inoculated well was positive for the viral p27 protein by ELISA. Infectivity was also tested on cells from low producer animal M0898, which gave identical results. P27 values were scored as + or - only. NA = sample not available.

Composition of PBMC cultures throughout *in vitro* culture. We have previously shown that the differences in virus production *in vitro* occur in both PBMC and $CD4^+$ T cell cultures (Chapter 3, Figure 11) (180). However, since some of our experiments were conducted using PBMC, a concern was the evolution of the cell populations during *in vitro* culture, specifically, whether or not an alternative cell population (CD8, B-cells, NK cells) outgrew $CD4^+$ cells in a differential manner. Flow cytometric analysis revealed that the percentage of $CD4^+$ lymphocytes decreased throughout the culture period; this was concomitant with a rise in the percentage of $CD8^+$ lymphocytes (Figure 12 A and B). The decrease in $CD4^+$ cells was significantly greater in high producer cultures than in low producer cultures ($P = 0.012$; repeated measured ANOVA). There was essentially no change in the percentage of double-positive $CD4^+CD8^+$ cells and a slight increase in CD4-CD8- cells (Figure 12 C and D). The rise in CD4-CD8- cells may have been due to a loss of CD4 expression as a result of viral infection (19). The presence of monocytes, B cells, and NK cells throughout the culture was negligible (data not shown and Figure 13).

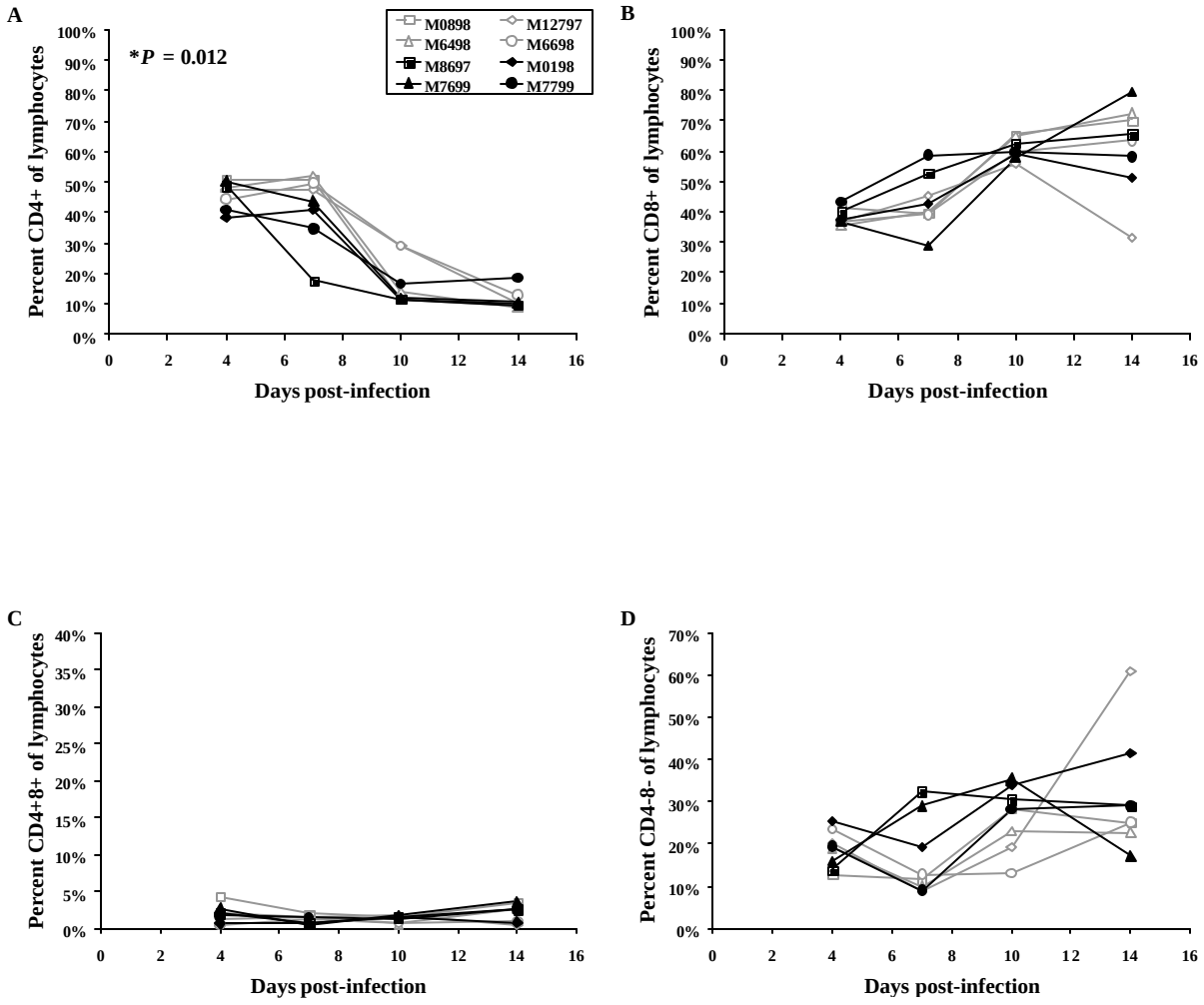

Figure 12. Evolution of CD4$^+$ and CD8$^+$ cell populations throughout *in vitro* culture.

The expression of CD4 and CD8 cell markers were monitored on gated lymphocytes by flow cytometry. High producers are shown in black with solid symbols; low producers are shown in gray with open symbols. The percentage of lymphocytes expressing (A) CD4, (B) CD8, (C) both CD4 and CD8, and (D) neither CD4 nor CD8 is shown. The decline in the percentage of CD4$^+$ cells (A) was statistically significant by repeated measures ANOVA and the *P*-value is indicated on the graph.

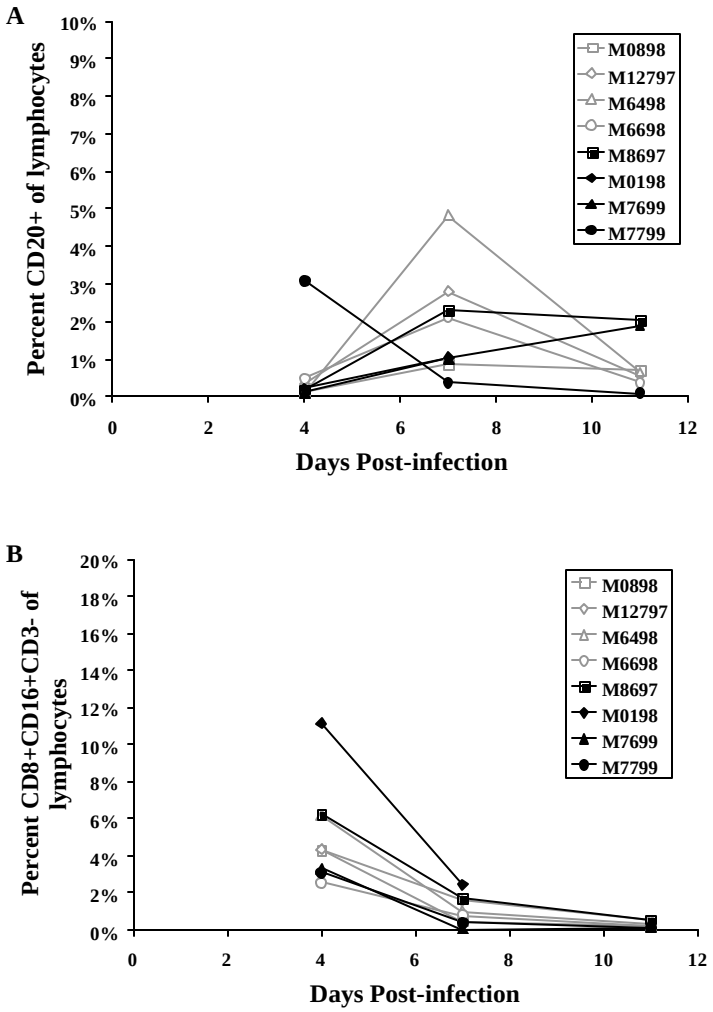

Figure 13. Detection of B cells and NK cells throughout *in vitro* culture.

(A) $CD20^+$ B cells, and (B) $CD8^+CD16^+CD3$- NK cells were monitored through the first 11 days of *in vitro* culture by flow cytometry. High producers are shown in the black solid symbols; low producers are shown in the gray open symbols. There were no differences between the two groups for either cell type.

Differences in virus production *in vitro* occur irrespective of the mitogen used to activate the cells. Our standard *in vitro* viral growth kinetics assay uses the mitogen phytohemagglutinin (PHA) to activate the cells after infection with SIV (Figure 15 A). PHA is a glycoprotein that non-specifically activates lymphocytes by cross-linking cell surface molecules, including the T-cell receptor (TCR) (Figure 14). Because cellular activation is intimately linked to replication of both HIV-1 and SIV (162, 192, 216, 217), both viruses generally replicate better and more efficiently in activated T cells as compared to resting cells. To better define the relationship between cell activation and differential virus production, we pursued a more physiological method of activating the cells. Antibodies to CD3 (the signaling component of the T-cell receptor) and CD28 (a co-stimulatory molecule) in combination directly activate the cells through the TCR in a specific manner (Figure 14). We found compelling differences in virus production when the TCR is directly activated by this method (Figure 15 B).

Alternatively, cells can be activated using Phorbol 12-myristate 13-acetate (PMA) and ionomycin, the combination of which bypasses the upper part of the signaling cascade by directly activating protein kinase C and affecting calcium mobilization (Figure 14). Indeed, differences in virus production between high and low producer cells were evident after PMA and ionomycin stimulation (Figure 15 C), although the differences were much more remarkable when anti-CD3/CD28 antibodies were used. These results suggest that differential virus production is most likely mediated by the lower half of the activation cascade.

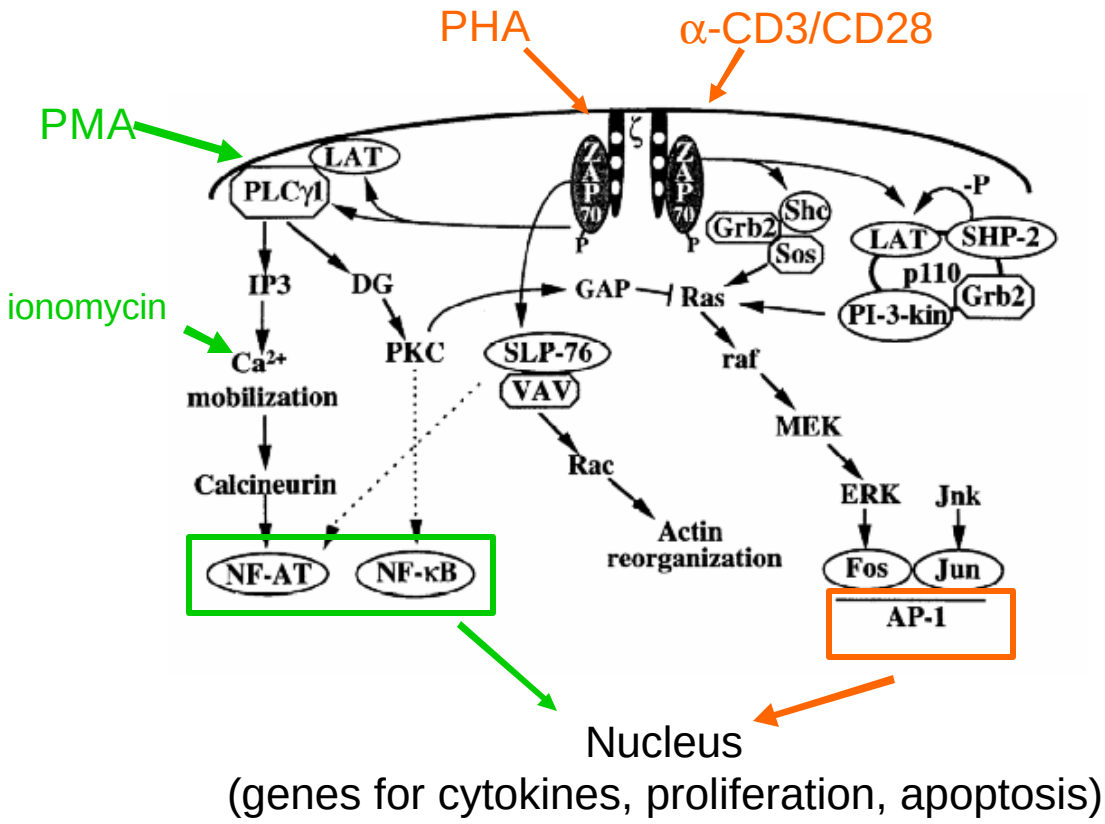

Figure 14. The effect of mitogens on signaling from the T-cell receptor.

T-cell activation involves numerous signaling molecules downstream of the TCR. PHA and anti-CD3/CD28 antibodies activate the cell directly through the TCR, while PMA and ionomycin affect PLC and calcium mobilization. The outcome of all three mitogens is activation of NF-AT, NF-kB, and AP-1 which result in proliferation and gene expression. (Modified with permission from Medema and Borst (128) © American Society for Human Immunology).

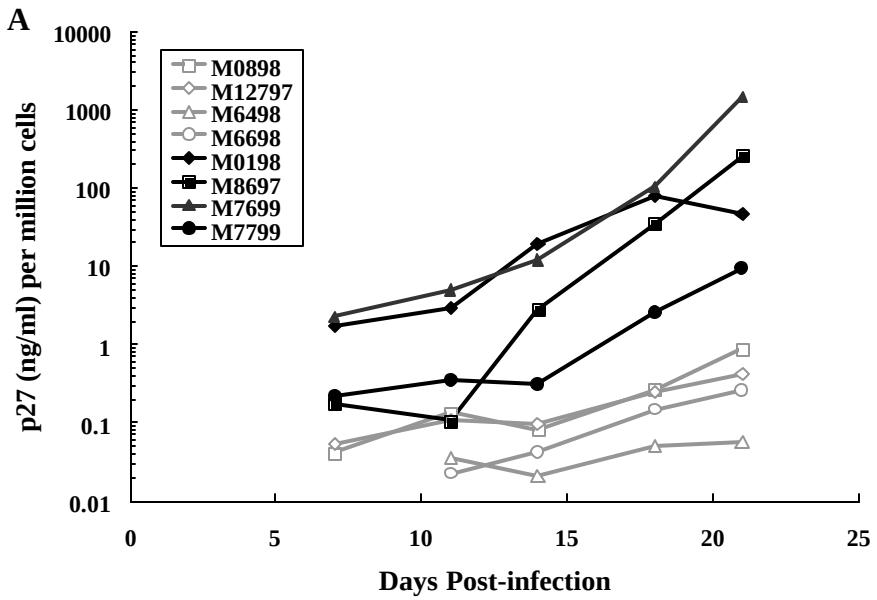

Figure 15. Growth of $SIV_{DeltaB670}$ on rhesus PBMC after activation with different mitogens.

Fresh PBMC were isolated and infected with SIV as per the *in vitro* growth kinetics assay. Twenty-four hours after infection, the cells were stimulated for 3 days with (A) 5 ug/ml PHA, (B) 5 ug/ml plate-bound anti-CD3/CD28 mAbs, or (C) 10 ng/ml PMA and 200 ng/ml ionomycin. Virus production was measured in supernatants samples using a p27 ELISA. Values are expressed as the amount of p27 (ng/ml) per 1 x 10^6 live cells at the time of the supernatant harvest. High producers are shown in black with closed symbols; low producers are shown in gray with open symbols. Panels (B) and (C) are shown on the following page.

Figure 15. (cont'd).

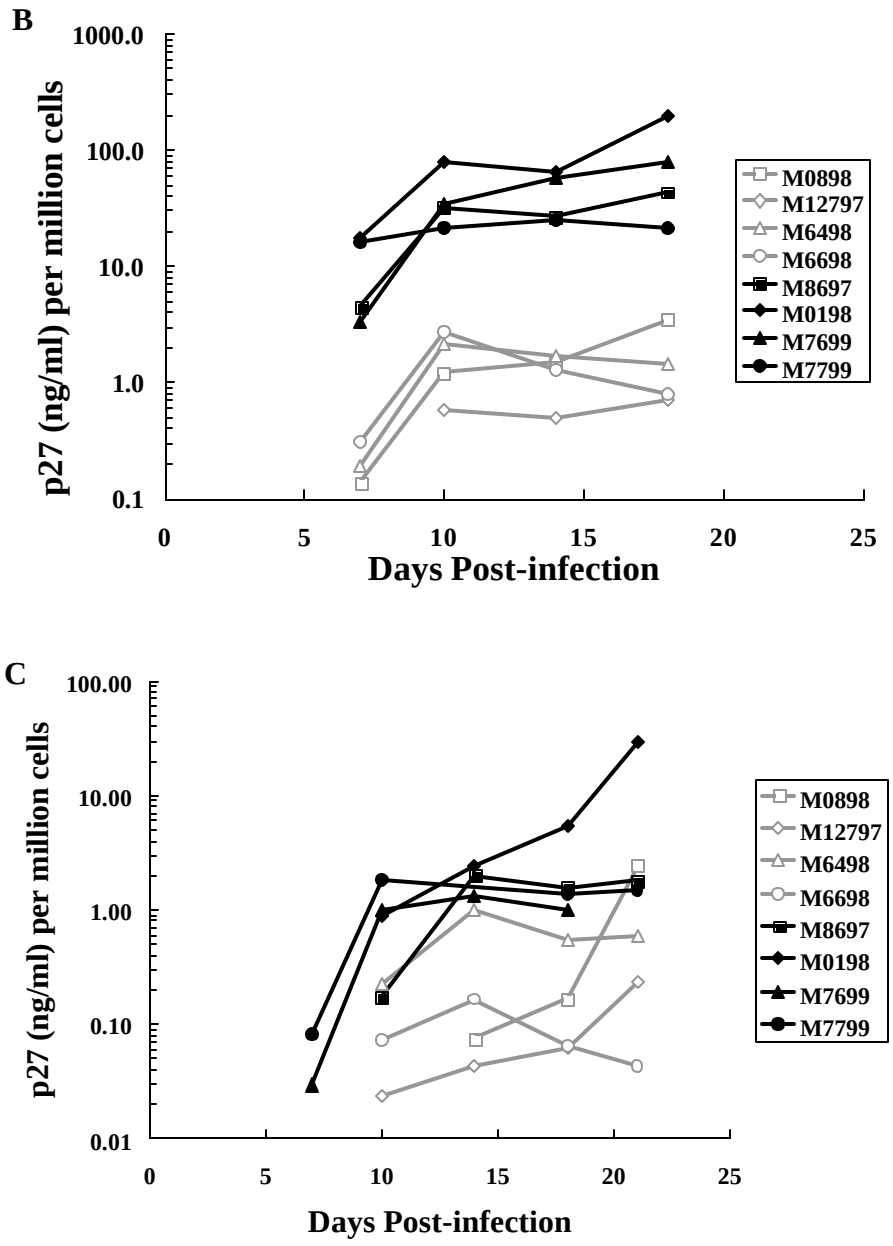

Cell viability during *in vitro* culture. An important component of *in vitro* virus production assays is the routine analysis of cell viability in both infected and mock-infected cultures so that virus production on a per cell basis can be determined. In the 8 animals studied here, greater numbers of viable cells accumulated in SIV-infected low producer cultures during the course of an *in vitro* infection than that routinely observed in high producer cultures (Figure 16 A). Surprisingly, a similar difference in cell growth was also seen in mock-infected cultures stimulated with mitogen alone (Figure 16 B). This difference was consistently observed during the numerous *in vitro* assays performed with these 8 animals. The one exception in this group, plotted separately in Figure 16, was the outlier high producer monkey M7799, whose cells continued to increase despite the large amounts of virus produced.

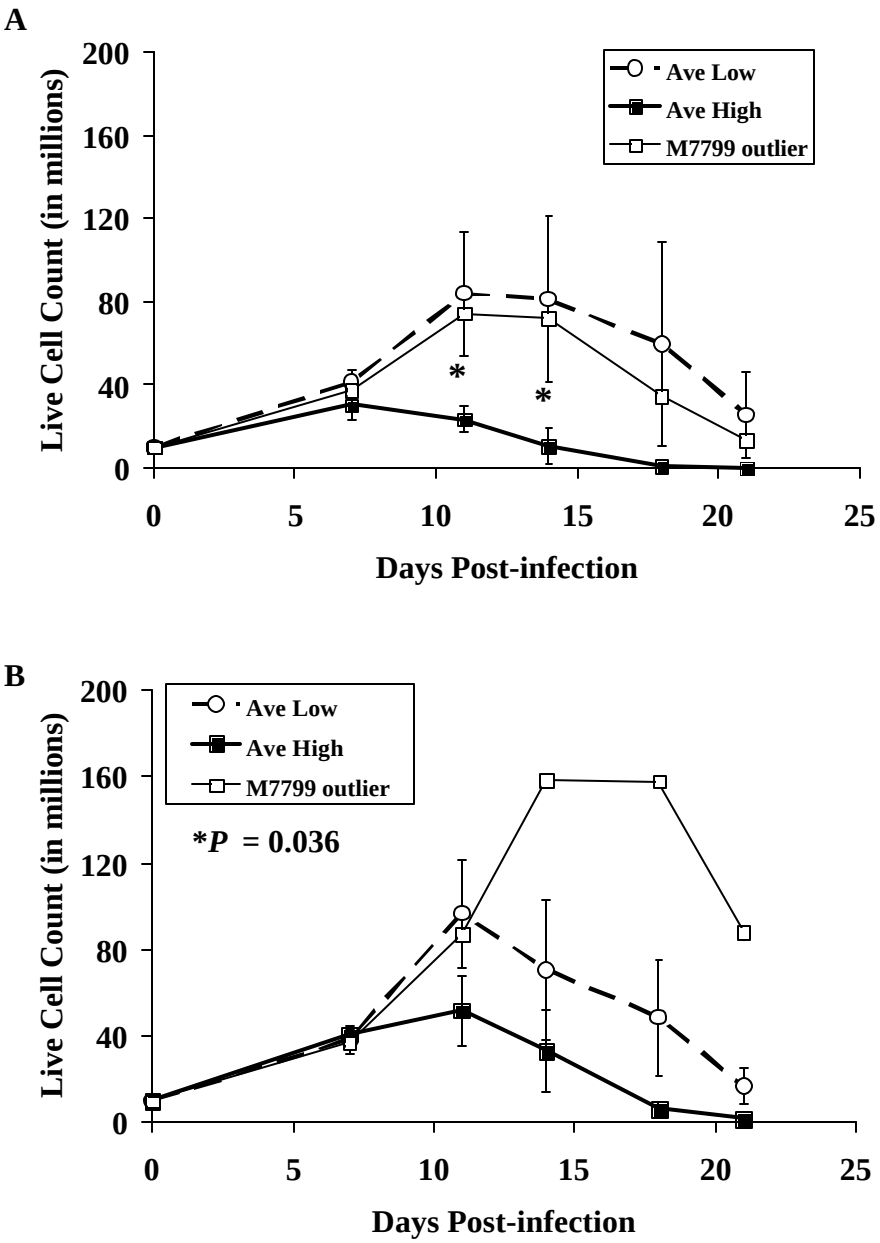

Figure 16. Both SIV- and mock-infected low producer PBMC cultures contain greater numbers of viable cells.

Viable cell numbers were determined by trypan blue exclusion in (A) SIV-infected and (B) mock-infected PBMC cultures stimulated with PHA during the standard *in vitro* assay. The average of the two groups is shown and the outlier, M7799, is represented separately. For panel (A), unpaired t-tests were used to determine significance at each time point. Significance ($P < 0.05$) is indicated by an asterisk. For panel (B), a repeated-measures ANOVA was used to determine statistical significance between the groups and the *P*-value is shown on the graph.

To determine whether differences in cell proliferation after activation were causing more live cells to accumulate in low producer cultures, the fluorescent dye carboxyfluorescein diacetate succinimidyl ester (CFSE) was used to measure the cell division rate after 6 days of anti-CD3/CD28 stimulation with or without virus infection (Figure 17). CFSE is a membrane-permeable dye that forms highly-stable amide bonds with intracellular molecules (154). Once cells are labeled, the amount of CFSE within cells remains stable and is halved with each successive cell division. It is therefore possible to track up to 8 cell divisions based on the relative fluorescent intensity of the dye (76). PBMC were isolated from each animal and half were infected with SIV. All cells were cultured overnight in culture media without IL-2. Twenty-four hours later, the cells were labeled with CFSE and subsequently activated with anti-CD3/CD28 antibodies. Some of the cells from each animal ($^{+}$/- SIV) were cultured without anti-CD3/CD28 stimulation as a control for non-dividing cells. Seven days after infection, the cells were removed, stained for expression of CD4, and analyzed for CFSE expression by flow cytometry. Six cell divisions were tracked in these assays, and there were no significant differences between the high and low producer animals in both SIV-infected and mock-infected cultures (Figure 17 A and B). This result was further supported by data showing that expression of the transferrin receptor (CD71), an activation marker expressed only on actively dividing cells, did not differ between the two groups of animals (Figure 18). Together, these data suggest that there was not a difference in the inherent rate of cell division after activation between high and low producer cells.

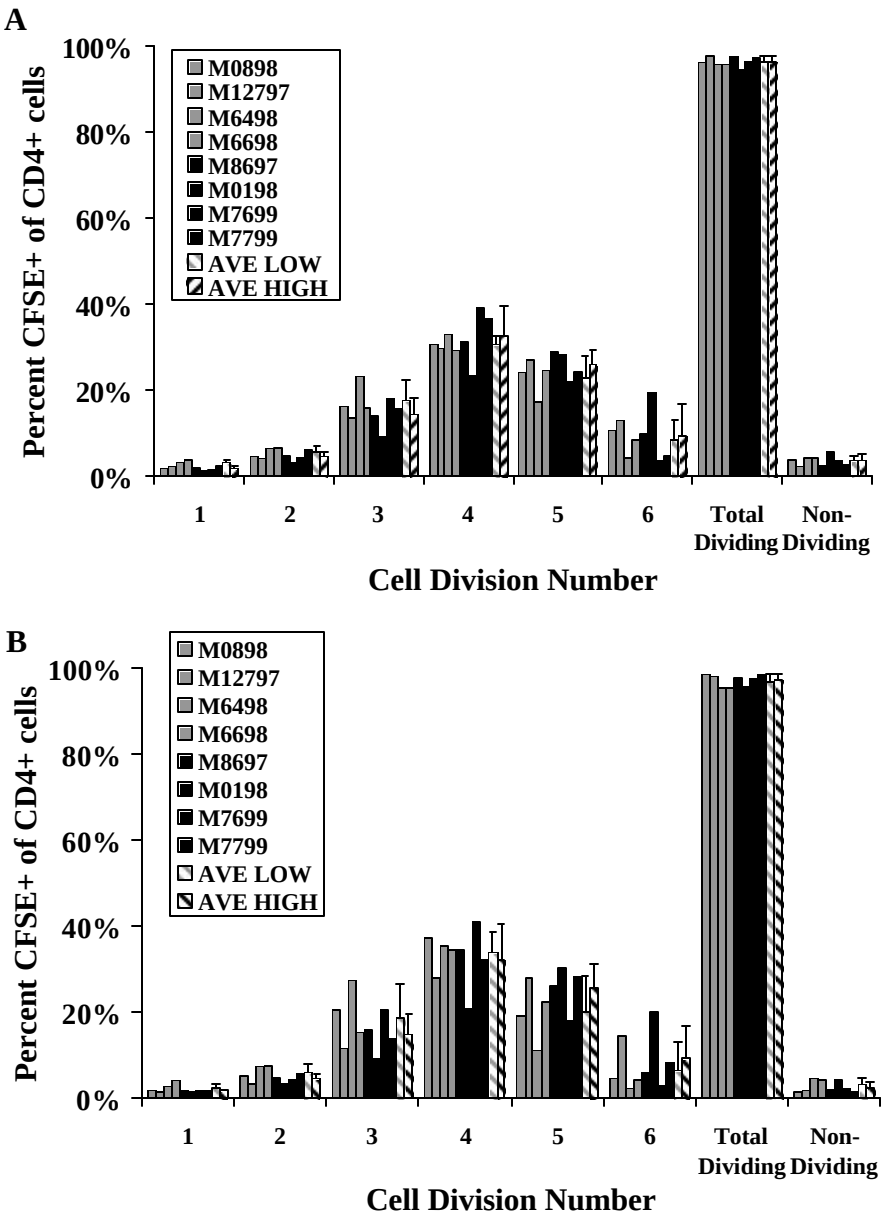

Figure 17. Similar levels of CD4$^+$ T cell proliferation after stimulation through the T-cell receptor.

Freshly isolated CD4$^+$ cells were infected with $SIV_{DeltaB670}$, labeled with CFSE, and then stimulated with plate-bound anti-CD3/28 antibodies for 3 days. On day 7, the cells were harvested and stained for surface markers by flow cytometry. The dividing and non-dividing cell gates were determined based on unactivated CFSE-stained cells. (A) SIV-infected cells; (B) mock-infected cells. High producers are shown in black; low producers are shown in gray.

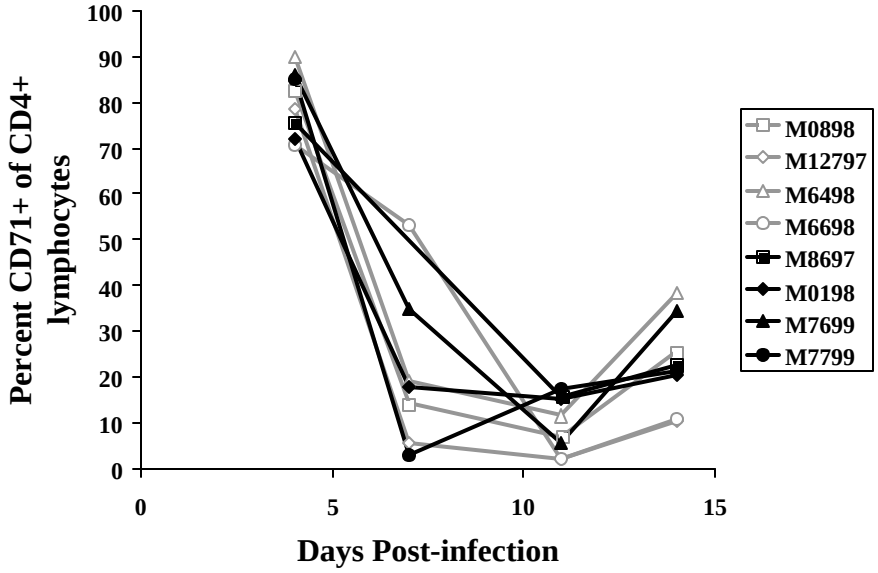

Figure 18. No differences in expression of CD71, a marker for actively proliferating cells.

Expression of the transferring receptor (CD71), an activation marker expressed only on proliferating cells, was measured by flow cytometry. No significant differences were seen between the two groups. High producers are shown in the black solid symbols; low producers are shown in the gray open symbols.

Since cell proliferation rate did not account for the differences in viable cell numbers, we determined whether the reduced number of live cells observed in the high producer cultures was due to apoptotic cell death. Caspase-3 proteases are the downstream effector enzymes of the apoptosis signaling cascade (173). Caspase-3 degrades cellular proteins by specific cleavage at GDEVDGI amino acid sequences. The substrate Phiphilux-G_1D_2 consists of a peptide with an amino acid sequence containing the GDEVDGI sequence; additionally, the peptide is homodoubly labeled with a fluorophore. Cleavage of this peptide by caspase-3 results in an increase in fluorescence as well as adsorption changes that are easily detectable using a flow cytometer. Therefore, Phiphilux can accurately detect caspase-3 activity within cells undergoing apoptosis. At intervals during *in vitro* culture, $CD4^+$ T lymphocytes from high and low producer animals were incubated with Phiphilux, and the percentage of $CD4^+$ cells undergoing apoptosis was monitored by flow cytometry. By 7 days p.i., significantly more apoptotic cells were observed in both SIV-infected (Figure 19 A) and mitogen-stimulated, uninfected high producer cultures (Figure 19 B) (P = 0.02 and 0.022, respectively; repeated measures ANOVA). The exception in these studies was the outlier high producer animal, M7799, who exhibited cell growth and apoptosis properties of low producer cells while at the same time producing large amounts of virus. These studies suggested that the differences in cell viability were due to increased apoptosis in high producer cultures rather than decreased proliferation.

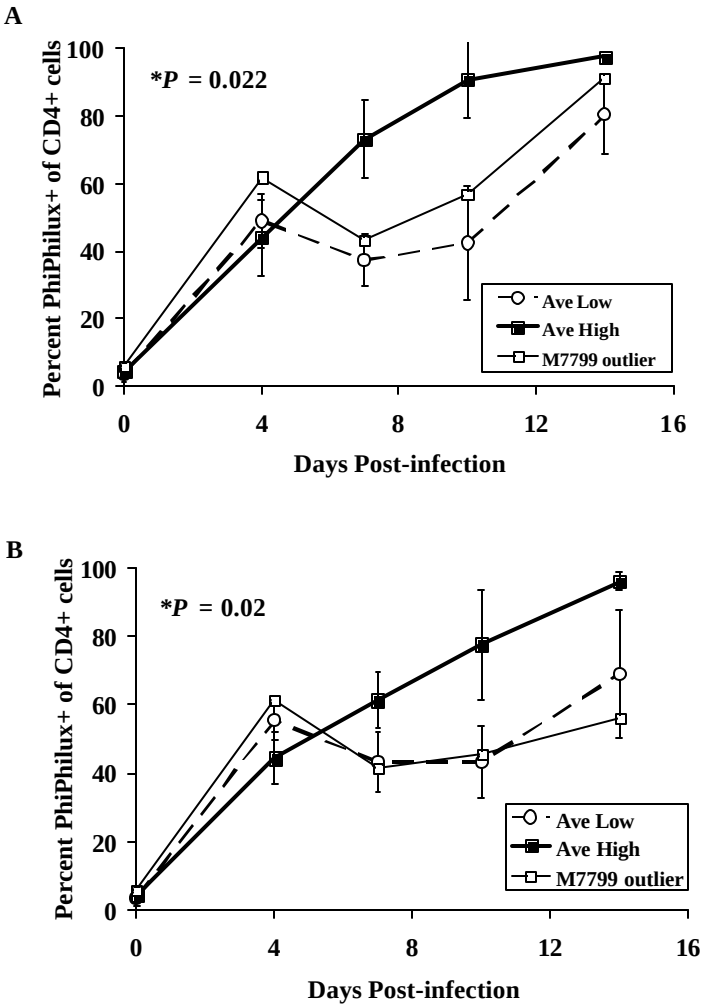

Figure 19. Low producer cultures have fewer cells undergoing apoptosis in both SIV- and mock-infected PBMC cultures.

Cells were infected according to the standard *in vitro* kinetics assay, and, at various time points, incubated with the caspase-3 substrate, Phiphilux. The percentage of $CD4^+$ cells staining positive for Phiphilux is shown for (A) SIV-infected and (B) mock-infected cultures. The average of the high and low producer groups is shown with bars representing one standard deviation. The outlier high producer animal M7799 is plotted separately. For both panels, a repeated-measures ANOVA was used to determine statistical significance between the groups and the *P*-value is shown on each graph.

Interestingly, expression of the death receptor Fas (CD95/APO-1) was consistently high on all cells throughout culture (Figure 20), indicating that variation in Fas expression on $CD4^+$ cells did not correlate with the amount of apoptosis occurring in the cultures. Expression of the memory cell marker CD29, the naïve cell marker CD45RA, or the activation marker CD69 did not differ between the two groups at any time point before or after infection (Figure 21). Expression of CD25, the IL-2 receptor, was equivalent at all time points except for 4 days p.i., at which time low producer cultures had a significantly higher percentage of $CD4^+$ cells expressing this receptor (Figure 22). This finding may be due to the lower number of apoptotic cells found in these same cultures. Together, these data suggest that intrinsic differences exist among the animals studied in their response to mitogen stimulation. The role that this finding plays in influencing virus production *in vitro* or disease progression *in vivo* is examined in the following chapters.

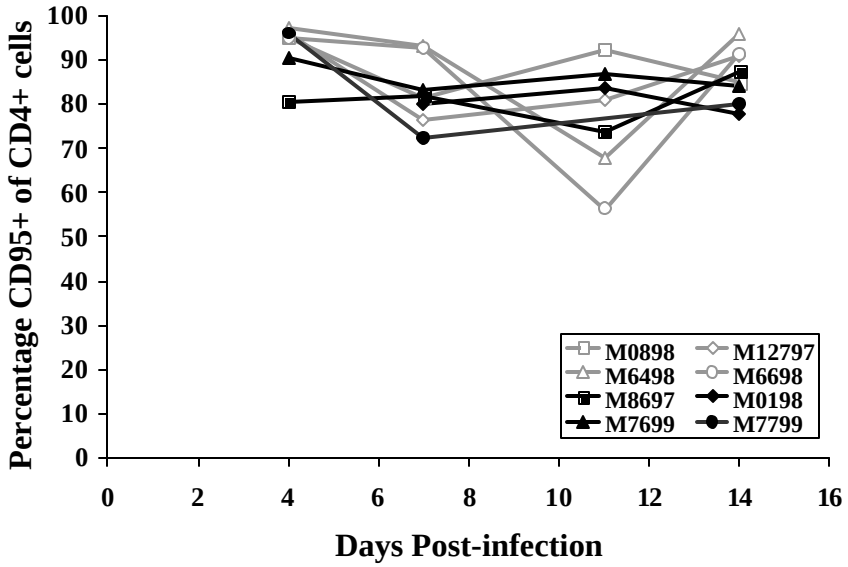

Figure 20. Expression of CD95 on $CD4^+$ T cells throughout *in vitro* culture.

Expression of Fas (APO-1/CD95) was measured on total $CD4^+$ T cells in SIV-infected PBMC cultures. High producers are shown in the black solid symbols; low producers are shown in the gray open symbols.

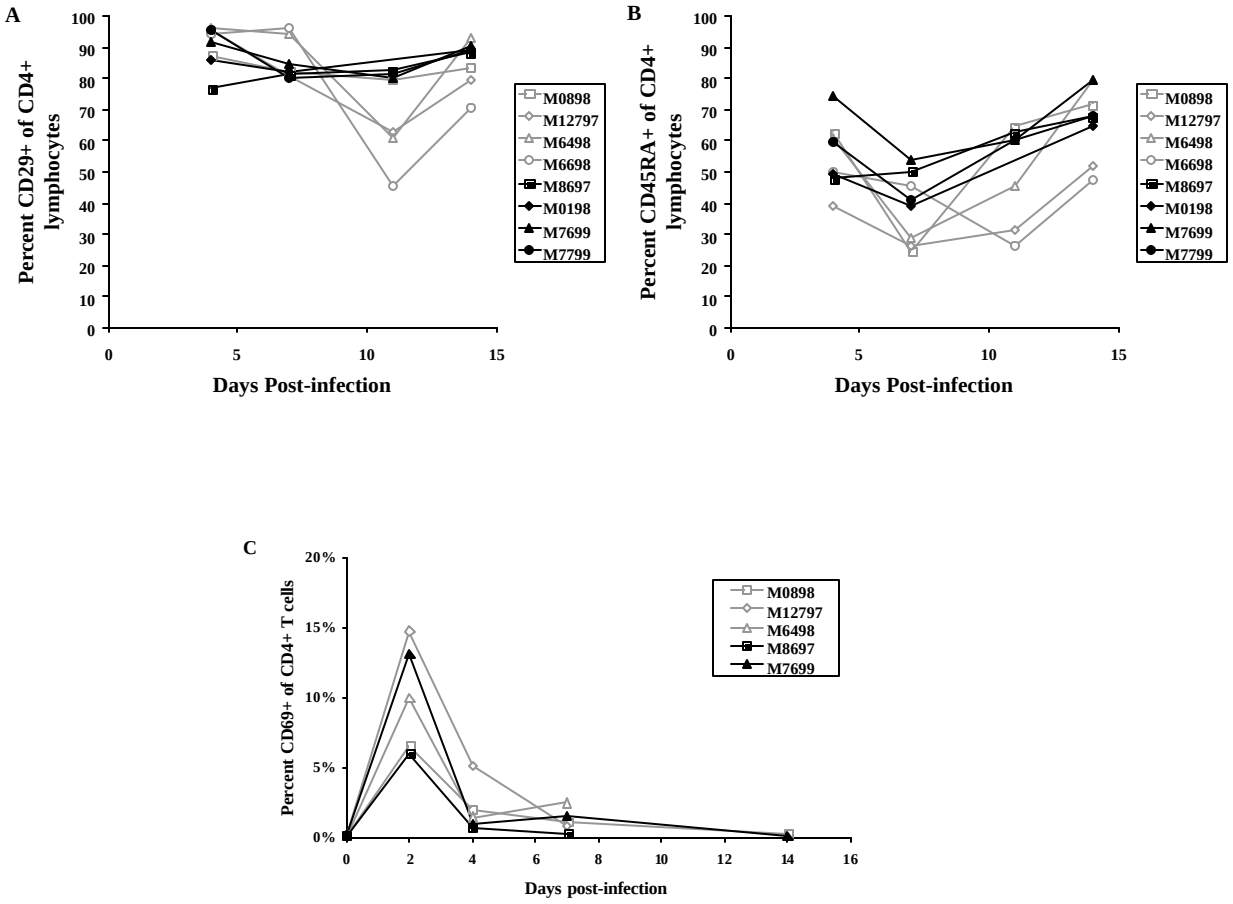

Figure 21. No differences in expression of activation and memory cell markers on CD4$^+$ cells during *in vitro* culture.

Expression of (A) CD29, a memory cell marker; and (B) CD45RA, naïve T-cell marker, and (C) CD69, an early activation marker were measured by flow cytometry. Cells were gated on CD4$^+$ cells and the percentage of these cells expressing each marker is shown. No significant differences were observed between the two groups for any of the markers. High producers are shown in the black solid symbols; low producers are shown in the gray open symbols.

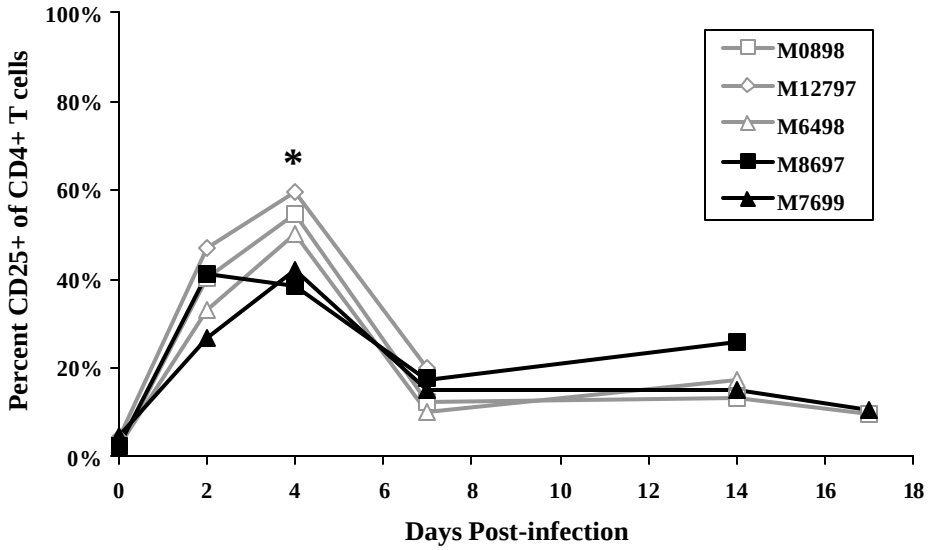

Figure 22. Expression of CD25 throughout *in vitro* culture.

Expression of CD25 was measured by flow cytometry. Cells were gated on $CD4^+$ cells and the percentage expressing CD25 is shown. An independent-samples T-test revealed that the two groups were significantly different and the day 4 time point (indicated by the asterisk). High producers are shown in the black solid symbols; low producers are shown in the gray open symbols.

The role of IFN-g and TNF-a in differential virus production *in vitro*. The secretion of cytokines and other small effector molecules can play key roles in both directly activating or inhibiting HIV-1/SIV replication and in the development of adaptive immune responses (34). Two cytokines in particular, IFN-γ and TNF-α, are known to influence virus replication, cellular activation, and apoptosis (34, 95, 103, 208, 212). To determine whether differential secretion of one of these cytokines was causing the different virus producer phenotypes, IFN-γ and TNF-α levels in the cell culture media during *in vitro* infection were measured by monkey-specific ELISAs (Figure 23). Two high producer animals (M8697 and M0198) secreted higher levels of IFN-γ than the other animals in both SIV-infected or mock-infected cultures (Figure 23 A and B). With the exception of these two animals, there were no consistent differences between high and low producers. Surprisingly, no TNF-α was detected in either SIV-infected or mock-infected cultures (data not shown), possibly because it may have been below the limit of detection of the ELISA assay.

Alternatively, intracellular flow cytometry was used to detect these same two cytokines after 5 hours of anti-CD3/CD28 stimulation in the absence of viral infection (Figure 24 A and B). IFN-γ was only detectable in $CD8^+$ cells, where expression was variable (Figure 24 A). For TNF-α, expression was detectable in both $CD8^+$ and $CD4^+$ (in this experiment $CD3^+CD8^-$) cells; however, this expression was also variable and did not correlate with high or low virus production (Figure 24 B). Taken together, these data suggest that IFN-γ and TNF-α, as measured by the methods described here, did not appear to have a significant correlation to the high/low producer phenotype.

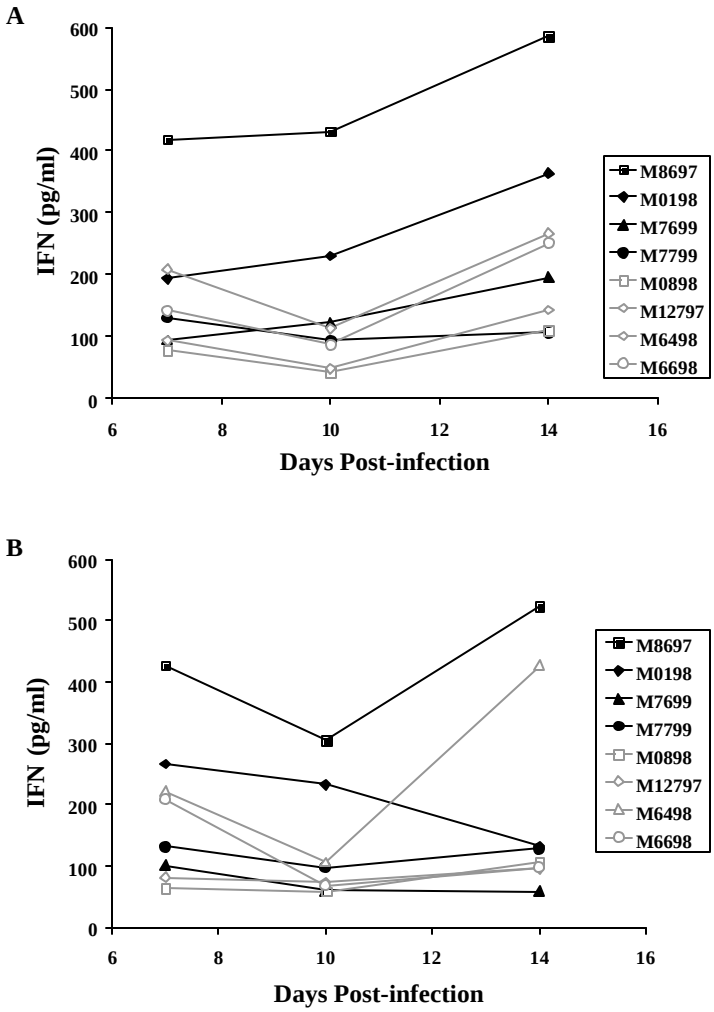

Figure 23. IFN-g secretion during *in vitro* culture.

PBMC from each animal were infected with SIV and subsequently activated with PHA. Supernatant samples were harvested at various time points after infection and IFN-γ was quantified by a monkey-specific ELISA. (A) SIV-infected cultures, (B) Mock-infected cultures. High producers are shown in the black solid symbols; low producers are shown in the gray open symbols.

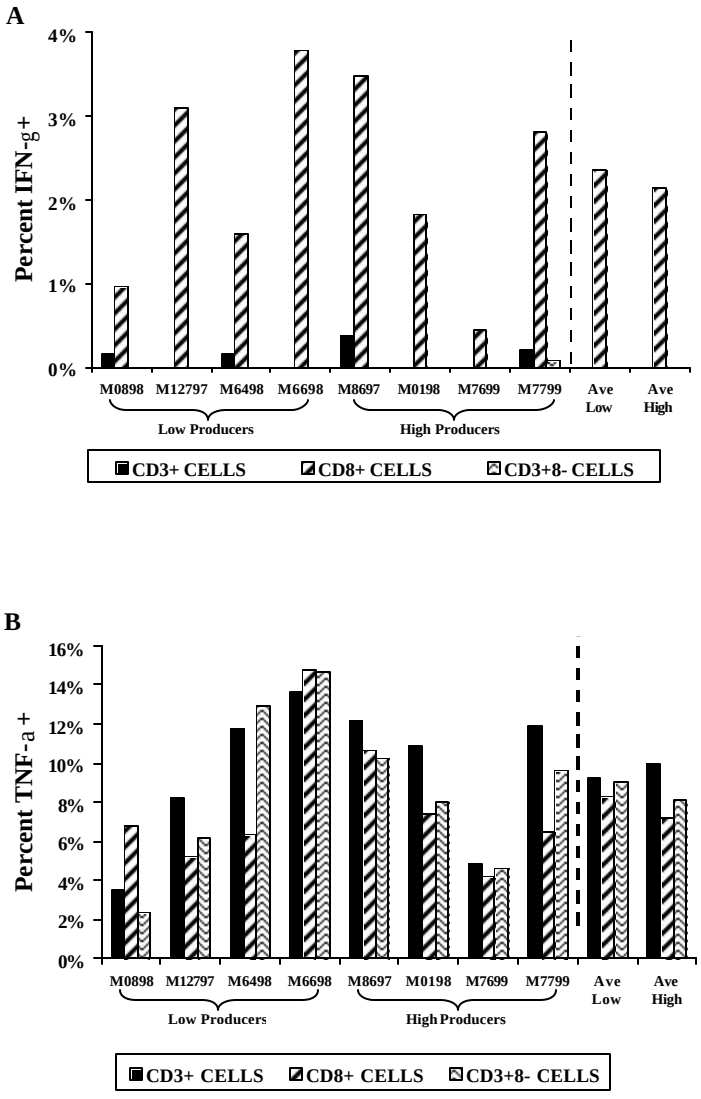

Figure 24. Intracellular IFN-g and TNF-a production uninfected PBMC cultures.

Fresh PBMC from each animal were stimulated with anti-CD3/CD28 antibodies for 5 hours and subsequently stained for intracellular (A) IFN-γ, and (B) TNF-α. Cytokine production for gated $CD3^+$ cells, $CD8^+$ cells, and $CD3^+CD8-$ cells (representative of the $CD4^+$ population) is shown. There are no significant differences between the two groups.

Global analysis of gene expression using cDNA arrays. Since numerous cytokines and chemokines are known to influence viral replication (164), a broader approach was used to identify possible genes liked to the high/low producer phenotype. Initially, global gene expression was performed using cDNA filter array analysis (R&D Systems). Each array contained 375 genes related to cytokines, chemokines, and cell surface molecules. Total RNA was harvested from purified $CD4^+$ T cells after 24 hours of infection with SIV in the absence of exogenous activation. RNA obtained from the two groups of animals was pooled for comparison analysis for several reasons: 1) sufficient quantities of RNA were more easily obtained in this manner, 2) cost-effectiveness, and 3) trends within the two groups could be more easily identified. RNA from each group was reverse transcribed with radiolabeled nucleotides to generate cDNA. The cDNA was hybridized to the filters, which were then exposed to a phosphorimager screen, scanned, and subsequently analyzed. A list of the most highly expressed genes for both groups of animals is shown in Appendix A, Table 6. As expected, cells from both types of animals expressed several characteristic markers of naïve and memory T cells, including CCR7 and L-selectin (39, 85). For comparison analyses, expression ratios were generated which represent the fold-increase in expression in one group over the other (Figure 25). A ratio of 2 or more indicates that a particular gene has a greater than 2-fold induction (highlighted in purple in Figure 25 C).

Only 2 genes, matrix metalloproteinase- (MMP)-1 and Leptin, had increased expression within the low producer cells. Of these genes, MMP-1 is a member of a family of proteolytic enzymes involved in the degradation of the extracellular matrix (214). With respect to lentivirus-induced disease, increased MMP expression has been shown to be associated with neurological diseases such as dimentia (87). Leptin is a plieotropic protein that plays key roles

in immune responses. It can affect cytokine production as well as induce proliferative and anti-apoptotic activities in T cells (55). Leptin dysregulation may indeed contribute to lipodystrophy and other metabolic disorders seen in HIV-1-infected humans (144). The contributions of these two proteins to the low producer phenotype remain to be confirmed with further analyses.

Several genes showed increased expression within the high producer cells, and these included IFN-γ, the interferon-inducible chemokine IP-10, IL-9, and the co-stimulatory molecules CD28, CD40L, and CD27. Since two of the genes expressed to a greater degree in high producer cells were related to the interferon system (IFN-γ and IP-10), cDNA microchip analysis was performed using glass arrays that contain approximately 300 genes related to interferons, cell signaling, and transcription. The cDNA microchip analyses were performed in collaboration with Dr. Neal DeLuca. Pooled RNA samples from high and low producer $CD4^+$ cells were compared under 3 conditions: 1) 24 hours after SIV infection (no activation), 2) 24 hours after anti-CD3/CD28 stimulation (no viral infection), and 3) 24 hours of culture without SIV infection or activation. Tables listing the differentially regulated genes are shown in Appendix A, Tables 7 - 12. While there were numerous genes differentially expressed, several corroborated the results from the filter array. For instance, in SIV-infected high producer $CD4^+$ cells, monokine induced by interferon gamma (MIG) was over-expressed according to the cDNA microchips, while IFN-γ and IP-10 both showed increased expression on the filter arrays. Both IP-10 and MIG are induced by IFN-γ and bind the same receptor, CXCR3 (168), indicating that their expression is probably highly coordinated.

Another similarity between the two types of arrays was in the number of over-expressed genes from each group. For both types of arrays, SIV-infected high producer cells had more over-expressed genes than the low producer cells (Figure 25 C and Appendix A, Tables 7 and 8).

Conversely, the opposite occurred for both anti-CD3/CD28 stimulated as well as unstimulated cells; low producer cells had a greater number of highly expressed genes than the high producer cells (Figure 25 C and Appendix A, Tables 9-12). This finding may imply that SIV infection of high producer cells induces activation of a number of genes that are repressed normally as compared to low producer cells.

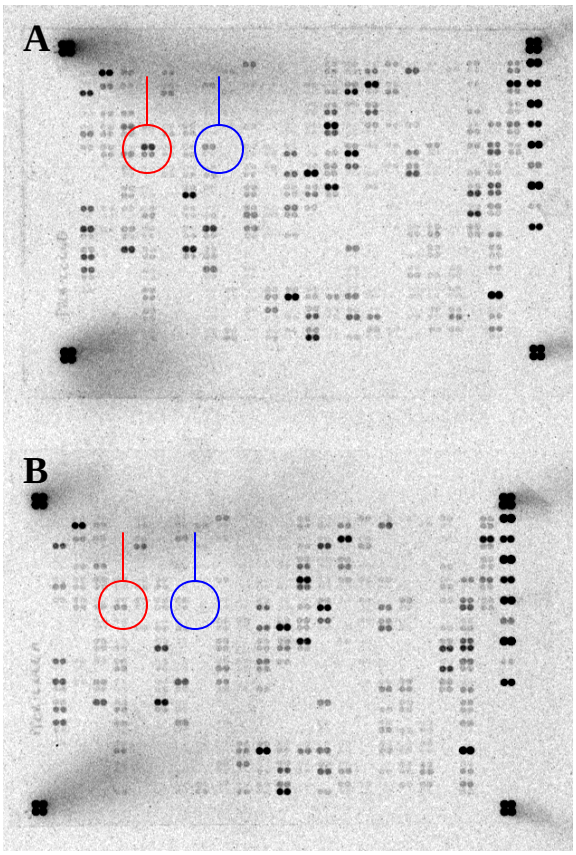

C

Low/High		High/Low	
MMP-1	2.332	IP-10	6.278
Leptin	2.129	CD28	3.405
MMP-10	1.990	CD40L	3.242
TNF-α	1.852	Genomic DNA	2.965
MMP-3	1.812	IL-9	2.786
TIMP-2	1.733	CD34	2.400
MIP-1α	1.691	IFN-γ	2.377
CD6	1.690	BMP RIB	2.119
TGF-β RII	1.669	CD27	2.112
NCAM	1.645	MSP	2.089
Midkine	1.603	CXCR-5	1.967
MIP-1β	1.587	CD30L	1.936
MMP-12	1.558	Integrin-αE	1.857
IL-1β	1.552	MCAM	1.856
AXL	1.543	PD-ECGF	1.848
MIC-1	1.536	CCR-3	1.801
MMP-9	1.535	GFRα3	1.763
EphA1	1.487	Endothelin-3	1.740
Decorin	1.483	MCP-2	1.737
CD64	1.475	IFN-α/β Rβ	1.666

Figure 25. Array analysis of cytokine/chemokine-related genes after 24 hours of infection with SIV.

Purified $CD4^+$ cells were infected with SIV, and RNA was harvested 24 hours later. RNA from the two groups of animals was pooled for analysis using the Cytokine cDNA Expression Array (R&D Systems). An image of the filter from (A) the four pooled high producer animals, and (B) the four pooled low producers is shown. (C) Data were adjusted for background and normalized. Expression ratios represent the ratio of the low producers to the high producers (left column) or the high:low (right column). An expression ratio of greater than 2 is considered significant. IP-10 (red circle) and IFN-γ (blue circle) are highlighted in (A) and (B).

The evaluation of molecular infectious clones of SIV in the *in vitro* viral growth kinetics assay. The virus used in all of these studies, $SIV_{DeltaB670}$, is a primary quasispecies that consists of several different clones, all of which are CD4-independent and utilize CCR5 for entry (51). Originally obtained from a rhesus monkey at end-stage AIDS (10), it has been passaged a limited number of times on primary rhesus PHA blasts. This virus is therefore pathogenic and optimally adapted for growth *in vivo.* The use of molecular infectious clones of SIV has advantages because they can be more easily manipulated *in vitro* and mutations are simple to engineer. However, the artificial manipulation required to generate these clones often results in the loss of pathogenic qualities and evolutionary fitness (52). To investigate whether the high/low virus producer phenotype is conserved when molecular infectious clones of SIV are used for *in vitro* infection, we tested a number of co-receptor-specific viruses (SIV_{mac239}, SIV_{macT3}, and SIV_{mac316}) that were generously obtained from Dr. Toshiaki Kodama (136). Their requirements for CD4 and co-receptor(s) are listed in Table 4 (127).

Table 4. Receptor and Co-receptor Usage of SIV Clones

Virus	Dependency on CD4	Co-receptor Usage	Human Stock	Rhesus Stock
B670	No	CCR5	Y	Y
239	Yes	CCR5	Y	Y
T3	Yes	CXCR4	Y	N
316	No	CCR5	N	Y

All three viruses were originally generated by transfection of the human T/B-cell hybrid line CEM x 174. Subsequently, the supernatant containing infectious virus was harvested and used to infect either primary rhesus or human PHA blasts to generate virus stocks. Supernatants from these cultures were harvested at 10 and 14 days post-infection, and the infectious titer was determined as described by Reed and Meunch (166). Successful stocks were generated for the viruses indicated in Table 4. Identical multiplicities of infection (m.o.i.) were then used to infect cells from 6 of the 8 animals described in this study (3 high producers and 3 low producers). Virus production was measured in supernatants at various intervals after infection. $SIV_{DeltaB670}$ generated on human cells behaved in a similar manner to that generated from rhesus cells, which is the standard virus stock used for all of these studies (Figure 26 A). Not surprisingly, for this virus, the three high producer animals secreted more p27 into the culture media than their low producer counterparts. However, for all of the molecular infectious clones, no differential virus production was seen regardless of whether human or rhesus cells were used to generate the stock (Figure 26 B-E). For these viruses, production from the low producer cells was similar to levels when B670 is used (50 – 100 ng/ml); however, surprisingly, the high producer cells also secreted 50 – 100 ng/ml of p27, which is 10-fold less than the typical 500 – 1000 ng/ml made by high producer cultures. Therefore, it appeared that virus replication was unaffected in low producer cells but was significantly inhibited in high producer cells. The common factor between these 4 viruses was that they were all cloned and generated by transfection of cell lines. It is possible that generation of viruses in this way alters them such that the high/low virus producer phenotype is no longer seen (52). Alternatively, the high/low virus production phenotype may be an observation specific to $SIV_{DeltaB670}$. Further analysis of other primary isolates is warranted to further explore the significance of these findings.

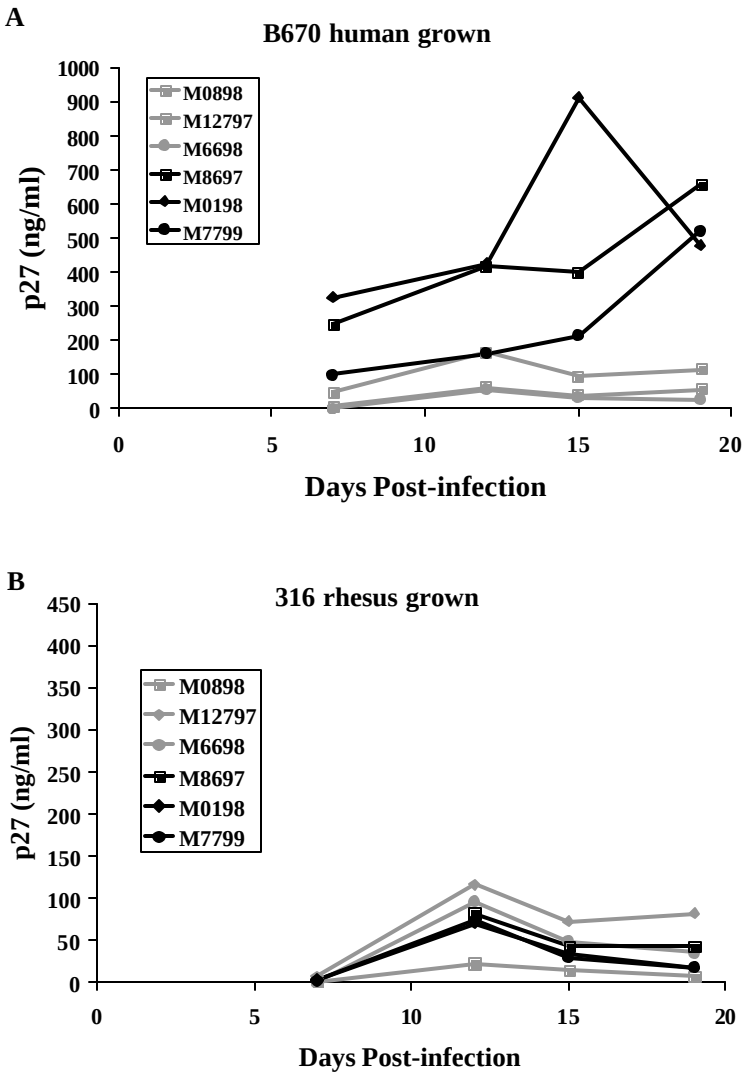

Figure 26. Cloned co-receptor-specific viruses and the *in vitro* kinetics assay.

Identically-prepared stocks of SIV_{mac239}, $_{macT3}$, $_{mac316}$, and $_{B670}$ were generated on both human and rhesus PHA blasts. Equivalent m.o.i. of each virus were used in the *in vitro* kinetics assay. (A) $SIV_{DeltaB670}$ grown on human cells; (B) SIV_{mac316} grown on rhesus cells; (C) and (D) SIV_{mac239} grown on rhesus and human cells respectively; and (E) SIV_{macT3} grown on human cells. The high producers are shown in black and the low producers are shown in gray. (C), (D), and (E) are shown on the following page.

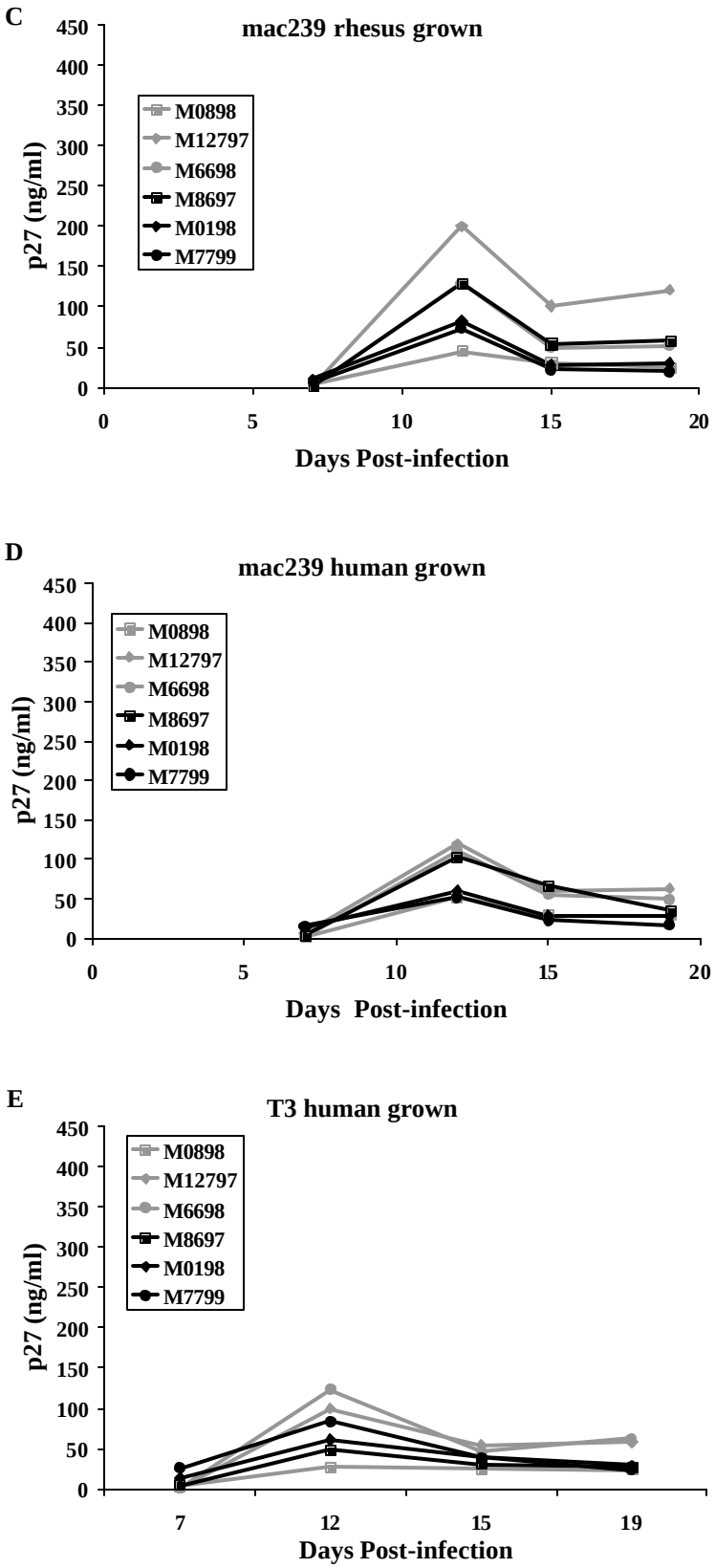

Figure 26. (cont'd).

Generation of transformed cell lines using *Herpesvirus saimiri*. All of the studies described thus far use primary cells which are limited in number and difficult to work with. Goldstein and colleagues (69) have demonstrated that susceptibility to infection with SIV was similar in PBMC or transformed T cell lines from the same animal. To evaluate this possibility in these 8 animals, $CD4^+$ T cells from each animal were transformed using *Herpesvirus saimiri* (129). Successful transformation is dependent on the Simian Foamy Virus-status of the animal; transformation is generally only successful in SFV-negative animals (59). Seven of the eight animals used in these studies were positive for SFV by a Group-Specific Antibody Screen (The Simian Diagnostic Laboratory, San Antonio, TX). The exception was high producer animal M0198. However, out of all 8 animals, a successful transformed cell line was generated from low producer animal M12797 and subsequently designated Line #9. The characteristics of this cell line, as determined by flow cytometry after 8 weeks of culture, are illustrated in Figure 27. The cell line consisted almost entirely of $CD3^+CD4^+$ cells, with approximately 25 % also expressing CD8, a common phenomenon noted in the literature (Figure 27 A-D) (59). Virtually 100 % of the cells expressed the activation marker CD71, while 28 % expressed CD25, the IL-2 receptor, suggesting that almost ¾ of the culture may be IL-2-independent (Figure 27 E and F).

Cell line #9 was infected with $SIV_{DeltaB670}$ as per the standard *in vitro* growth kinetics assay but without any subsequent mitogen activation. At various times after infection, ~20 ml of supernatant was harvested and frozen in 1 ml aliquots for virus stocks. The amount of p27 in the supernatant was measured using an ELISA and the results are shown in Figure 28. The kinetics of the emergence of virus in culture was similar to experiments with primary cells; however relatively high levels of p27 protein were secreted as compared to non-transformed PBMC from M12797. Because transformation of cells from the other 7 animals was unsuccessful, it remains

undetermined whether the high/low virus producer phenotype is maintained in transformed cell lines from these animals. However, the relatively high titer of virus generated from this cell line may render it useful in the future for the production of virus stocks. Because of the low success rate of transformation by *H. saimiri*, the routine generation of transformed cell lines from a large number of animals for experimental use is most likely not feasible.

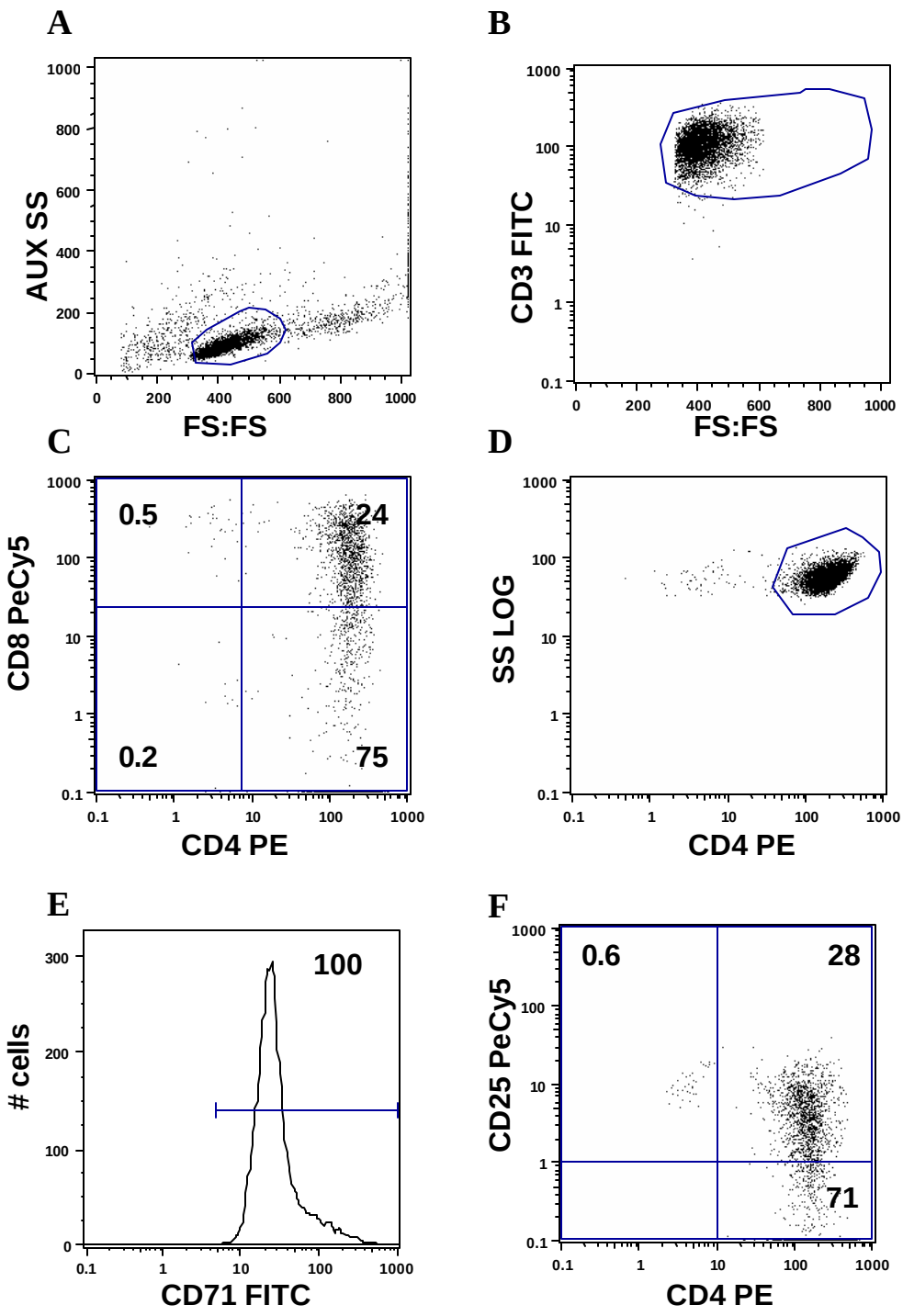

Figure 27. Legend on next page.

Figure 27. Characteristics of *H. saimiri*-transformed cell line #9 (from low producer animal M12797).

(previous page) Purified $CD4^+$ T cells were transformed with *Herpesvirus saimiri*, and the cell line was tested for purity and activation markers. (A) the whole cell population showing the lymphocyte gate; (B) gated lymphocytes showing CD3 cells; (C)(D)(E)(F) are gated on $CD3^+$ cells showing distribution of CD4, CD8, the proliferation marker CD71, and CD25, the IL-2 receptor. Percentages are indicated on each graph.

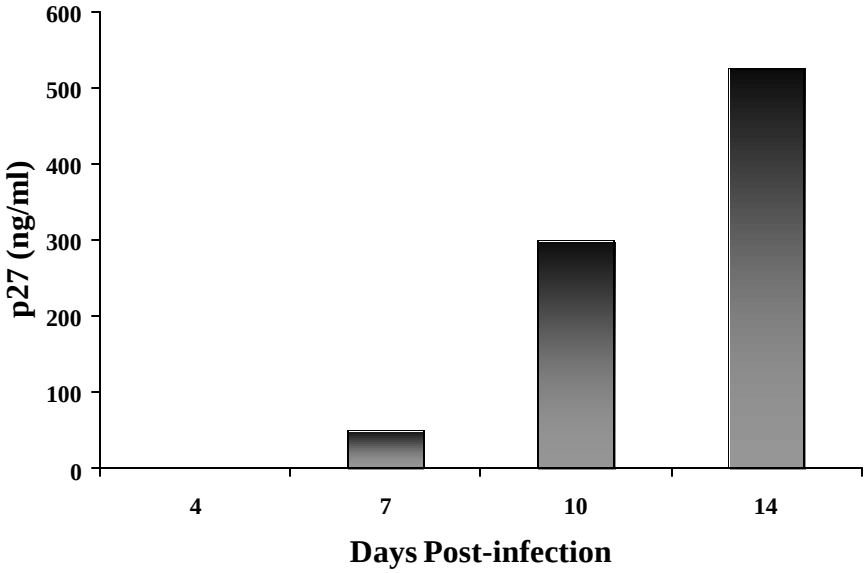

Figure 28. SIV production from transformed cell line #9.

Cells from Line #9 (low producer animal M12797) were infected with $SIV_{DeltaB670}$ as per the standard *in vitro* growth kinetics assay. At certain time points after infection, supernatants were removed and frozen for virus stocks. The amount of p27 antigen was measured using an ELSIA.

4.4. Discussion.

Identification of the mechanism causing differential virus production *in vitro* requires a solid knowledge of the basic properties of the *in vitro* assay. The studies within this chapter were designed to identify the properties of the cells in culture, to test several early hypotheses, and to determine the applicability of our assay to other model systems.

Hypothesis 1: Virus secreted into the cell culture media from low producer cells is infectious. We have shown that virus secreted into the cell culture media from low producer cells is infectious. This is an important finding because retroviruses can have an infectious to total particle ratio as low as 1:1000 (92). Therefore, virus replication is not functionally aborted in low producer cells. Rather, infectious virus is produced at lower levels than that from high producer cells.

Hypothesis 2: Cell populations other than $CD3^+$ lymphocytes do not predominate the PBMC cultures. Most of the experiments presented in this chapter were performed on whole PBMC cultures due to the availability of these cells. Other experiments were performed using purified $CD4^+$ T cells. Even though purified $CD4^+$ T cell cultures are >95 % pure by flow cytometry, it was possible that a cell population specifically susceptible or resistant to virus infection was overgrowing high or low producer cultures, respectively. Analysis of PBMC cultures revealed that the predominant cell population during *in vitro* infection was $CD3^+$ T cells. Very few monocytes, B cells, or NK cells persisted in the culture after the first 3 – 4 days post-infection. Of the $CD3^+$ cells, the percentage of CD4-expressing cells decreased over time, as

would be expected in an infected culture. This resulted in a concomitant increase in the percentage of $CD8^+$ cells. Interestingly, we also found a doubling in the percentage of $CD3^+$CD4-CD8- cells over time. This may represent infected $CD4^+$ cells that have lost expression of the CD4 marker (19). These data suggest that, based on the markers examined here, there was not a differential predominance of a specific cell population in either high or low producer cultures that could account for differential virus production.

Hypothesis 3: The high/low producer phenotype persists irrespective of the method used to activate the cells. Three different mechanisms used to activate the PBMC during the *in vitro* assay all lead to differential virus production. PHA and anti-CD3/CD28 antibodies both activate cells by signaling through the T-cell receptor; however, anti-CD3/CD28 antibodies do this in a specific manner, while PHA does not. Indeed, bypassing the upper part of the signaling cascade through the use of PMA and ionomycin still resulted in differential virus production. Therefore, the high/low virus producer phenotype is mediated by the lower half of the activation cascade.

This is a noteworthy finding because the viral Nef protein can modulate T-cell signaling by interacting with the TCR ζ chain, thereby enhancing activation of the cell and priming it for viral replication (11, 183). It was possible that the interaction of Nef with various cellular proteins involved in T-cell signaling may be different within high and low producer cells, and this therefore results in differential virus replication. However, since we found that the phenotype persists in cells stimulated with PMA and ionomycin, which activates cells at a point below the interaction of Nef with the TCR cascade, Nef most likely does not play a role in our observations.

Hypothesis 4: High producer cells secrete more virus because they are at a higher activation state than low producer cells. Because SIV preferentially replicates in activated T cells (162, 192, 216, 217), one early hypothesis was that high producer cells may be hyper-activated as a result of an identical activation stimulus as compared to low producer cells. This would result in more virus production because T-cell signaling leads to activation of many transcription factors, including NF-κB, NFAT, and AP-1, all of which can bind to sites within the LTR region of the virus and stimulate transcription (117, 192). Initially, examination of the cells in culture revealed that low producer cultures accumulated significantly greater numbers of viable cells than high producer cultures. Surprisingly, a trend was also seen in mock-infected cultures activated by either PHA or anti-CD3/CD28 antibodies, with the exception of one outlier high producer animal M7799. However, for all animals, measurement of cell proliferation after PHA or anti-CD3/CD28 stimulation was not significantly different, indicating that the inherent rate of cell division was similar. In addition, expression of several memory and activation markers (CD29, CD45RA, CD69, CD71, CD95) after mitogen stimulation did not differ between the two groups. Because the cell division rate and expression of activation markers were identical between the two phenotypes, signaling from the TCR appeared to be the same.

However, detection of apoptotic cells using the caspase-3 substrate Phiphilux revealed more apoptotic cells in high producer lymphocyte cultures as compared to their low producer counterparts, even in the absence of detectable differences in Fas (CD95) expression. This finding was highly significant, with the exception of one outlier (monkey M7799), who had decreased apoptosis compared to the other 3 high producers and consequently accumulated increased numbers of viable cells in the culture despite producing large amounts of virus. Together, these data suggest that $CD4^+$ lymphocytes from 3 of the 4 high producer animals

undergo more apoptosis in response to identical activation stimuli than low producer cells, and the presence of viral infection appears to enhance this effect. Indeed, recent data have shown that death receptors, such at the TNF receptor (TNFR) and CD95 (FAS/APO-1), can lead to either apoptosis or survival, depending on whether the intracellular signal proceeds via caspase-8 or FLIP, respectively (23, 121). These findings suggest a plausible scenario in which TNFR/Fas signaling in low producer cells leads to a survival signal, while the same signal in cells from 3 high producer animals leads to apoptosis. Further analysis is required to test this hypothesis and is discussed in the following chapters.

Hypothesis 5: The high/low phenotype is consistent with differential expression of a cytokine or chemokine known to influence viral replication. The cytokines IFN-γ and TNF-α are known to play key roles in directly influencing HIV-1 and SIV replication as well as in affecting the development of adaptive immune responses *in vivo* (34, 164). Of all known cytokines, the role of TNF-α in stimulating virus replication is the most clear (83, 95, 103, 164, 208). TNF-α binds to the TNF receptor (TNFR1) and initiates a signaling cascade that results in activation of the transcription factor NF-κB. NF-κB, in turn, binds to sites within the promotor region of the viral LTR, thereby increasing viral transcription (47). Concurrently, TNF-α binding to TNFR1 can result in apoptosis by a signaling cascade related to Fas-FasL (121). Indeed, it was possible that differential expression of TNF-α could result in both the increase in viral replication as well as apoptosis seen in high producer cultures. However, the results presented in this chapter failed to find differential expression of TNF by either ELISA of cell culture media or intracellular cytokine staining of activated cells.

The role of IFN-γ in viral replication is less well-defined because this cytokine can have both enhancing and inhibiting effects on viral replication, depending on the cell culture system used (95, 103, 208). However, given that this cytokine is important for the generation of immune responses *in vivo,* ELISA assays and intracellular cytokine staining were used to determine whether differential expression of this pivotal cytokine was associated with high or low virus production. There was no clear association between the two groups of animals, although two high producers secreted more IFN than all the other animals in both SIV-infected and mock-infected cultures as determined by ELISA assay. Using these assays, there is no apparent association of IFN-γ or TNF-α production with the high/low virus producer phenotype.

Microarray analysis of cytokine and chemokine-specific genes led to several interesting results. In high producer cells infected with SIV for 24 hours, there were increased levels of IFN-γ and the IFN-inducible chemokine IP-10, both of which can stimulate HIV-1 and SIV replication (103, 104). However, because these studies were performed with pooled high and low producer RNA samples, conclusions from these results must take into consideration the fact that only 2 of the 4 high producers showed increased IFN-γ protein production by flow cytometry or ELISA. Therefore, the increase in RNA expression seen in the microarray results may be skewed by these two animals and may not be a general property of high producers.

A second set of microarray analyses revealed higher expression of the interferon-induced monokine, MIG, which binds to the same receptor as IP-10. While these results are still preliminary, the consistently increased expression of IFN-inducible genes on the two types of arrays suggests that high expression of these genes may be inducing virus replication in high producer cells *in vitro,* despite the fact that no differences in protein expression were found. Additionally, these results were remarkably consistent with those of Reinhart and colleagues

(168) who have shown that IFN-inducible chemokines are highly expressed in lymphoid tissues of SIV-infected rhesus monkeys with high levels of localized virus replication. Indeed, it is possible that IFN-γ and genes induced by it may act to directly enhance virus replication *in vitro*, while affecting localized IFN-γ-driven positive feedback loops in the lymphoid tissue of the infected animal (168). To further evaluate the role of IFN-γ in contributing to high virus production *in vitro*, it is necessary to: 1) confirm the increased expression of IFN-γ, IP-10, and MIG by real-time RT-PCR of the same pooled RNA samples as well as individual RNA samples from each animal; 2) confirm that the level of RNA expression correlates with an increased expression of these same proteins; 3) demonstrate that neutralization of each of these proteins can convert high producer cells into low producer cells. These pilot microarray analyses highlight potential directions for further study into the role of IFN-γ in the high/low virus producer phenotype.

A second interesting result from the cDNA array studies was that pooled high producer RNA also had increased levels of mRNA encoding co-stimulatory molecules such as CD28, CD40L, and CD27, indicating possibly a higher state of general immune activation, despite the fact that no differences in the expression level of other activation markers or proliferation were found. Indeed, flow cytometry may not have been sensitive enough to detect subtle differences in the expression level of the activation markers examined here. Alternatively, while expression of common activation markers was not different between the two groups, a selective difference in expression of these co-stimulatory molecules may point to a more specific difference in activation status of the cells. Because these results are preliminary, confirmation of the differences in expression between the two groups needs to be conducted using real-time RT-PCR, as well as assays that can sensitively measure protein expression. Therefore, while global

gene expression as measured by microarray analysis has the potential to identify the role of novel genes in this process, further investigation into these findings is required to determine the exact role in virus production *in vitro* and disease progression.

Hypothesis 6: The high/low phenotype occurs when molecular infectious clones of SIV are used in the *in vitro* kinetics assay. The applicability of our *in vitro* model to other SIV systems is important. In particular, the use of molecular infectious clones of SIV, generated by transfection of cell lines such as CEMx174, is widespread in the field. Using a different but related *in vitro* assay, Goldstein and colleagues (69) have shown up to a 4-5 log difference in the susceptibility of individual rhesus monkeys' cells to infection with both $SIV_{smE543\text{-}3}$ (a molecular infectious clone) and SIV_{mac251} (a primary isolate). Here, we determined the usefulness of our *in vitro* assay for monitoring the replication of a series of molecular infectious clones of SIV that use specific co-receptors for entry. Infection of high and low producer cells with these viruses resulted in identical quantities of virus secreted from both high and low producer cells. Interestingly, replication of all the cloned viruses was unaffected in low producer cells, but was significantly inhibited in high producer cells as compared to the replication of $SIV_{DeltaB670}$. The common factor between these 3 viruses is that they are all cloned and generated by transfection of cell lines. Generation of molecular infectious clones by transfection of human T-cell lines may have sufficiently altered the virus such that the high/low producer phenotype was no longer seen in primary rhesus cells (52). These results may suggest that the high/low virus producer phenotype is a property particular to $SIV_{DeltaB670}$. However, it is most likely a property of uncloned primary isolates of virus. Further studies evaluating other primary isolates of virus is required to test this hypothesis.

Hypothesis 7: The high/low producer phenotype is maintained in $CD4^+$ T cells transformed by *Herpesvirus saimiri*. Because primary cells are limited in number and difficult to work with, we evaluated whether the high/low virus production phenotype was maintained when transformed $CD4^+$ T cell lines made from each animal were used instead of primary PBMC from the same animal. Transformation of rhesus monkey $CD4^+$ T cells using *Herpesvirus saimiri* has been demonstrated to be a useful tool in HIV/SIV research (129). Establishment of cell lines would make more complicated assays feasible due to a greater number of available cells. However, transformation can be hampered if the animal is infected with Simian Foamy Virus (SFV) (59). Seven of the eight animals used in these studies were positive for SFV except for high producer animal M0198. However, a successful transformed cell line was generated from low producer animal M12797, designated Line #9, in spite of a positive SFV status of this animal. Flow cytometric analysis revealed that it was a pure $CD4^+$ cell line with approximately 25 % also expressing CD8. In the literature, *H. saimiri*-transformed cell lines often become double-positive for CD4 and CD8 after numerous passages in culture (59). Infection of this cell line revealed that it may be suitable for the production of virus stocks because the amount of virus generated from these cells was relatively high. Since no other transformed lines were successful after numerous attempts, it remains undetermined whether the high/low producer phenotype is maintained in transformed cell lines. However, these results are useful because they highlight the fact that, due to the low success rate of transformation by *H. saimiri*, the routine generation of transformed cell lines from a large number of animals for experimental use is not feasible.

Conclusion:

While there is a clear and distinct connection between the amount of virus produced from an animal's $CD4^+$ T lymphocytes after infection *in vitro* and survival of that animal after *in vivo* infection, the reasons behind this observation are not clear. The studies described in this chapter have identified basic properties and applications of our *in vitro* assay which will enable a more focused approach to identification of the mechanism responsible for differential virus production *in vitro*. Specifically, the finding that cells from the two types of animals respond differently to mitogen activation may help to pinpoint a mechanism for these observations. The impact of the results presented here is examined in more detail in the following chapters.

4.5. Acknowledgements.

I would like to acknowledge Toshi Kodama for generously providing the molecular infectious clones for testing in the *in vitro* assay. I also appreciate the technical help and advice on transforming the rhesus $CD4^+$ cells from Julius Youngner and Patricia Dowling. Albert Donnenberg provided much technical assistance in the flow cytometric studies. Todd Reinhart and Todd Schaefer dedicated valuable time in teaching me the cDNA filter protocols, as well as in providing help with data analysis. Neal DeLuca and Brian Manning also spent significant amounts of time in collaboration with the cDNA microchip analyses.

CHAPTER 5

MOLECULAR ANALYSIS OF SIV REPLICATION WITHIN HIGH- AND LOW-PRODUCER $CD4^+$ T LYMPHOCYTES.

This chapter was modified from the following manuscript:

Amy L. Hartman, Premeela A. Rajakumar, Tara L. Washko, Toshiaki Kodama, and Michael Murphey-Corb. 2003. "The Effects of Intrinsic Differences in Regulation of Viral Reverse Transcription and Activated $CD4^+$ T Cell Death on Simian Immunodeficiency Virus (SIV) Production *In vitro*"

Virology (manuscript submitted)

5.1. Introduction.

The interplay between host and virus that controls disease progression in HIV-1/SIV infected individuals is undoubtedly complex. Host factor(s) play a major role in this process, however, because in the SIV-infected macaque, differences in disease progression and survival persist even though identical virus stocks, doses, and routes of inoculation are used for infection (108, 112, 134, 219). In humans infected with HIV, survival can vary from 5 to 20 years after infection (115, 140, 152). A similar variation in survival is seen in SIV-infected rhesus macaques, where the time from infection to death can be as short as 2 months post-infection (p.i.) to as long as 5 years (46, 93, 219).

Whereas it is difficult to study a phenomenon such as this due to the complexity and cost of *in vivo* studies, an *in vitro* assay has been developed that can be used to study these events in a more controlled environment. We (141, 180) and others (69, 156) have shown that the ability of primary $CD4^+$ T cells from an uninfected macaque to support SIV replication *in vitro* correlates significantly with the rate of disease progression of the animal after intravenous infection. Infected primary $CD4^+$ T lymphocytes that support little *in vitro* virus production (low producers) predict slow disease progression whereas cells that produce large amounts of virus (high producers) predict rapid disease progression.

Identification of the stage(s) of the virus life cycle at which host cell factors are exerting their effect is a crucial next step in understanding this process. A post-entry block was recently implicated by Robert-Guroff and colleagues (156) who found differences between the two phenotypes in the accumulation of reverse transcription intermediates as measured by semi-quantitative autoradiographic detection of PCR products. Although this result provides

compelling evidence that post-entry events may be at least in part responsible for the differences observed in *in vitro* virus production, the impact of post-entry events on subsequent steps in the virus life cycle, as well as an examination of the properties of the host cell itself, remain to be evaluated.

In this study, we find that $CD4^+$ T cells from low producer animals are more refractory to infection with SIV, and, similar to previous studies (156), that this impairment is mediated by a block prior to, or at the first step of, viral reverse transcription. However, synthesis of second strand DNA, as well as viral mRNA expression and protein synthesis thereafter, appeared to occur at a similar rate in both phenotypes. Therefore, the lower template copy number resulted in fewer viral particles and a subsequent slower spread of the virus through the culture. Indeed, spread of the virus throughout three of the four high producer cultures was linear as compared to a biphasic increase in infected cells within low producer cultures. Together, these findings support the concept that a rather modest interference with virus replication during the early stages of infection has a profound effect on the accumulation and spread of virus in the culture.

5.2. Materials and Methods.

Isolation of PBMC. 10-40 ml blood was collected via the femoral vein from individual rhesus macaques using acid citrate dextrose (ACD) as the anticoagulant. Peripheral blood mononuclear cells (PBMC) were isolated from whole blood by Ficoll-Paque (Pharmacia Biotech, Uppsala, Sweden) density-gradient centrifugation. One tube (~10 ml) whole blood was diluted in 20 ml RPMI containing penicillin-streptomycin (100 U/ml; 100 U/ml) and L-glutamine (2 mM). This was layered on 10 ml Ficoll at a 45º angle. The tubes were centrifuged for 40 minutes at 2000 rpm at room temperature (RT) without the brake. The white cell layer was carefully removed with a transfer pipet (~7-8 ml) and placed in a new tube. The cells were washed once for 15 minutes at 1500 rpm, and then two more times for 12 minutes at 1200 rpm. For all studies involving PBMC, these washes were done with 30 ml RPMI containing 15% fetal bovine serum. For $CD4^+$ cell isolation, these washes were done with 30 ml Dulbecco's PBS (DPBS; w/o Ca or Mg) (Mediatech). Complete culture media consisted of RPMI containing penicillin-streptomycin, L-glutamine, 15% FBS, 10 mM HEPES buffer, and 40 U/ml human IL-2 (Hoffman-LaRoche, Nutley, NJ).

Isolation of purified $CD4^+$ cells by column selection. PBMC were obtained as above and washed 3 times in DPBS. After the third wash, the cells were resuspended in 20 ml MACS buffer (PBS containing 5 mM EDTA, 10 mM HEPES, 0.5% BSA; pH 7.2-7.4) and counted on a hemocytometer. Cells were kept cold from this point forward. The cells were then pelleted by centrifugation (12 min, 1200 rpm). For every 1 x 10^6 cells, 20 ul CD4 beads and 80 ul MACS buffer were added and mixed. The cells were incubated in the refrigerator (4 ºC) for 30 minutes.

After the incubation, 10 ml MACS buffer was added, and the cells were pelleted as above. One MS^+ column was used for every 3 x 10^7 total PBMC. The pellets were resuspended in 500 ul buffer for every column needed and then passed through the column. The columns were then washed 3 times with 500 ul fresh MACS buffer. After the final wash, the column was removed from the magnet and placed in a new 15 ml conical tube. 3 ml fresh buffer was added to the column and pushed through with plunger. This was repeated two more times using 1 ml fresh MACS buffer.

Reed-Meunch analysis for calculating infectivity titer endpoints. Rhesus PBMC or $CD4^+$ cells were obtained as described previously. Immediately following isolation, the cells were cultured in complete media (described above) and stimulated with PHA (5 ug/ml; GibcoBRL) or plate-bound anti-CD3/CD28 Abs (5 ug/ml; Pharmingen clone SP34 and CD28.2, respectively). For coating the plates, the antibodies were diluted to the appropriate concentration in sodium bicarbonate buffer (pH 8.5) and added to the plates for at least 1 hour at 37 °C. The plates were washed several times with cold bicarbonate buffer prior to adding the cells. Three days after stimulation, the cells were removed from the antibodies or PHA by washing the cells twice in RPMI containing 15 % FBS and culturing in complete media. On day 7, the cells were counted, and 5 x 10^5 cells were aliquoted into each well of a 48-well plate. The cells were incubated with 100 ul of virus (5-fold dilutions from 5 x 10^{-2} to 1.6 x 10^{-6}), with 6 replicates at each dilution, and incubated for 2 hrs at 37 °C. After virus adsorption, the plates were placed in zip-loc bags and centrifuged at 1600 rpm in plate carriers for 12 minutes. After aspirating the supernatant, 1 ml of complete media containing IL-2 was added to each well. Twice weekly, 50% of the media was removed and new media was added. Both the supernatant and cells from day 14 were saved

and frozen to be tested for p27 antigen or viral DNA sequences, respectively. Virus production in supernatants was measured using a p27 ELISA. Wells were scored as positive or negative only for calculation of $TCID_{50}$.

DNA was isolated from p27-negative samples by lysis of cell pellets in 100 ul of DNA lysis buffer (10 mM Tris-HCl pH 8.0, 1 mM EDTA, 200 uM CaCl2, 0.001% Triton X-100, 0.001% SDS, and 1 mg/ml Proteinase K) for 1 hr at 58 °C, followed by 15 minutes in a 95 °C heat block (150). To detect viral DNA sequences, nested PCR was performed using primers within the *gag* gene (220). PCR conditions were as follows: For each 50 ul reaction, 5 ul 10X PCR buffer, 3.5 ul $MgCl_2$ (25 mM), 4 ul dNTP mix (10 mM), 0.5 ul each primer (20 pmol/ul), 0.5 ul AmpliTaq Gold, and 5 ul of each DNA sample were mixed (all reagents from Applied Biosystems). The thermocycler profile for both rounds was as follows: 95 °C for 10 min and 35 cycles of 95 °C for 15 sec, 55 °C for 15 sec, and 72 °C for 1 min. PCR results were analyzed on 1% agarose gel. For the second round, 1 ul of the first round was used and the same conditions were applied.

Based on the results from p27 ELISA and PCR, the endpoint titer ($TCID_{50}$) was calculated as described by Reed and Meunch (166). Statistical analysis was performed on the log transformed values using an unpaired T-test for equal variances. Based on the known titer of the virus stock, the minimal infectious units required to establish infection was calculated.

Co-receptor polymorphism analysis. The rhesus macaque genes for CCR5, CCR3, and BOB were amplified using previously published primer sequences (156). The PCR conditions per 50 ul reaction were as follows: 4 ul dNTP mix (10 mM), 1 ul each primer (20 pmol/ul), 0.75 ul Expand High Fidelity Taq Polymerase (Roche), 5 ul 10 x PCR buffer, 5 ul $MgCl_2$ (25 mM)(all

reagents except Taq from Applied Biosystems). The CCR5 samples were amplified in a Perkin-Elmer 9600 Thermocycler under the following conditions: 1) 94 °C for 2 minutes; 2) 10 cycles of 94 °C for 15 seconds, 53 °C for 30 seconds, and 72 °C for 1 minute; 3) 20 cycles consisting of: 94 °C for 15 seconds, 53 °C for 30 seconds, and 72 °C for 1 minute with an auto-extension of 5 seconds for each cycle; and finally 4) 72 °C for 7 minutes. The PCR conditions and cycling profile for BOB and CCR3 were identical, except that the annealing temperature for PCR was 51 °C for both genes. The PCR products were analyzed on a 1% agarose gel.

Immediately after PCR amplification, 2 ul of the PCR product was used in the TOPO TA cloning vector kit (Invitrogen) according to the manufacturer's instructions. Plasmid DNA was isolated from single colonies using the WizardPLUS Miniprep kit (Promega). The plasmids were sequenced using the T3 (forward) and T7 (reverse) primers. Automatic sequencing was performed at the MGB Departmental Core Facility. At least 5 clones from each animal were sequenced. Sequence alignments were made using ClustalX software program.

Real-time PCR analysis of CCR5 expression. Real-time RT-PCR primers and probe for the rhesus CCR5 gene were designed using PrimerExpress software (Applied Biosystems) and are as follows: primers: forward 5'-AACCCTGCCAAAAAATCAATGT-3' and reverse 5'-TATGTTGCCCACAAAACCAAAG-3'; probe: 6-FAM-AACAAATCGCAGCCCGCCTCC-TAMRA. For the RT reaction (20 ul total volume): 0.75 ul dH_20, 2 ul 10X PCR Buffer, 4 ul $MgCl_2$ (25 mM), 6 ul dNTP mix (10 mM), 1 ul Random Hexamers (50 uM), 1 ul RNase Inhibitor, and 1.25 ul MuLV Reverse Transcriptase (all reagents from Applied Biosystems) were mixed together and 4 ul of RNA (1 ug) was subsequently added. The PCR cycle for the RT reaction was 10 minutes at RT, 42 °C for 15 minutes, 99 °C for 5 minutes and 4 °C for 5

minutes. To the existing 20 ul reaction, 6.5 ul dH_20, 5 ul 10X Taqman Buffer A, 11 ul $MgCl_2$ (25 mM), 4 ul dNTP (10 mM) mix, 0.5 ul Taq Gold, 1 ul of each primer and 1 ul of the probe (20 pmol/ul each) was added (total volume was 50 ul). The real-time reaction conditions were as follows: 95 °C for 10 minutes, followed by 40 cycles of 95 °C for 15 seconds, 55 °C for 15 seconds, and 72 °C for 30 seconds.

Measurement of viral entry. This assay was modified from the one described previously (80). Essentially, 4 x 10^5 freshly isolated $CD4^+$ T cells were incubated with $SIV_{DeltaB670}$ at an m.o.i. of 1.0 in triplicate for 2 hours at 37 °C (most of these experiments used Pat Dowling's A60 stock of virus; titer = 1 x 10^7 infectious units/ml). The infections were performed in 5 ml snap-cap FACS tubes. After the incubation, the cells were washed 3 times with 1 x Dulbecco's PBS w/o Ca or Mg (GibcoBRL). After the final wash, 200 ul of 0.25% trypsin containing 1 mM EDTA (GibcoBRL) was added to each tube, which was then incubated 10 minutes at 37 °C. To stop the reaction, 1 ml PBS containing 15% FBS was added to each tube. The samples were washed twice more with PBS/FBS and then transferred to a 1.5 ml tube after the second wash. These tubes were centrifuged at 6,000 rpm in a microfuge. The supernatant was carefully removed (pellet was sometimes loose) and the cells were resuspended in 250 ul of cell lysis buffer (100 mM Tris, pH 7.5, 0.5% Triton X-100). Samples were immediately run in the p27 Core Antigen ELISA assay using the Optimum Sensitivity Protocol (Coulter). The following controls were used: adsorption at 4 °C or heat-inactivated virus (60 °C, 30 min).

Quantification of Reverse Transcription. Prior to infection of cells, the $SIV_{DeltaB670}$ virus stock (8-9-01 stock; titer = 1 x 10^6 infectious units/ml) was treated with RNase-free DNase 1 (Ambion). For every 100 ul of virus, 10 ul of DNase (~10 U) and 10 ul of 10 X DNase I Buffer were added, and the tubes were incubated at 37 °C for 30 min. The virus was subsequently passed through a 0.2 uM membrane filter. Freshly isolated $CD4^+$ cells were infected at an m.o.i. of 0.2 (titer determined prior to DNase treatment) at 37 °C for 2 hrs (200 ul of virus per 1 x 10^6 cells). As a control, the virus was heat-inactivated at 60 °C for 30 min. After adsorption, the cells were washed 3 times and cultured in complete media with IL-2 (40 U/ml) at a concentration of 1 x 10^6 cells/ml. 2 x 10^5 cells were harvested at various times post-infection, and DNA was isolated as described above (in a total volume of 100 ul). After isolation of DNA, each sample was passed 20 times through a 25-guage needle to shear the DNA prior to subjecting them to real-time PCR.

Reverse transcription was quantified using real-time PCR and the Prism 7700 sequence detection system (Applied Biosystems). Early reverse transcripts were quantified using primers and probes within the LTR region, which have been described previously (64). Late reverse transcripts were quantified using primer and probes within the U5 and PBS regions, which were generously obtained from Dr. Toshiaki Kodama. The sequences are as follows: forward primer: 5'-GAA ACC GAA GCA GGA AAA TCC-'3, reverse primer: 5'-CTG CCT TCA CTC AGC CGT ACT-'3, and probe: 6-FAM-AGG AGT CTC TCA CTC TCC TTC AAG TCC CTG TT-TAMRA.

Conditions for real-time PCR have been described previously (64). For each sample, 10 µl (1/10 volume) was run in triplicate in the real-time PCR assay. Serial dilutions of a plasmid

containing the LTR and PBS regions were amplified in triplicate to generate a standard curve with a sensitivity of 10 copies per reaction.

Spinoculation of $CD4^+$ T cells. Freshly isolated $CD4^+$ T cells were isolated and spinoculated as described previously (150). Essentially, 1.6 x 10^6 $CD4^+$ cells were aliquoted into 48-well plates and the plate was centrifuged using plate carriers for 12 minutes at 1600 rpm. The supernatant was aspirated using a Pasteur pipet and vacuum. The virus stock (8-9-01 stock) was treated with DNase I as described above and filtered through a 0.2 uM syringe filter. To each well, 100 ul virus was added (m.o.i. = 0.06) and the plate was placed in plastic Ziploc bags and centrifuged at 2600 rpm (1200 x g) for 2 – 3 hours at room temperature. After centrifugation, the plate was washed 4 times using cold RPMI containing 15 % FBS (12 minutes at 1600 rpm each wash). After the last wash, 800 ul fresh culture media containing IL-2 was added to each well, and the cells were cultured. 2 x 10^5 cells were harvested at various times post-infection (0, 12, 24, 48, and 72 hours post-infection), and DNA was isolated as described in a total volume of 100 ul. After isolation of DNA, each sample was passed 20 times through a 25-guage needle prior to subjecting them to real-time PCR.

Quantification of viral RNA transcripts. Total RNA was isolated from 6 x 10^5 cells harvested in parallel with the DNA samples described above. Upon harvesting, the cells were washed 2 times in PBS, treated with 0.25% trypsin/1 mM EDTA for 10 minutes at room temperature, and then washed several more times in complete media before freezing the cell pellet in 800 ul Trizol (GibcoBRL) in siliconized individually wrapped Eppendorf tubes (Fisher).

The following method of isolating RNA gave the best results with small sample sizes in the shortest amount of time. The samples were thawed to room temperature (RT) and homogenized 10 times with an 18-guage syringe attached to a 1 ml barrel, followed by 10 times with a 23-guage syringe. Each sample was then incubated for 5-10 minutes at RT. To each tube, 160 ul Chloroform:isoamyl alchohol (24:1) was added and immediately vortexed for 1 minute. This was followed by a RT incubation for 2-3 minutes and then centrifugation at 12,000 x g (14,000 rpm) for 15 minutes at 4 °C. The aqueous phase (~400 ul) was removed and put in a new siliconized tube. To each tube, 5 ul glyco-blue (Ambion; 2 mg/ml) and 400 ul isopropanol were added. The tubes were inverted several times and incubated at RT for 20 minutes. Following precipitation, the tubes were centrifuged at 12,000 x g (14,000 rpm) for 10 minutes at 4 °C. The supernatant was decanted and each tube was blotted on a kimwipe. Next, 1 ml 75% EtOH was added to each tube, followed by a quick vortex and centrifugation at 7,500 x g (8700 rpm) for 5 minutes at 4 °C. The supernatant was again poured off. The tubes were inverted and allowed to dry for 10 minutes. Each pellet was resuspended in 10 ul RNase-free water (Quality Biologicals) and incubated in a 60 °C heat block for 5 - 10 minutes to solubilize the RNA pellet. To each tube, 1 ul 10X DNase buffer and 1 ul Rnase-free DNase-I (Ambion) was added. The tubes were mixed and incubated at 37 °C for 30 minutes. Following this, 1 ul 50 mM EDTA was added, and the DNase reaction was stopped by heating the tubes in a 75 °C heating block for 10 minutes. The samples were kept on ice from this point forward. To determine the RNA concentration, 1 ul was removed and diluted 1:100 in water for O.D. (in duplicate). Samples were stored at –80 °C.

Cell-associated viral RNA was measured using two-step real-time RT-PCR as described previously (64). The primer and probe set was directed at the U5 and PBS regions of the SIV

genome, which detects all RNA transcripts. For each sample, 400 ng and 200 ng were separately reverse transcribed in duplicate reactions. Serial dilutions of RNA obtained by *in vitro* transcription of a plasmid containing the LTR and PBS regions, ranging from 10^8 to 10^0 copies/ reaction, were subjected to reverse transcription-PCR in triplicate, along with the samples, to generate a standard curve with a sensitivity threshold of 10 copies/ reaction. RNA copy numbers from the samples were calculated from the standard curve and expressed as RNA copies per ug of RNA.

As a control, expression of cellular β-glucuronidase (β-GUS) was measured in 400 ng RNA for each sample, and the appropriate RT-negative controls were also run. The primer and probe sequences for β-GUS were identical to those described previously (67). Data are expressed as a ratio of U5-PBS copies to β-GUS copies.

Flow cytometry. CD4-PE (Pharmingen; clone M-T477) and CD8-PeCy5 (Coulter; clone B9.11) were used to determine cell surface phenotype by flow cytometry using a Coulter XLS machine. Infected cells were detected by intracellular flow cytometry using a mouse monoclonal antibody to the p27 Gag protein (Advanced Biotechnologies; cat# 13-113-100). The purified antibody was first biotinylated and used to indirectly stain infected cells using a streptavidin-FITC secondary antibody (Coulter).

For biotinylation of the antibody, a 25 mg/ml solution of Biotin long arm NHS (Vector Labs cat. #SP-1200) was made in DMSO. Of this solution, 1 ul (25 ug) was added to the vial of antibody (~100 ul), and the tube was mixed well and subsequently incubated for 3 hours at room temperature with periodic mixing. The antibody was then carefully transferred to a small dialysis cassette (Slide-A-Lyzer; Pierce; 2500 m.w. cutoff), placed in a floating rack, and

dialyzed in a 1 L beaker of PBS with a slow stirbar for 1 hr. This was repeated with 2 more fresh liters of PBS, with the last wash being overnight at 4 °C. The antibody was then removed and stored at 4 °C.

The optimal concentration of this antibody for use in intracellular staining was empirically determined to be a 1:10 dilution. Streptavidin-FITC was also used at a 1:10 dilution. The intracellular staining protocol is as follows: for each animal, 0.5 - 1.0 x 10^6 cells were placed into each of two 5 ml FACS tubes. The cells were washed once with FACS buffer (PBS containing 5 % FBS, 2 % Normal Human Serum, 2 % Goat Serum, and 0.1 % Sodium Azide; filter sterilized) by filling the tube and centrifuging at 1400 rpm for 10 min at 4 °C. After decanting the supernatant, 5 ul of each surface antibody (CD4-PE and CD8-PeCy5) was added, and the tubes were mixed and incubated for 30 minutes on ice in the dark. The cells were washed two times with 1 ml FACS buffer each, using centrifuge conditions above. After decanting the supernatant, 500 ul 1% paraformaldehyde (PFA) was added per tube, and the tubes were incubated for 20 minutes at room temperature. After the incubation, the tubes were centrifuged and decanted. They were then washed once more in FACS buffer, followed by one wash in permeabilization buffer (FACS buffer $^+$ 0.1 % Saponin). After decanting the supernatant, 5 ul of the primary biotinylated anti-p27 mAb or the control IgG antibody was added per tube (1:10 dilution made in perm buffer for both antibodies). The tubes were mixed and incubated for 15 minutes at RT in the dark. The cells were than washed cells once with 1 ml permeabilization buffer. Then, 5 ul of the secondary SA-FITC (1:10 dilution made in perm buffer) was added, mixed, and incubated 15 min at RT in the dark. Following this, the cells were washed once in permeabilization buffer and once in FACS buffer before being fixed by the addition of 500 ul 1 % PFA.

5.3. Results.

Low producer $CD4^+$ cells are more refractory to infection than high producer cells. Our previous work has shown a strong and consistent correlation between the ability of an individual animal's PBMC and $CD4^+$ T cells to support viral replication *in vitro* and survival of that animal after intravenous inoculation (180). In these studies, primary cells from a group of randomly selected animals displayed a wide range of virus production. However, the amount of virus produced by cells from a given individual was highly consistent. We chose 8 animals at the opposite ends of the spectrum for further study so that differences between the two phenotypes would be readily visible. Four of these animals consistently exhibited high virus production when either PBMC or $CD4^+$ cells were infected with $SIV_{DeltaB670}$, and four of these animals exhibited low virus production. This outcome was seen irrespective of whether the cells were stimulated with phytohemagglutinin (PHA), plate-bound anti-CD3 and anti-CD28 antibodies, or Phorbol 12-myristate 13-acetate (PMA) and ionomycin (Chapter 4). Identification of the point at which replication differs within low and high producer $CD4^+$ T cells is key to pinpointing a mechanism for these observations.

Previously, it was demonstrated that cells from individual rhesus monkeys varied in their permissiveness for infection with the molecular infectious clone $SIV_{smE543-3}$ (69). To determine whether the $CD4^+$ T lymphocytes from the low producer animals studied here were more refractory to infection with the pathogenic primary isolate $SIV_{DeltaB670}$, the multiplicity of infection (m.o.i.) required to infect these cells was determined using the method of Reed and Meunch (166). PHA-stimulated PBMC from each animal were infected with 5-fold dilutions of SIV and cultured. At 14 days post-infection (p.i.), the supernatants were harvested and frozen

for measurement of p27 antigen, and the cells were frozen for DNA isolation and PCR. All wells were scored as either positive or negative based on p27 ELISA of culture medium or nested *gag* PCR of PBMC DNA.

The results in Figure 29 are presented as the log of the $TCID_{50}$ dilution, which represents the minimum dilution of virus required to infect 50 % of the wells. A log $TCID_{50}$ dilution of -4, for example, means that a 1:10,000 (10^{-4}) dilution of virus will result in half of the wells becoming positive for either p27 or *gag* sequences, whereas a -6 value means the virus can be diluted an additional 100-fold and still result in infection of half the wells. Based on these calculations, 10-fold more input virus was required to infect cells from low producer animals when compared to their high producer counterparts, and this finding was true for both the p27 ELISA (log $TCID_{50}$ = -4.24 and -5.30 for the average of the low and high producer animals, respectively) and the *gag* PCR results (log $TCID_{50}$ = -4.46 and -5.48, respectively). The average log $TCID_{50}$ for the high and low producer groups was significantly different (unpaired t-test, P = 0.006 for p27 ELISA, and P = 0.032 for *gag* PCR) (Figure 29 A). This experiment was repeated using purified $CD4^+$ T cells activated with anti-CD3/CD28 antibodies, and identical results were obtained (unpaired t-test, P = 0.003 for p27 results, and P = 0.003 for *gag* PCR results) (Figure 29 B). Because the difference in $TCID_{50}$ was not alleviated when *gag* PCR results were used for calculation, the difference between the two groups is most likely not in the virus production stage of the life cycle, but rather lies prior to completion of reverse transcription.

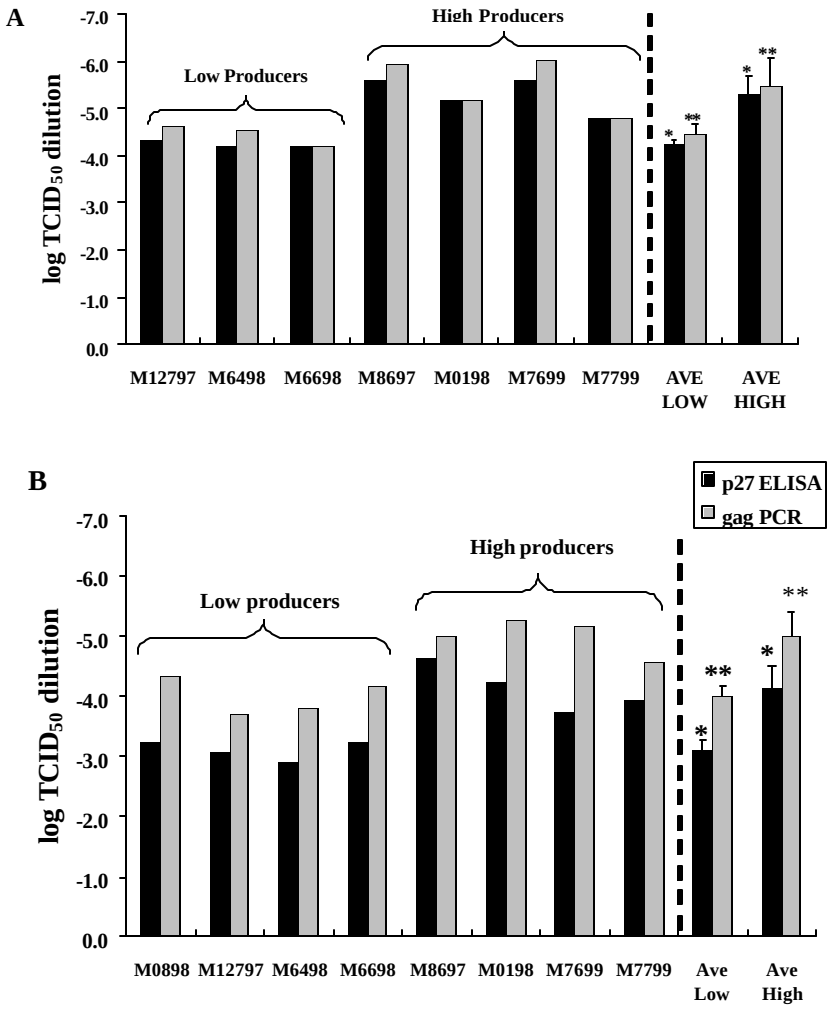

Figure 29. Low producer cells are more refractory to infection compared to high producer cells.

$SIV_{DeltaB670}$ was titered on PHA-stimulated PBMC (A) or anti-CD3/CD28-stimulated primary $CD4^+$ T cells (B) from high and low producer animals. Results are expressed as the log transformation of the $TCID_{50}$ dilution, which was calculated based on the presence or absence of p27 in the supernatant (black bars) or *gag* sequences by PCR (gray bars) at 14 days post-infection. The average of the two groups is also shown, including bars representing one standard deviation. For panel (A), unpaired T-tests revealed that the average log $TCID_{50}$ from each group was significantly different at the p27 (*P = 0.006) and *gag* PCR (**P = 0.032) levels. In panel (B), the results were also significantly different at the p27 (*P = 0.003) and *gag* PCR (**P = 0.003) levels.

Viral entry into high and low producer $CD4^+$ cells is identical. To determine whether viral entry could account for the differences observed in the amount of virus required to support infection, we measured the ability of $SIV_{DeltaB670}$ to enter freshly-isolated $CD4^+$ cells by measuring the amount of p27 internalized during a 2 hour adsorption period at either 37 °C or 4 °C (80). As expected, when heat-inactivated virus was used at either 37 °C or 4 °C, no viral entry occurred (data not shown). When viable virus was used, the amount of internalized p27 was significantly higher in cells incubated at 37 °C than 4 °C (Figure 30). However, when values from the two phenotypic groups were compared, no significant difference in viral entry was observed. These results were consistent among several repeated experiments using 2 different stocks of virus and 2 different multiplicities of infection (m.o.i.) (data not shown).

Both flow cytometric evaluation of surface protein expression and real-time RT-PCR of mRNA transcripts for CCR5, the major receptor for $SIV_{DeltaB670}$ (50), further supported these results. The density of expression of CCR5 on the surface of susceptible cells may affect the ability of virus to enter and initiate an infection. After activation of PBMC with the mitogen PHA, expression levels of CCR5 on the $CD4^+$ T cell surface, as measured by the mean fluorescence intensity of CCR5 staining, were identical between high and low producer animals (Figure 31 A). Clearly, PHA activation alone does not differentially alter CCR5 expression on the cells over time, indicating that $CD4^+$ T cells from both groups of animals should be equally susceptible to CCR5-mediated viral entry. To confirm this finding, real-time RT-PCR analysis revealed that the number of intracellular CCR5-specific mRNA transcripts in both infected and uninfected cells from the two phenotypes were not significantly different (Figure 31 B). Therefore, variations in the expression level of CCR5 were not a contributing factor to the resistance of low producer cells to infection with SIV.

To further prove that viral entry differences were not responsible for the high/low virus producer phenotype, extensive sequence analysis of receptor genes was undertaken. Polymorphisms have been noted within the genes encoding receptors for both HIV and SIV that affect virus binding, entry, and, as a consequence, disease progression (101, 135). Therefore, the coding regions of CCR5 and two other potential alternative receptors, CCR3 and GPR15/BOB (50, 51), were sequenced. Analysis of the coding region of CCR5 revealed 2 nucleotide changes that segregated between high and low producer animals (see Appendix B, Figure 46). Both mutations were synonymous, and therefore did not affect the amino acid sequence. Interestingly, the G to A transition at position 786 lead to insertion of a new EcoRI restriction site. This mutation has been noted in the literature and has not been associated with disease progression in SIV-infected monkeys (156). Further screening of 9 other well-characterized animals for the presence of this mutation revealed that some animals were heterozygous; however, there was no association with producer status as there was in this group of 8 animals (See Appendix B, Table 13). Therefore, the segregation of these two mutations between this group of high and low producer animals was most likely coincidental.

Sequence analysis of CCR3 and GPR15/BOB (50, 51) revealed no nucleotide polymorphisms that could be associated with high or low virus production (see Appendix B, Figures 47 and 48). Together, these data failed to reveal any difference at the level of virus entry between the two phenotypes that could account for the relative resistance of low producer cells to infection.

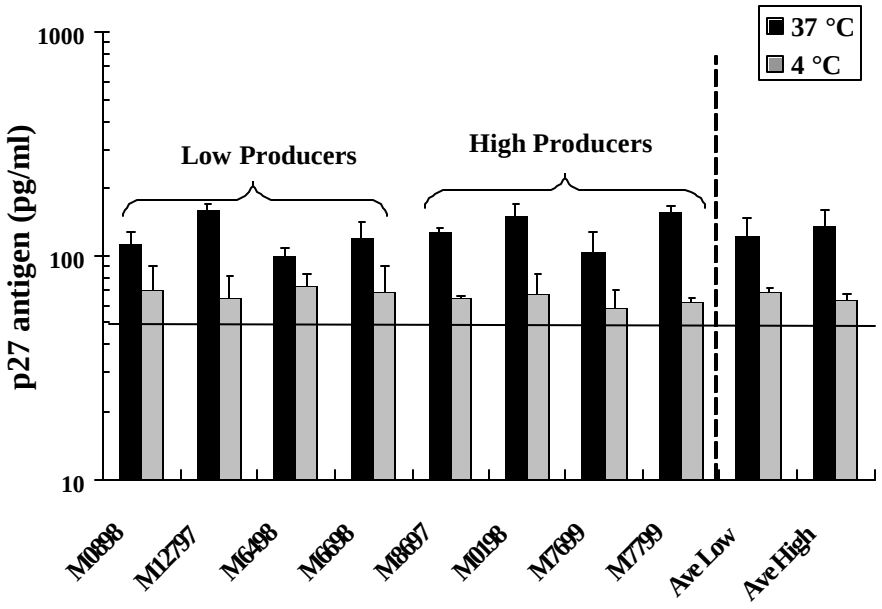

Figure 30. There are no differences in viral entry into high and low producer cells.

Viral entry into fresh $CD4^+$ cells was measured by quantifying intracellular p27 core antigen after 2 hours of adsorption (m.o.i. = 1.0) at 37 °C (black bars) or 4 °C as a control (gray bars). The bar for each animal represents the average of 3 replicates. The average of the high and low producer cells is shown on the right with bars representing one standard deviation. The sensitivity of the p27 ELISA is 50 pg/ml (indicated by the black horizontal line). Results shown are representative of 5 different experiments using different doses of virus. The average of the two groups is not statistically significant.

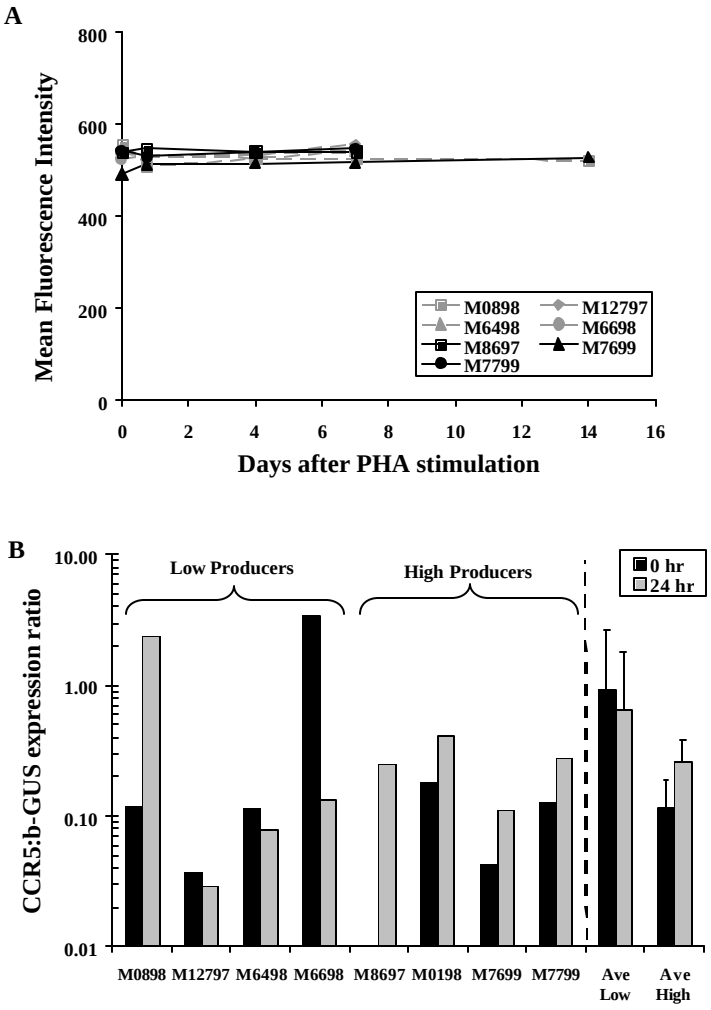

Figure 31. Measurement of CCR5 expression levels on $CD4^+$ T cells.

(A) The mean fluorescence intensity of CCR5 staining on gated $CD4^+$ T cells from PHA-stimulated, uninfected PBMC cultures. (B) CCR5 mRNA levels were measured in freshly isolated $CD4^+$ cells using real-time RT-PCR prior to infection with SIV (black bars) and 24 hours after infection (gray bars). An internal standard (β-GUS) was run for each sample and used for normalization. All values are expressed as a ratio between CCR5 and β-GUS expression. There were no significant differences between the groups at either time point.

The reverse transcription process is less efficient in low producer $CD4^+$ T cells. Analysis of receptor expression and viral entry failed to identify any distinct differences between high and low producer animals. Consequently, analysis of reverse transcription, the subsequent step in the virus life cycle, was undertaken to identify any differences between high and low producer cells with regard to this crucial step in the virus life cycle. One of the earliest detectable products of the reverse transcription process is strong-stop DNA, which is a short fragment of cDNA generated after inititation at the primer binding site (PBS) through the first strand-transfer (see Figure 4; step #1). These early reverse transcription cDNA products were measured by real-time PCR using primers and a probe within the LTR itself (R and U5 regions). Additionally, fully reverse-transcribed cDNA was detected using one primer within the LTR U5 region and the other within the primer binding site (PBS), which forms a product only after the reverse transcription process is mostly complete (see Figure 4; step #9). For accurate quantification, standard curves were generated from serial dilutions of a plasmid containing the LTR and PBS regions and had a sensitivity of 10 copies per reaction (see Appendix C, Figures 49 and 50).

Freshly-isolated $CD4^+$ cells were infected with DNase-treated virus stock (m.o.i. = 0.2), and samples were harvested at intervals within the first 72 hours of infection. Consistent over several repeated experiments, a modest (1.5 to 2-fold) greater increase in strong-stop DNA products was observed in high producer cells that was detectable by 6 hours post-infection (p.i.) (Figure 32 A) and persisted through 72 hours (Figure 32 B). A similar difference was observed when full-length transcripts were measured (Figure 32 D), and as expected, this difference followed a later time course and was not evident until 8 hours p.i. (Figure 32 C).

The results described in this section were consistent over several repeated experiments. Independent sample T-tests of the differences between the two groups at each individual time

point revealed *P* -values that approached significance (0.07 – 0.1) for all time points after 6 hours p.i. Repeated measures ANOVA, which generates a *P* -value for each group as a whole, and not for individual time points, revealed *P*-values that approached significance as well (*P* = 0.08 and *P* = 0.1 for LTR and U5-PBS results, respectively). While the *P*-values for these studies did not reach the standard 0.05 cutoff for significance, these results are noteworthy because they were very consistent over several repeated experiments. Despite our attempts to select animals at the opposite ends of the spectrum of virus production, the out bred nature of rhesus monkeys makes experiments using only 4 animals per group difficult to analyze statistically.

Spinoculation, or centrifugal infection, of $CD4^+$ cells with HIV-1 has been shown to increase virus binding in a CD4-dependent manner without affecting fusion (150). This technique has been used to enhance the infection of cells by HIV-1 and other pathogens that are difficult to culture (81, 159). $CD4^+$ T cells from the 8 animals studied here were spinoculated with SIV, and a similar 2-fold difference in accumulation of strong-stop DNA products was seen as in the results presented above (Figure 33). This finding again argues for a block after virus binding.

To determine whether the difference in number of reverse transcription intermediates between the two phenotypes was dependent on the virus dose used for infection, 2-fold dilutions of $SIV_{DeltaB670}$ were used to infect $CD4^+$ cells as described above, and the DNA was harvested at 24 hours post-infection for analysis. High producers had significantly more early strong-stop cDNA copies throughout the range of doses employed to infect the cells (Figure 34), indicating that observed differences were not a phenomenon of one specific dose. These results are consistent with the $TCID_{50}$ measurements (Figure 29).

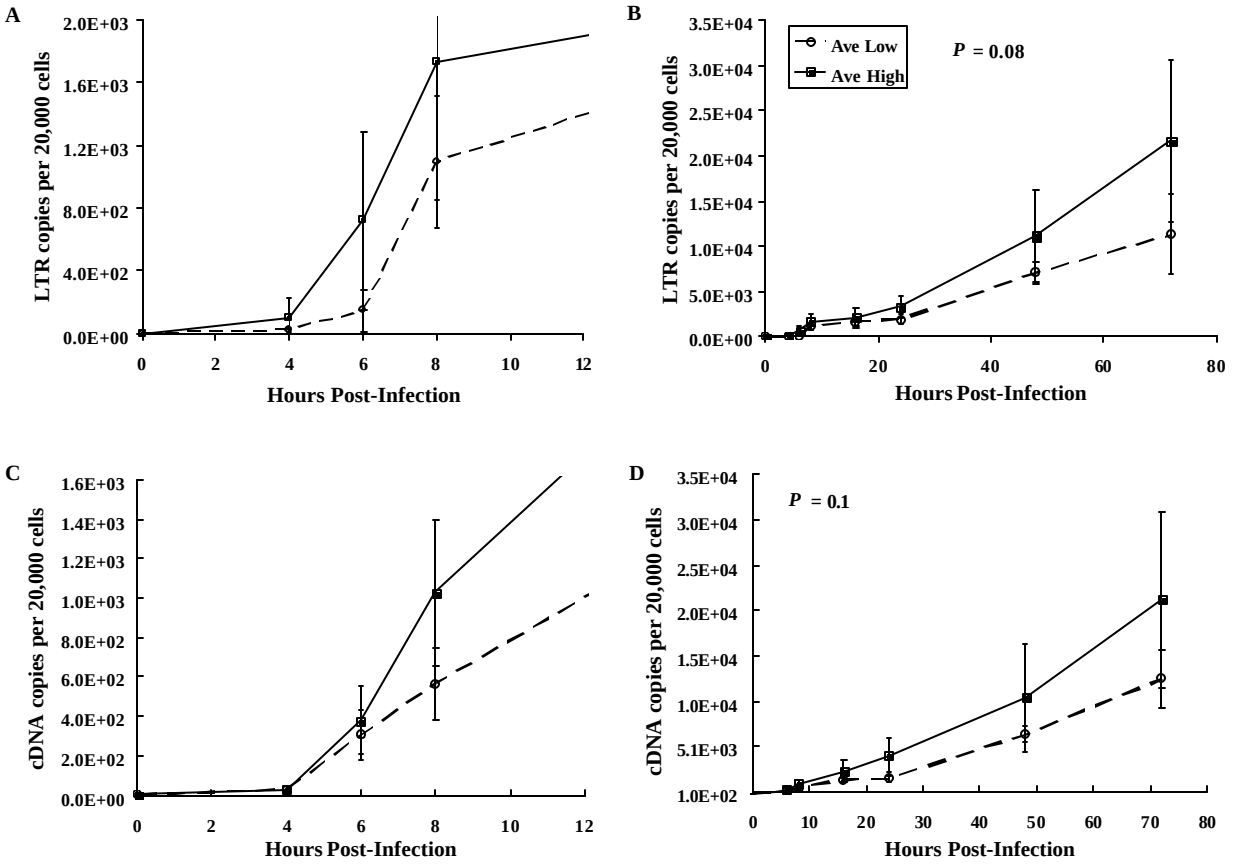

Figure 32. Low producer CD4$^+$ cells have a slower accumulation of early and late reverse transcription intermediates than high producer cells.

Freshly isolated CD4$^+$ cells were infected with $SIV_{DeltaB670}$ (m.o.i. = 0.1) and cells were harvested at various time points post-infection for measurement of cDNA intermediates by real-time PCR. (A) Early reverse transcription products (strong-stop DNA) through the first 12 hours post-infection were measured using primers and probe within the LTR region. (B) A later time course of early reverse transcripts through 72 hours after infection. (C) Full-length reverse transcription products through the first 12 hours post-infection were measured using primers and probe within the U5 and PBS regions. (D) A later time course of full-length reverse transcripts through 72 hours after infection. Results shown are representative of several experiments. For each graph, the average of the two groups is shown including bars that represent ±1 standard deviation. The high producers are represented by the solid line and solid squares, while the low producers are represented by the dashed lines and open circles. A repeated measures ANOVA was used to determine statistical significance and the *P*-value is indicated on (B) and (D).

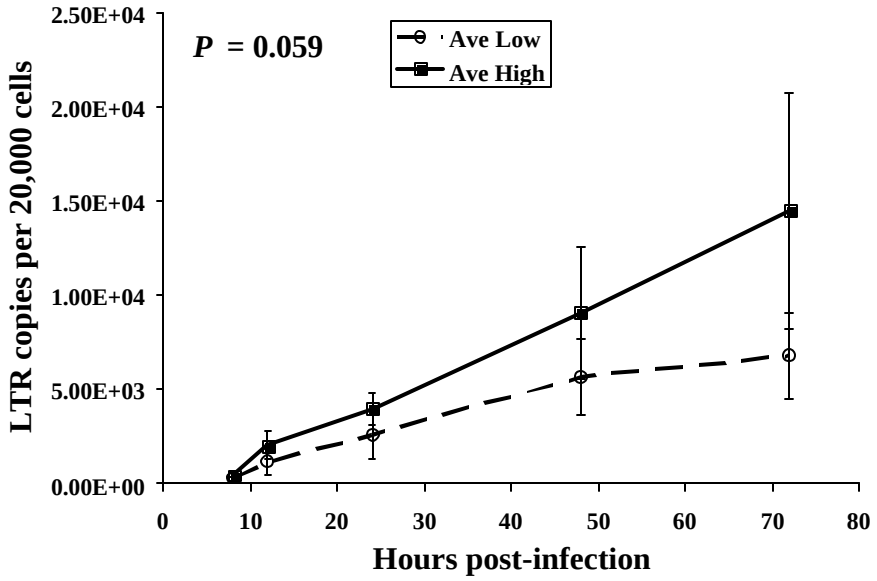

Figure 33. Spinoculation of CD4$^+$ T cells results in 2-fold differences in early reverse transcripts.

CD4$^+$ T cells from each animal were infected with SIV via 'spinoculation', whereby the virus was added to the cells in 48-well plates, and the plates were subsequently centrifuged at 2600 rpm (1200 x g) for 2 – 3 hours at room temperature. DNA was harvested at intervals after infection and real-time PCR was used to determine the LTR (strong-stop) copy number.

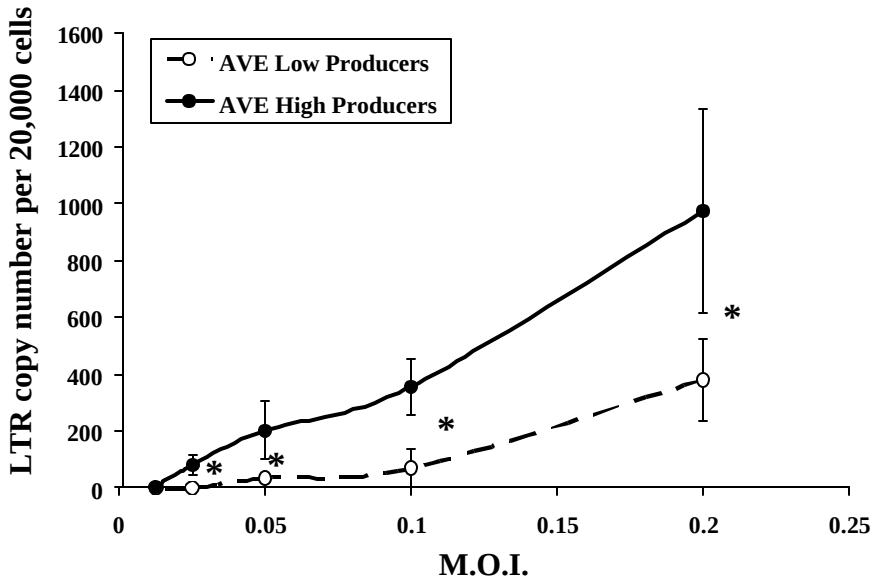

Figure 34. Differences in early reverse transcripts are independent of the dose of virus used for infection.

Freshly isolated $CD4^+$ cells were infected with 2-fold dilutions of SIV. Twenty-four hours after infection, cells were harvested and the number of early reverse transcription products (LTR; strong-stop) was quantified by real-time PCR. An unpaired T-test for comparison of means was run for each time point and significance ($P < 0.05$) is indicated by an asterisk (*).

Low producer CD4$^+$ cells have fewer numbers of cell-associated viral RNA transcripts than high producer cells. To determine whether the two phenotypes differed with respect to virus-specific transcription, cell-associated viral RNA was quantified using real-time RT-PCR. Purified CD4$^+$ cells were infected with SIV as described above. At various intervals after infection, the cells were harvested, trypsinized, and then washed extensively prior to RNA extraction to remove virions bound to the cell surface. Real-time RT-PCR was performed using primers/probe within the U5 and PBS regions of the viral genome because this region is included in all viral RNA transcripts. Serial dilutions of RNA obtained by *in vitro* transcription of a plasmid containing the LTR-PBS regions, ranging from 10^8 to 10^0 copies/ reaction, were used to generate a standard curve with a sensitivity threshold of 10 copies/ reaction (See Appendix C, Figure 51). The cellular β-glucuoronidase (β-GUS) gene was used as an internal control for quantification and integrity of the RNA sample. β-GUS is an ideal control for assaying mRNA transcription in primary CD4$^+$ lymphocytes because its expression is constitutive in SIV-infected, uninfected, activated, or resting cells (See Appendix C, Figure 52). Results are expressed as a ratio of the number of U5-PBS to β-GUS transcripts.

As expected, SIV DNA within cells from both phenotypes was transcriptionally active. Analysis of an early time course of infection (Figure 35 A) showed no significant difference in the number of RNA copies present immediately after adsorption of the virus (0 timepoint). Since viral RNA in the cell at this time represents RNA associated with incoming virions, these results again confirm no difference in viral entry between high and low producer phenotypes. The RNA copy number decreased at 6 to 8 hours post-infection in both groups, a finding consistent with the conversion of incoming RNA to DNA (91). Thereafter, both infections proceeded similarly during the first 24 hours p.i. However, later in the infection, an average of 2- to 3-fold more

viral RNA transcripts were evident in high producer cells when compared to their low producer counterparts (Figure 35 B). This increase was similar to the 2- fold increase in DNA templates observed in high producer cells (Figure 32). Expression of β-GUS was not significantly different at any time point (data not shown). Although the assay used to measure viral DNA did not discriminate between extra-chromosomal and integrated forms, the lack of an obvious difference in the number of viral RNA copies per to DNA template suggests that viral RNA transcription was not intrinsically different between the two groups. Rather, the greater template copy number in the high producer cells appeared to result in more mRNA being produced.

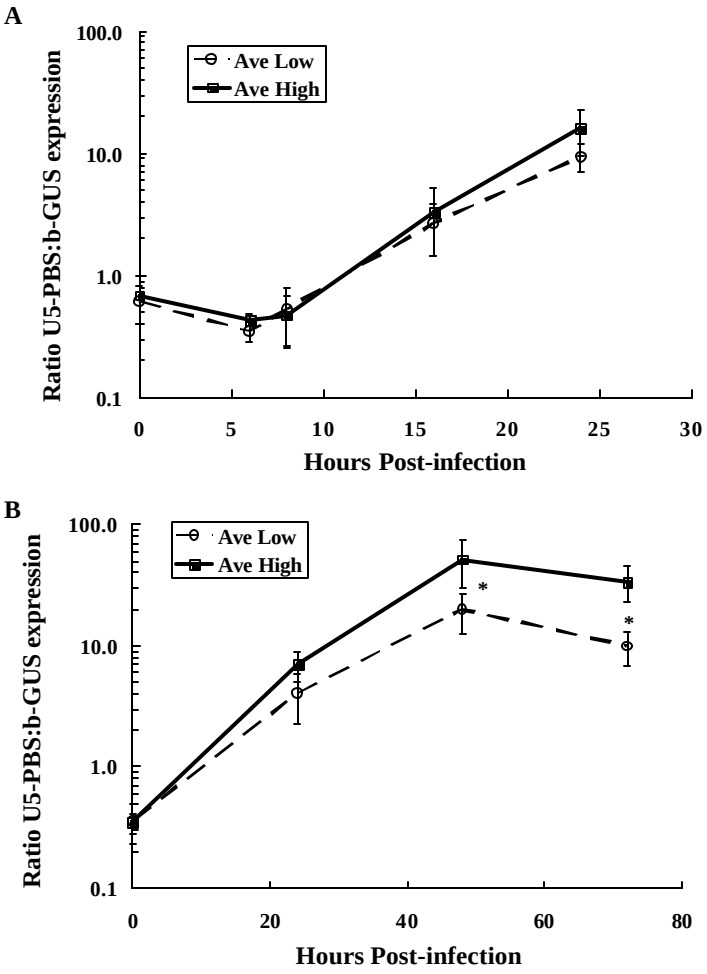

Figure 35. Low producer CD4$^+$ cells have fewer numbers of cell-associated viral RNA transcripts than high producer cells.

Primary CD4$^+$ T cells were infected with $SIV_{DeltaB670}$ (m.o.i. = 0.1), and RNA was harvested at various time points post-infection. Cell-associated viral RNA was measured by real-time RT-PCR using primers and probe within the U5 and PBS regions of the viral genome. Data are expressed as the ratio between the expression of U5-PBS and an internal standard, β-GUS. (A) RNA transcripts through 24 hours post-infection. (B) RNA transcripts at 24, 48, and 72 hours post-infection. For all graphs, the average of the two groups is shown including bars that represent ±1 standard deviation. There was no significant difference in the amount of RNA transcripts present immediately after adsorption (0 hr time point), confirming that there are no differences in viral entry as shown in Figure 3.2. An unpaired T-test was performed on 48 and 72 hr samples and is statistically significant (*P = 0.03; *P = 0.006, respectively).

The efficiency of reverse transcription is associated with the rate of viral spread throughout the culture. To determine how the different levels of viral DNA synthesis and RNA transcription observed in the two phenotypes relate to the number of productively infected cells, an intracellular staining procedure was employed to accurately detect and quantify p27-expressing cells. Histograms of intracellular p27 staining are shown for all 8 animals in Appendix D, Figure 53. Not surprisingly, high producer cultures had a higher percentage of infected $CD4^+$ cells than low producer cells throughout the entire 18 day culture period (P = 0.005, repeated measures ANOVA) (Figure 36 A). Virus dissemination in the two types of cultures did not follow the same rate kinetics, however. The increase in infected cells within 3 of the 4 high producer cultures was linear through day 11, at which point the percentage of infected cells leveled off at ~80 %, most likely because all viable susceptible cells within the culture were infected by this time. In contrast, a biphasic increase in the number of productively infected cells was observed in all 4 low producer cultures and one of the high producer cultures (cells from animal M7799, depicted separately in Figure 36 A). A more gradual increase in the number of infected cells was observed in these cultures for the first 7 days, which then increased dramatically thereafter. After 7 days, the number of infected cells in the culture from high producer M7799 rapidly reached the levels obtained by the other high producers. The low producer cultures, however, did not peak until day 18, 7 days after the peak achieved in the high producer cultures. Even then, this level (70% of the cells) was less than that of their high producer counterparts. Repeated measures ANOVA of the results with or without animal M7799 included within the high producer group resulted in P-values that were very similar (P = 0.005 without M7799; P = 0.003 with M7799).

The amount of p27 made per infected cell, determined by examining the fluorescence intensity of the p27 staining, was similar in all cultures, regardless of the number of infected cells in the culture at the time of analysis (Figure 36 B). Together with the kinetics of viral RNA expression, these data suggest that despite the inhibition in the production of early reverse transcription intermediates and the delayed kinetics of virus spread in the culture, RNA transcription and protein expression on a per cell basis proceeded similarly in the two phenotypes. The end result was that significantly less virion-associated p27 protein accumulated in the supernatant of the low producer cultures when compared to their high producer counterparts (Figure 36 C; $P = 0.003$, repeated measures ANOVA) .

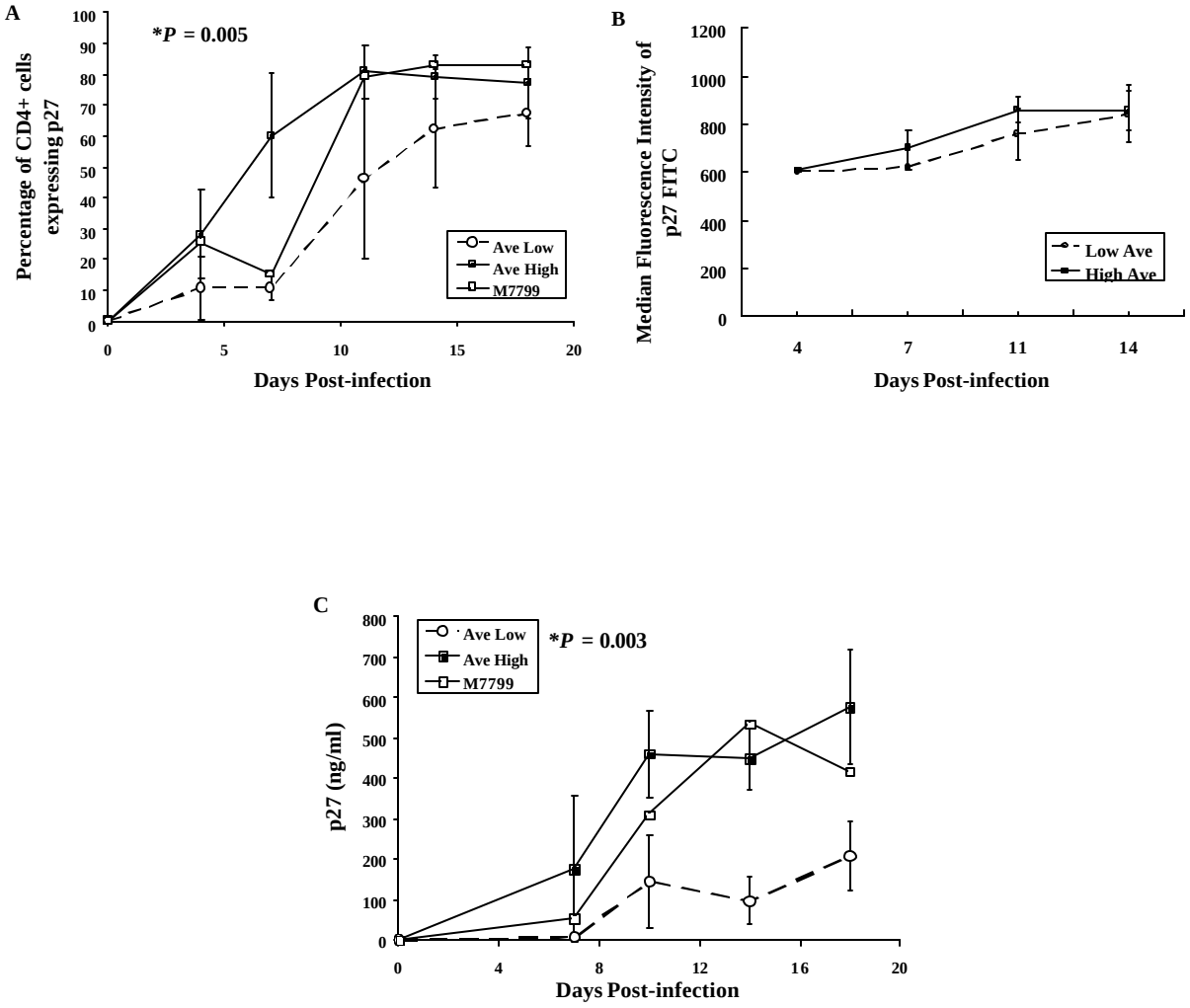

Figure 36. Virus production and spread is significantly inhibited in low producer cultures.

At various time points after infection *in vitro*, cells were removed and stained for cell surface markers and intracellular p27 antigen. (A) Percentage of gated $CD4^+$ cells expressing p27 antigen. (B) Median fluorescent intensity of p27 FITC staining. (C) Amount of p27 secreted into the supernatant as measured by p27 ELISA. For (A) and (C), the average of 3 high producers is shown in the thick black line with a solid square, while the average of the 4 low producers is shown in the dashed black line with an open circle; both include bars that represent one standard deviation. The outlier high producer animal, M7799, is represented separately by the solid black line with the open square. For each graph, a repeated measures ANOVA was used to determine statistical significance between the 4 low producers and 3 high producers and the *P*-value is indicated on each graph. *P*-values generated after including animal M7799 in the analysis were very similar ($P = 0.003$ for (A) and $P = 0.002$ for (C)).

Intracellular levels of glutathione are equivalent in high and low producer cells. In Chapter 4, we noted that greater numbers of viable cells accumulated in the 4 SIV-infected low producer cultures and one high producer culture (M7799) during the course of an *in vitro* infection as compared to the remaining 3 animals with the high producer phenotype (Figure 16 A). Surprisingly, a similar difference in cell growth was also seen in mock-infected, mitogen-stimulated cultures (Figure 16 B). The decreased number of viable cells was due to more apoptosis in these three high producer cultures (Figure 19) in the absence of detectable differences in proliferation rate or activation marker expression. The kinetics of virus spread through the culture shown in this chapter (Figure 36 A) paralleled the apoptosis results; a faster, linear spread of virus through 3 high producer cultures was associated with increased $CD4^+$ cell apoptosis within cultures from these same animals.

Differences in apoptosis in the absence of detectable differences in T cell activation or proliferation suggest that signaling from apoptosis-inducing receptors, such as Fas or the TNF receptor, may differ between the two groups. Death receptors, such as TNFR and CD95 (FAS/APO-1), have been shown to lead to either apoptosis or proliferation, depending on whether the intracellular signal proceeds via caspase-8 or FLIP, respectively (23, 121). These findings suggest a plausible scenario in which TNFR/Fas signaling in some lymphocytes leads to a survival signal, while the same signal in cells from another individual leads to apoptosis. A key determining factor in the switch between apoptosis or death are intracellular levels of glutathione (GSH), a necessary antioxidant which reduces harmful reactive oxygen species (ROS) within cells, thereby protecting the cell from apoptosis and prolonging survival. Interestingly, HIV-infected humans have reduced levels of intracellular GSH, and the level of GSH reduction correlates with the stage of disease (191).

To determine whether the differences observed in cell survival could be accounted for by differential levels of GSH, intracellular GSH was quantified in primary PBMC using the glutathione-specific fluorescent dye monochlorobimane (MCB) (Figure 37). Cryopreserved PBMC from each animal were thawed and stimulated with anti-CD3/CD28 antibodies for 3 days, and continued in culture for 2 more days. On day 5, half of the cells from each animal were infected with $SIV_{DeltaB670}$ (m.o.i. = 0.01). Twenty-four hours after infection, intracellular glutathione levels were measured using MCB. No apparent difference in GSH levels were found among the animals tested (Figure 37). However, because activity of GSH is controlled by its oxidation-reduction state, apparent differences in levels of active GSH may be masked. Further investigation to examine the role of GSH in this phenomenon is ongoing.

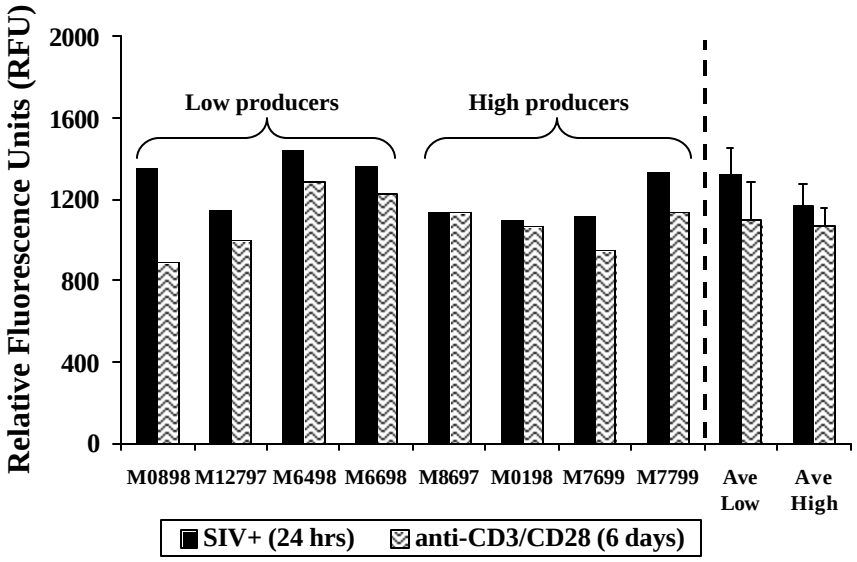

Figure 37. Intracellular glutathione levels are equivalent between high and low producer cells.

Cryopreserved PBMC from each animal were thawed and stimulated with anti-CD3/CD28 antibodies for 3 days and cultured. On day 5, half of the cells from each animal were infected with $SIV_{DeltaB670}$ (m.o.i. = 0.01). Twenty-four hours after infection, intracellular glutathione levels were measured using monochlorobimane (MCB). Intracellular glutathione levels after 24 hours of SIV infection (black bars) or 6 days of anti-CD3/CD28 stimulation alone (striped bars) is shown. There were no significant differences between the two groups.

5.4. Discussion.

The relative amount of SIV produced during *in vitro* infection of rhesus monkey primary $CD4^+$ T lymphocytes is highly predictive of the rate of progression to AIDS following *in vivo* infection (69, 156, 180). Specifically, host factors that exert their effects on virus replication within $CD4^+$ T cells *in vitro* could potentially have a significant impact on disease progression and survival *in vivo*. Identification of the host factor(s) responsible for controlling *in vitro* virus production, and the possible association of these factor(s) with survival *in vivo*, is dependent on a clear understanding of how virus replication differs within cells from high and low virus producing animals. In this chapter, we have delineated the point in the virus life cycle at which the lymphocyte differentially controls virus replication and how this control may impact the subsequent stages of replication. In addition, we have begun a preliminary examination of the phenotypic properties of the host cell that may be associated with this phenomenon.

Primary $CD4^+$ lymphocytes from 8 rhesus monkeys representing the extreme high and low ends of the spectrum of *in vitro* virus production (4 high producers and 4 low producers) were used for this study. Since the differences in virus production occur when equal numbers of $CD4^+$ T cells from each animal are infected with the same dose of virus, the control of virus replication is at the level of the $CD4^+$ T lymphocyte itself (180). Based on Reed-Muench analysis, 10-fold more input virus was required to infect $CD4^+$ cells from low virus producing animals than was required for infection of high producer lymphocytes. This 10-fold difference was seen not only at the level of p27 antigen production (a late step of the virus life cycle), but at the cDNA level, indicating that the effect on the virus life cycle was prior to generation of full-length viral DNA.

The virus we used for these and previous studies is $SIV_{DeltaB670}$, which was obtained from a rhesus monkey at end-stage AIDS (10), and is therefore evolutionarily fit and adapted for pathogenic growth in an animal. It has subsequently been passaged a limited number of times on primary rhesus PHA blasts. For these reasons, it is pathogenically and phenotypically relevant as a model for the viral diversity and fitness seen in HIV-infected humans. Our *in vitro* viral replication assay (180) requires infection of fresh PBMC with high doses of $SIV_{DeltaB670}$ followed by mitogen stimulation (PHA or anti-CD3/CD28 antibodies) of the cells after 24 hours of infection. This assay results in consistent virus production from individual animals that varies from animal to animal and encompasses a 10-fold difference in virus production between the two extremes. In a previous study, Hirsch and colleagues (69) measured the susceptibility of PBMC from different animals to infection with $SIV_{smE543-3}$, a molecular infectious clone generated by transfection of the human cell line CEM x 174, and found a 4-log difference in infectious dose between the most and least susceptible cells. The discrepancy between our finding of a 10-fold maximum difference in susceptibility and that of Hirsch and colleagues may lie in the fact that the virus used for their study was a molecular clone that was passed on a human cell line, and may implicate phenotypic properties of the virus itself that were altered during growth in human cells (52).

Here, detailed analysis of various steps in the viral life cycle was undertaken to determine the point at which the lymphocyte differentially controls virus replication. Differences in viral entry were ruled out at several levels. First, analysis of CCR5 expression, the major receptor for $SIV_{DeltaB670}$ (50), failed to identify differences in either protein or mRNA expression. Genetic analysis further revealed no sequence polymorphism(s) in the genes for either CCR5 or the two other putative co-receptors of SIV, CCR3 and GPR15/BOB (51), that

might be associated with a differential binding of the virus envelope to the receptor(s). Importantly, two methods of measuring viral entry, an ELISA which quantifies intracellular p27 antigen, and real-time RT-PCR which measures the number of internalized, cell-associated viral RNA copies, revealed no difference in the number of virions inside cells from the two phenotypes immediately after adsorption.

Analysis of the accumulation of reverse transcription products using real-time PCR demonstrated, however, that modest, but consistently higher levels of both early (strong-stop) and late (full-length) reverse transcription products were observed in high producer lymphocytes when compared to their low producer counterparts. Furthermore, these differences were independent of the dose of virus used to infect the cells. These data confirm the previous observations of Robert-Guroff and colleagues (156) who reported similar results in an analysis of a rhesus monkey resistant to mucosal infection with SIV. In our studies, analysis of subsequent steps in the virus life cycle revealed no obvious differential ability to express viral RNA or p27 protein. The partial inhibition at the level of early reverse transcription appeared to be the only defect in low producer cells; this was enough to result in decreased RNA and protein production.

Examination of the kinetics of virus spread in the culture and the growth properties of activated cells revealed other phenotypic differences among the cells studied. Flow cytometric enumeration of virus infected cells using an intracellular p27 staining assay revealed a biphasic increase in the accumulation of productively infected cells in all 4 low producer cultures that was characterized by a slow, gradual increase in infected cells for the first 7 days p.i. Subsequently, the number of infected cells increased dramatically to a level of 70 % by the end of the culture period (18 days p.i.). In contrast, 3 of the high producer cultures displayed a rapid, linear increase in the number of infected cells that reached a peak level of 80 % of the cells infected by

11 days p.i., which was 7 days earlier than that observed in the low producer cultures. Interestingly, one of the high producer cultures displayed the delayed kinetics of virus spread observed in the low producer cultures during the first week p.i. However, unlike the low producer cultures, after the 7 day lag period, the number of infected cells quickly reached levels identical to that of the other high producers, and large amounts of virus were detected in the culture medium.

The linear increase in virus-infected cells observed in three of the high producers was further found to be associated with a higher rate of apoptotic cell death triggered by either virus infection, or, interestingly, by mitogen stimulation of mock-infected cultures using either PHA or anti-CD3/CD28 antibodies (Chapter 4). The inherent rate of T cell activation and cell division was apparently not responsible because no significant difference in surface expression of CD29, CD45RA, CD69, CD71, and CD95, or proliferation as measured by CSFE staining, respectively, was observed.

The relationship between high virus production and increased apoptosis observed in 3 of the high producer animals examined in this study is an intriguing finding. A plausible explanation for this observation that also addresses suppression of viral reverse transcription is that high producer cells may have a reduced level of glutathione (GSH). GSH is a necessary antioxidant that reduces harmful reactive oxygen species (ROS) that are known to induce apoptosis (158). HIV-1-infected patients have been shown to have reduced levels of GSH (191). Conversely, high levels of GSH are also known to block HIV-1 reverse transcription (88), an observation consistent with the suppression of viral reverse transcription observed in low producer cultures. Although the levels of GSH *per se* did not appear to differ among the animals tested, other factors that control GSH activity may nevertheless be responsible. The outcome of

in vivo infection of the one outlier animal which had low levels of apoptosis despite high virus production may be key to understanding the interplay between these two phenomena.

Other mechanisms known to block virus replication independent of apoptotic cell death are also plausible. Inhibition of the early stages of the HIV-1 life cycle after entry but before viral RNA synthesis can have effects on virus production, tropism, permissivity, and/or cytopathicity (26, 118, 156). After fusion of the virus with the host cell membrane, the viral core is released into the cytoplasm and an ill-defined uncoating process occurs. While not yet completely understood, a rearrangement of viral proteins must occur at this time to allow for efficient reverse transcription and formation of the pre-integration complex, which consists of the viral DNA, reverse transcriptase (RT), integrase (IN), matrix (MA), nucleocapsid (NC), and Vpr proteins (56). The virus is very vulnerable to the effects of host-cell antiviral mechanisms during this time period.

Restricted growth of retroviruses after entry but before completion of reverse transcription has been shown to be due to the presence of endogenous retroviral *gag* sequences such as *Fv1* in mice and *Ref1* in humans (199). The inability of HIV-1 to replicate in rhesus monkey cells is due to the presence of *Ref1*, which acts through interaction with the incoming viral capsid (p24) protein in a dominant-negative manner, leading possibly to decreased stability of the pre-integration complex and inhibited nuclear importation (38, 68). The primate form of *Ref1* (*Lv1*) has not been identified to date. While restriction of HIV-1 replication in monkey cells is complete, it is possible that partial restriction occurring in a similar manner in low producer cells, perhaps due to a polymorphism that leads to increased expression of the *Lv1* gene, can account for the differences observed in accumulation of reverse transcription products (38). While further analysis of the putative roles that *Ref1*-like factors may play in this process is

being pursued, the biphasic increase in infected cells in the low producer cultures is consistent with a *Ref1*-mediated event because the block can be overcome by increasing amounts of input virus (38).

Another recently identified cellular antiviral factor, CEM15, has been shown to inhibit replication at the level of reverse transcription; however, the activity of CEM15 is usually inhibited by the viral Vif protein (120, 181). Vif has long been known to have a role in the reverse transcription process by modulating the stability of the nucleoprotein complex thereby influencing initiation (44, 70, 71, 184). The Vif protein of primate immunodeficiency viruses is critical in regulating infectivity and host-range of these viruses (186), and this is presumably due to its ability (or inability) to overcome the antiviral activity of the CEM15 protein. Altered expression of CEM15, or alternatively, polymorphisms within CEM15 that affect interactions with Vif, may lead to individual differences in susceptibility to infection by lentiviruses. Identification of the primate version of CEM15 as well as expression levels of CEM15 in humans and primate species remains to be examined.

Regardless of the intrinsic mechanism(s) employed, we have shown that a surprisingly modest suppression of reverse transcription within $CD4^+$ T cells appears to impart a dramatic effect on virus spread during *in vitro* infection. Furthermore, the fate of the T cell in response to activation can vary significantly among individuals. Analysis of the interplay of these two phenotypes on infection *in vivo* in these same animals is a vital next step in determining the significance of these findings with respect to disease progression.

5.5. Acknowledgements.

The work presented in this chapter would not have been possible without the contributions of many people. I would especially like to thank Premi Rajakumar for excellent technical advice and for helping with the real-time PCR assays. Tara Washko, a rotating graduate student, performed the sequencing analyses of the co-receptor genes, as well as developed and optimized a real-time RT-PCR assay for detection of CCR5 mRNA transcripts. Patricia Dowling gave technical advice for the Reed-Meunch assays. Todd Reinhart and Sonali Songhavi provided technical advice for the β-GUS internal standard. Albert Donnenberg provided advice and technical support for the flow cytometric assays.

CHAPTER 6

MOLECULAR DISSECTION OF ACUTE SIMIAN IMMUNODEFICIENCY VIRUS (SIV) INFECTION IN RHESUS MACAQUES WITH HIGH VERSUS LOW INTRINSIC SUSCEPTIBILITY TO VIRUS INDUCED AIDS-LIKE DISEASE.

This chapter has been modified from:

Amy L. Hartman, Premeela A. Rajakumar, Chris McMahon, Deborah Heydenburg Fuller, and Michael Murphey-Corb. 2003. "Molecular Dissection of Acute Simian Immunodeficiency Virus (SIV) Infection in Rhesus Macaques with High versus Low Intrinsic Susceptibility to Virus Induced AIDS-like Disease."

Virology (manuscript submitted)

6.1. Introduction.

Detailed, informative analysis of the events contributing to the variable rate of disease progression and length of survival of humans infected with HIV (115, 140, 152) as well as rhesus macaques infected with its simian relative, SIV (46, 93, 219), is hampered by the complexity and expense of the required studies in both humans and monkeys. A simplified *in vitro* assay (69, 141, 156, 180) that significantly correlates with disease progression after infection *in vivo* can be used to overcome this obstacle. The amount of virus produced from primary $CD4^+$ T cells obtained from uninfected monkeys and infected *in vitro* correlates significantly with the rate of disease progression and survival. Infected primary $CD4^+$ T lymphocytes that support little virus production (low producers) predict a slow disease phenotype, whereas cells that produce large amounts of virus (high producers) predict a rapid disease phenotype.

We (Chapter 5) and others (156) have recently demonstrated that suppression of virus production in low producer $CD4^+$ T cells occurs during the initial step of reverse transcription at the creation of "strong-stop" DNA. Although subsequent events did not appear to be additionally hampered, this delay was sufficient to significantly affect overall virus production and spread through the culture. Furthermore, we have shown a differential susceptibility of high and low producer $CD4^+$ cells to apoptosis induced by T cell activation (Chapter 4). Although the difference in apoptosis was apparent in uninfected $CD4^+$ T cells activated by mitogen alone, it was enhanced by virus infection. Using the same 8 animals that have been extensively characterized in our previous studies, we examined the impact of these *in vitro* findings on both virus infection and dissemination during acute infection, as well as induction of host immune responses *in vivo.*

Detailed analyses of infected cell populations during acute infection *in vivo* of 8 animals revealed a striking correlation between the rate of virus replication *in vitro* and dissemination of virus within both $CD4^+$ and $CD14^+$ cell populations *in vivo*. High producer animals had an earlier emergence of cell-associated virus in both $CD4^+$ T cells and monocytes. These events were associated with significantly more virus infected cells in the periphery overall and a higher viral load by 28 days post-infection (p.i.). Interestingly, the peak plasma virus burden was not significantly different between the two groups. Furthermore, high producer monkeys that displayed an increased rate of apoptosis *in vitro* (Chapter 4) appeared to be the most severely affected and had the highest virus loads overall. Therefore, early events affecting virus replication rate and the susceptibility of the cells to apoptosis were associated with the rate of dissemination of the virus through the host as well as possibly the induction of an adaptive immune response thereafter. This study confirms our previous *in vitro* observations and strengthens the use of our *in vitro* assay for future studies directed at the identification of specific host factors responsible for these findings.

6.2. Materials and Methods.

Animal infections and measurement of viral loads. Intra-rectal and intravenous animal infections were performed as described previously (64, 180). Plasma viral loads were determined by real-time RT-PCR with a limit of detection of 10 copies/reaction (64).

Flow cytometric analysis of peripheral blood cell populations. A whole blood staining technique was used to enumerate various cell populations within the peripheral blood. Prior to obtaining the blood sample, 3 tubes per animal were aliquoted with 5 ul of the following antibodies (clones and manufacturers are given in Table 2): 1) CD3-FITC/CD20-PE/CD14-ECD/CD45-Pe-Cy5; 2) CD29-FITC/CD4-PE/CD45RA-ECD/CD45-PeCy5; and 3) CD3-FITC/CD4-PE/-/CD8-Pe-Cy5. For each animal, 2.5 ml of whole blood was obtained in EDTA (purple-top) tubes. The tubes were mixed thoroughly and 100 ul of blood was pipetted into each tube of antibodies. The tubes were mixed and incubated for 20 minutes at room temperature (RT) in the dark. After the incubation, 600 ul BD FACSLyse solution (1:10 dilution made in water) was added to each tube. After vortexing, the tubes were incubated for 12 minutes at RT in the dark with occasional mixing. Finally, 200 ul of 4 % paraformaldehyde was added to each tube. Prior to acquisition, 100 ul of Flow-Count Fluorospheres (Coulter) were added to each tube for accurate determination of absolute numbers.

Isolation of $CD4^+$ and $CD14^+$ cells. $CD4^+$ and $CD14^+$ cell populations were isolated using the Miltenyi Biotec magnetic cell selection system. Detailed description of this protocol is given in Chapter 5. PBMC obtained from 10 ml of whole blood were incubated first with CD14 beads

and passed over 1 MS^+ column. The negative fraction was subsequently incubated with CD4 beads and again passed over 1 column. The entire $CD14^+$ fraction was pelleted and frozen for DNA isolation. For the $CD4^+$ fraction, 1/3 of the cells were pelleted and frozen for DNA isolation, while 2/3 were frozen in 800 ul trizol for RNA isolation. DNA and RNA were isolated as described in Chapter 5.

Measurement of viral cDNA and RNA transcripts. Both viral DNA and RNA transcripts were detected using real-time PCR and RT-PCR, respectively, exactly as described in Chapter 5. For measurement of viral cDNA, 500 ng of DNA from each sample was amplified in triplicate. For measurement of RNA, 200 ng of RNA from each sample was amplified in duplicate using both U5-PBS and β-GUS primers and probe.

Intracellular p27 flow cytometry. Infected cells were detected by intracellular flow cytometry using a mouse mAb to the p27 Gag protein (Advanced Biotechnologies, Columbia, MD). A detailed protocol for staining is given in Chapter 5. Cells were simultaneously stained with CD4-PE and CD29-FITC. Apoptosis was measured in $CD4^+$ cells using the PhiPhiLux-G_1D_2 caspase-3 substrate according to the manufacturer's instructions (OncoImmunin, Gaithersburg, MD). Samples were analyzed using FlowJo software (Tree Star, Inc., San Carlos, CA).

Measurement of PBMC and $CD8^+$ immune responses by ELISPOT. 96-well plates were coated with 50 ul of a rhesus INF-γ capture mAb (U-Cytech, clone MD-1) overnight at 4^oC. The plate was then washed 5 times with 150 ul of sterile PBS and blocked with 200ul of complete RPMI-10% FCS for 1-2 hrs at room temperature. $CD4^+$ T-cells were isolated from PBMCs

using Dynal CD4 selection kit according to manufacturer's protocol. The cells not attached to beads were used as CD8 cells for the ELISPOT analysis. Whole PBMC were also run in parallel. To each well, 100ul of media containing 30 ug/ml of each peptide set (Env, Gag, or Pol), irrelevant control peptide, or no peptide was added to the appropriate wells to achieve final peptide concentration of 1 ug/ml. For each stimulation condition, $4x10^5$ and $2x10^5$ cells were added to each well and incubated at 37^oC for 24 hours. The following day, the plates were washed 5 times with PBS. To each well, 50 ul of the biotinylated anti-INF-gamma Ab was added and the plates were incubated for 2 hrs at RT or overnight at 4^0C. After washing the plates 5 times with PBS, 50 ul of strepavidin-ALP conjugate (diluted 1:1000 in PBS) was added, and the plates were incubated at 1 h at room temperature. After another 5 washes with PBS, 50 ul of a chromogenic alkaline phosphatase substrate was added and allowed to incubate for 2-10 minutes or until dark spots emerge. The reaction was stopped by washing plate with tap water. The plate was allowed to air dry, and the spots were counted spots under a microscope (x40).

6.3. Results.

Using a cohort of 8 Indian rhesus monkeys (4 high producers and 4 low producers) selected on the basis of virus production *in vitro* in primary $CD4^+$ T lymphocyte cultures, we sought to determine the *in vivo* relevance of several phenotypic properties identified in these cultures: 1) the modest two-fold suppression in synthesis of strong-stop cDNA observed in low producer cells, 2) the enhanced apoptosis induced by T cell activation observed in 3 of the high producer cultures, and 3) the biphasic versus linear kinetics of infected cell spread identified in apoptotic resistant versus susceptible phenotypes, respectively. The effects of these phenotypic differences on virus spread, plasma set point, $CD8^+$ CTL responses, and $CD4^+$ T cell loss after *in vivo* infection were investigated.

Low producer animals are more refractory to mucosal infection than high producer animals. Approximately 1×10^3 tissue-culture infectious doses were delivered intra-rectally in a 2 ml total volume to each of the 8 animals. All four high producer animals and two low producer animals became infected as determined by detection of virus in plasma (Figure 38). On the other hand, the two remaining low producer animals (M12797 and M6698) appeared to be resistant to mucosal infection as determined by an inability to identify viral sequences in either plasma or PBMC by 14 days after inoculation. The resistance to infection noted in these two low producer monkeys was not surprising given the results of our previous Reed-Meunch analyses (Figure 29). Cells from these two animals required a 10-fold higher dose of virus to establish infection *in vitro* when compared to the four high producer animals. Following an intravenous inoculation with the same virus stock 21 days after the initial inoculation, these two animals were successfully infected, a finding not unexpected given that 6,000-fold less virus is required to

infect monkeys intravenously than intra-rectally (6). Values for these two intravenously inoculated animals are depicted by the dashed lines in each figure to reflect their i.v. route of infection.

Low producer animals have lower plasma virus loads than high producer animals. Plasma virus loads, as determined by an LTR-directed real-time RT-PCR assay developed in our laboratory (64), were determined three times weekly for the first two weeks post-infection (p.i.), followed by weekly for the next two weeks and monthly thereafter. As expected, by 56 days p.i. (the typical set-point in SIV-infected macaques), all 4 high producer animals had higher virus loads than their low producer counterparts (Figure 38 A), although the differences were not statistically significant due to the wide spread within each group. The amount of virus present at the first positive time point (day 5) as well as the peak virus load differed among the animals, but, surprisingly, there was no correlation to the viral set-point or the virus producer status of the animals (Figure 38 B). Thus, the immune system of all monkeys received a similar antigen "dose" during the inductive phase of the immune response. Importantly, although the plasma virus loads at 5 days p.i. were higher in the 2 low producer animals inoculated intravenously, a finding that likely reflects the higher dose given these animals, no difference was observed among all 4 low producer animals in the viral set point at 56 days p.i. This finding reinforces the concept of strong host control of virus replication during the early phase of infection within these two low producer animals.

One high producer animal, M0198, died of simian AIDS at 42 days p.i. Not surprisingly, this animal had the highest plasma virus load at the time of death. It is interesting to note that in our previous *in vitro* studies, $CD4^+$ cells from this animal required the lowest $TCID_{50}$ for

productive infection, a finding that implies that these cells were the most susceptible to infection of those analyzed. In addition, high producer animal M7699 died at 125 days post-infection, and cells from this animal were also very susceptible to infection (Figure 39). In contrast, cells from high producer animal M7799 were the most resistant to *in vitro* infection when compared to the other 3 high producer animals; this animal had the lowest viral set point among the high producer cohort (Figure 38 A). Indeed, measurement of the susceptibility of the cells from each animal to infection with SIV correlated with the viral load at 8 weeks p.i. (Figure 39).

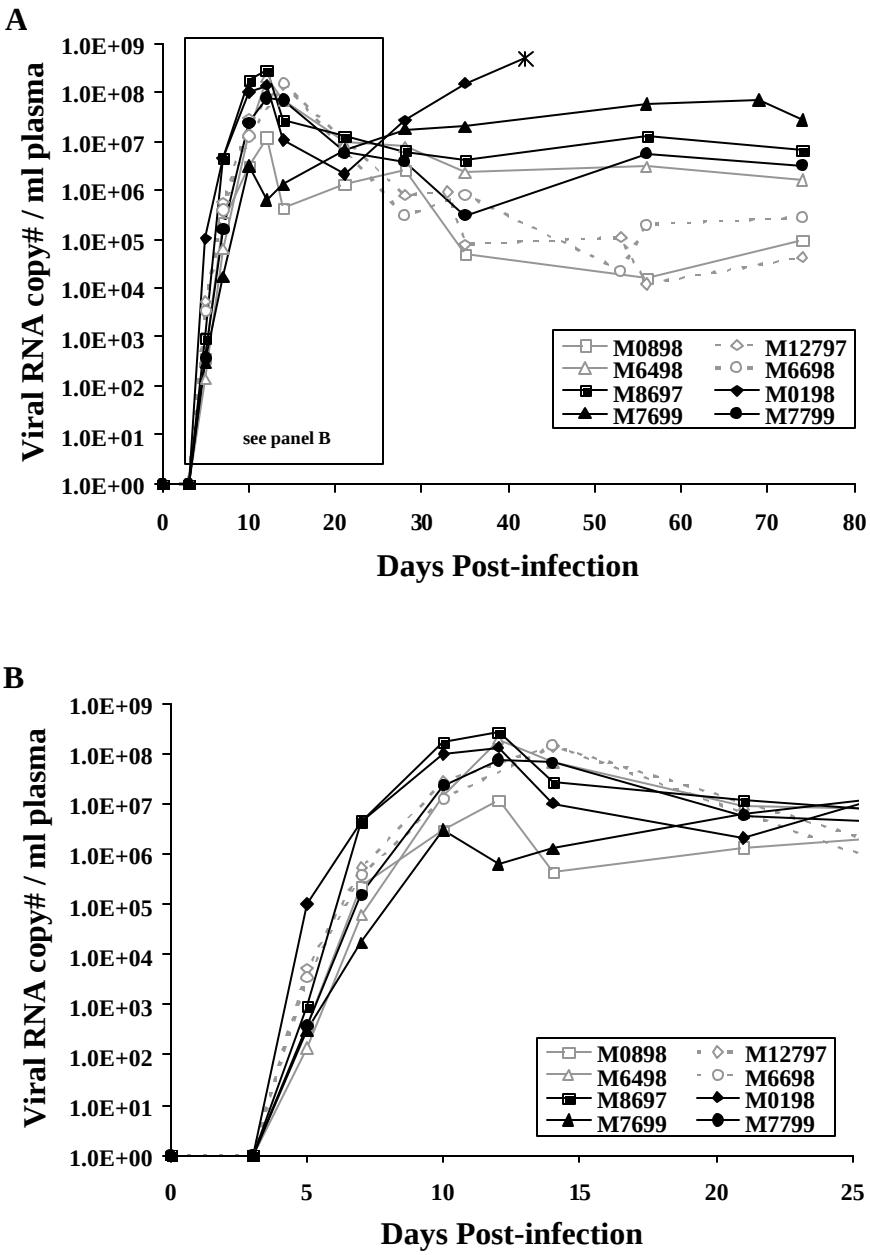

Figure 38. Low producer animals have lower plasma viral loads by 56 days post-infection.

Plasma virus loads were measured by real-time RT-PCR at various time points after infection with $SIV_{DeltaB670}$. (A) Virus loads through the first 11 weeks of infection; (B) Virus loads through 21 days of infection. High producers are shown in the black lines and low producers are shown in the gray lines. The two low producers that were re-infected i.v. (M12797 and M6698) are shown in the gray dotted lines. The "x" symbol at day 42 post-infection for animal M0198 indicates death from simian AIDS.

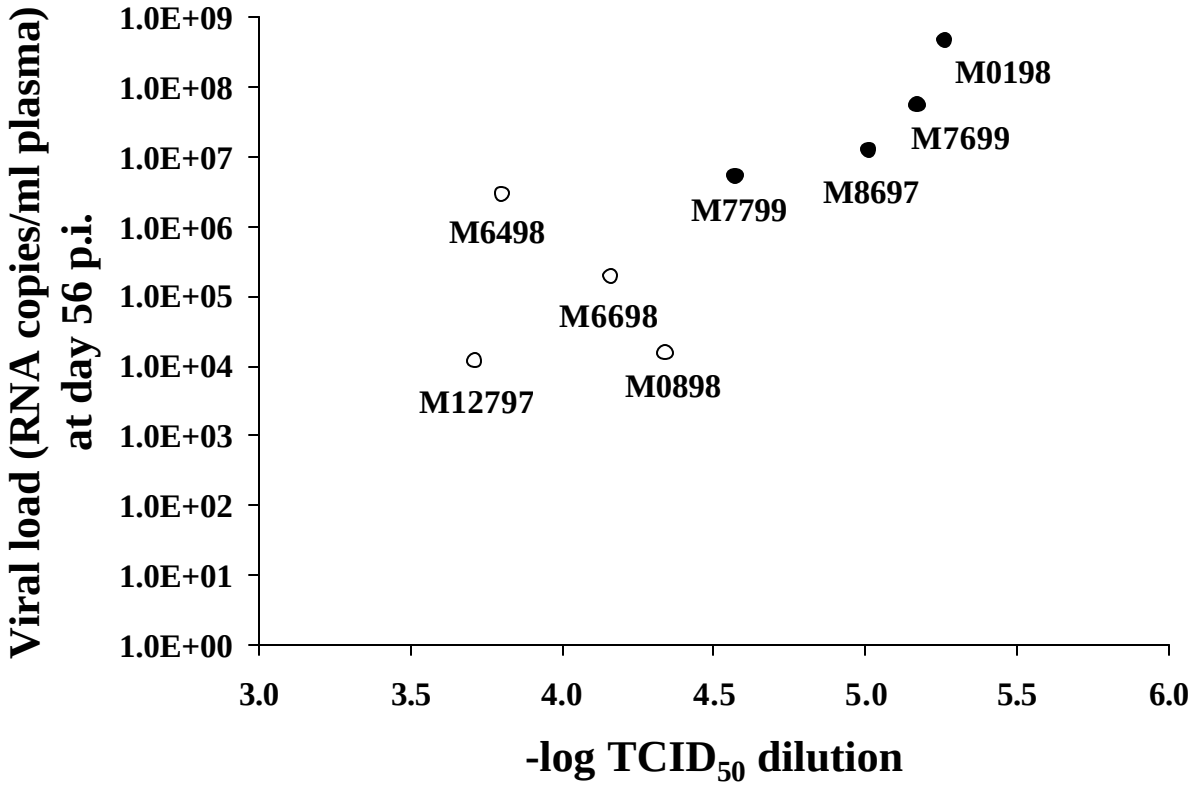

Figure 39. Correlation between the susceptibility of cells to infection *in vitro* and viral load during the set-point.

The log $TCID_{50}$ dilution, or the amount of virus required to infect cells as determined by *gag* PCR at 14 days p.i. (Figure 29), was plotted versus the viral load at 56 days post-infection. The low producers are shown in the open circles and the high producers are shown in the closed circles. For animal M0198, the viral load at time of necropsy (42 days p.i.) is shown.

Low producer animals have a less severe decline in memory $CD4^+$ T cells in the peripheral blood. $CD4^+$ T cell loss is a hallmark of AIDS in both HIV-1-infected humans and SIV-infected macaques. An early, selective decline in the memory subset of $CD4^+$ lymphocytes identified by dual expression of CD4 and CD29 is also highly predictive of rapid disease induced by $SIV_{DeltaB670}$ infection (123-125, 201). To determine the response of these cell populations to virus infection in the animals studied here, peripheral blood mononuclear cells were evaluated by flow cytometry throughout the course of infection using a whole blood staining method (Figure 40). As expected, no animals were lymphopenic during the observation period of this study, and no difference in absolute $CD4^+$ T cell counts was observed in high and low producer animals during the first 3 months p.i. (Figure 40 A). However, high producer animals showed a significantly greater decline in the percentage of $CD4^+$ cells expressing the memory cell marker CD29 by 8 weeks post-infection than low producer animals (Figure 40 B; $P = 0.002$; t-test based on change in percentage from 0 days to 56 days p.i.). Despite the sharp decrease in the absolute number of $CD4^+$ cells observed in low producer monkey M12797 (Figure 40 A), this animal retained a significant percentage of the $CD29^+$ population by 56 days p.i. onward (Figure 40 B). Supporting the results of others (123), this finding suggests that a better maintenance of memory $CD4^+$ T cells may be associated with a slower disease progression. Tracking of other cell populations as well as absolute cell numbers for these populations can be found in Appendix E, Figures 54 and 55.

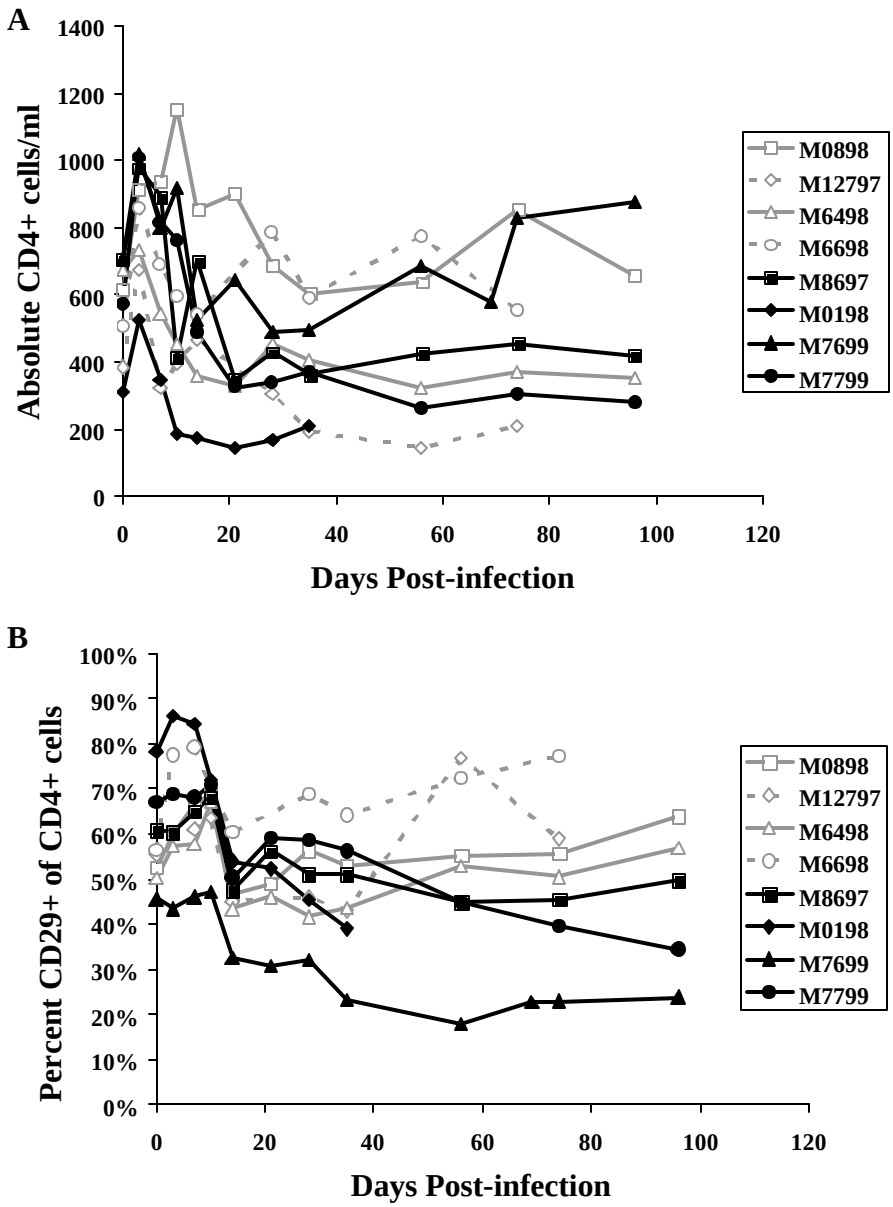

Figure 40. Low producer animals have a slower decline in the percentage memory CD4$^+$ T cells.

Whole blood staining was used to determine (A) the absolute number of CD4$^+$ cells per ml of peripheral blood, and (B) the percentage of CD4$^+$ cells expressing the memory cell marker CD29. High producers are shown in the black lines with closed symbols and low producers are shown in the gray lines with open symbols. The two low producers that were re-infected i.v. (M12797 and M6698) are shown in the gray dotted lines. In (B), a t-test was used to determine the significance of the change in percentage of CD29-expressing CD4+ cells from 0 days to 56 days p.i. (*P = 0.002).

Detection of viral sequences in $CD4^+$ T cells and $CD14^+$ monocytes is both delayed and maintained at lower levels in low producer animals. $SIV_{DeltaB670}$ is a CD4-independent, CCR5-utilizing primary isolate that is dual tropic and therefore efficiently infects both $CD4^+$ T cells and monocytes (50, 169). To determine whether the modest difference in virus replication observed *in vitro* between high and low producer cells affects the dissemination of the virus within these two target cell populations *in vivo*, viral sequences were quantified in both cell types during acute infection. While $CD4^+$ cells are generally thought of as the main target of lentiviruses such as HIV-1 and SIV, infection of the monocyte population was also of interest because infection of these cells can potentially affect the subsequent development of an effective immune response by impairing antigen presentation and macrophage effector functions (89).

At various intervals after infection of the animals, $CD4^+$ T cells and $CD14^+$ monocytes were positively selected from freshly isolated PBMC. To detect and accurately quantify infected cells, the number of viral DNA copies within both cell populations was measured using real-time PCR. The primers and probe used for this assay were within the U5 region of the LTR and the primer binding site (PBS), a combination that detects only full-length viral double-stranded DNA (216). In addition, using the same primers and probe, real-time RT-PCR was used to measure the number of viral RNA copies within $CD4^+$ cells to determine the level of productive infection in these cells. This pair of primers and probe will detect all forms of viral RNA transcripts, including spliced mRNA and full-length genomic RNA (216).

The emergence of detectable viral DNA sequences in $CD4^+$ T cells of all 4 low producer animals occurred on day 10 p.i., while emergence in 2 of the high producers (M0198 and M8697) occurred 3 days earlier, at day 7 p.i. (Figure 41 A). Strikingly, all 4 high producer animals, regardless of the day at which viral sequences were first detectable, had significantly

more viral DNA copies at day 10 p.i. ($P = 0.03$; t-test) than the 4 low producer animals. Indeed, the high producer animals had more viral DNA copies at nearly all time points examined, and the difference between the two groups approached significance by day 35 p.i. ($P = 0.12$; t-test). Thus, the low producer animals not only had a significant delay in the initial spread of virus throughout CD4+ cells of the peripheral blood, but they also maintained a lower level of infection of these cells during the set-point.

Quantification of cell-associated viral RNA within $CD4^+$ cells yielded similar results, with high producer animals having significantly more viral RNA copies present within these cells by day 35 p.i. (Figure 41 B; $P = 0.02$; t-test), indicating that the differences in viral DNA copy number may have resulted in differences in viral RNA synthesis, as suggested by our *in vitro* studies. The differences observed in the number of infected cells, both at the DNA and RNA levels, persisted throughout the acute phase as well as during the viral set-point. In addition, the number of infected cells over the course of infection followed a very similar pattern as the viral load (Figure 38), with a peak in the number of viral sequences detected at 10 – 14 days p.i. Interestingly, while there were no differences in the peak plasma virus loads, there were significant differences in the peak number of infected cells in the peripheral blood as determined by real-time PCR at these same time points (Figure 41). Taken together, these studies suggest that the number of infected cells and the timing of their emergence may be more predictive of the eventual viral set-point than the peak viral load during the acute phase.

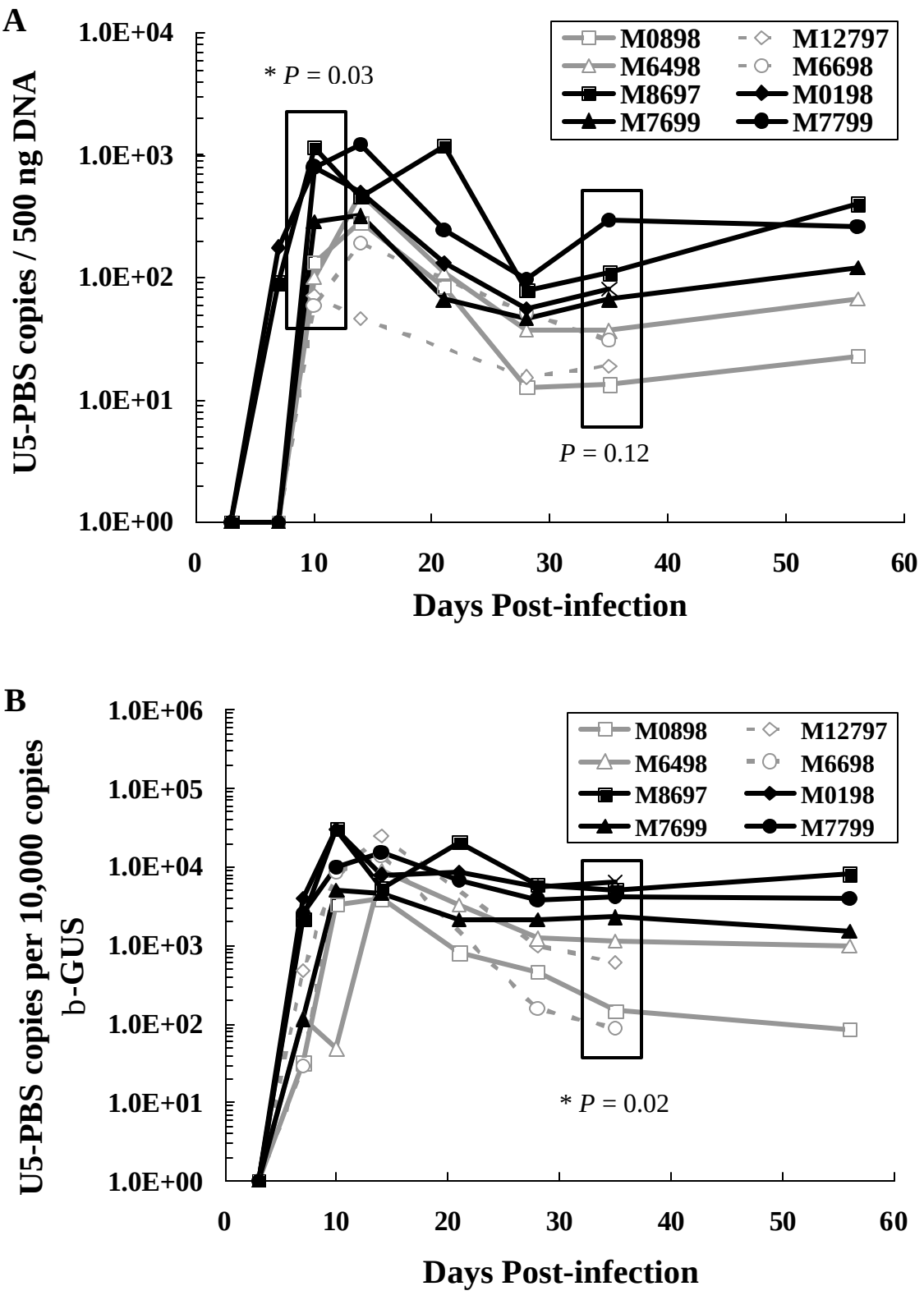

Figure 41. Legend on next page.

Figure 41. The emergence of viral sequences within CD4$^+$ T cells is delayed and decreased in low producer animals.

(previous page) CD4$^+$ T cells were isolated from PBMC during infection *in vivo.* (A) Viral DNA sequences were detected by real-time PCR using primers and probe within the PBS and U5 regions of the viral genome, which detects fully reverse transcribed viral DNA. (B) Viral RNA sequences were detected by real-time RT-PCR using primers and probe within the PBS and U5 regions of the viral genome, which detects all viral RNA species. High producers are shown in the black lines with closed symbols and low producers are shown in the gray lines with open symbols. The two low producers that were re-infected i.v. (M12797 and M6698) are shown in the gray dotted lines. Statistical significance, as determined by a t-test, is indicated by an asterisk (*) followed by the corresponding *P*-value.

When viral DNA copies were quantified within $CD14^+$ cells, similar findings were observed (Figure 42). The emergence of viral sequences within $CD14^+$ cells on day 10 was significantly delayed ($P = 0.03$) and decreased at nearly all time points in low producer animals. Despite this delay, the i.v. infected low producer animals (M12797 and M6698) had a higher viral DNA copy number at 14 days post-infection than the intra-rectally infected low producer animals. This finding may be due to the higher dose given these animals directly into the bloodstream where these cells reside. However, despite this advantage, the copy number within the cells from these two animals still declined to levels below that of the high producers. By 28 days p.i., the number of infected $CD14^+$ cells in low producer animals was below the detectable limit of the real-time PCR assay (10 copies/reaction). In contrast, infected $CD14^+$ cells remained detectable in all of the high producer animals through 8 weeks p.i.

The finding that the emergence of virus as well as its spread was significantly diminished in low producer animals is particularly striking given the small number of animals used in each group. These findings are reminiscent of our earlier observations during the very first rounds of infection *in vitro*, implying that very early events may have a significant impact on virus dissemination *in vivo.* In addition, the number of viral sequences detected in low producer animals remained below that of the high producer animals through the first 8 weeks of infection, a finding that further emphasizes the significant delay in viral spread.

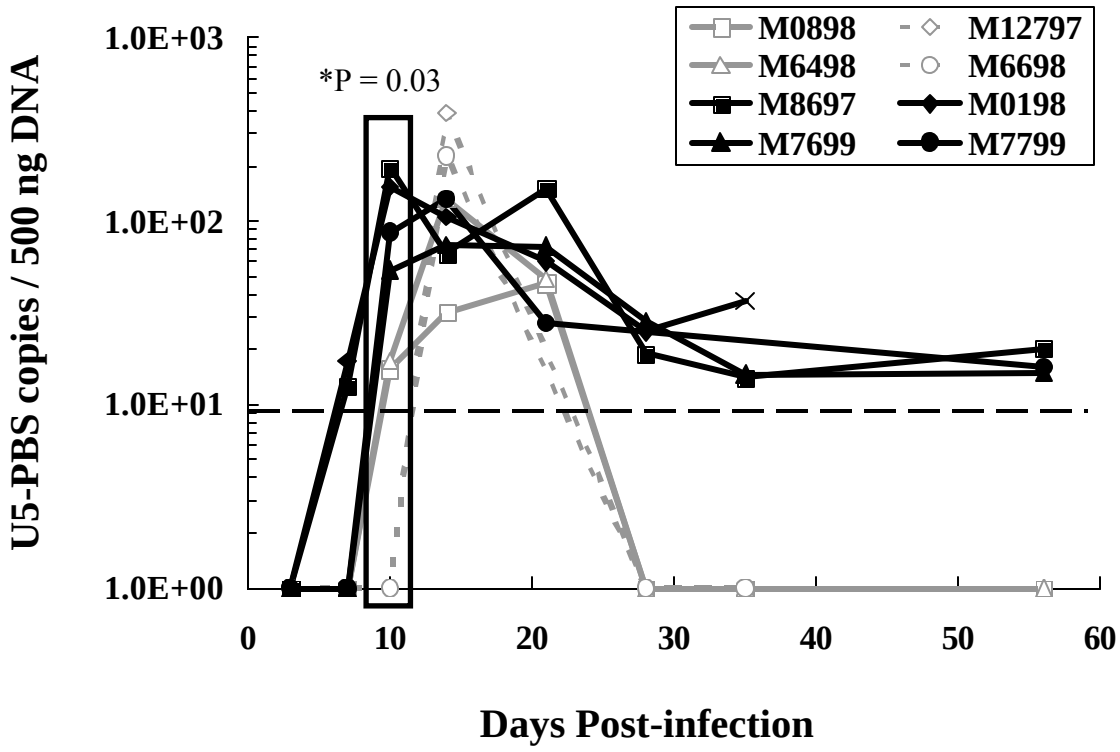

Figure 42. The emergence of viral sequences within CD14$^+$ monocytes is delayed and decreased in low producer animals.

During infection *in vivo*, CD14$^+$ cells were isolated from PBMC and viral DNA sequences were detected by real-time PCR using primers and probe within the PBS and U5 regions as described above. High producers are shown in the black lines with closed symbols and low producers are shown in the gray lines with open symbols. The two low producers that were re-infected i.v. (M12797 and M6698) are shown in the gray dotted lines. The limit of detection of the real-time RT-PCR assay (10 copies/reaction) is indicated by the horizontal dashed black line. There was a significant delay in the emergence of viral DNA sequences at 10 days p.i. (*P = 0.03; t-test)

The emergence of productively infected cells within the peripheral blood is delayed in low producer animals. During our *in vitro* studies, enumeration of productively infected cells by intracellular p27 flow cytometry was highly informative in elucidating the kinetics of the dissemination of infected cells in the culture (Chapter 5). Since a detailed analysis of viral infection during acute infection of monkeys has never been reported using this method, we monitored p27-expressing cells in the peripheral blood of these animals throughout the first 8 weeks of infection (Figure 43). Interestingly, no p27-expressing cells were detected within the first 7 days post-infection in any animal even though significant plasma virus loads had been achieved by this time. By day 10, however, productively infected $CD4^+$ cells were readily detectable in three of the high producer animals (Figure 43 A), and peak percentages were achieved in two of these by this day. A peak percentage of infected cells was not achieved in the third animal (monkey M7799) until 4 days later, a time at which infected cells emerged in low producer animals. Interestingly, unlike the other high producer animals, cells from animal M7799 had a biphasic, rather than a linear dissemination of virus following *in vitro* infection (Chapter 5). Cells expressing p27 were detectable in all 4 low producer animals on day 14, which was 4 days later than most of the high producer animals. The high producer that had the highest plasma virus load and died rapidly after infection had only nominal numbers of infected cells in the periphery. Although the significance of this observation is unknown at present, it may reflect a combination of extremely high virus production and rapid turnover of infected cells associated with the increased susceptibility to apoptosis (Chapter 4). In both groups, a significant decline in infected cells was observed by 21 days p.i. that resulted in nearly undetectable infected cells by 35 days p.i. The two i.v. inoculated low producer animals had a higher percentage of infected cells than the other animals most likely because they received a

higher dose. Interestingly, however, despite the greater infectious dose used to infect these animals, the peak in the number of infected cells was still delayed as compared to the high producer animals. In summary, low producers appeared to have a significant delay in the dissemination of virus infected cells as measured by viral DNA, RNA, and protein levels than their high producer counterparts.

The selective loss of the $CD4^+CD29^+$ memory cell population observed in high producer animals (Figure 40 B), could be explained by preferential infection of this cell population in these animals when compared to their low producer counterparts. To determine whether this is indeed true, we selectively analyzed the $CD4^+CD29^+$ population for p27 protein expression (Figure 43 B). No difference in the pattern of infection was observed between total $CD4^+$ lymphocytes and the $CD29^+$ subset of these cells. The 3-day delay in infected low producer cells was seen in both cell populations. Thus, the selective loss of the $CD4^+CD29^+$ population in high producer animals does not appear to be due to a preferential infection of this cell type but, rather, may more likely reflect the more rapid expansion of virus *per se* observed in the high producer animals.

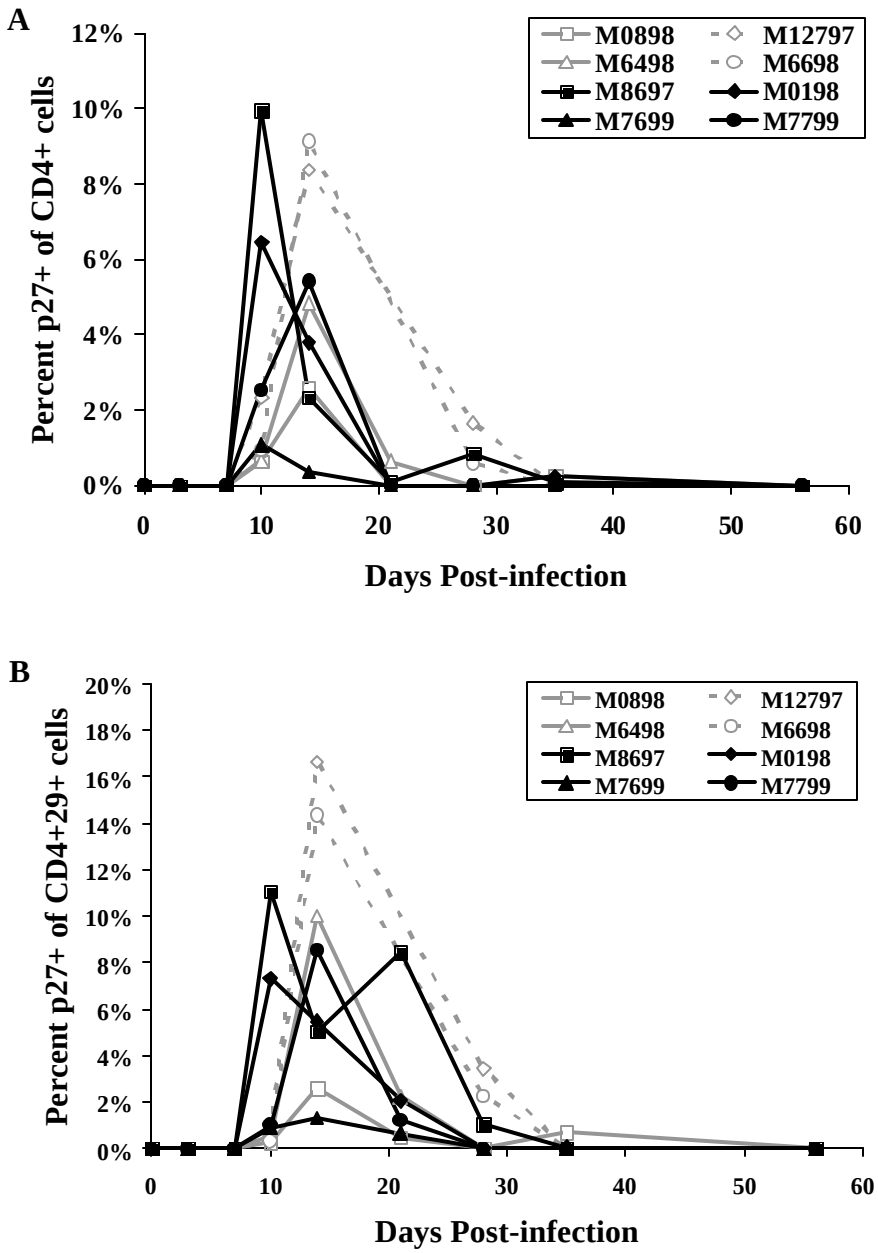

Figure 43. The emergence of p27 antigen-positive cells is delayed by 3-4 days in low producer animals.

$CD4^+$ T cells expressing p27 were detected using intracellular flow cytometry. (A) Total $CD4^+$ cells expressing p27, and (B) $CD4^+CD29^+$ memory cells expressing p27. High producers are shown in the black lines with closed symbols and low producers are shown in the gray lines with open symbols. The two low producers that were re-infected i.v. (M12797 and M6698) are shown in the gray dotted lines.

The delay in virus dissemination in low producer animals is associated with the development of a stronger T cell-mediated immune response. Infection of both $CD4^+$ T cells and $CD14^+$ monocytes can adversely affect the development of an appropriate and effective immune response (18, 89, 176). To determine whether the more rapid dissemination of virus observed in high producer animals was associated with an impaired induction of SIV-specific T cell responses, PBMC and $CD8^+$ T cell IFN-γ ELISPOT analyses were conducted using peptide pools representing *gag*, *pol*, and *env* regions of the viral genome. Assays were performed prior to infection, and at 2 and 4 weeks p.i. (Figure 44). Despite having only 4 animals per group, examination of the total responses to all peptides revealed that low producer animals tended to respond more rapidly (2 weeks p.i.) and mount more robust T cell responses (4 weeks p.i.) than the high producer animals. These results were evident in both whole PBMC and purified $CD8^+$ cells and approached statistical significance (Figure 44 A and B; t-test; $P = 0.14$ and $P = 0.13$, respectively, based responses to all peptide pools). High producer animal M0198, which died at 42 days p.i., had the poorest response at all time points. This result is consistent with this animal being a true rapid progressor, which characteristically respond to infection with very high viral loads concomitant with little or undetectable virus-specific immune responses (18, 49, 57, 134, 211).

The breadth of the ELISPOT responses also appeared to be greater in low producer animals. A breakdown of the responses to the Gag, Pol, and Env peptides revealed that while all animals had responses to Gag, Pol responses were predominantly found in the low producer animals, in which there was a trend toward significance (t-test; $P = 0.14$ and $P = 0.19$, respectively, for PBMC and $CD8^+$ cell responses to Pol only). The slower kinetics of virus spread may have permitted immune recognition of a wider repertoire of antigens which may

have, in turn, enabled a greater control of virus replication. Regardless of the mechanism, these data suggest that the apparent retardation of virus dissemination in the low producer animals was associated with the development of a stronger cell-mediated immune response, which could have, in turn, reduced the virus burden at the viral set point (Figure 38 A).

Figure 44. Low producer animals have stronger virus-specific cellular immune responses than high producer animals.

(following page) IFN-γ ELISPOT analysis of (A) whole PBMC, and (B) $CD8^+$ cells at 0, 2, and 4 weeks post-infection. Pools containing peptides from the *gag*, *pol*, and *env* regions of the viral genome were used to differentiate the virus-specific responses. Data are expressed as spot-forming-units (SFU) per 1 x 10^6 cells. T-tests were used to determine significance between the two groups for total and *pol*-specific responses at 4 weeks p.i., and the *P*-values are indicated in the text.

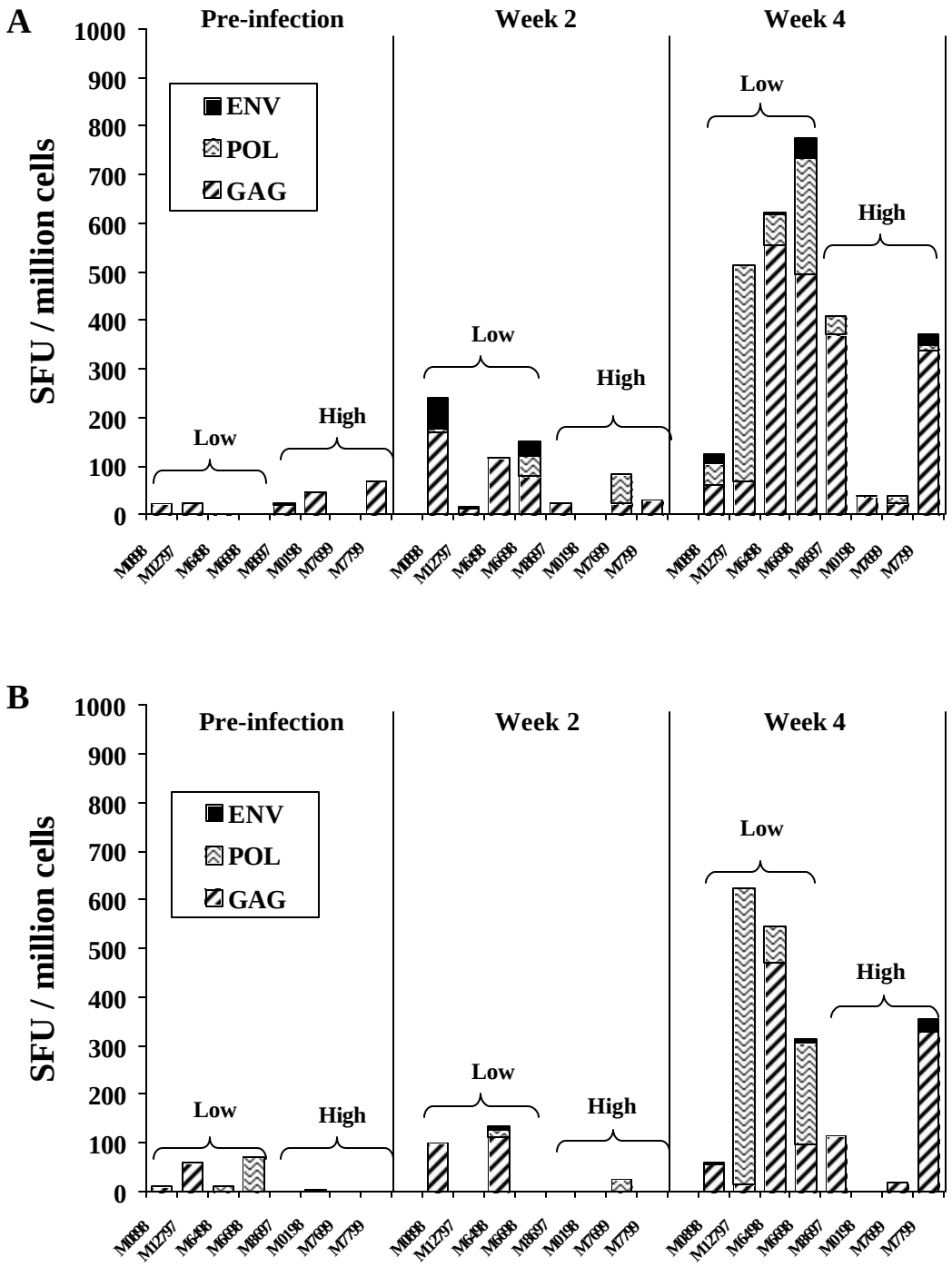

Figure 44. Legend on previous page.

Detection of apoptotic cells in the peripheral blood reveals no differences between high and low producer animals. During virus infection *in vitro*, high producer $CD4^+$ T cells underwent significantly more caspase-3-mediated apoptosis than their low producer counterparts (Figure 19). Interestingly, this finding was also true in mock-infected, mitogen-stimulated cultures, indicating that cell activation alone was enough to induce differences in apoptosis. In an attempt to evaluate this finding during infection *in vivo*, PBMC were harvested at intervals post-infection and incubated with the fluorescent caspase-3 substrate, Phiphilux. In most of the animals, there was a peak in Phiphilux staining in $CD4^+$ T cells at day 7 p.i. (Figure 45 A), which coincided with the rise in viral loads during acute infection (Figure 38). Interestingly, a similar peak in apoptosis was seen in $CD8^+$ T cells at this time (Figure 45 B). However, there were no apparent differences between the two groups of animals. In hindsight, these results may be due to technical artifacts because Phiphilux may not have been the most appropriate and effective method to measure apoptosis *in vivo*. Cells stained with Phiphilux must be analyzed within 1 hour of staining. Due to constraints by other experiments going on at the same time, the time between isolation of the cells from the animals and staining for Phiphilux was variable, and often as long as 10 – 12 hours. During this time, the cells were placed in culture media in an incubator. However, the cells may have been adversely affected during this time period, and therefore the measurement of apoptosis in this manner may not be an accurate reflection of true events within the animal. An assay that permits staining and fixing of cells immediately after isolation would be more appropriate. Further analysis of this finding is required to obtain conclusive results.

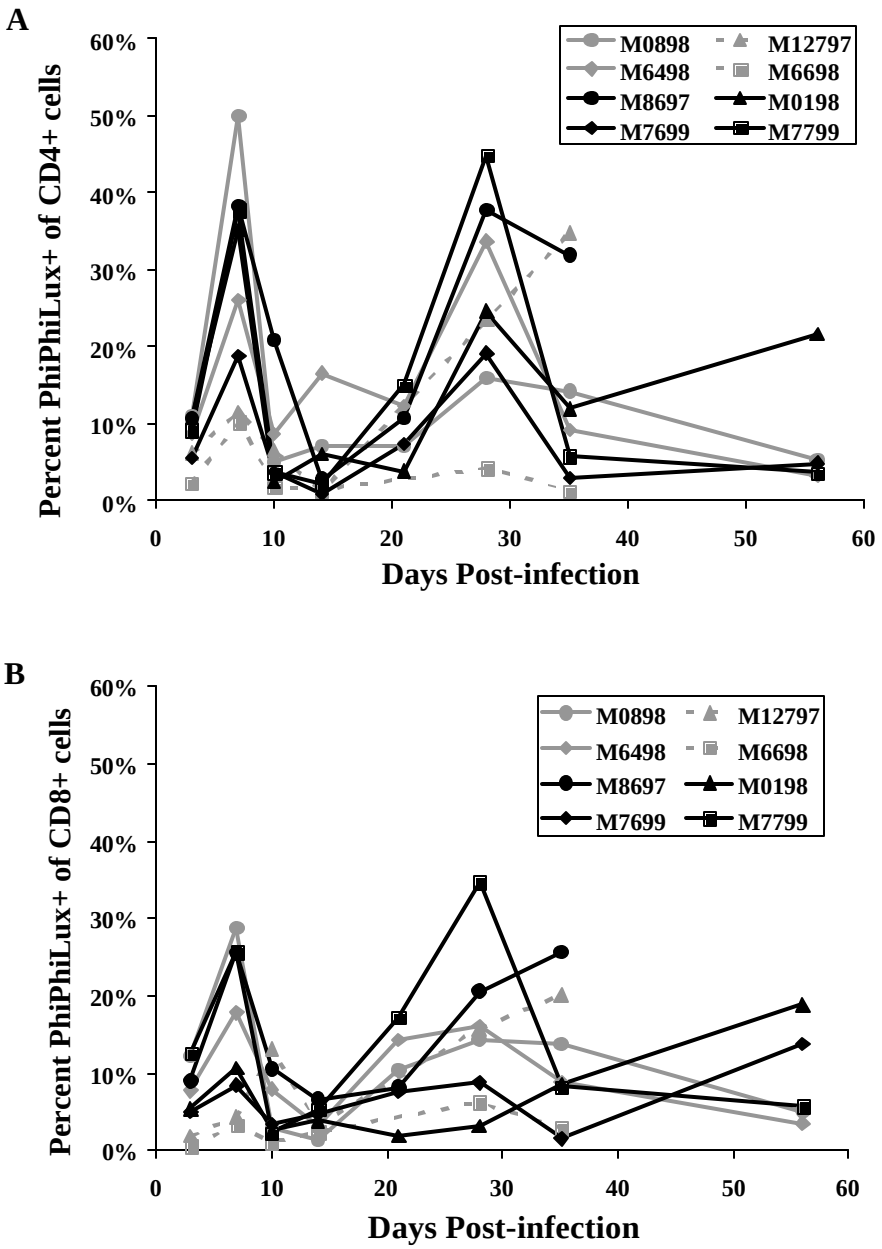

Figure 45. No apparent differences in apoptosis of $CD4^+$ T cells during *in vivo* infection.

At intervals post-infection, PBMC were incubated with the caspase-3 substrate, Phiphilux, and stained for CD4 and CD8. (A) the percentage of $CD4^+$ cells positive for Phiphilux; (B) the percentage of $CD8^+$ cells positive for Phiphilux. High producers are shown in the black lines and low producers are shown in the gray lines. The two low producers that were re-infected i.v. (M12797 and M6698) are shown in the gray dotted lines.

6.4. Discussion.

The viral set-point, the rate of progression to AIDS, and survival of SIV-infected monkeys can be predicted by both the amount of virus required to initiate a productive infection (69, 156) and the amount of virus produced thereafter from primary $CD4^+$ T lymphocytes infected *in vitro* (141, 180). T lymphocytes from low producer animals require 1 (Chapter 5) to 3 logs (69) more input virus to become productively infected than their high producer counterparts. A partial block at the initial step of reverse transcription (Chapter 5) (156) appears to be responsible for this observation. This difference is modest, however, and is associated with only a 2-fold reduction in viral DNA copy number. Later steps in reverse transcription and viral mRNA synthesis do not appear to be additionally affected.

Differential suppression of reverse transcription is not the only difference observed in monkey primary lymphocyte cultures, however. In our study, 3 of 4 high producer lymphocyte cultures were also significantly more susceptible to apoptosis after mitogen activation both in the presence of absence of viral infection (Chapter 4). These cultures had a rapid, linear increase in virus infected cells. In contrast, in low producer cultures, which undergo little apoptosis, virus spread was biphasic, with an initial gradual increase in the number of infected cells that then increased dramatically after 7 days.

This study was designed to determine the potential impact of these *in vitro* properties on the acute phase of infection *in vivo*, as well as the role that these events may play in the induction of virus-specific immunity and subsequent disease progression. Intra-rectal inoculation of the 8 previously-characterized animals (4 high producers and 4 low producers) resulted in 6 successful infections. Not surprisingly, two low producers were resistant to mucosal infection, as suggested by our Reed-Meunch data and the anecdotal study of a monkey that resisted mucosal infection

described by others (156). These results correlated well with our previous observation wherein cells from these two animals required a significantly higher dose of virus to establish infection *in vitro* relative to the high producer animals. Subsequently, these two animals were inoculated intravenously with a higher dose of virus and became persistently infected.

As predicted by previous reports (113, 180), the four high producer animals had higher viral loads by 56 days post-infection, with one animal dying as early as 6 weeks post-infection. $CD4^+$ T cells from this animal had the lowest *in vitro* $TCID_{50}$ of all animals, a finding that effectively predicted that this animal would have the most rapid disease progression. The four high producer animals also had a significantly more rapid decline in $CD4^+$ $CD29^+$ memory cells, a finding that has been documented as a hallmark of rapid progressors infected with $SIV_{DeltaB670}$ (123-125).

Quantification of virus-infected $CD4^+$ T cells and $CD14^+$ monocytes in the peripheral circulation harboring SIV DNA, RNA, and protein during acute infection using highly quantitative, unique methodology not only provided additional insight into the nature of virus dissemination in the host, but also revealed newer predictors of disease progression. Not surprisingly, there was a significant delay in the emergence of $CD4^+$ T cells containing SIV DNA and RNA in low producer animals. Low producer animals also had lower numbers of both cell-associated viral RNA and DNA than that seen in high producer animals at all time points examined.

The number of infected cells over the course of infection followed a very similar pattern as the viral load, with a peak in the number of cell-associated viral sequences detected at 10 – 14 days p.i. It was somewhat puzzling, however, that even though there were clearly significant differences in the number of infected cells at both this time point and the set point later on, no

differences in peak plasma virus load were detected. While some studies have shown that the viral load 7 days p.i. is predictive of the viral set point (113), our study suggests that the number of infected cells, rather than the viral load, during acute infection may be a more accurate indicator of the eventual set-point. Because DNA samples are more easily stored than cryopreserved plasma, this finding may provide a more accurate and manageable predictor of the viral set-point and hence disease progression.

The appearance of viral DNA sequences in $CD14^+$ monocytes mirrored that observed in $CD4^+$ T cells, with low producers exhibiting a 4-day delay in the detection of viral sequences within these cells. Quantitatively, the viral DNA copy number also remained lower than that observed in high producer animals at all time points. Strikingly, viral DNA sequences were undetectable in low producer CD14+ cells by 28 days p.i., while they remained detectable in high producer animals throughout the time points examined. If hit early and hard by virus infection, monocytes may be unable to fulfill the critical function of antigen presentation during the inductive phase of the immune response. Once the function of these infected macrophages is disrupted, antigen presentation, cytokine secretion, phagocytosis, and intracellular killing could all be impaired, thus preventing the development of a strong immune response (89). Infected $CD14^+$ cells also traffic to lymph nodes where they provide a conduit for dissemination of virus to the large number of susceptible $CD4^+$ T cells harbored by these organs (89). Evidence that this may have occurred is suggested by the significantly impaired virus-specific T cell responses in high producer animals. Strong immune responses, both T cell and antibody-mediated, are critical in curtailing the initial burst of viral replication and establishing the set point (18, 98, 167, 176).

The 3-day delay in infection of $CD4^+$ and $CD14^+$ cells in low producer animals is reflected in a similar delay in detection of p27-expressing $CD4^+$ cells by flow cytometry. The peak of p27-expressing cells occurred at day 10 in high producer animals and at day 14 in low producer animals. Even the two animals that were re-infected intravenously with a higher dose of virus had a delayed peak in p27 expression. While we were able to detect productively-infected cells by this method only from days 10 to 28 post-infection, differential detection of viral DNA sequences in both $CD4^+$ and $CD14^+$ cells persisted beyond the acute phase of infection, suggesting that both of these cell populations are potential reservoirs for virus infection.

The failure to detect a difference in peak viral loads between the high and low producer animals described in this report may be explained by our finding that high producer cells are more susceptible to apoptosis *in vitro*. Apoptosis can potentially have both beneficial and detrimental effects on virus replication (77), and both HIV-1 and SIV encode pro- and anti-apoptotic genes. The regulation of this mode of cell death by retroviruses is highly complex. The high virus replication *in vitro* observed in three of the high producer animals in this report was associated with increased susceptibility to apoptosis, thereby suggesting that apoptosis in these cells is beneficial to virus replication, at least *in vitro*. However, *in vivo*, during acute infection, massive virus replication and dissemination is taking place, which is known in some individuals to induce a primary acute syndrome (31, 40, 58). The rapid and robust virus replication, coupled with the enhanced susceptibility to apoptosis (of both infected and uninfected activated bystander cells), observed in these animals may actually limit the number of available target cells in high producers to a point where low producers, due to their resistance to activated cell death, may "catch up". Thus, the difference between the two groups during acute

infection may not be the amount of virus *per se*, but the speed with which the virus-infected cell disseminates in the host. After the chaos of the acute phase dwindles, the true differences between the two groups could then be seen as a relative difference in SIV-specific T cell responses associated with control of virus burden. Evidence to support this comes from high producer animal M7799, whose profile of apoptosis paralleled that of the low producers *in vitro*, had the lowest viral load, and appeared to be the least affected by SIV infection out of this group.

While the amount of virus produced after infection of cells *in vitro* is an accurate predictor of survival (180), there is not an absolute correlation. Other factors, such as susceptibility to apoptosis, can modulate this effect. Therefore, while *in vitro* virus production alone would have predicted animal M7799 to be a true rapid progressor, the phenotype of this animal was more intermediate, potentially due to the decreased susceptibility of the cells to apoptosis as compared to the other high producer animals. Clearly, *in vitro* virus production and susceptibility to apoptosis work in concert, and their combined effect may ultimately influence the outcome of an infection. An understanding of the interplay between these events will enable a more in-depth comprehension of events leading to rapid or slow disease onset.

In summary, this study provides compelling evidence that a modest decrease in reverse transcription within $CD4^+$ T cells, coupled with an intrinsic resistance to mitogen-induced apoptosis, may result not only in decreased viral spread throughout an *in vitro* culture, but also may have a direct impact on dissemination of infected cells as well as the virus burden in the infected host. Although it is known that early events can control the development of a strong, effective immune response required to control virus replication during the chronic phase of infection (18, 98, 167, 176), it is surprising that relatively subtle differences in the rate of virus spread appear to have such a profound impact on this process. Such data provide encouragement

for the development of prophylactic vaccines that, despite their inability to provide sterilizing protection, can effectively dampen virus replication during acute infection. The exact host factor(s) responsible for these events are under investigation. This study highlights the usefulness of our *in vitro* assay in the analysis of host factor(s) critical to understanding the pathogenesis of SIV-induced disease and for the development of potential new therapies and vaccines to combat HIV-1-infection in humans.

6.5. Acknowledgements.

I would like to acknowledge the many contributions that others have made with regards to the data presented within this chapter. Specifically, Premi Rajakumar provided the real-time PCR analysis, including viral loads. Chris McMahon and Deborah Fuller at Powderject Vaccines, Inc. in Madison, Wisconsin performed the ELISPOT analyses. Afrouz Bazmi helped with flow cytometric analysis, as well as with the processing of blood samples. Dawn McClemens-McBride coordinated the entire animal study. Stephanie Casino, Holly Warnock, Dave Meleason, and Anita Trichel took exceptional care of the animals during and prior to this study.

CHAPTER 7

DISCUSSION

In the past 20 years, the AIDS epidemic has exploded across the continent of Africa and is now rapidly descending upon Asia. Countries that were already struggling with poverty and famine are now decimated by this disease. Even though HIV-1 infection is completely preventable through limiting body fluid exchange, vaccines and therapies to prevent and eliminate the infection, respectively, are still necessary.

Study of the immunology and virology behind this disease has taught scientists an incredible amount about the human immune system and its response to viral pathogens. The complex interaction of HIV-1 with the immune system, particularly the fact that the virus infects immune cells, poses enormous scientific problems for eradicating the infection. A greater understanding of the host-virus interactions is essential for the development of novel vaccines and therapies.

In particular, the genetic makeup of the host plays a significant role in the outcome of human infection with HIV-1 (126, 133, 148, 171). The identification of a number of host genes and their role in controlling disease progression has been extremely valuable for understanding the complex interplay between host and virus. In addition, both human and monkey studies have revealed that not all individuals respond identically to a particular vaccine, and protection has yet to be demonstrated to be universal for any given vaccine candidate (106). In fact, the design of some newer vaccine candidates takes the particular genetic makeup of the host into account, such as the major histocompatibility complex (HLA) (13, 138), indicating that researchers now have a greater appreciation of the impact of host genetics on disease outcome.

In contrast to human studies, SIV-infected rhesus monkeys enable a more detailed analysis of lentiviral infection, particularly during the early events which are difficult to monitor in humans. Extensive analysis of virus replication during the acute phase of SIV infection has

provided insight into early immunological and virological events and their influence on disease outcome (112, 113, 209). Despite the usefulness of the SIV-infected macaque model, many questions remain unanswered due to the complexity of *in vivo* monkey studies. The studies described in this dissertation provide a solid framework for identification of host genes that control disease progression and survival using a simplified *in vitro* setting. In addition, we provide evidence to suggest that extremely early events may shape the outcome of an infection, a finding which underscores the importance of host factors in these processes.

A simplified way to predict disease progression profiles based on virus replication within primary CD4$^+$ T cell cultures. In a survey of rhesus monkeys infected intravenously with the primary virulent isolate $SIV_{DeltaB670}$, the ability of virus to replicate in a naïve animal's PBMC or CD4$^+$ T cells following *in vitro* infection was highly predictive of disease progression and survival *in vivo* following experimental inoculation. Monkeys whose cells were high producers of SIV following an *in vitro* infection were significantly more likely to develop simian AIDS sooner and die more quickly than those animals whose cells supported little virus replication. This relationship was particularly intriguing in view of the likelihood that *in vitro* control of virus did not involve virus-specific immunity. As expected in an out bred group of animals, there was a continuum of virus production and survival that spanned high virus production/early death to low virus production/long-term survival.

These findings, together with that of others (69, 113, 156), clearly identify an innate property of individual macaques that controls virus replication both *in vitro* and *in vivo*. The intrinsic ability of macaque PBMC to support the replication of SIV *in vitro* may be analogous to the differences in replicative capacity observed for human PBMC infected *in vitro* with HIV-1

(151, 190, 210). In HIV-1-infected humans, a variable length of time from infection to death is also seen that is similar to SIV-infected monkeys (22, 27, 112, 134, 139, 152). Therefore, the data reported here are highly relevant to the pathogenesis of HIV-1, fulfilling an important goal of research in the field of primate lentiviruses. The simple *in vitro* assay described here should enable the identification of specific host gene(s) responsible for this phenomenon as well as provide crucial information for the development of effective strategies for disease intervention.

In addition to the ability to identify novel host factors, this assay presents the researcher with the advantage of accurately predicting survival prior to selection of monkeys for SIV studies, which is particularly useful in experiments where both control and test groups are infected and more subtle parameters of efficacy are required. Since limited numbers of animals are often used in macaque trials due to the expense, optimal stratification of groups is crucial so that differences in delays in disease progression can be appropriately identified. In this regard, it is important to note that *in vitro* virus production not only predicted overall survival in the animals reported here, but also correlated with other parameters such as antigenemia, the rate of T cell decline (180), and plasma virus loads (113), all of which are indicative of the rate of disease progression before death.

Summary of three main findings from the work presented in this dissertation:

1) The efficiency of early reverse transcription appears to be the mechanism behind differential virus production *in vitro*. To better understand the cause of differential virus replication within $CD4^+$ cells from individual animals, detailed analyses of various steps of the viral life cycle were undertaken to determine the point at which the $CD4^+$ T cell differentially controls virus replication. Surprisingly, inhibition of viral entry into low virus producing cells was not the basis of our observations. Rather, we observed a consistent partial inhibition of the early stage of reverse transcription within low producer cells that was independent of the dose of virus used to infect the cells. After analysis of subsequent steps in the virus life cycle, we determined that there were no additional impairments to virus replication in low producer cells as compared to their high producer counterparts. Viral RNA and protein expression on a per cell basis appeared to be equivalent between high and low producer cells. Partial inhibition at the level of early reverse transcription alone resulted in fewer cells getting infected at the outset and a slower spread of the virus through culture, while the remainder of the virus life cycle proceeded normally.

Because lentiviruses utilize the cellular transcription machinery, RNA transcription represents an evident step at which cellular proteins can influence viral replication (33). Therefore, at first glance, the impairment in virus replication after entry and before completion of reverse transcription may not appear to be an obvious step affected by host proteins. However, after fusion of the virus with the host cell membrane, the viral core is released into the cytoplasm and an ill-defined uncoating process occurs. While this process is not yet completely understood, a rearrangement of viral proteins occurs to allow for efficient reverse transcription

and formation of the pre-integration complex (PIC) (56). During this time period, the virus is highly susceptible to the effects of host-cell antiviral mechanisms. Indeed, host proteins such as Ref1, CEM15, IFN-α, glutathione, and subunits of the proteasome complex, among others, all specifically inhibit viral replication after entry and before reverse transcription (38, 88, 177, 181, 195). The *in vitro* assay studied here represents a simple way to study how these known proteins, as well as yet unidentified host proteins, play a role in controlling *in vitro* virus production as well as their possible association with disease progression *in vivo.*

One of the future aims of this study is to directly evaluate the role of some of these potential proteins in the high/low virus producer phenotype. Even prior to that, our findings are fairly consistent with the involvement of the *Ref1* gene. As discussed in the Introduction section to this dissertation, Ref1 functions to restrict HIV-1 infection within monkey cells in a similar manner as MuLV-infection is restricted in mammalian cells by Fv1 (199). Characteristics of *Ref1*-like sequences and how they may be consistent with our observations are listed below:

1) *Ref1* appears to act after viral entry but before reverse transcription (199); indeed, this is the point at which viral replication is partially inhibited in low producer cells.

2) Restriction has varying degrees of severity ranging from complete inhibition (e.g. HIV-1 replication in monkey cells) to partial inhibition of viral replication from 50 – 1000-fold (14, 38, 73). Our studies using individual rhesus macaques demonstrate partial inhibition of reverse transcription within cells from low producer animals as compared to cells from high producer animals.

3) Titration of the virus on non-permissive cells shows second-order (two-hit) kinetics, indicating that the incoming Gag protein is able to saturate the block caused by Ref1 (68). We measured the number of early reverse transcripts after titration of input virus. While a true biphasic increase in the number of viral DNA copies was not seen within low producer cultures, the highest achievable dose of virus (m.o.i. = 0.2) may not have been sufficiently great enough to overcome the potential action of Ref1. Further investigation of this observation is required. However, our studies using intracellular p27 staining showed that the spread of infected cells throughout low producer cultures displayed biphasic kinetics. However, this result is tempered by the fact that we were specifically looking at the spread of infected cells through the culture after infection, rather than the number of infected cells (as measured by reporter gene expression) after varying input viral doses (38).

4) Restriction acts in a dominant-negative manner meaning that very few Ref1 molecules are needed to mediate restriction (68).

Evaluation of the last characteristic of Ref1 function, as well as a direct examination of *Ref1* expression levels in monkey cells is warranted. It is feasible that a slight variation among individual monkeys in the expression level of *Ref1*-like elements could affect the permissivity of cells to infection and give rise to our *in vitro* observations.

2) Cells from individual animals have differential responses to mitogen stimulation. In these studies, an intriguing connection was made between virus production *in vitro* and response of the cells to mitogen stimulation in the absence of viral infection. Activation of cells from 3 high producer animals with either anti-CD3/CD28 antibodies or PHA resulted in increased $CD4^+$ T cell apoptosis and therefore fewer viable cells as compared to their low producer counterparts. Despite this finding, there were no differences in the rate of cell division or T cell activation between the two groups. One high producer animal, M7799, was the exception to this finding; cultures of cells from this animal accumulated large numbers of viable cells, had a relatively low number of cells undergoing apoptosis, and yet secreted large amounts of virus into the supernatant.

Interestingly, the apoptotic properties of the cultures correlated with different patterns of virus spread in the culture. In the 3 high producer cultures susceptible to apoptosis, a rapid and linear increase in the number of infected cells was observed that peaked at 80% of the cells infected by 11 days post-infection. In contrast, cells that were more refractory to apoptotic cell death had a biphasic spread of infected cells, and the low producer cultures never achieved the high percentage of infected cells observed in the high producer cultures. In the one high producer culture that was more resistant to apoptosis (animal M7799), a biphasic spread was seen which eventually reached that of the other high producers. While the relationship between virus production and the apoptotic response to mitogen stimulation was consistent in the animals studied here, future studies should be directed at determining if this is a consistent observation among other rhesus macaques. The potential interplay between this observation and virus replication during acute infection is discussed below.

3) The *in vitro* observations correlate with the rate of virus dissemination and disease progression. Our *in vitro* assay is useful and biologically relevant only if the results obtained can be extrapolated to an SIV-infected animal. As predicted, after intra-rectal infection, the four high producer animals had higher viral loads during the asymptomatic phase, or set-point, with one animal dying as early as 6 weeks post-infection and another by 18 weeks. Surprisingly, the peak viral load during the acute phase did not predict the viral load at the set point. However, detection of infected cells by highly quantitative methods during the acute phase did correlate with the post-acute set point. During the acute phase, low producer animals had a significantly delayed emergence of infected $CD4^+$ and $CD14^+$ cells in addition to having fewer infected cells overall, indicating that virus dissemination may have been slower in these animals. This finding was remarkably reminiscent of our *in vitro* data which showed that a 2-fold decrease in the efficiency of reverse transcription resulted in significantly slower spread of the virus through an *in vitro* culture. The apparently slower dissemination of virus during acute infection of the low producer animals could potentially be a direct result of slower viral replication during the very first few rounds of infection. Here, the number of infected cells and the timing of their emergence, rather than the peak viral load, was an accurate indicator of the eventual set point, and therefore survival time (130). Measurement of virus infected cells during the acute phase, therefore, may be a newer predictor of disease progression and survival. The slower emergence of virus in low producer animals was associated with the development of stronger cell-mediated immune responses, which could have contributed to a more effective control of viremia during the asymptomatic phase (18, 98). The fact that incredibly early events during *in vivo* infection appeared to play a dominant role in the disease outcome underscores the studies of others who

have shown, both in humans and monkeys, that a better clinical prognosis can be achieved the earlier that antiretroviral treatment is initiated after infection (79, 170).

A potential relationship exists between reverse transcription efficiency, susceptibility to mitogen-induced apoptosis, and dissemination of the virus during acute infection *in vivo*. To more closely examine the interplay between these three main observations, the animals were ranked relative to their placement in the group based the results from a number of parameters examined throughout this dissertation (Table 5). The parameters listed in this table were the most relevant to our observations. An overall rank in the group was created for each of the 8 animals studied, with the first animal listed (M12797) representing the lowest producer and the last (M0198) representing the highest producer. The rank order for various parameters is given in each column.

The reverse transcription and apoptosis observations noted above may be linked; that is, the differential response to mitogens, which result in increased apoptosis, may directly cause higher levels of virus replication *in vitro*. However, evidence presented here suggests that the two observations work in concert. In these studies, efficient reverse transcription in conjunction with an increased susceptibility to mitogen-induced apoptosis was associated with the highest level of virus production *in vitro*, as well as the most severe disease phenotype after *in vivo* infection. For instance, cells from animals M0198 and M8697 made the most virus after infection *in vitro*, were the most susceptible to infection, and underwent the most apoptotic cell death after mitogen stimulation. Interestingly, these animals had the highest viral loads at the post-acute set-point as well as the earliest emergence of infected cells in the periphery, which culminated in the death of animal M0198 on day 42 p.i (Table 5), suggesting a possible link

between our *in vitro* observations and disease outcome. Indeed, M0198 had the highest rank order for almost all assays examined and was therefore our 'highest' high producer.

On the other hand, efficient reverse transcription without an increased susceptibility to mitogen-induced apoptosis was associated with a more intermediate phenotype, such as seen in high producer animal M7799. Ranked among the high producers with respect to virus production *in vitro* and susceptibility to infection, this animal was often considered an outlier because it exhibited cell growth properties and a susceptibility to apoptosis that was similar to the low producers. This animal ultimately had an intermediate disease phenotype, with a viral load at 56 days p.i. that was higher than all the low producers but was the lowest of the 4 high producers.

Finally, two low producer animals had the lowest overall rank (M12797 and M6698) because their cells produced the least amount of virus and underwent the least amount of apoptosis *in vitro*. Interestingly, these animals appeared to be resistant to intra-rectal infection and also had the lowest viral loads at set point.

While the amount of virus produced after *in vitro* infection is a very good predictor of survival (180), it is not 100 % correlative. We found that virus production *in vitro* significantly correlates with disease progression profile and survival, and this indicates that it is most likely the predominant mechanism. However, other factors, namely the susceptibility of the cells to apoptosis, may modulate this effect. This is exemplified by animal M7799. Measurement of *in vitro* virus production alone would have predicted animal M7799 to be a true rapid progressor, but the disease phenotype of this animal was more intermediate potentially due to the decreased susceptibility of cells from this animal to apoptosis compared to the other high producer animals.

These studies have provided a better understanding of the interplay between two events and their possible relationship to rapid or slow disease onset.

In summary, there are two overall conclusions from this dissertation: 1) the efficiency of reverse transcription and the response of the cell to mitogen stimulation work in concert to determine how much virus is produced from a cell *in vitro*, and 2) very early events during acute infection (i.e. potentially the first round or two of infection) may have an astonishing effect on virus dissemination, development of a virus-specific immune response, and eventually survival of the infected animal. While we have presented compelling evidence, a direct link between reverse transcription efficiency, susceptibility to mitogen-induced apoptosis, and dissemination of the virus during acute infection *in vivo* still remains to be unambiguously demonstrated. However, it does appear that both *in vitro* virus production and susceptibility to apoptosis work in concert, at least in *in vitro* culture, and may potentially have an influence on the outcome of the infection *in vivo.*

Table 5. The rank order of animals and implications for disease outcome

Animal #	Producer Status	Virus production in vitro[1]	Susceptibility to infection[1]	Cell Growth[2] SIV+	Cell Growth[2] SIV-	Apoptosis[1] SIV+	Apoptosis[1] SIV-	Viral Load[1] at 56 d.p.i.	Overall Average Rank
M12797[3]	**Low**	1	1	4	6	2	1	1	2.3
M6698[3]	**Low**	2	3	2	4	1	2	3	2.4
M6498	**Low**	3	2	1	2	3	4	4	2.7
M0898	**Low**	4	4	5	3	4	5	2	3.9
M7799	**High**	6	5	3	1	5	3	5	4.0
M7699[5]	**High**	5	6	7	7	6	6	7	6.3
M8697	**High**	7	7	6	5	7	8	6	6.6
M0198[4]	**High**	8	8	8	8	8	7	8	7.9

[1]rank orders are listed as 1 through 8 with 1 being the lowest value for the given assay and 8 being the highest

[2]rank orders are listed as 1 through 8 with 1 being the highest cell growth and 8 being the lowest

[3]resistant to i.r. challenge

[4]death at 42 d.p.i.

[5]death at 125 d.p.i.

APPENDICES

APPENDIX A

MICROARRAY RESULTS

Table 6. List of highly expressed genes in rhesus macaque $CD4^+$ T cells after 24 hours of SIV infection.

High Producers		Low Producers	
Expression	**Gene**	**Expression**	**Gene**
1.259	Lymphotoxin b	1.240	FGF basic
1.236	Integrin-b1	1.215	Lymphotoxin b
1.226	cysteine-rich FGF R	1.190	Integrin-b1
1.210	L19	1.181	b-Actin
1.187	FGF basic	1.174	a-Tubulin
1.140	TRAIL	1.166	cysteine-rich FGF R
1.134	HLA-A 0201 heavy chain	1.160	TRAIL
1.129	Integrin-b7	1.151	IL-16
1.103	IL-7 Ra	1.138	Cyclophilin A
1.087	b-Actin	1.121	Integrin-b7
1.085	GAPDH	1.102	IL-7 Ra
1.080	IL-16	1.101	GAPDH
1.064	a-Tubulin	1.085	Integrin-a6
1.050	CCR-7	1.038	HLA-A 0201 heavy chain
1.021	Cyclophilin A	1.010	L-Selectin
0.989	Genomic DNA	1.000	CXCR-4
0.961	CXCR-4	0.992	b2M
0.938	L-Selectin	0.865	L19
0.913	b2M	0.847	CCR-7
0.908	TOSO	0.800	CD40
0.908	Integrin-a6	0.787	TGF-b1
0.846	IP-10	0.769	IL-10
0.839	MIF	0.760	Genomic DNA
0.829	IL-10	0.744	TGF-b RI
0.808	Genomic DNA	0.669	Genomic DNA
0.783	CAD-12	0.665	PECAM
0.773	TGF-b1	0.652	MIF
0.773	PECAM	0.636	CAD-12
0.760	TGF-b RI	0.635	CD27
0.659	CD30L	0.626	PIN
0.647	ICAM-2	0.617	Genomic DNA
0.639	IL-17	0.617	CD30L
0.628	CD27	0.607	TOSO
0.627	Caspase-1	0.593	IL-2 Rg
0.620	ICAM-3	0.584	Integrin-a4
0.609	PIN	0.565	IL-17
0.598	IL-10 Rb	0.565	ICAM-3
0.586	IL-2 Rg	0.516	IL-2 Ra
0.567	ALCAM	0.511	HPRT
0.542	CD40	0.509	EphA7
0.539	Genomic DNA	0.488	Integrin-b2
0.539	Integrin-a4	0.486	Integrin-aL
0.510	PBEF	0.483	Caspase-1
0.509	EphA7	0.476	TRAIL R4
0.503	Genomic DNA	0.472	ALCAM
0.489	April	0.465	April
0.486	HPRT	0.464	EphA4

*Results were based on R&D System's Human Cytokine Array

Table 7. List of genes over-expressed in high producer cells after 24 hours of SIV infection

Gene ID	Expression ratio	Signal Intensity	
	High:Low	High	Low
TATA box binding protein (TBP)-associated factor, RNA polymerase I, C, 110kD Hs.153022 AA454218	3.14	1.39	0.44
interferon gamma receptor 2 (interferon gamma transducer 1) Hs.177559 AA969475 | AI733305 1572614	3.09	3.17	1.03
interferon, alpha-inducible protein (clone IFI-6-16) Hs.179972	2.77	1.56	0.56
cofactor required for Sp1 transcriptional activation, subunit 8 (34kD) Hs.28166 AA490614	2.69	0.99	0.37
TBP-like 1 Hs.13993 AA448001	2.66	0.92	0.35
Human clone 137308 mRNA, partial cds Hs.159255	2.51	5.60	2.24
activated RNA polymerase II transcription cofactor 4 Hs.74861 AA099534	2.43	1.18	0.49
RNA polymerase I subunit Hs.5409 AA733038	2.39	1.55	0.65
TATA boxbinding protein Hs.1100 N50549	2.39	4.34	1.82
cofactor required for Sp1 transcriptional activation, subunit 2 (150kD) Hs.21586 AA150093	2.38	0.41	0.17
polymerase (RNA) II (DNA directed) polypeptide A (220kD) Hs.171880 AA479052	2.29	0.44	0.19
laminin receptor 1 (67kD, ribosomal protein SA) Hs.181357 AA777192	2.25	1.77	0.79
ELL-RELATED RNA POLYMERASE II, ELONGATION FACTOR Hs.173334 AA884897	2.24	1.24	0.55
TATA element modulatory factor 1 Hs.267632 AA252318	2.24	1.45	0.65
ATP-binding cassette, sub-family B (MDR/TAP), member 2 Hs.158164 AI346384 1925995	2.23	2.14	0.96
polymerase (RNA) II (DNA directed) polypeptide L (7.6kD) Hs.71618 AA873691	2.09	0.81	0.39
proteasome subunit, beta type, 8 (large multifunctional protease 7) Hs.180062 AA181300 624360	2.04	1.17	0.57
N/A N51625	2.01	1.14	0.57
monokine induced by gamma interferon Hs.77367	1.99	0.68	0.34
superoxide dismutase 2, mitochondrial Hs.177781	1.99	6.35	3.19
interferon gamma receptor 1 Hs.180866	1.98	1.05	0.53
protein kinase, interferon-inducible double stranded RNA dependent activator Hs.18571	1.94	0.62	0.32
cadherin 11 (OB-cadherin, osteoblast) Hs.249176 N64628	1.93	5.05	2.62
TATA box binding protein (TBP)-associated factor, RNA polymerase II, B, 150kD Hs.122752 AA705134	1.86	1.45	0.78
interferon regulatory factor 4 Hs.82132	1.85	7.08	3.82
TATA box binding protein (TBP)-associated factor, RNA polymerase II, F, 55kD Hs.155188 AA036649	1.82	1.12	0.62
Homo sapiens pRGR1 mRNA, partial cds Hs.284265 H89912	1.79	1.07	0.60
general transcription factor IIF, polypeptide 2 (30kD subunit) Hs.58593 N72223	1.71	1.09	0.63
interferon gamma receptor 2 (interferon gamma transducer 1) Hs.177559	1.71	0.79	0.46

Table 8. List of genes over-expressed in low producer cells after 24 hours of SIV infection.

Gene ID	Expression ratio	Signal Intensity	
	Low:High	High	Low
interferon induced transmembrane protein 1 (9-27) Hs.146360 AA058323 509641	4.2806	0.8783	3.7595
interferon-stimulated transcription factor 3, gamma (48kD) Hs.1706	3.1562	0.2009	0.6339
signal transducer and activator of transcription 1, 91kD Hs.21486	2.89	0.3296	0.9524
vascular endothelial growth factor C Hs.79141 H07899 45138	2.7167	0.8509	2.3116
collagen, type XVI, alpha 1 Hs.26208 AA088202 488258	2.6109	0.0658	0.1719
myosin, heavy polypeptide 9, non-muscle Hs.146550	2.5124	1.7404	4.3725
interferon-induced protein 17 Hs.146360	2.5096	2.8528	7.1594
down-regulator of transcription 1, TBP-binding (negative cofactor 2) Hs.16697 AA043503	1.9294	0.4242	0.8185
ESTs, Highly similar to S17112 interferon alpha/beta receptor Hs.20474 AA074230 383197	1.9219	0.0641	0.1233
interferon, gamma-inducible protein 16 Hs.155530	1.8936	1.3216	2.5025
polymerase (RNA) II (DNA directed) polypeptide C (33kD) Hs.79402 AA430656	1.8077	2.8658	5.1805
interferon-inducible Hs.182241	1.7938	4.2058	7.5442
interferon stimulated gene (20kD) Hs.183487	1.774	1.0894	1.9326
interferon-inducible Hs.174195	1.7034	3.5911	6.117
splicing factor, arginine/serine-rich 2, interacting protein Hs.51957 H78241	1.6912	3.0845	5.2165
B Actin	1.517	0.8023	1.2171

Table 9. List of genes over-expressed in high producer cells after 24 hours of anti-CD3/CD28 stimulation in the absence of viral infection

Gene ID	Expression Ratio	Signal Intensity	
	High:Low	High	Low
integrin, alpha 2 (CD49B, alpha 2 subunit of VLA-2 receptor) Hs.1142	1.91	2.08	1.09
adrenal gland protein AD-004 Hs.279586 AA150301	1.74	0.62	0.35
interferon-induced protein 75, 52kD Hs.38125	1.67	0.16	0.10
polymerase (RNA) II (DNA directed) polypeptide A (220kD) Hs.171880 AA010216	1.67	0.94	0.56
proteasome (prosome, macropain) subunit, beta type, 8 (large multifunctional protease 7) Hs.180062 AA181300 624360	1.66	0.58	0.35
interferon, alpha-inducible protein 27 Hs.2867	1.66	0.11	0.07
TATA box binding protein (TBP)-associated factor, RNA polymerase II, A, 250kD Hs.1179 N75438	1.61	0.85	0.53
guanylate binding protein 1, interferon-inducible, 67kD Hs.62661	1.58	0.89	0.56
interferon gamma receptor 2 (interferon gamma transducer 1) Hs.177559 AA969475 | AI733305 1572614	1.56	0.70	0.45
ESTs, Highly similar to IFT2_HUMAN INTERFERON-INDUCED PROTEIN [H.sapiens] Hs.169274 AA143609 588492	1.56	0.17	0.11

Table 10. List of genes over-expressed in low producer cells after 24 hours of anti-CD3/CD28 stimulation in the absence of viral infection.

Gene ID	Expression Ratio	Signal Intensity	
	Low:High	High	Low
interferon gamma receptor 1 Hs.180866	4.88	0.12	0.59
lectin, galactoside-binding, soluble, 3 binding protein (galectin 6 binding protein) Hs.73614 AA191488	4.41	0.05	0.21
polymerase (RNA) II (DNA directed) polypeptide B (140kD) Hs.148027 N63783	4.18	0.11	0.47
TATA box binding protein (TBP)-associated factor, RNA polymerase II, D, 100kD Hs.96103 AA977222	4.06	0.08	0.33
general transcription factor IIF, polypeptide 2 (30kD subunit) Hs.58593 N72223	3.85	0.05	0.20
Human transformer-2 alpha (htra-2 alpha) mRNA, complete cds Hs.184601 AA419177	3.75	0.08	0.30
Homo sapiens pRGR1 mRNA, partial cds Hs.284265 H89912	3.70	0.13	0.47
transcription factor 7-like 2 (T-cell specific, HMG-box) Hs.78305 T82415	3.62	0.06	0.22
retinoblastoma-binding protein 4 Hs.16003 AA428365 773599	3.24	1.16	3.77
interferon-stimulated transcription factor 3, gamma (48kD) Hs.1706	3.14	0.16	0.51
major histocompatibility complex, class I, C Hs.182225 AA480866	3.03	0.09	0.26
interferon (alpha, beta and omega) receptor 2 Hs.86958	2.81	0.11	0.30
general transcription factor II, i Hs.184122 AA400128	2.66	0.12	0.31
polymerase (RNA) II (DNA directed) polypeptide E (25kD) Hs.24301 AA027042	2.25	0.13	0.30
monokine induced by gamma interferon Hs.77367	2.07	0.11	0.23
general transcription factor IIH, polypeptide 3 (34kD subunit) Hs.90304 AA460838	1.92	0.27	0.51
ring finger protein 21, interferon-responsive" Hs.125300 H50872 194351	1.85	0.64	1.19
superoxide dismutase 2, mitochondrial Hs.177781	1.79	1.37	2.45
polymerase (RNA) II (DNA directed) polypeptide H Hs.3128 AI554561	1.78	0.25	0.45
TATA box binding protein (TBP)-associated factor, RNA polymerase II, I, 28kD Hs.83126 N92711	1.75	0.19	0.33
retinoblastoma-binding protein 4 Hs.16003 AA705035 461465	1.72	4.32	7.41
interferon regulatory factor 4 Hs.82132	1.57	2.48	3.90
thyroid hormone receptor-associated protein, 150 kDa subunit Hs.108319 W85832	1.54	0.30	0.47
protein-kinase, interferon-inducible double stranded RNA dependent inhibitor Hs.177574 AI222468 1761715	1.54	0.19	0.29

Table 11. List of genes over-expressed in high producer cells after 24 hours of culture in the absence of viral infection or cellular activation.

Gene ID	Expression Ratio High:Low	Signal Intensity High	Signal Intensity Low
interferon-related developmental regulator 1 Hs.7879 AA676598 882483	3.01	0.78	0.26
ESTs, similar to protein activator of the interferon-induced protein kinase Hs.144946 AI218355 1845366	1.89	0.49	0.26
guanylate binding protein 1, interferon-inducible, 67kD Hs.62661	1.63	0.67	0.41
general transcription factor IIB Hs.255464 H23978	1.63	16.94	10.43
superoxide dis mutase 2, mitochondrial Hs.177781	1.62	1.98	1.22
interferon (alpha, beta and omega) receptor 2 Hs.86958	1.41	0.19	0.13

Table 12. List of genes over-expressed in low producer cells after 24 hours of culture in the absence of viral infection or cellular activation.

Gene ID	Expression Ratio Low:High	Signal Intensity High	Signal Intensity Low
B Actin	4.20	0.12	0.52
general transcription factor II, i Hs.184122 AA400128	3.16	0.34	1.07
interferon-induced protein 75, 52kD Hs.38125	3.00	0.09	0.27
TATA-binding protein-binding protein Hs.109428 AA480876	2.93	0.11	0.31
ESTs, Highly similar to CREB-binding protein [H.sapiens] Hs.110134 W88746	2.78	0.18	0.49
TATA box binding protein (TBP)-associated factor, RNA polymerase II, B, 150kD Hs.122752 R34694	2.61	0.12	0.30
caspase 1, apoptosis-related cysteine protease (interleukin 1, beta, convertase) Hs.2490	2.53	0.17	0.43
splicing factor, arginine/serine-rich 2, interacting protein Hs.51957 R85367	2.47	0.22	0.55
interferon-induced protein 35 Hs.50842	2.31	0.15	0.35
SUMO-1 activating enzyme subunit 1 Hs.250747 AA620917 1055607	2.26	0.15	0.34
related RAS viral (r-ras) oncogene homolog Hs.9651	2.20	0.20	0.44
major histocompatibility complex, class I, C Hs.182225 AA480866	2.19	0.21	0.45
cyclin-dependent kinase 8 Hs.25283 R59697	2.14	0.23	0.49
interferon regulatory factor 7 Hs.166120 AA443090 809456	1.94	0.23	0.44
glucosidase, alpha; acid (Pompe disease, glycogen storage disease type II) Hs.167017 N70841	1.94	0.17	0.32
transcription elongation factor A (SII)-like 1 Hs.95243 AA451969	1.76	0.28	0.49
general transcription factor IIH, polypeptide 1 (62kD subunit) Hs.89578 AA455003	1.75	0.25	0.45
TATA box binding protein (TBP)-associated factor, RNA polymerase II, B, 150kD Hs.122752 AA705134	1.65	0.24	0.39
polymerase (RNA) II (DNA directed) polypeptide L (7.6kD) Hs.71618 AA873691	1.63	0.26	0.42
interferon, gamma-inducible protein 30 Hs.14623	1.62	0.29	0.46
alkaline phosphatase, intestinal Hs.37009 AA190871	1.61	0.34	0.55
BCL2-associated athanogene Hs.41714 AI017240 1636251	1.61	0.24	0.39
interferon gamma receptor 1 Hs.180866	1.60	0.25	0.40

APPENDIX B

SEQUENCE ANALYSIS OF CCR5, CCR3, AND GPR15/BOB GENES

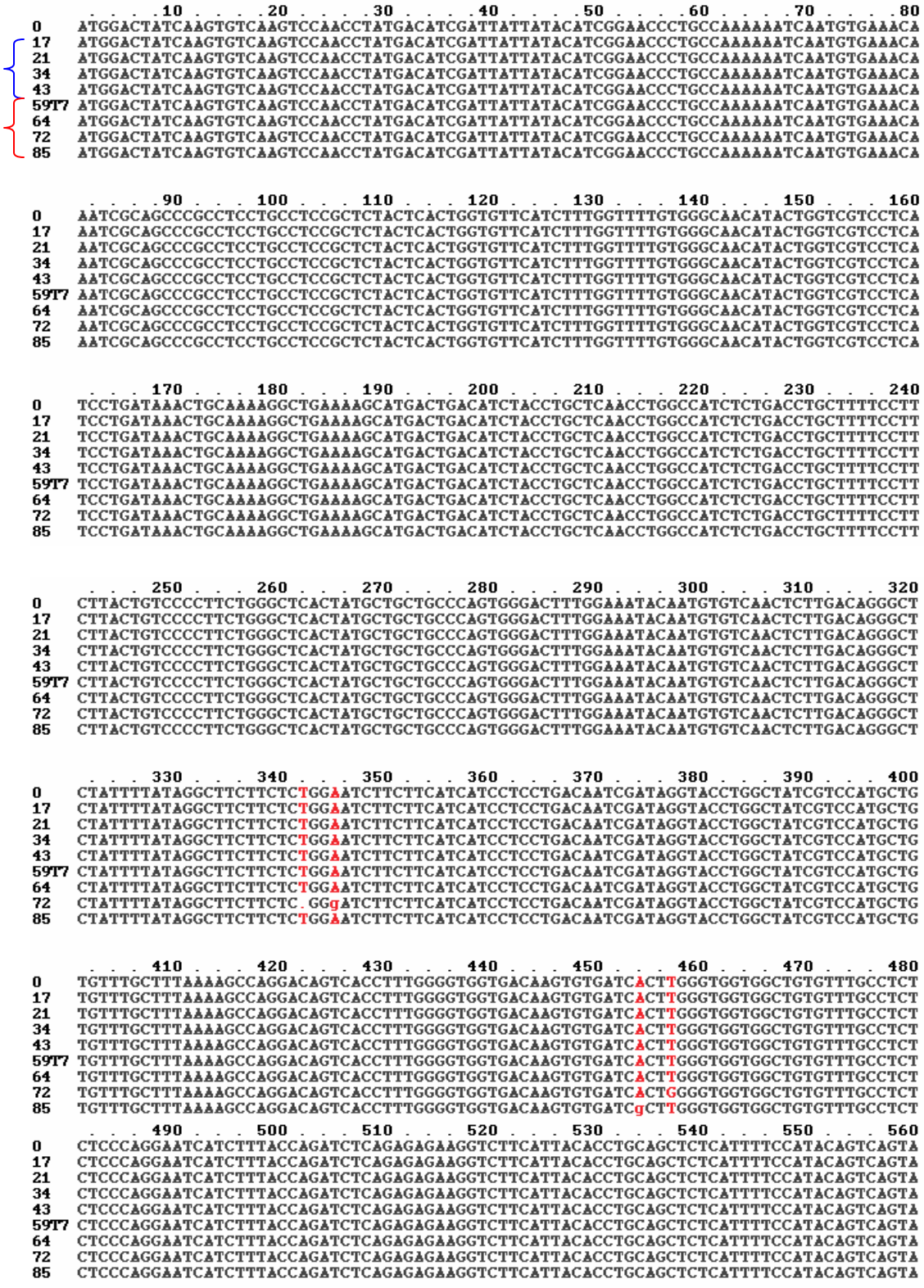

Figure 46. Legend on following page.

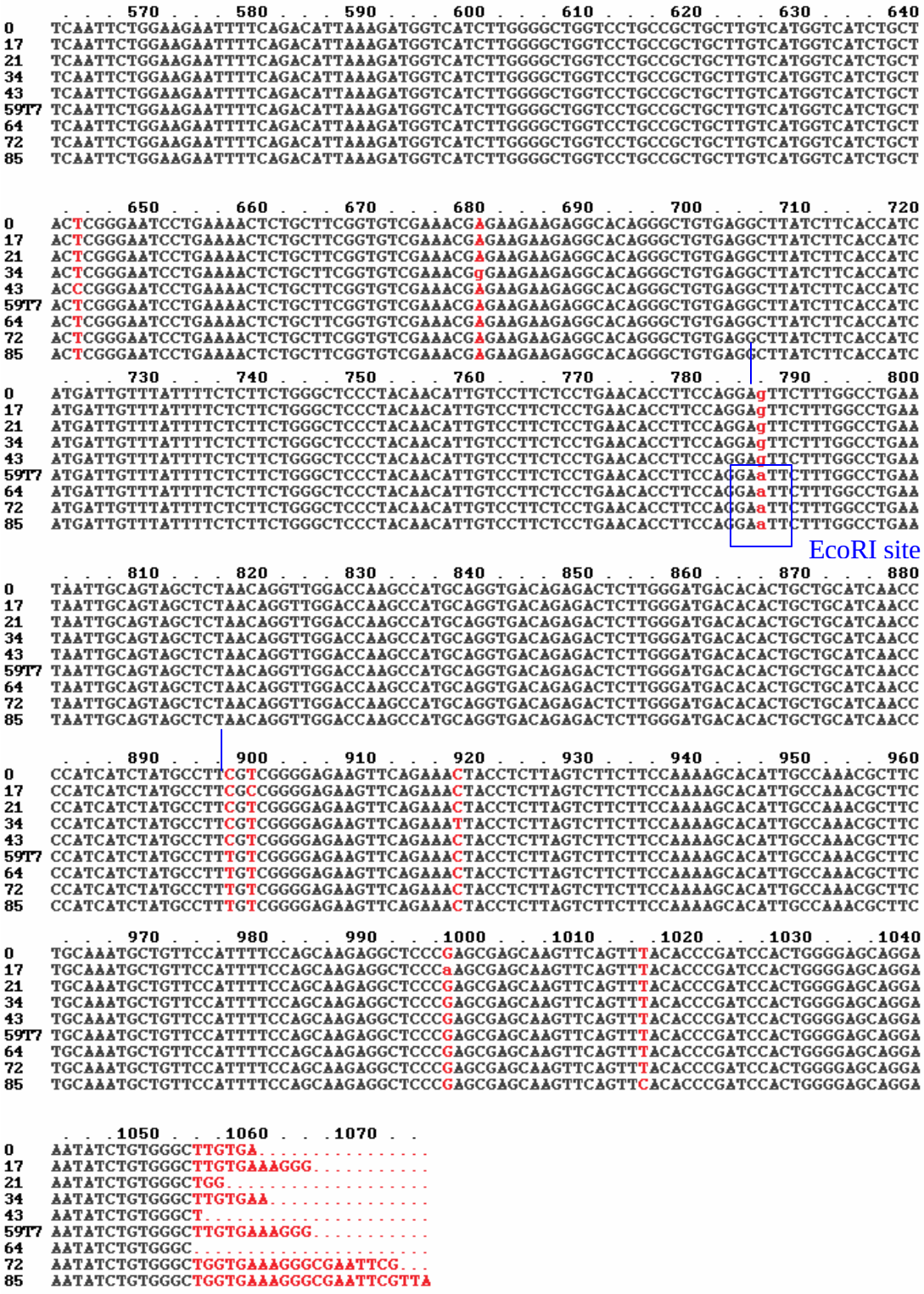

Figure 46. continued.

Figure 46. CCR5 sequence alignments from all 8 animals.

(previous 2 pages) Top line represents the human coding sequence for CCR5. All other sequences represent the following animals in order: M0898, M12797, M6498, M6698, M8697, M0198, M7699, and M7799. Beneath the human sequence, the first four animals are low producers (indicated by the blue bracket on the first line), and the last four animals are high producers (indicated by the red bracket on the first line). Nucleotides in black are identical and nucleotides in red indicate sequence divergence. Positions 786 and 897 (indicated by blue arrows) show a nucleotide change that segregates between the high and low producer animals. The G to A transition at position 786 leads to insertion of a new EcoRI restriction site.

Table 13. Polymorphism[a] analysis of the rhesus CCR5 gene at position 786.

Animal #[b]	Producer Status	Cut w/ EcoRI?[c]
J991	Low	Y
H822	Low	Y / N
I369	Low	N
I510	Low	Y
I855	Intermediate	Y / N
H737	Intermediate	N
N277	High	Y
H779	High	Y
H695	High	Y / N

[a]The presence of a G to A transition at position 786 was indicated by the presence of a functional EcoRI restriction site.
[b]These animals were previously characterized for their virus producer status (180).
[c]Y/N denotes heterozygosity at this position.

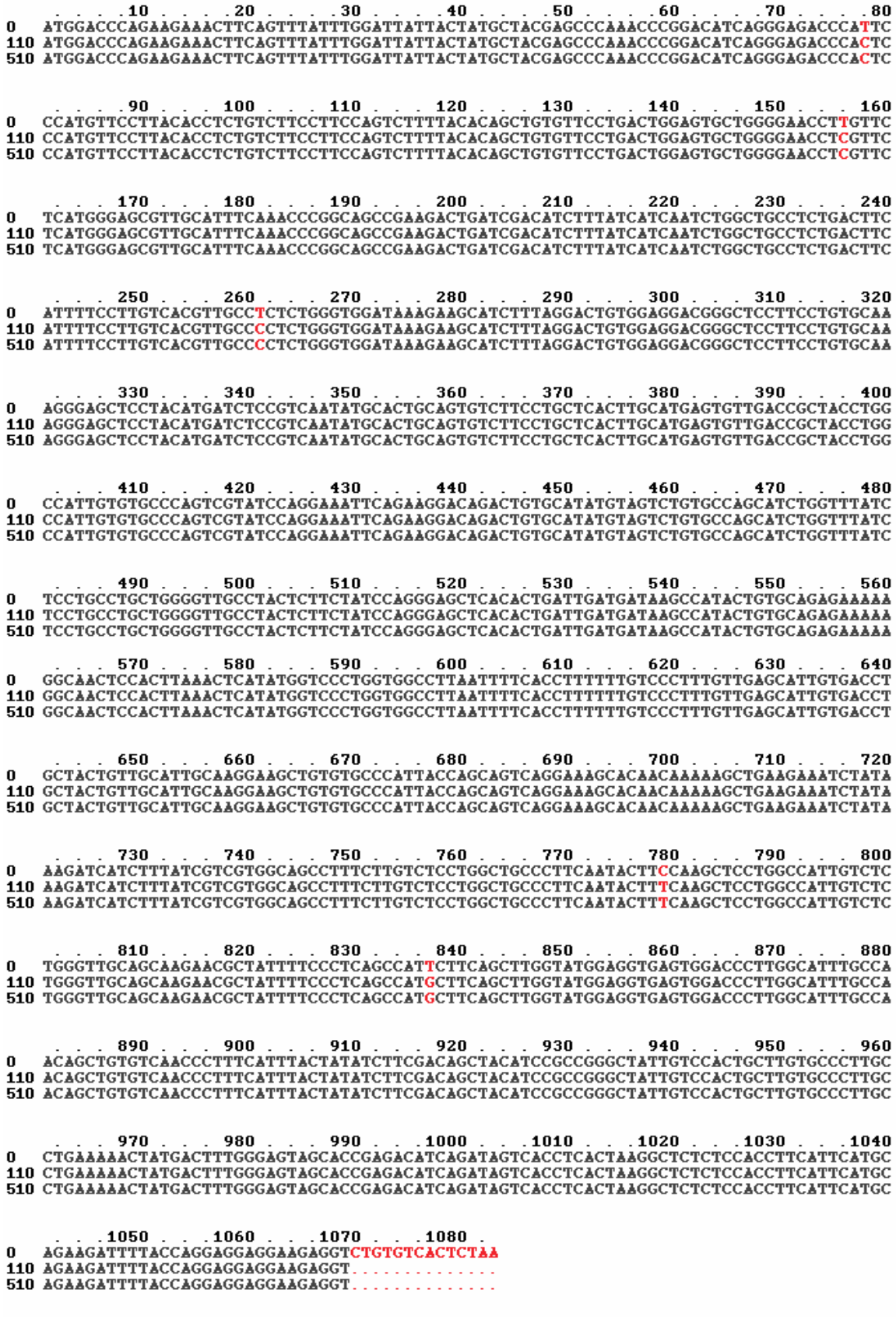

Figure 47. Legend on next page

Figure 47. GPR15/BOB sequence alignment from one representative low and high producer animal.

(previous page) Top line (#0) represents the human sequence. #110 is low producer animal M0898, and #510 is high producer animal M8697. Divergent nucleotides are indicated in red.

Figure 48. CCR3 sequence alignment from one representative low and high producer animal.

(following page) Bottom line (#0) represents the human sequence. #16 is low producer animal M0898, and #59 is high producer animal M8697. Divergent nucleotides are indicated in red.

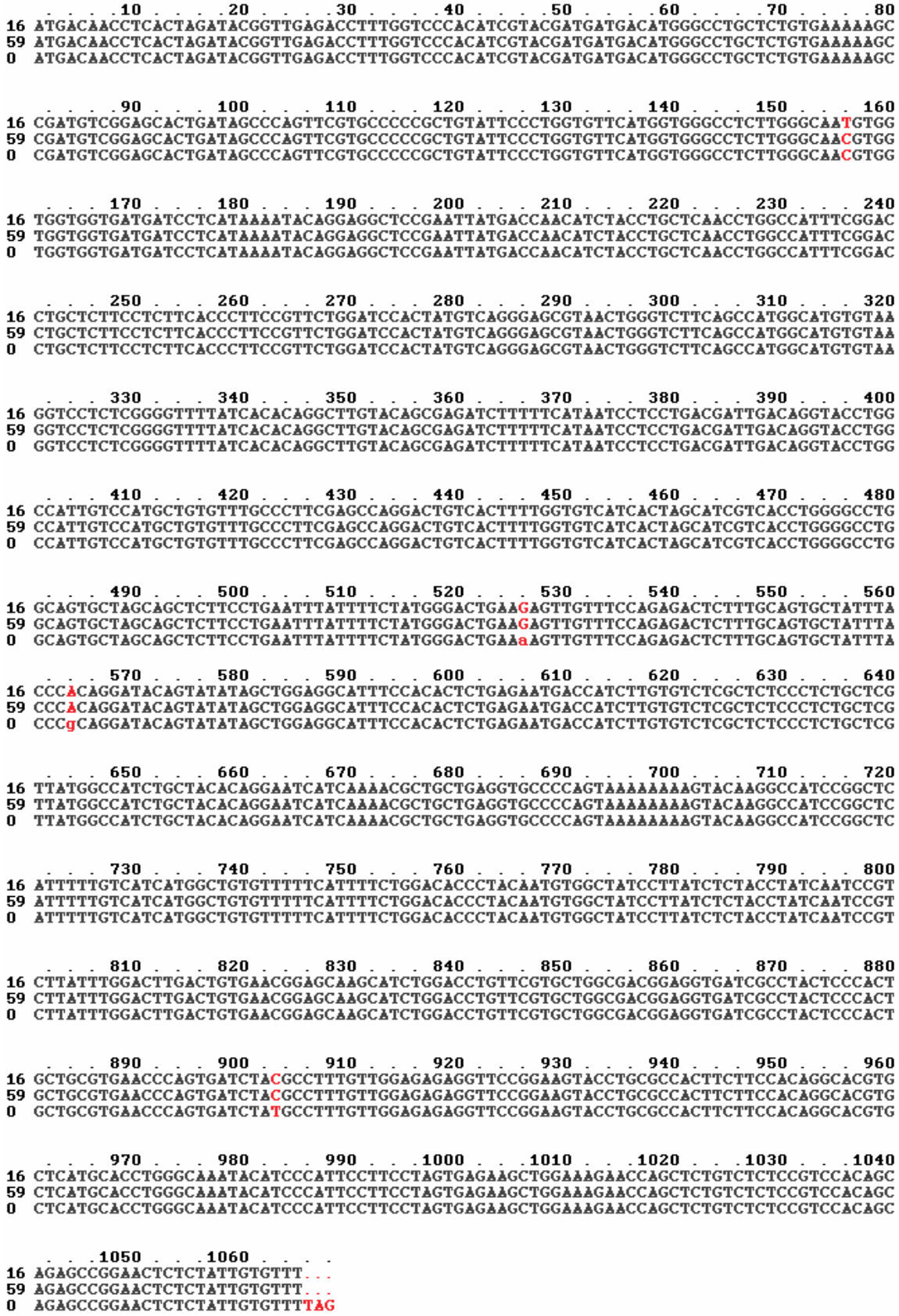

Figure 48. Legend on previous page

APPENDIX C

STANDARD CURVES AND b -GUS CONTROL USED FOR REAL-TIME PCR ANALYSIS

A

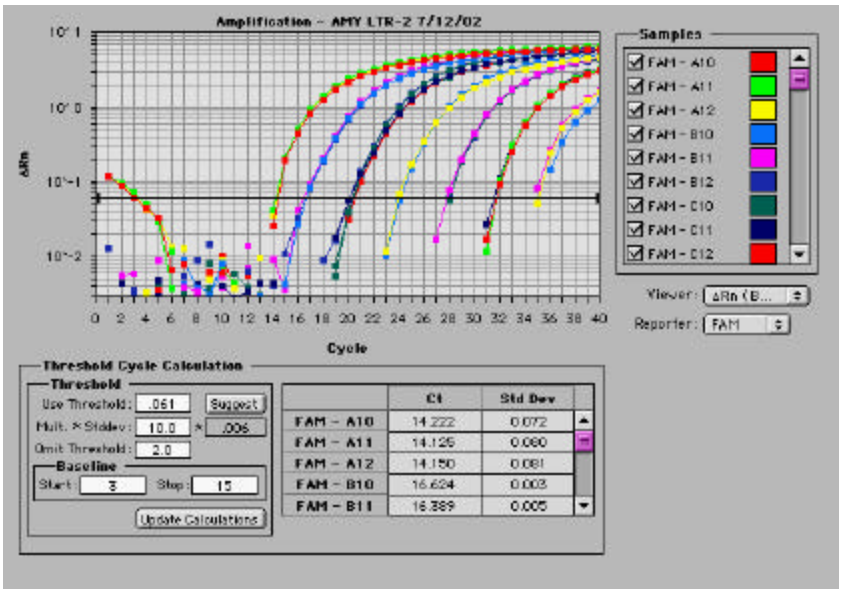

B

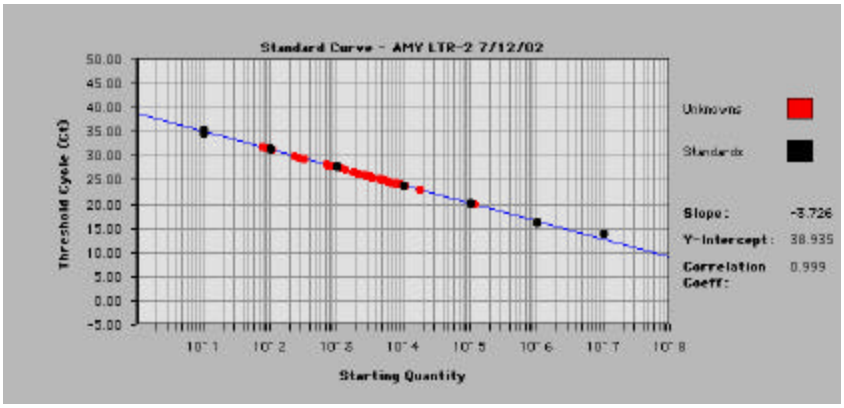

Figure 49. Standard curves used for real-time PCR analysis of early reverse transcripts.

Primers and a probe within the LTR region of the viral genome were used to amplify early ('strong-stop') reverse transcription products. Serial dilutions of a plasmid containing the LTR region were amplified in triplicate to generate a standard curve with a sensitivity of 10 copies per reaction. (A) the amplification plot, and (B) the standard curve from one representative experiment.

A

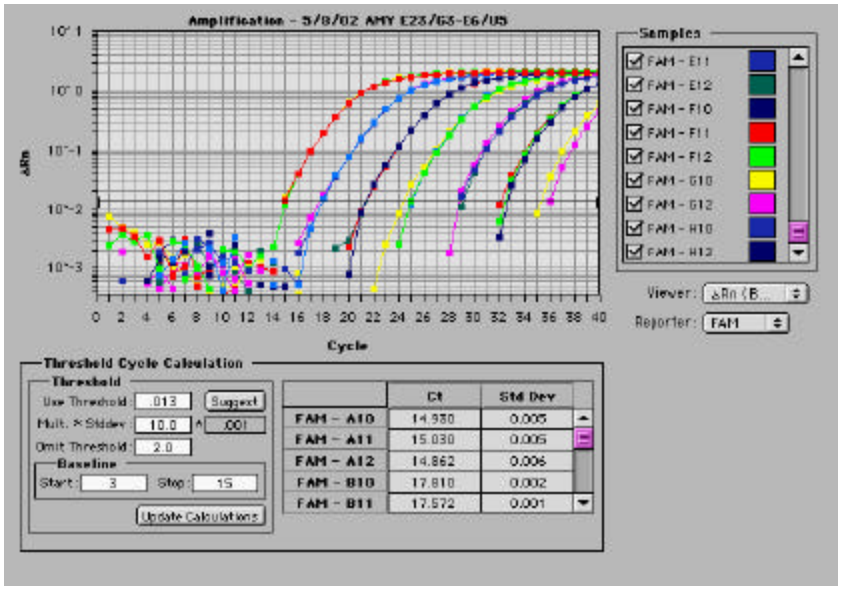

B

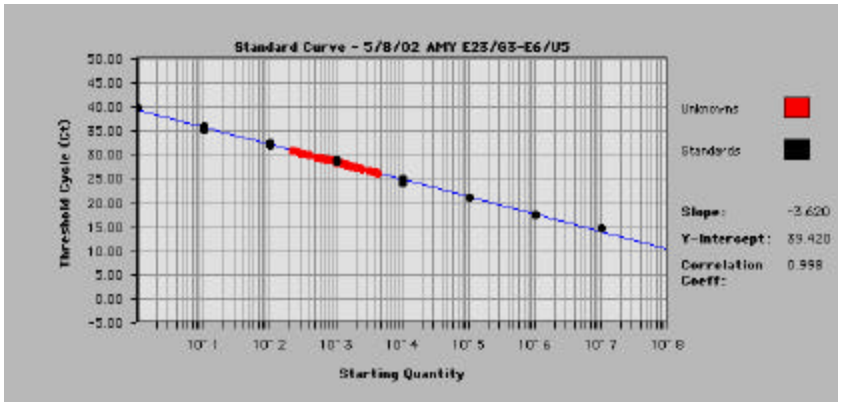

Figure 50. Standard curves used for real-time PCR analysis of full-length reverse transcripts.

Primers and a probe within the LTR-U5 and primer binding site (PBS) regions of the viral genome were used to amplify full-length reverse transcription products. Serial dilutions of a plasmid containing the U5-PBS region were amplified in triplicate to generate a standard curve with a sensitivity of 10 copies per reaction. (A) the amplification plot, and (B) the standard curve from one representative experiment.

A

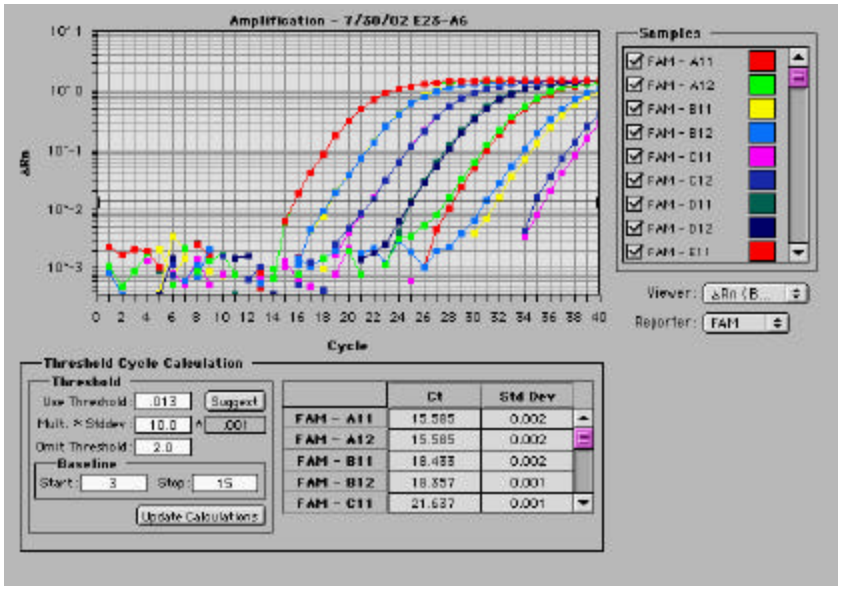

B

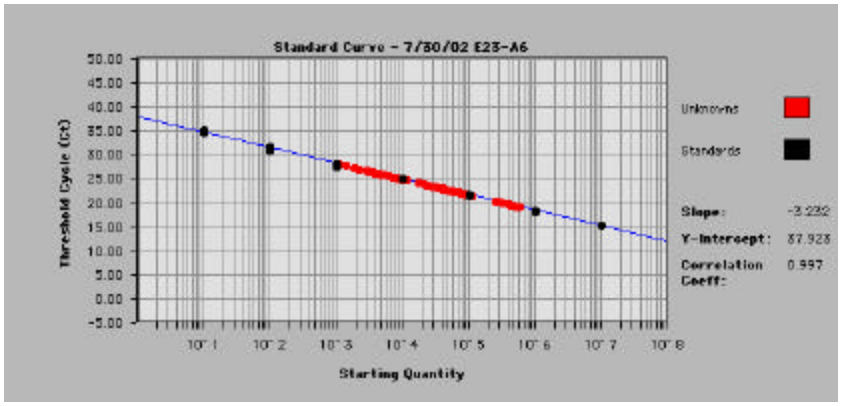

Figure 51. Standard curves used for real-time RT-PCR analysis of RNA transcripts.

Primers and a probe within the LTR-U5 and primer binding site (PBS) regions of the viral genome were used to amplify viral RNA transcripts. Serial dilutions of RNA obtained by *in vitro* transcription of a plasmid containing the LTR-PBS regions, ranging from 10^8 to 10^0 copies/ reaction, were subjected to reverse transcription-PCR in triplicate, along with the samples, to generate a standard curve with a sensitivity threshold of 10 copies/ reaction. (A) the amplification plot, and (B) the standard curve from one representative experiment.

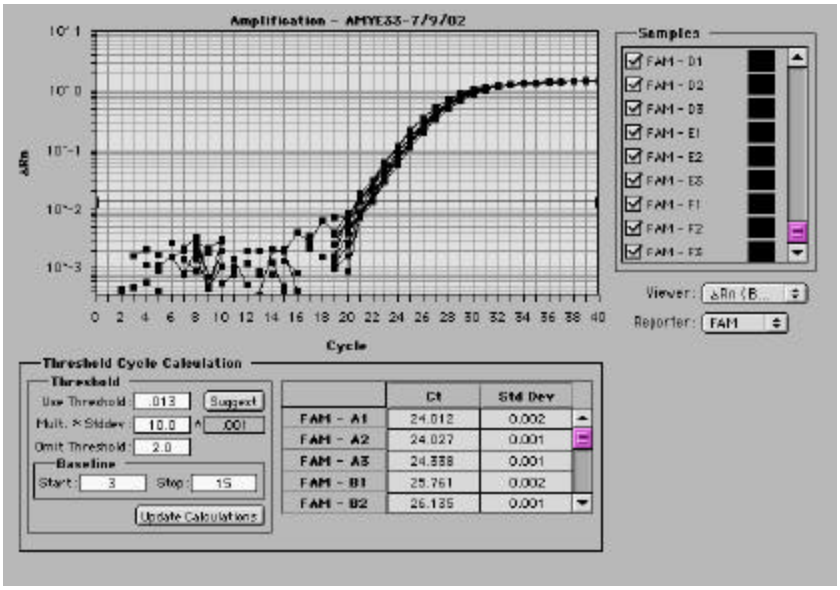

Figure 52. The use of b-GUS expression as an internal control for real-time RT-PCR analysis.

High and low producer $CD4^+$ T cell RNA from SIV-infected, uninfected, anti-CD3/CD28-stimulated cells were analyzed for β-GUS expression by real-time RT-PCR. The amplification plots of the samples are shown. Threshold cycles were very similar irrespective of producer status of the animal or whether the cells were infected or stimulated.

APPENDIX D

DEVELOPMENT OF INTRACELLULAR STAINING PROTOCOL FOR SIV P27 CAPSID PROTEIN.

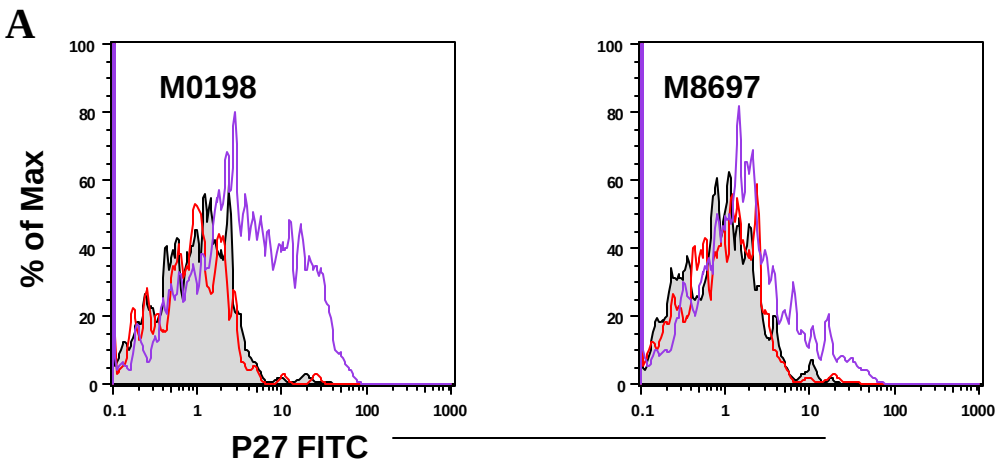

Figure 53. Detection of infected cells using intracellular flow cytometry.

Intracellular flow cytometry was performed using a biotinylated anti-p27 antibody followed by detection with streptavidin-FITC. (A) The staining procedure was validated using SIV-infected cells stained with anti-p27 followed by SA-FITC (purple line), infected cells stained with control antibody followed by SA-FITC (red line), and uninfected cells stained with anti-p27 and SA-FITC (gray shaded area). Two representative high producer animals are shown. (B) Histograms showing high producer animal $CD4^+$ cells stained with anti-p27 (red shaded area) or control antibody (black dotted line) on days 7, 11, or 14 post-infection. Value in upper right corner of histogram is the percentage of cells that are positive for p27. Cells are gated on lymphocytes and $CD4^+$ cells. (C) Same as (B), but for low producer animals (shaded areas are blue).

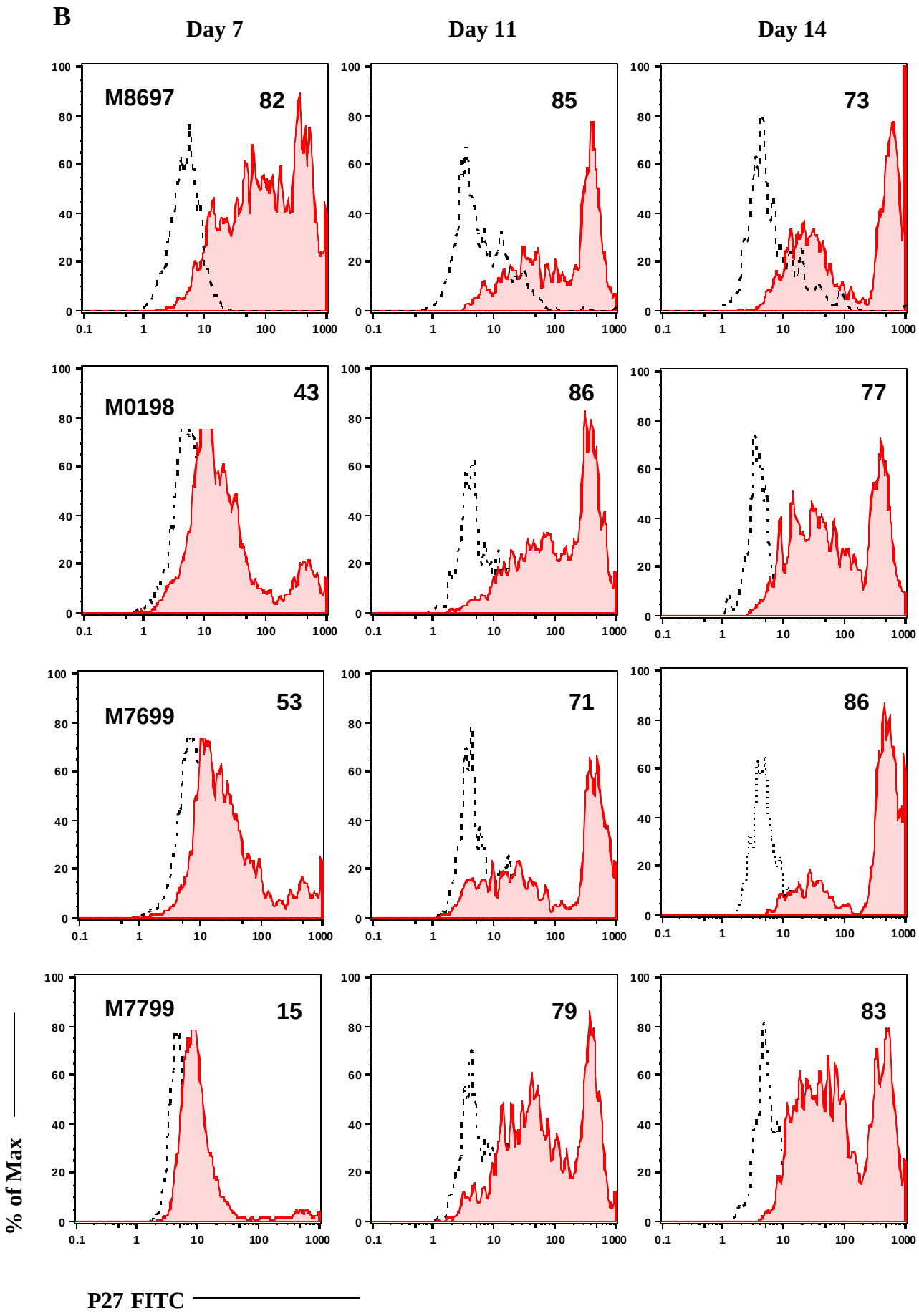
B
Day 7
Day 11
Day 14
M8697
82
85
73
M0198
43
86
77
M7699
53
71
86
M7799
15
79
83
% of Max
P27 FITC

C

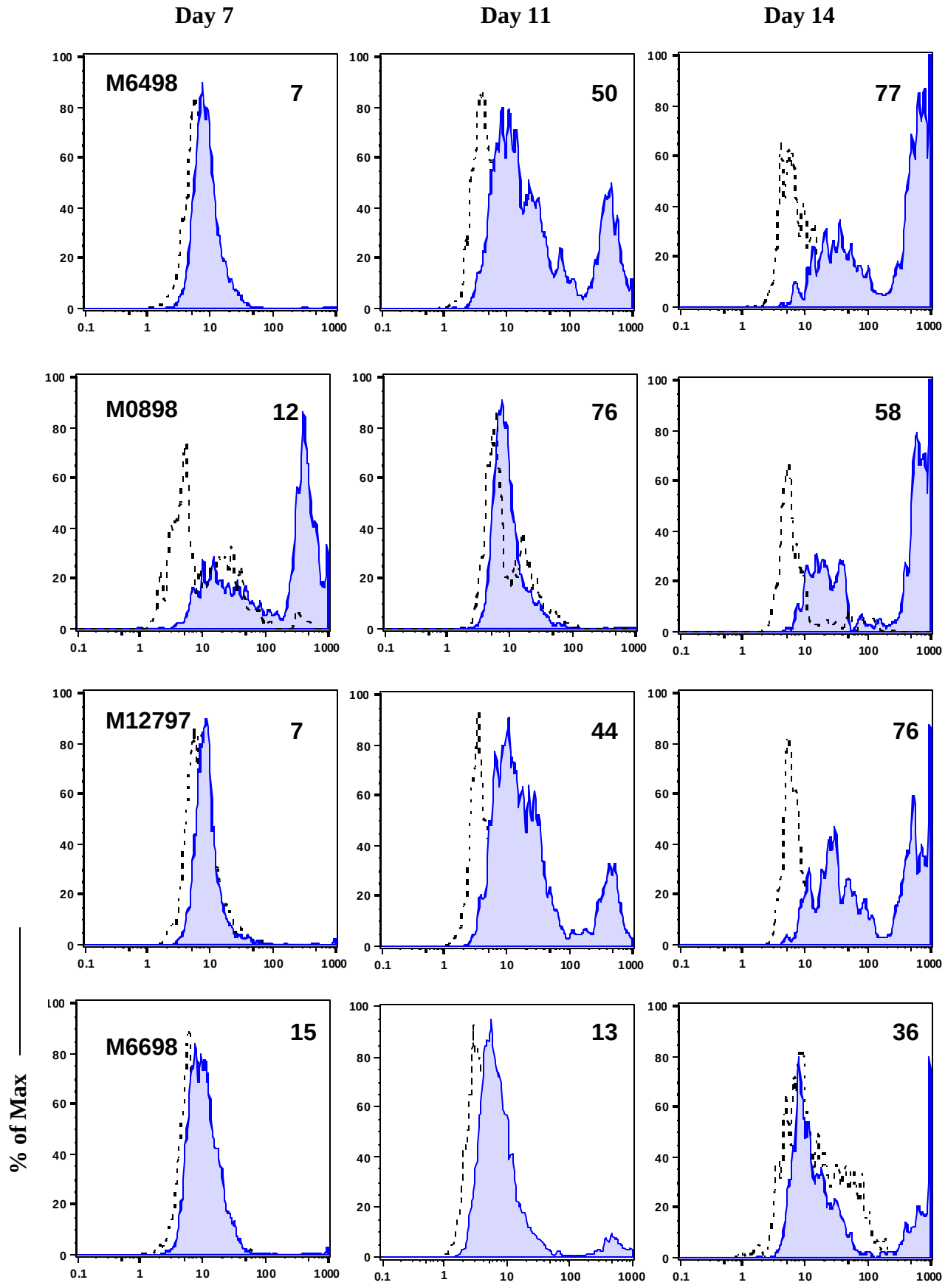
Day 7
Day 11
Day 14
M6498
7
50
77
M0898
12
76
58
M12797
7
44
76
M6698
15
13
36
% of Max
P27 FITC

APPENDIX E

CELL POPULATIONS IN THE PERIPHERAL BLOOD DURING INFECTION *IN VIVO*.

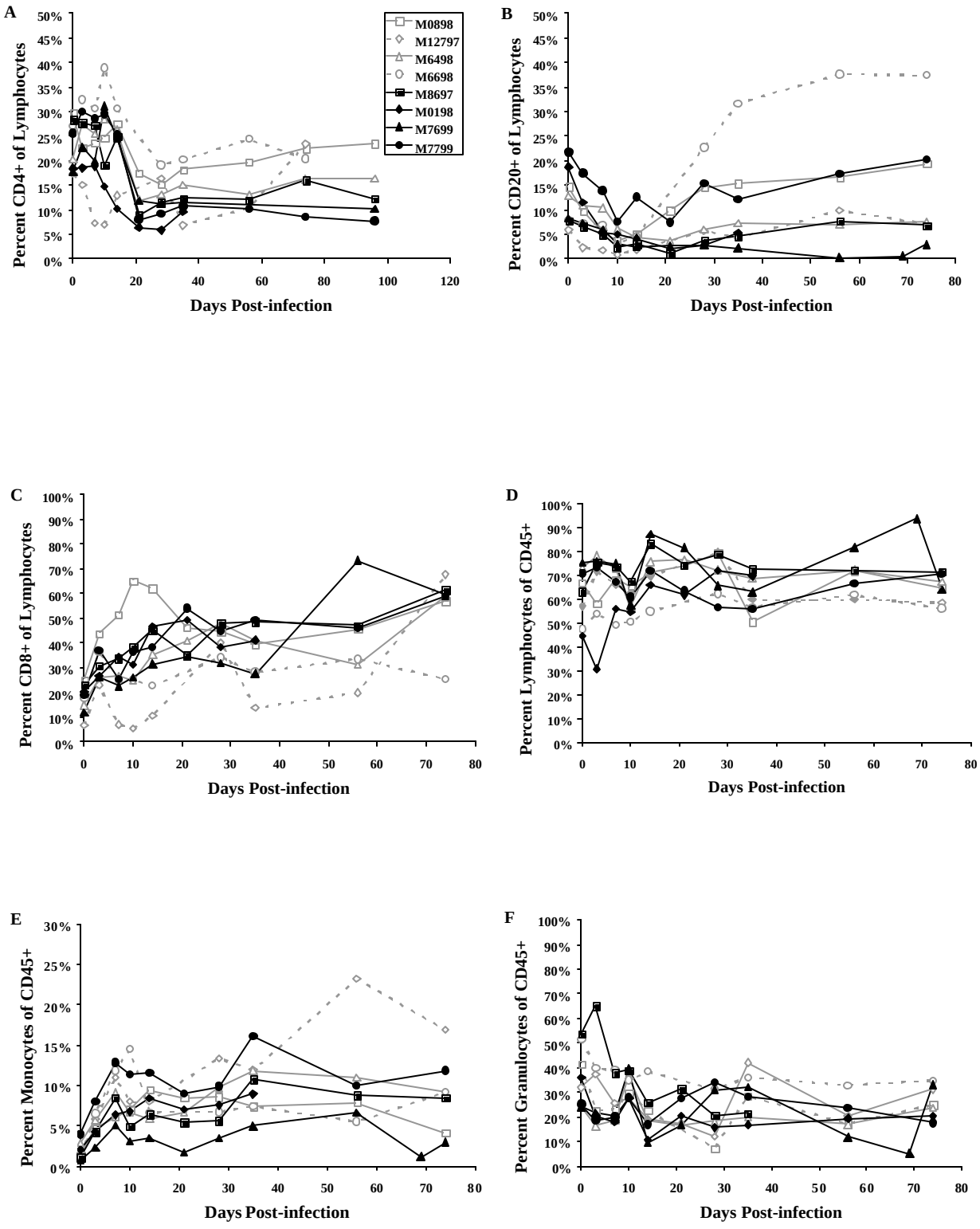

Figure 54. Legend on next page.

Figure 54. Cell populations in the peripheral blood during infection *in vivo*.

(previous page) Whole blood staining and flow cytometry was used to enumerate cell populations during infection. (A) Percent $CD4^+$ of lymphocytes; (B) Percent $CD20^+$ of lymphocytes; (C) Percent $CD8^+$ of lymphocytes; (D) Percent lymphocytes of $CD45^+$ leukocytes; (E) Percent monocytes of $CD45^+$ leukocytes; and (F) Percent granulocytes of $CD45^+$ leukocytes.

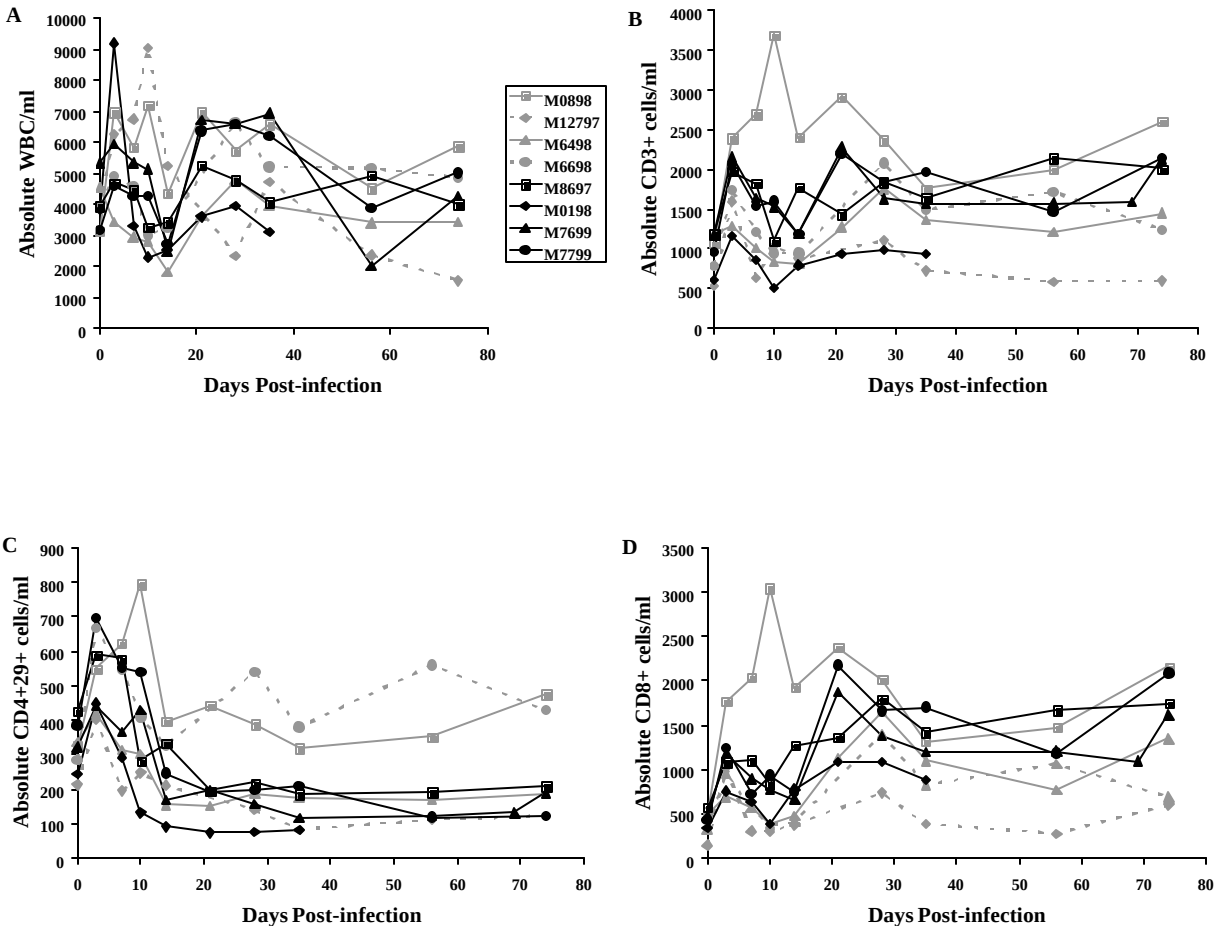

Figure 55. Absolute number of various cell populations in the peripheral blood during infection *in vivo*.

Whole blood staining using Flow-Count Fluorospheres (Coulter) was used to enumerate the absolute number of various cell populations during infection. (A) absolute white blood cell count; (B) number of $CD3^+$ cells/ml blood; (C) number of $CD4^+CD29^+$ cells/ml blood; and (D) number of $CD8^+$ cells/ml blood.

BIBLIOGRAPHY

1. **Abel, K., M. J. Alegria-Hartman, K. Rothaeusler, M. Marthas, and C. J. Miller.** 2002. The relationship between simian immunodeficiency virus RNA levels and the mRNA levels of alpha/beta interferons (IFN-alpha/beta) and IFN-alpha/beta-inducible Mx in lymphoid tissues of rhesus macaques during acute and chronic infection. J. Virol. **76:**8433-45.

2. **Al Jabri, A. A.** 2001. HLA and in vitro susceptibility to HIV infection. Molecular Immunology **38:**959-967.

3. **Asderakis, A., V. Pravica, P. A. Dyer, P. J. Sinnott, and I. V. Hutchinson.** 1997. CA-repeat polymorphism in the first intron of the interferon-gamma (IFN-gamma) gene. Immunology **92:**15.8.

4. **Awad, M. R., A. El-Gamel, P. Hasleton, D. M. Turner, P. J. Sinott, and I. V. Hutchinson.** 1998. Genotypic variation in the Transforming growth factor-beta 1 gene: association with transforming growth factor -beta 1 production, fibrotic lung disease, and graft fibrosis after lung transplantation. Transplantation **66:**1014-1020.

5. **Awad, M. R., V. Pravica, P. A. Dyer, P. J. Sinnott, and I. V. Hutchinson.** 1999. CA-repeat allele in the first intron of the IFN-gamma gene is associated with lung allograft fibrosis. Human Immunology **60:**343-346.

6. **Baba, T. W., A. M. Trichel, L. An, V. Liska, L. N. Martin, M. Murphey-Corb, and R. M. Ruprecht.** 1996. Infection and AIDS in adult macaques after nontraumatic oral exposure to cell-free SIV. Science **272:**1486-9.

7. **Badley, A. D., A. A. Pilon, A. Landay, and D. H. Lynch.** 2000. Mechanisms of HIV-associated lymphocyte apoptosis. Blood **96:**2951-64.

8. **Baltimore, D.** 1970. RNA-dependent DNA polymerase in virions of RNA tumor viruses. Nature **226:**1209.

9. **Barker, E., K. N. Bossart, and J. A. Levy.** 1998. Primary CD8+ cells from HIV-infected individuals can suppress productive infection of macrophages independent of beta chemokines. Proc. Nat. Acad. Sci. U.S.A. **95:**1725-1729.

10. **Baskin, G. B., M. Murphey-Corb, E. A. Watson, and L. N. Martin.** 1988. Necropsy findings in rhesus monkeys experimentally infected with cultured simian immunodeficiency virus (SIV)/delta. Vet. Pathol. **25:**456-67.

11. **Baur, A. S., E. T. Sawai, P. Dazin, W. J. Fantl, C. Cheng-Mayer, and B. M. Peterlin.** 1994. HIV-1 Nef leads to inhibition or activation of T cells depending on its intracellular localization. Immunity **1:**373-84.

12. **Benveniste, R. C., W. R. Morton, E. A. Clark, C. C. Tsai, H. D. Ochs, J. M. Ward, L. Kuller, W. B. Knott, R. W. Hill, M. J. Gale, and M. E. Thouless.** 1988. Inoculation of baboons and macaques with simian immunodeficiency virus/Mne, a primate lentivirus closely related to human immunodeficiency virus type 2. J. Virol. **62:**2091.

13. **Berzofsky, J. A., J. D. Ahlers, M. A. Derby, C. D. Pendleton, T. Arichi, and I. M. Belyakov.** 1999. Approaches to improve engineered vaccines for human immunodeficiency virus and other viruses that cause chronic infections. Immunol. Rev. **170:**151-72.

14. **Besnier, C., Y. Takeuchi, and G. Towers.** 2002. Restriction of lentivirus in monkeys. Proc. Natl. Acad. Sci. USA **99:**11920-5.

15. **Best, S., P. Le Tissier, G. Towers, and J. P. Stoye.** 1996. Positional cloning of the mouse retrovirus restriction gene Fv1. Nature **382:**826-9.

16. **Blackwell, J. M.** 2001. Genetics and genomics in infectious disease susceptibility. Trends Mol. Med. **7:**521-6.

17. **Bontrop, R. E., N. Otting, H. Niphuis, R. Noort, V. Teeuwsen, and J. L. Heeney.** 1996. The role of major histocompatibility complex polymorphisms on SIV infection in rhesus macaques. Immunology Letters **51:**35-38.

18. **Borrow, P., H. Lewicki, B. H. Hahn, G. M. Shaw, and M. B. Oldstone.** 1994. Virus-specific CD8+ cytotoxic T-lymphocyte activity associated with control of viremia in primary human immunodeficiency virus type 1 infection. J. Virol. **68:**6103-10.

19. **Bour, S., R. Geleziunas, and M. A. Wainberg.** 1994. The role of CD4 and its downmodulation in establishment and maintenance of HIV-1 infection. Immunol. Rev. **140:**147-71.

20. **Brinchmann, J. E., G. Gaudernack, and F. Vartdal.** 1990. CD8+ T cells inhibit HIV replication in naturally infected CD4+ T cells: evidence for a soluble inhibitor. J. Immunol. **144:**2961-2966.

21. **Brinkman, B. M., I. P. Keet, F. Miedema, C. L. Verweij, and M. R. Klein.** 1997. Polymorphisms within the human tumor necrosis factor-alpha promoter region in human immunodeficiency virus type 1-seropositive persons. J. Infect. Dis. **175:**188-90.

22. **Buchbinder, S. P., M. H. Katz, N. A. Hessol, P. M. O'Malley, and S. D. Holmberg.** 1994. Long-term HIV-1 infection without immunologic progression. AIDS **8:**1123-1128.

23. **Budd, R. C.** 2002. Death receptors couple to both cell proliferation and apoptosis. J. Clin. Invest. **109:**437-41.

24. **Bukrinskaya, A., B. Brichacek, A. Mann, and M. Stevenson.** 1998. Establishment of a functional human immunodeficiency virus type 1 (HIV-1) reverse transcription complex involves the cytoskeleton. J. Exp. Med. **188:**2113-25.

25. **Burns, D. P., and R. C. Desrosiers.** 1994. Envelope sequence variation, neutralizing antibodies, and primate lentivirus persistence. Curr. Top. Microbiol. Immunol. **188:**185-219.

26. **Cann, A. J., J. A. Zack, A. S. Go, S. J. Arrigo, Y. Koyanagi, P. L. Green, S. Pang, and I. S. Chen.** 1990. Human immunodeficiency virus type 1 T-cell tropism is determined by events prior to provirus formation. J. Virol. **64:**4735-42.

27. **Cao, Y., L. Qin, L. Zhang, J. Safrit, and D. D. Ho.** 1995. Virologic and immunologic characterization of long-term survivors of human immunodeficiency virus type 1 infection. N. Engl. J. Med. **322:**201-208.

28. **Carrington, M., G. W. Nelson, M. P. Martin, T. Kissner, D. Vlahov, J. J. Goedert, R. Kaslow, S. Buchbinder, K. Hoots, and S. J. O'Brien.** 1999. HLA and HIV-1: heterozygote advantage and B*35-Cw*04 disadvantage. Science **283:**1748-52.

29. **CDC.** 2001. HIV/AIDS Update. www.cdc.gov.

30. **Chackerian, B., E. M. Long, P. A. Luciw, and J. Overbaugh.** 1997. Human immunodeficiency virus type 1 coreceptors participate in postentry stages in the virus replication cycle and function in simian immunodeficiency virus infection. J. Virol. **71:**3932-9.

31. **Clark, S. J., M. S. Saag, W. E. Decker, S. Campbell-Hill, J. L. Robertson, P. H. Veldkamp, J. C. Kappes, B. H. Hahn, and G. M. Shaw.** 1991. High titers of cytopathic virus in plasma of patients with symptomatic primary HIV-1 infection. N. Engl. J. Med. **324:**954-960.

32. **Cocci, F., A. DeVico, A. Garazino-Demo, S. K. Arya, R. C. Gallo, and P. Lusso.** 1995. Identification of RANTES, MIP-1alpha, and MIP-1beta as the major HIV-supressive factors produced by CD8+ T cells. Science **270:**1811-1815.

33. **Coffin, J. M.** 1996. Retroviridae: The viruses and their replication, p. 763-843. *In* B. N. Fields, D. M. Knipe, and P. M. Howley (ed.), Fundamental Virology, 3rd ed. Lippincott-Raven, Philadelphia.

34. **Cohen, O., D. Weissman, and A. S. Fauci.** 1999. The Immunopathogenesis of HIV infection. *In* W. E. Paul (ed.), Fundamental Immunology. Lippincott-Raven, Philadelphia.

35. **Cohen, O. J., S. Paolucci, S. M. Bende, M. Daucher, H. Moriuchi, M. Moriuchi, C. Cicala, R. T. Davey, Jr., B. Baird, and A. S. Fauci.** 1998. CXCR4 and CCR5 genetic polymorphisms in long-term nonprogressive human immunodeficiency virus infection: lack of association with mutations other than CCR5-Delta32. J. Virol. **72:**6215-7.

36. **Conley, A. J., J. A. Kessler, 2nd, L. J. Boots, J. S. Tung, B. A. Arnold, P. M. Keller, A. R. Shaw, and E. A. Emini.** 1994. Neutralization of divergent human immunodeficiency virus type 1 variants and primary isolates by IAM-41-2F5, an anti-gp41 human monoclonal antibody. Proc. Natl. Acad. Sci. USA **91:**3348-52.

37. **Conti, L., P. Matarrese, B. Varano, M. C. Gauzzi, A. Sato, W. Malorni, F. Belardelli, and S. Gessani.** 2000. Dual role of the HIV-1 vpr protein in the modulation of the apoptotic response of T cells. J. Immunol. **165:**3293-300.

38. **Cowan, S., T. Hatziioannou, T. Cunningham, M. A. Muesing, H. G. Gottlinger, and P. D. Bieniasz.** 2002. Cellular inhibitors with Fv1-like activity restrict human and simian immunodeficiency virus tropism. Proc. Natl. Acad. Sci. USA **99:**11914-9.

39. **Cyster, J. G.** 2000. Leukocyte migration: scent of the T zone. Curr. Biol. **10:**R30-3.

40. **Daar, E. S., T. Moudgil, R. D. Meyer, and D. D. Ho.** 1991. Transient high levels of viremia in patients with primary human immunodeficiency virus type 1 infection. N. Engl. J. Med. **324:**961-964.

41. **Daniel, M. D., N. L. Letvin, N. W. King, M. Kannagi, P. K. Sehgal, R. D. Hunt, P. J. Kanki, M. Essex, and R. C. Desrosiers.** 1985. Isolation of T-cell tropic HTLV-III-like retrovirus from macaques. Science **228:**1201-1204.

42. **Dean, M., M. Carrington, C. Winkler, G. A. Huttley, M. W. Smith, R. Allikmets, J. J. Goedert, S. P. Buchbinder, E. Vittinghoff, E. Gomperts, S. Donfield, D. Vlahov, R. Kaslow, A. Saah, C. Rinaldo, R. Detels, and S. J. O'Brien.** 1996. Genetic restriction of HIV-1 infection and progression to AIDS by a deletion allele of the CKR5 structural gene. Science **273:**1856-62.

43. **Desrosiers, R. C., J. D. Lifson, J. S. Gibbs, S. C. Czajak, A. Y. Howe, L. O. Arthur, and R. P. Johnson.** 1998. Identification of highly attenuated mutants of simian immunodeficiency virus. J. Virol. **72:**1431-7.

44. **Dettenhofer, M., S. Cen, B. A. Carlson, L. Kleiman, and X. F. Yu.** 2000. Association of Human Immunodeficiency Virus Type 1 Vif with RNA and its role in reverse transcription. J. Virol. **74:**8938-8945.

45. **Dittmer, U., and G. Hunsmann.** 1997. Long-term non-progressive human immunodeficiency virus infection: new insights from the simian immunodeficiency virus model. J. Gen. Virol. **78 (5):**979-84.

46. **Dittmer, U., W. Luke, C. Stahl-Hennig, C. Coulibaly, H. Petry, W. Bodemer, G. Hunsmann, and G. Voss.** 1994. Early helper T cell dysfunction in SIV-but not HIV-2-infected macaques. J. Med. Primatol. **23:**298-303.

47. **Duh, E. J., W. J. Maury, T. M. Folks, A. S. Fauci, and A. B. Rabson.** 1989. Tumor necrosis factor alpha activates human immunodeficiency virus type 1 through induction of nuclear factor binding to the NF-kappa B sites in the long terminal repeat. Proc. Natl. Acad. Sci. USA **86:**5974-8.

48. **Dworkin, B. M.** 1994. Selenium deficiency in HIV infection and the acquired immunodeficiency syndrome (AIDS). Chem. Biol. Interact. **91:**181-6.

49. **Dykhuizen, M., J. L. Mitchen, D. C. Montefiori, J. Thomson, L. Acker, H. Lardy, and C. D. Pauza.** 1998. Determinants of disease in the simian immunodeficiency virus-infected rhesus macaque: characterizing animals with low antibody responses and rapid progression. J. Gen. Virol. **79:**2461-2467.

50. **Edinger, A. L., A. Amedee, K. Miller, B. J. Doranz, M. Endres, M. Sharron, M. Samson, Z. H. Lu, J. E. Clements, M. Murphey-Corb, S. C. Peiper, M. Parmentier, C. C. Broder, and R. W. Doms.** 1997. Differential utilization of CCR5 by macrophage and T cell tropic simian immunodeficiency virus strains. Proc. Natl. Acad. Sci. USA **94:**4005-10.

51. **Edinger, A. L., T. L. Hoffman, M. Sharron, B. Lee, B. O'Dowd, and R. W. Doms.** 1998. Use of GPR1, GPR15, and STRL33 as coreceptors by diverse human immunodeficiency virus type 1 and simian immunodeficiency virus envelope proteins. Virology **249:**367-78.

52. **Edmonson, P., M. Murphey-Corb, L. N. Martin, C. Delahunty, J. Heeney, H. Kornfeld, P. R. Donahue, G. H. Learn, L. Hood, and J. I. Mullins.** 1998. Evolution of a simian immunodeficiency virus pathogen. J. Virol. **72:**405-14.

53. **El-Gamel, A., M. R. Awad, P. S. Hasleton, N. A. Yonan, J. A. Hutchinson, C. S. Campbell, A. H. Rahman, A. K. Deiraniya, P. J. Sinnott, and I. V. Hutchinson.** 1999. Transforming growth factor-beta (TGF-beta1) genotype and lung allograft fibrosis. Journal of Heart and Lung Transplantation **18:**517-523.

54. **Eskdale, J., G. Gallagher, C. L. Verweij, V. Keijsers, R. G. J. Westendorf, and T. W. J. Huizinga.** 1998. Interleukin 10 secretion in relation to human IL-10 locus haplotypes. Proc. Natl. Acad. Sci. USA **95:**9465-9470.

55. **Fantuzzi, G., and R. Faggioni.** 2000. Leptin in the regulation of immunity, inflammation, and hematopoiesis. J. Leukoc. Biol. **68:**437-46.

56. **Farnet, C. M., and W. A. Haseltine.** 1991. Determination of viral proteins present in the human immunodeficiency virus type 1 preintegration complex. J. Virol. **65:**1910-5.

57. **Farzadegan, H., D. R. Henrard, C. A. Kleeberger, L. Schrager, A. J. Kirby, A. J. Saah, C. R. J. Rinaldo, M. O'Gorman, R. Detels, E. Taylor, J. P. Phair, and J. B. Margolick.** 1996. Virologic and serologic markers of rapid progression to AIDS after HIV-1 seroconversion. J. Acquired Immune Defic. Syndr. **13:**448-455.

58. **Fauci, A. S., and H. C. Lane.** 1998. Human immunodeficiency virus (HIV) disease: AIDS and related disorders., p. 1791–1856. *In* A. S. Fauci, K. J. Isselbacher, and J. D. Wilson (ed.), Harrison's Principles of Internal Medicine, 14th ed. McGraw-Hill, New York.

59. **Feldmann, G., H. Fickenscher, W. Bodemer, M. Spring, T. Niblein, G. Hunsmann, and U. Dittmer.** 1997. Generation of herpes virus saimiri-transformed T-cell lines from macaques is restricted by reactivation of simian spuma viruses. Virology **229:**106-12.

60. **Fisher, A. G., B. Ensoli, L. Ivanoff, M. Chamberlain, S. Petteway, L. Ratner, R. C. Gallo, and F. Wong-Staal.** 1987. The sor gene of HIV-1 is required for efficient virus transmission in vitro. Science **237:**888-93.

61. **Fortin, A., M. M. Stevenson, and P. Gros.** 2002. Susceptibility to malaria as a complex trait: big pressure from a tiny creature. Hum. Mol. Genet. **11:**2469-78.

62. **Francis, M. L., M. S. Meltzer, and H. E. Gendelman.** 1992. Interferons in the persistence, pathogenesis, and treatment of HIV infection. AIDS Res. Hum. Retroviruses **8:**199-207.

63. **Freed, E. O.** 1998. HIV-1 gag proteins: diverse functions in the virus life cycle. Virology **251:**1-15.

64. **Fuller, D. H., P. A. Rajakumar, L. A. Wilson, A. M. Trichel, J. T. Fuller, T. Shipley, M. S. Wu, K. Weis, C. R. Rinaldo, J. R. Haynes, and M. Murphey-Corb.** 2002. Induction of mucosal protection against primary, heterologous simian immunodeficiency virus by a DNA vaccine. J. Virol. **76:**3309-3317.

65. **Gardner, M. B., M. Endres, and P. Barry.** 1992. The Simian Retroviruses: SIV and SRV, p. 133-236. *In* J. A. Levy (ed.), The Retroviridae, vol. 3. Plenum Press, New York.

66. **Gardner, M. B., and P. A. Luciw.** 1988. Simian Immunodeficiency Viruses and their Relationship to the Human Immunodeficiency Virus. AIDS **2:**S3.

67. **Godfrey, T. E., S.-H. Kim, M. Chavira, D. W. Ruff, R. S. Warren, J. W. Gray, and R. H. Jensen.** 2000. Quantitative mRNA expression analysis from formalin-fixed, parrafin-embedded tissues using 5' nuclease quantitative reverse transcription polymerase chain reaction. Journal of Molecular Diagnostics **2:**84-91.

68. **Goff, S. P.** 1996. Operating under a Gag order: a block against incoming virus by the Fv1 gene. Cell **86:**691-3.

69. **Goldstein, S., C. R. Brown, H. Dehghani, J. D. Lifson, and V. M. Hirsch.** 2000. Intrinsic susceptibility of rhesus macaque peripheral CD4+ T cells to simian immunodeficiency virus in vitro is predictive of in vivo viral replication. J. Virol. **74:**9388-9395.

70. **Goncalves, J., Y. Korin, J. Zack, and D. Gabuzda.** 1996. Role of Vif in Human Immunodeficiency Virus Type 1 reverse transcription. J. Virol. **70:**8701-8709.

71. **Goncalves, J., F. Silva, A. Freitas-Vieira, M. Santa-Marta, R. Malho, X. Yang, D. Gabuzda, and C. Barbas.** 2002. Functional neutralization of HIV-1 Vif protein by intracellular immunization inhibits reverse transcription and viral replication. J. Biol. Chem. **277:**32036-45.

72. **Habis, A., G. B. Baskin, M. Murphey-Corb, and L. S. Levy.** 1999. SAIDS-associated lymphoma (SAL) in rhesus and cynomolgus monkeys recapitulates the primary pathobiological features of AIDs-associated non-Hodgkin's lymphoma (AAL). AIDS Res. Hum. Retroviruses **15:**1389-1398.

73. **Hartley, J. W., W. P. Rowe, and R. J. Huebner.** 1970. Host-range restrictions of murine leukemia viruses in mouse embryo cell cultures. J. Virol. **5:**221-5.

74. **Hartman, A. L., P. A. Rajakumar, C. McMahon, D. H. Fuller, and M. Murphey-Corb.** 2003. Molecular dissection of acute Simian Immunodeficiency Virus (SIV) infection in rhesus macaques with high versus low intrinsic susceptibility to virus-induced AIDS-like disease. J. Virol. **manuscript submitted**.

75. **Hartman, A. L., P. A. Rajakumar, T. L. Washko, T. Kodama, and M. Murphey-Corb.** 2003. The effects of intrinsic differences in regulation of viral reverse transcription and activated CD4+ T cell death on Simian Immunodeficiency Virus (SIV) production in vitro. J. Virol. **manuscript submitted**.

76. **Hasbold, J., A. V. Gett, J. S. Rush, E. Deenick, D. Avery, J. Jun, and P. D. Hodgkin.** 1999. Quantitative analysis of lymphocyte differentiation and proliferation in vitro using carboxyfluorescein diacetate succinimidyl ester. Immunol. Cell. Biol. **77:**516-22.

77. **Hay, S., and G. Kannourakis.** 2002. A time to kill: viral manipulation of the cell death program. J. Gen. Virol. **83:**1547-64.

78. **Haynes, B. F., G. Pantaleo, and A. S. Fauci.** 1996. Toward an understanding of the correlates of protective immunity to HIV infection. Science **271:**324-328.

79. **Hel, Z., D. Venzon, M. Poudyal, W. P. Tsai, L. Giuliani, R. Woodward, C. Chougnet, G. Shearer, J. D. Altman, D. Watkins, N. Bischofberger, A. Abimiku, P. Markham, J. Tartaglia, and G. Franchini.** 2000. Viremia control following antiretroviral treatment and therapeutic immunization during primary SIV251 infection of macaques. Nat. Med. **6:**1140-6.

80. **Himathongkham, S., and P. A. Luciw.** 1996. Restriction of HIV-1 (subtype B) replication at the entry step in rhesus macaque cells. Virology **219:**485-488.

81. **Ho, W. Z., R. Cherukuri, S. D. Ge, J. R. Cutilli, L. Song, S. Whitko, and S. D. Douglas.** 1993. Centrifugal enhancement of human immunodeficiency virus type 1 infection and human cytomegalovirus gene expression in human primary monocyte/macrophages in vitro. J. Leukoc. Biol. **53:**208-12.

82. **Huang, Y., W. A. Paxton, S. M. Wolinsky, A. U. Neumann, L. Zhang, T. He, S. Kang, D. Ceradini, Z. Jin, K. Yazdanbakhsh, K. Kunstman, D. Erickson, E. Dragon, N. R. Landau, J. Phair, D. D. Ho, and R. A. Koup.** 1996. The role of a mutant CCR5 allele in HIV-1 transmission and disease progression. Nat. Med. **2:**1240-3.

83. **Israel, N., U. Hazan, J. Alcami, A. Munier, F. Arenzana-Seisdedos, F. Bachelerie, A. Israel, and J. L. Virelizier.** 1989. Tumor necrosis factor stimulates transcription of HIV-1 in human T lymphocytes, independently and synergistically with mitogens. J. Immunol. **143:**3956-60.

84. **Jacque, J. M., A. Mann, H. Enslen, N. Sharova, B. Brichacek, R. J. Davis, and M. Stevenson.** 1998. Modulation of HIV-1 infectivity by MAPK, a virion-associated kinase. Embo J. **17:**2607-18.

85. **Janeway, C. A.** 1997. Immunobiology: The immune system in health and disease., 3rd ed. Garland Publishing, New York.

86. **Johnson, R. P.** 2002. Mechanisms of protection against simian immunodeficiency virus infection. Vaccine **20:**1985-7.

87. **Johnston, J. B., Y. Jiang, G. van Marle, M. B. Mayne, W. Ni, J. Holden, J. C. McArthur, and C. Power.** 2000. Lentivirus infection in the brain induces matrix metalloproteinase expression: role of envelope diversity. J. Virol. **74:**7211-20.

88. **Kameoka, M., Y. Okada, M. Tobiume, T. Kimura, and K. Ikuta.** 1996. Intracellular glutathione as a possible direct blocker of HIV type 1 reverse transcription. AIDS Res. Hum. Retroviruses **12:**1635-8.

89. **Kedzierska, K., and S. M. Crowe.** 2002. The role of monocytes and macrophages in the pathogenesis of HIV-1 infection. Curr. Med. Chem. **9:**1893-903.

90. **Khatissian, E., M. G. Tovey, M. C. Cumont, V. Monceaux, P. Lebon, L. Montagnier, B. Hurtrel, and L. Chakrabarti.** 1996. The relationship between the interferon alpha response and viral burden in primary SIV infection. AIDS Res. Hum. Retroviruses **12:**1273-8.

91. **Kim, S., R. Byrn, J. Groopman, and D. Baltimore.** 1989. Temporal Aspects of DNA and RNA Synthesis During Human Immunodeficiency Virus Infection: Evidence for Differential Gene Expression. J. Virol. **63:**3708-3713.

92. **Kimpton, J., and M. Emerman.** 1992. Detection of replication-competent and pseudotyped human immunodeficiency virus with a sensitive cell line on the basis of activation of an integrated beta-galactosidase gene. J. Virol. **66:**2232-9.

93. **Kindt, T. J., V. M. Hirsch, P. R. Johnson, and S. Sawasdikosol.** 1992. Animal models for acquired immunodeficiency syndrome. Advances in Immunology **52:**425-474.

94. **Kinter, A. L., M. Ostrowski, D. Goletti, A. Oliva, D. Weissman, K. Gantt, E. Hardy, R. Jackson, L. Ehler, and A. S. Fauci.** 1996. HIV replication in CD4+ T cells of HIV-infected individuals is regulated by a balance between the viral suppressive effects of endogenous beta-chemokines and the viral inductive effects of other endogenous cytokines. Proc. Natl. Acad. Sci. USA **93:**14076-81.

95. **Kinter, A. L., G. Poli, L. Fox, E. Hardy, and A. S. Fauci.** 1995. HIV replication in IL-2-stimulated peripheral blood mononuclear cells is driven in an autocrine/paracrine manner by endogenous cytokines. J. Immunol. **154:**2448-59.

96. **Knuchel, M. C., T. J. Spira, A. U. Neumann, L. Xiao, D. L. Rudolph, J. Phair, S. M. Wolinsky, R. A. Koup, O. J. Cohen, T. M. Folks, and R. B. Lal.** 1998. Analysis of a biallelic polymorphism in the tumor necrosis factor alpha promoter and HIV type 1 disease progression. AIDS Res. Hum. Retroviruses **14:**305-9.

97. **Korth, M. J., M. D. Taylor, and M. G. Katze.** 1998. Interferon inhibits the replication of HIV-1, SIV, and SHIV chimeric viruses by distinct mechanisms. Virology **247:**265-273.

98. **Koup, R. A., J. T. Safrit, Y. Cao, C. A. Andrews, G. McLeod, W. Borkowsky, C. Farthing, and D. D. Ho.** 1994. Temporal association of cellular immune responses with initial control of viremia in primary human immunodeficiency virus type 1 syndrome. J. Virol. **68:**4650-4655.

99. **Kozak, C. A., and A. Chakraborti.** 1996. Single amino acid changes in the murine leukemia virus capsid protein gene define the target of Fv1 resistance. Virology **225:**300-5.

100. **Kuhmann, S. E., N. Madani, O. M. Diop, E. J. Platt, J. Morvan, M. C. Muller-Trutwin, F. Barre-Sinoussi, and D. Kabat.** 2001. Frequent substitution polymorphisms in African green monkey CCR5 cluster at critical sites for infections by simian immunodeficiency virus SIVagm, implying ancient virus-host coevolution. J. Virol. **75:**8449-60.

101. **Kuhmann, S. E., E. J. Platt, S. L. Kozak, and D. Kabat.** 1997. Polymorphisms in the CCR5 genes of African green monkeys and mice implicate specific amino acids in infections by simian and human immunodeficiency viruses. J. Virol. **71:**8642-56.

102. **Lackner, A.** 1994. Pathology of simian immunodeficiency virus infection. Curr. Top. Micro. Immunol. **188:**35-64.

103. **Lairmore, M. D., A. A. Post, C. S. Goldsmith, and T. M. Folks.** 1991. Cytokine enhancement of simian immunodeficiency virus (SIV/mac) from a chronically infected cloned T-cell line (HuT-78). Arch. Virol. **121:**43-53.

104. **Lane, B. R., S. R. King, P. J. Bock, R. M. Strieter, M. J. Coffey, and D. M. Markovitz.** 2003. The C-X-C chemokine IP-10 stimulates HIV-1 replication. Virology **307:**122-34.

105. **Lathey, J. L., R. D. Pratt, and S. A. Spector.** 1997. Appearance of autologous neutralizing antibody correlates with reduction in virus load and phenotype switch during primary infection with human immunodeficiency virus type 1. J. Infect. Dis. **175:**231-2.

106. **Letvin, N. L., D. H. Barouch, and D. C. Montefiori.** 2002. Prospects for vaccine protection against HIV-1 infection and AIDS. Annu. Rev. Immunol. **20:**73-99.

107. **Letvin, N. L., M. D. Daniel, P. K. Sehgal, R. C. Desrosiers, R. D. Hunt, L. M. Waldron, J. J. MacKey, D. K. Schmidt, L. V. Chalifoux, and N. W. King.** 1985. Induction of AIDS-like disease in macaque monkeys with T-cell tropic retrovirus STLV-III. Science **230:**71-3.

108. **Letvin, N. L., and N. W. King.** 1990. Immunologic and pathologic manifestations of the infection of rhesus monkeys with simian immunodeficiency virus of macaques. J. Acquired Immune Defic. Syndr. **3:**1023-1040.

109. **Letvin, N. L., J. E. Schmitz, H. L. Jordan, A. Seth, V. M. Hirsch, K. A. Reimann, and M. J. Kuroda.** 1999. Cytotoxic T lymphocytes specific for the simian immunodeficiency virus. Immunol. Rev. **170:**127-34.

110. **Levy, J. A., J. Shimabukuro, T. McHugh, C. Casavant, D. Stites, and L. Oshiro.** 1985. AIDS-associated retroviruses (ARV) can productively infect other cells besides human T helper cells. Virology **147:**441-8.

111. **Li, L., J. M. Olvera, K. E. Yoder, R. S. Mitchell, S. L. Butler, M. Lieber, S. L. Martin, and F. D. Bushman.** 2001. Role of the non-homologous DNA end joining pathway in the early steps of retroviral infection. Embo J. **20:**3272-81.

112. **Lifson, A. R., G. W. Rutherford, and H. W. Jaffe.** 1988. The natural history of human immunodeficiency virus infection. J. Infect. Dis. **158:**1360-1367.

113. **Lifson, J. D., M. A. Nowak, S. Goldstein, J. L. Rossio, A. Kinter, G. Vasquez, T. A. Wiltrout, C. Brown, D. Schneider, L. Wahl, A. L. Lloyd, J. Williams, W. R. Elkins, A. S. Fauci, and V. M. Hirsch.** 1997. The extent of early viral replication is a critical determinant of the natural history of simian immunodeficiency virus infection. J. Virol. **71:**9508-9514.

114. **Liu, R., W. A. Paxton, S. Choe, D. Ceradini, S. R. Martin, R. Horuk, M. E. MacDonald, H. Stuhlmann, R. A. Koup, and N. R. Landau.** 1996. Homozygous defect in HIV-1 coreceptor accounts for resistance of some multiply-exposed individuals to HIV-1 infection. Cell **86:**367-77.

115. **Liu, S. L., T. Schacker, L. Musey, D. Shriner, M. J. McElrath, L. Corey, and J. I. Mullins.** 1997. Divergent patterns of progression to AIDS after infection from the same source: human immunodeficiency virus type 1 evolution and antiviral responses. J. Virol. **71:**4284-4295.

116. **Lodish, H., A. Berk, S. L. Zipursky, P. Matsudaira, D. Baltimore, and J. Darnell.** Molecular Cell Biology, 4th ed. W.H. Freeman and Company, New York.

117. **Luciw, P. A.** 1996. Human Immunodeficiency Viruses and their Replication, p. 845-916. *In* B. N. Fields, D. M. Knipe, and P. M. Howley (ed.), Fundamental Virology, 3rd ed. Lippincott-Raven, Philadelphia.

118. **Ma, X., K. Sakai, F. Sinangil, E. Golub, and D. J. Volsky.** 1990. Interaction of a noncytopathic Human Immunodeficiency Virus Type 1 (HIV-1) with yarget cells: efficient viral entry followed by delayed expression of its RNA and protein. Virology **176:**184-194.

119. **MacDonald, K. S., K. R. Fowke, J. Kimani, V. A. Dunand, N. J. Nagelkerke, T. B. Ball, J. Oyugi, E. Njagi, L. K. Gaur, R. C. Brunham, J. Wade, M. A. Luscher, P. Krausa, S. Rowland-Jones, E. Ngugi, J. J. Bwayo, and F. A. Plummer.** 2000. Influence of HLA supertypes on susceptibility and resistance to human immunodeficiency virus type 1 infection. J. Infect. Dis. **181:**1581-9.

120. **Madani, N., and D. Kabat.** 1998. An endogenous inhibitor of human immunodeficiency virus in human lymphocytes is overcome by the viral Vif protein. J. Virol. **72:**10251-5.

121. **Magnusson, C., and D. L. Vaux.** 1999. Signalling by CD95 and TNF receptors: not only life and death. Immunol. Cell Biol. **77:**41-6.

122. **Makropoulos, V., T. Bruning, and K. Schulze-Osthoff.** 1996. Selenium-mediated inhibition of transcription factor NF-kappa B and HIV-1 LTR promoter activity. Arch. Toxicol. **70:**277-83.

123. **Martin, L. N., M. Murphey-Corb, P. Mack, G. B. Baskin, G. Pantaleo, M. Vaccarezza, C. H. Fox, and A. S. Fauci.** 1997. Cyclosporin A Modulation of Early Virologic and Immunologic Events during Primary Simian Immunodeficiency Virus infection in Rhesus Monkeys. J. Infect. Dis. **176:**374-383.

124. **Martin, L. N., M. Murphey-Corb, K. F. Soike, B. Davison-Fairburn, and G. B. Baskin.** 1993. Effects of Initiation of 3'-Azido,3'-Deoxythymidine (Zidovudine) Treatment at Different Times after Infected of Rhesus Monkeys with Simian Immunodeficiency Virus. J. Infect. Dis. **168:**825-835.

125. **Martin, L. N., K. F. Soike, M. Murphey-Corb, R. P. Bohn, E. D. Roberts, K. T.J., S. Thaisrivongs, T. J. Vidmar, M. J. Ruwart, S. R. Davio, and W. G. Tarpley.** 1994. Effects of U-75875, a Peptidomimetic Inhibitor of Retroviral Proteases, on Simian Immunodeficiency Virus Infection in Rhesus Monkeys. Antimicrobial Agents and Chemotherapy **38:**1277-1283.

126. **McNicholl, J. M., and K. T. Cuenco.** 1999. Host genes and infectious diseases. HIV, other pathogens, and a public health perspective. Am. J. Prev. Med. **16:**141-54.

127. **Means, R. E., T. Matthews, J. A. Hoxie, M. H. Malim, T. Kodama, and R. C. Desrosiers.** 2001. Ability of the V3 loop of simian immunodeficiency virus to serve as a target for antibody-mediated neutralization: correlation of neutralization sensitivity, growth in macrophages, and decreased dependence on CD4. J. Virol. **75:**3903-15.

128. **Medema, J. P., and J. Borst.** 1999. T cell signaling: a decision of life and death. Hum. Immunol. **60:**403-11.

129. **Meinl, E., H. Fickenscher, R. M. Hoch, R. D. Malefyt, R. de Waal Malefyt, B. A. Hart, H. Wekerle, R. Hohlfeld, and B. Fleckenstein.** 1997. Growth transformation of antigen-specific T cell lines from rhesus monkeys by herpesvirus saimiri. Virology **229:**175-82.

130. **Mellors, J. W., C. R. Rinaldo, Jr., P. Gupta, R. M. White, J. A. Todd, and L. A. Kingsley.** 1996. Prognosis in HIV-1 infection predicted by the quantity of virus in plasma. Science **272:**1167-1170.

131. **Meyer, L., M. Magierowska, J. B. Hubert, C. Rouzioux, C. Deveau, F. Sanson, P. Debre, J. F. Delfraissy, and I. Theodorou.** 1997. Early protective effect of CCR-5 delta 32 heterozygosity on HIV-1 disease progression: relationship with viral load. AIDS **11:**F73-8.

132. **Mi, J., Z. Y. Li, S. Ni, D. Steinwaerder, and A. Lieber.** 2001. Induced apoptosis supports spread of adenovirus vectors in tumors. Hum. Gene Ther. **12:**1343-52.

133. **Michael, N. L.** 1999. Host genetic influences on HIV-1 pathogenesis. Curr. Op. Immunol. **11:**466-474.

134. **Michael, N. L., A. E. Brown, R. F. Voigt, S. S. Frankel, J. R. Mascola, K. S. Brothers, M. Louder, D. L. Birx, and S. A. Cassol.** 1997. Rapid disease progression without seroconversion following primary human immunodeficiency type 1 infection - evidence for highly susceptible human hosts. J. Infect. Dis. **174:**1352-1359.

135. **Michael, N. L., G. Chang, L. G. Louie, J. R. Mascola, D. Dondero, D. L. Birx, and H. W. Sheppard.** 1997. The role of viral phenotype and CCR-5 gene defects in HIV-1 transmission and disease progression. Nat. Med. **3:**338-40.

136. **Mori, K., D. J. Ringler, T. Kodama, and R. C. Desrosiers.** 1992. Complex determinants of macrophage tropism in env of simian immunodeficiency virus. J. Virol. **66:**2067-75.

137. **Morrow, W. J., J. Homsy, J. W. Eichberg, J. Krowka, L. Z. Pan, I. Gaston, H. Legg, N. Lerche, J. Thomas, and J. A. Levy.** 1989. Long-term observation of baboons, rhesus monkeys, and chimpanzees inoculated with HIV and given periodic immunosuppressive treatment. AIDS Res. Hum. Retroviruses **5:**233-45.

138. **Mothe, B. R., J. Weinfurter, C. Wang, W. Rehrauer, N. Wilson, T. M. Allen, D. B. Allison, and D. I. Watkins.** 2003. Expression of the major histocompatibility complex class I molecule Mamu-A*01 is associated with control of simian immunodeficiency virus SIVmac239 replication. J. Virol. **77:**2736-40.

139. **Munoz, A., A. J. Kirby, Y. D. He, J. B. Margolick, B. R. Visscher, C. R. Rinaldo, R. A. Kaslow, and J. P. Phair.** 1995. Long-term survivors with HIV-1 infection: incubation period and longitudinal patterns of CD4+ lymphocytes. J. Acquired Immune Defic. Syndr. **8:**496-505.

140. **Munoz, A., M. C. Wang, S. Bass, J. M. Taylor, L. A. Kingsley, J. S. Chmiel, and B. F. Polk.** 1989. Acquired immunodeficiency syndrome (AIDS)-free time after human immunodeficiency virus type 1 (HIV-1) seroconversion in homosexual men. American Journal of Epidemiology **130:**530-539.

141. **Murphey-Corb, M., L. Martin, and B. Davison-Fairburn.** 1989. The susceptibility of rhesus PBL to SIV/Delta infection in vitro is predictive of in vivo disease. Presented at the 8th Annual Symposium on Non-human Primate Models for AIDS.

142. **Murphey-Corb, M., L. N. Martin, B. Davison-Fairburn, R. C. Montelaro, M. Miller, M. West, S. Ohkawa, G. B. Baskin, J. Y. Zhang, and S. D. Putney.** 1989. A formalin-inactivated whole SIV vaccine confers protection in macaques. Science **246:**1293-7.

143. **Murphey-Corb, M., L. N. Martin, S. R. S. Rangan, G. B. Baskin, B. J. Gormus, R. H. Wolf, W. A. Andes, M. West, and R. C. Montelaro.** 1986. Isolation of an HTLV-III-related retrovirus from macaques with simian AIDS and its possible origin in asymptomatic mangabeys. Nature **321:**435-437.

144. **Nagy, G. S., S. Tsiodras, L. D. Martin, A. Avihingsanon, A. Gavrila, W. C. Hsu, A. W. Karchmer, and C. S. Mantzoros.** 2003. Human immunodeficiency virus type 1-related lipoatrophy and lipohypertrophy are associated with serum concentrations of leptin. Clin. Infect. Dis. **36:**795-802.

145. **Naidu, Y. M., H. W. I. Kestler, Y. Li, C. V. Butler, D. P. Silva, D. K. Schmidt, C. D. Troup, P. K. Sehgal, P. Sonigo, M. D. Daniel, and R. C. Desrosiers.** 1988. Characterization of infectious molecular clones of simian immunodeficiency virus (SIVmac) and human immunodeficiency virus type 2: Persistent infection of rhesus monkeys with molecularly cloned SIVmac. J. Virol. **62:**4691.

146. **Nicholson, J. K., T. J. Spira, C. H. Aloisio, B. M. Jones, M. S. Kennedy, R. C. Holman, and J. S. McDougal.** 1989. Serial determinations of HIV-1 titers in HIV-infected homosexual men: association of rising titers with CD4 T cell depletion and progression to AIDS. AIDS Research & Human Retroviruses **5:**205-215.

147. **O'Brien, S. J., X. Gao, and M. Carrington.** 2001. HLA and AIDS: a cautionary tale. Trends Mol. Med. **7:**379-81.

148. **O'Brien, S. J., G. W. Nelson, C. A. Winkler, and M. W. Smith.** 2000. Polygenic and multifactorial disease gene association in man: Lessons from AIDS. Annu. Rev. Genet. **34:**563-591.

149. **O'Brien, T., W. A. Blattner, D. Waters, E. Eyster, M. W. Hilgartner, A. R. Cohen, N. Luban, A. Hatzakis, L. M. Aledort, P. S. Rosenberg, W. J. Miley, B. L. Kroner, and J. J. Goedert.** 1996. Serum HIV-1 RNA levels and time to development of AIDS in the multicenter hemophilia cohort study. JAMA **276:**105-110.

150. **O'Doherty, U., W. J. Swiggard, and M. H. Malim.** 2000. Human immunodeficiency virus type I spinoculation enhances infection through virus binding. J. Virol. **74:**10074-10080.

151. **Ondoa, P., D. Davis, L. Kestens, C. Vereecken, S. Garcia Ribas, K. Fransen, J. Heeney, and G. van der Groen.** 2002. In vitro susceptibility to infection with SIVcpz and HIV-1 is lower in chimpanzee than in human peripheral blood mononuclear cells. J. Med. Virol. **67:**301-11.

152. **Operskalski, E. A., M. P. Busch, J. W. Mosley, D. O. Stram, and T. S. S. Group.** 1997. Comparative rates of disease progression among persons infected with the same or different HIV-1 strains. J. Acquired Immune Defic. Syndr. **15:**145-150.

153. **Pantaleo, G., and A. S. Fauci.** 1996. Immunopathogenesis of HIV infection. Ann. Rev. Micro. **50:**825-54.

154. **Parish, C. R.** 1999. Fluorescent dyes for lymphocyte migration and proliferation studies. Immunol. Cell Biol. **77:**499-508.

155. **Patel, C. A., M. Mukhtar, and R. J. Pomerantz.** 2000. Human immunodeficiency virus type 1 Vpr induces apoptosis in human neuronal cells. J. Virol. **74:**9717-26.

156. **Peng, B., R. Voltan, L. Lim, Y. Edghill-Smith, S. Phogat, D. S. Dimitrov, K. Arora, M. Leno, S. Than, R. Woodward, P. D. Markham, M. Cranage, and M. Robert-Guroff.** 2002. Rhesus macaque resistance to mucosal simian immunodeficiency virus infection is associated with a postentry block in viral replication. J. Virol. **76:**6016-6026.

157. **Perl, A., and K. Banki.** 2000. Genetic and metabolic control of the mitochondrial transmembrane potential and reactive oxygen intermediate production in HIV disease. Antioxid. Redox Signal. **2:**551-73.

158. **Perl, A., P. Gergely, Jr., F. Puskas, and K. Banki.** 2002. Metabolic switches of T-cell activation and apoptosis. Antioxid. Redox. Signal. **4:**427-43.

159. **Pietroboni, G. R., G. B. Harnett, and M. R. Bucens.** 1989. Centrifugal enhancement of human immunodeficiency virus (HIV) and human herpesvirus type 6 (HHV-6) infection in vitro. J. Virol. Methods **24:**85-90.

160. **Pincus, T., W. P. Rowe, and F. Lilly.** 1971. A major genetic locus affecting resistance to infection with murine leukemia viruses. II. Apparent identity to a major locus described for resistance to friend murine leukemia virus. J. Exp. Med. **133:**1234-41.

161. **Polaciano, P. S., H. A. Liang, and E. A. Clark.** 1995. Formation of simian immunodeficiency virus long terminal repeat circles in resting T cells requires both T cell receptor- and IL-2-dependent activation. J. Exp. Med. **182:**617-21.

162. **Polaciano, P. S., H. A. Liang, E. J. Firpo, and E. A. Clark.** 1993. T-Cell activation influences initial DNA synthesis of simian immunodeficiency virus in resting T lymphocytes from macaques. J. Virol. **67:**7008-7016.

163. **Poli, G., P. Biswas, and A. S. Fauci.** 1994. Interferons in the pathogenesis and treatment of human immunodeficiency virus infection. Antiviral. Res. **24:**221-33.

164. **Poli, G., A. L. Kinter, E. Vicenzi, and A. S. Fauci.** 1994. Cytokine regulation of acute and chronic HIV infection in vitro: from cell lines to primary mononuclear cells. Res. Immunol. **145:**578-82.

165. **Pravica, V., A. Askerakis, C. Perrey, A. Hajeer, P. J. Sinnott, and I. V. Hutchinson.** 1999. In vitro production of IFN gamma correlates with CA repeat polymorphism in the human IFN gamma gene. Eur. J. Immunogen. **26:**1-3.

166. **Reed, L. J., and H. Meunch.** 1938. A simple method of estimating fifty percent endpoints. American Journal of Hygeine **27:**493-497.

167. **Reimann, K. A., K. Tenner-Racz, P. Racz, D. C. Montefiori, Y. Yasutomi, W. Lin, B. J. Ransil, and N. L. Letvin.** 1994. Immunopathogenic events in acute infection of rhesus monkeys with simian immunodeficiency virus of macaques. J. Virol. **68:**2362-70.

168. **Reinhart, T. A., B. A. Fallert, M. E. Pfeifer, S. Sanghavi, S. Capuano, 3rd, P. Rajakumar, M. Murphey-Corb, R. Day, C. L. Fuller, and T. M. Schaefer.** 2002. Increased expression of the inflammatory chemokine CXC chemokine ligand 9/monokine induced by interferon-gamma in lymphoid tissues of rhesus macaques during simian immunodeficiency virus infection and acquired immunodeficiency syndrome. Blood **99:**3119-28.

169. **Reinhart, T. A., M. J. Rogan, A. M. Amedee, M. Murphey-Corb, D. M. Rausch, L. E. Eiden, and A. T. Haase.** 1998. Tracking members of the simian immunodeficiency virus deltaB670 quasispecies population in vivo at single-cell resolution. J. Virol. **72:**113-20.

170. **Rosenberg, E. S., M. Altfeld, S. H. Poon, M. N. Phillips, B. M. Wilkes, R. L. Eldridge, G. K. Robbins, R. T. D'Aquila, P. J. Goulder, and B. D. Walker.** 2000. Immune control of HIV-1 after early treatment of acute infection. Nature **407:**523-6.

171. **Rowland-Jones, S., S. Pinheiro, and R. Kaul.** 2001. New insights into host factors in HIV-1 pathogenesis. Cell **104:**473-476.

172. **Rusche, J. R., K. Javaherian, C. McDanal, J. Petro, D. L. Lynn, R. Grimaila, A. Langlois, R. C. Gallo, L. O. Arthur, and P. J. Fischinger.** 1988. Antibodies that inhibit fusion of human immunodeficiency virus-infected cells bind a 24-amino acid sequence of the viral envelope, gp120. Proc. Natl. Acad. Sci. USA **85:**3198-202.

173. **Saikumar, P., Z. Dong, V. Mikhailov, M. Denton, J. M. Weinberg, and M. A. Venkatachalam.** 1999. Apoptosis: definition, mechanisms, and relevance to disease. Am. J. Med. **107:**489-506.

174. **Samson, M., F. Libert, B. J. Doranz, J. Rucker, C. Liesnard, C. M. Farber, S. Saragosti, C. Lapoumeroulie, J. Cognaux, C. Forceille, G. Muyldermans, C. Verhofstede, G. Burtonboy, M. Georges, T. Imai, S. Rana, Y. Yi, R. J. Smyth, R. G. Collman, R. W. Doms, G. Vassart, and M. Parmentier.** 1996. Resistance to HIV-1 infection in caucasian individuals bearing mutant alleles of the CCR-5 chemokine receptor gene. Nature **382:**722-5.

175. **Sauermann, U., C. Stahl-Hennig, N. Stolte, T. Muhl, M. Krawczak, M. Spring, D. Fuchs, F. J. Kaup, G. Hunsmann, and S. Sopper.** 2000. Homozygosity for a conserved Mhc class II DQ-DRB haplotype is associated with rapid disease progression in simian immunodeficiency virus-infected macaques: results from a prospective study. J. Infect. Dis. **182:**716-24.

176. **Schmitz, J. E., M. J. Kuroda, S. Santra, M. A. Simon, M. A. Lifton, W. Lin, R. Khunkhun, M. Piatak, J. D. Lifson, G. Grosschupff, R. S. Gelman, P. Racz, K. Tenner-Racz, K. A. Mansfield, N. L. Letvin, D. C. Montefiori, and K. A. Reimann.** 2003. Effect of humoral immune responses on controlling viremia during primary infection of rhesus monkeys with simian immunodeficiency virus. J. Virol. **77:**2165-73.

177. **Schwartz, O., V. Marechal, B. Friguet, F. Arenzana-Seisdedos, and J. M. Heard.** 1998. Antiviral activity of the proteasome on incoming human immunodeficiency virus type 1. J. Virol. **72:**3845-50.

178. **Sei, Y., P. H. Tsang, F. N. Chu, I. Wallace, J. P. Roboz, P. S. Sarin, and J. G. Bekesi.** 1989. Inverse relationship between HIV-1 p24 antigenemia, anti-p24 antibody and neutralizing antibody response in all stages of HIV-1 infection. Immunol. Lett. **20:**223-30.

179. **Sei, Y., P. H. Tsang, J. P. Roboz, P. S. Sarin, J. I. Wallace, and J. G. Bekesi.** 1988. Neutralizing antibodies as a prognostic indicator in the progression of acquired immune deficiency syndrome (AIDS)-related disorders: a double-blind study. J. Clin. Immunol. **8:**464-72.

180. **Seman, A. L., W. F. Pewen, L. F. Fresh, L. N. Martin, and M. Murphey-Corb.** 2000. The replicative capacity of rhesus macaque peripheral blood mononuclear cells for simian immunodeficiency virus in vitro is predictive of the rate of progression to AIDS in vivo. J. Gen. Virol. **81:**2441-2449.

181. **Sheehy, A. M., N. C. Gaddis, J. D. Choi, and M. H. Malim.** 2002. Isolation of a human gene that inhibits HIV-1 infection and is suppressed by the viral Vif protein. Nature **418:**646-50.

182. **Shin, H. D., C. Winkler, J. C. Stephens, J. Bream, H. Young, J. J. Goedert, T. R. O'Brien, D. Vlahov, S. Buchbinder, J. Giorgi, C. Rinaldo, S. Donfield, A. Willoughby, S. J. O'Brien, and M. W. Smith.** 2000. Genetic restriction of HIV-1 pathogenesis to AIDS by promoter alleles of IL10. Proc. Natl. Acad. Sci. USA **97:**14467-72.

183. **Simmons, A., V. Aluvihare, and A. McMichael.** 2001. Nef triggers a transcriptional program in T cells imitating single-signal T cell activation and inducing HIV virulence mediators. Immunity **14:**763-77.

184. **Simon, J. H., and M. H. Malim.** 1996. The human immunodeficiency virus type 1 Vif protein modulates the postpenetration stability of viral nucleoprotein complexes. J. Virol. **70:**5297-305.

185. **Simon, J. H. M., N. C. Gaddis, R. A. M. Fouchier, and M. H. Malim.** 1998. Evidence for a newly discovered cellular anti-HIV-1 phenotype. Nat. Med. **4:**1397-1400.

186. **Simon, J. H. M., D. L. Miller, R. A. M. Fouchier, M. A. Soares, K. W. C. Peden, and M. H. Malim.** 1998. The regulation of primate immunodeficiency virus infectivity by Vif is cell species restricted: a role for Vif in determining virus host range and cross-species transmission. EMBO Journal **17:**1259-1267.

187. **Skoog, T., F. M. van't Hooft, B. Kallin, S. Jovinge, S. Boquist, J. Nilsson, P. Eriksson, and A. Hamsten.** 1999. A common functional polymorphism (C to A substitution at position -863) in the promotor region of the tumor necrosis factor alpha (TNF-a) gene associated with reduced circulating levels of TNF-a. Human Molecular Genetics **8:**1443.

188. **Smith, M. W., M. Carrington, C. Winkler, D. Lomb, M. Dean, G. Huttley, and S. J. O'Brien.** 1997. CCR2 chemokine receptor and AIDS progression. Nat. Med. **3:**1052-3.

189. **Sodeik, B.** 2002. Unchain my heart, baby let me go--the entry and intracellular transport of HIV. J. Cell Biol. **159:**393-5.

190. **Spira, A., and D. D. Ho.** 1995. Effect of different donor cells on human immunodeficiency virus type 1 replication and selection in vitro. J. Virol. **69:**422-429.

191. **Staal, F. J., S. W. Ela, M. Roederer, M. T. Anderson, and L. A. Herzenberg.** 1992. Glutathione deficiency and human immunodeficiency virus infection. Lancet **339:**909-12.

192. **Stevenson, M., T. L. Stanwick, M. P. Dempsey, and C. A. Lamonica.** 1990. HIV-1 replication is controlled at the level of T cell activation and proviral integration. EMBO Journal **9:**1551-60.

193. **Strebel, K., and S. Bour.** 1999. Molecular interactions of HIV with host factors. AIDS **13:**S13-S24.

194. **Strebel, K., D. Daugherty, K. Clouse, D. Cohen, T. Folks, and M. A. Martin.** 1987. The HIV 'A' (sor) gene product is essential for virus infectivity. Nature **328:**728-30.

195. **Taylor, M. D., M. J. Korth, and M. G. Katze.** 1998. Interferon treatment inhibits the replication of simian immunodeficiency virus at an early stage: evidence for a block between attachment and reverse transcription. Virology **241:**156-162.

196. **Temin, H. M.** 1992. Origin and General Nature of Retroviruses, p. 1-17. *In* J. A. Levy (ed.), The Retroviridae, vol. 1. Plenum Press, New York.

197. **Temin, H. M., and D. Baltimore.** 1972. RNA-directed DNA synthesis and RNA tumor viruses. Advances in Virus Research **17:**129.

198. **Temin, H. M., and S. Mizutani.** 1970. RNA-directed DNA polymerase in virions of Rous sarcoma virus. Nature **226:**1211.

199. **Towers, G., M. Bock, S. Martin, Y. Takeuchi, J. P. Stoye, and O. Danos.** 2000. A conserved mechanism of retrovirus restriction in mammals. Proc. Natl. Acad. Sci. USA **97:**12295-9.

200. **Towers, G., M. Collins, and Y. Takeuchi.** 2002. Abrogation of Ref1 retrovirus restriction in human cells. J. Virol. **76:**2548-50.

201. **Trichel, A. M., P. A. Rajakumar, and M. Murphey-Corb.** 2002. Species-specific variation in SIV disease progression between Chinese and Indian subspecies of rhesus macaque. J. Med. Primatol. **31:**171-8.

202. **Turner, D. M., D. Sankaran, and S. C. D. Grant.** 1997. The effect of polymorphism in the TNF-alpha and IL-10 genes on heart transplant rejection. International Journal of Heart and Lung Transplantation **16:**108.

203. **UNAIDS/WHO.** 2002. AIDS Epidemic Update: 2002. www.unaids.org.

204. **Vella, C., and R. S. Daniels.** 2003. CD8(+) T-cell-mediated Non-cytolytic Suppression of Human Immuno-deficiency Viruses. Curr. Drug Targets Infect. Disord. **3:**97-113.

205. **Vilcek, J., and G. C. Sen.** 1996. Interferons and other cytokines., p. 341-365. *In* B. N. Fields, D. M. Knipe, and P. M. Howley (ed.), Fundamental Virology, 3rd ed. Lippincott - Raven Publishers, Philadelphia.

206. **Villinger, F., T. M. Folks, S. Lauro, J. D. Powell, J. B. Sundstrom, A. Mayne, and A. A. Ansari.** 1996. Immunological and virological studies of natural SIV infection of disease-resistant nonhuman primates. Immunol. Lett. **51:**59-68.

207. **Vogel, T. U., D. T. Evans, J. A. Urvater, D. H. O'Connor, A. L. Hughes, and D. I. Watkins.** 1999. Major histocompatibility complex class I genes in primates: co-evolution with pathogens. Immunol. Rev. **167:**327-337.

208. **Walsh, D. G., C. J. Horvath, A. Hansen-Moosa, J. J. MacKey, P. K. Sehgal, M. D. Daniel, R. C. Desrosiers, and D. J. Ringler.** 1991. Cytokine influence on simian immunodeficiency virus replication within primary macrophages. TNF-alpha, but not GMCSF, enhances viral replication on a per-cell basis. Am. J. Pathol. **139:**877-87.

209. **Watson, A., J. Ranchalis, J. McClure, W. Sutton, P. R. Johnson, S. Hu, and N. L. Haigwood.** 1997. Plasma viremia in macaques infected with simian immunodeficiency virus: plasma viral load early in infection predicts survival. J. Virol. **71:**284-290.

210. **Williams, L. M., and M. W. Cloyd.** 1991. Polymorphic human gene(s) determines differential susceptibility of CD4 lymphocytes to infection by certain HIV-1 isolates. Virology **184:**723-728.

211. **Wilson, L. A., M. Murphey-Corb, L. N. Martin, R. M. Harrison, M. S. Ratterree, and R. P. Bohm.** 2000. Identification of SIV env-specific CTL in the jejunal mucosa in vaginally exposed, seronegative rhesus macaques (Macaca mulatta). J. Med. Primatol. **29:**173-81.

212. **Yang, Y. C., T. Y. Hsu, R. H. Lin, I. J. Su, J. Y. Chen, and C. S. Yang.** 2002. Resistance to tumor necrosis factor-alpha-induced apoptosis in human T-lymphotropic virus type I-infected T cell lines. AIDS Res. Hum. Retroviruses **18:**207-12.

213. **Yasutomi, Y., K. A. Reimann, C. I. Lord, M. D. Miller, and N. L. Letvin.** 1993. Simian immunodeficiency virus-specific CD8+ lymphocyte response in acutely infected rhesus monkeys. J. Virol. **67:**1707-11.

214. **Yong, V. W., C. A. Krekoski, P. A. Forsyth, R. Bell, and D. R. Edwards.** 1998. Matrix metalloproteinases and diseases of the CNS. Trends Neurosci. **21:**75-80.

215. **Youngner, J. S., and W. R. Stinebring.** 1965. Interferon appearance stimulated by endotoxin, bacteria, or viruses in mice pre-treated with Escherichia coli endotoxin or infected with Mycobacterium tuberculosis. Nature **208:**456-8.

216. **Zack, J. A., S. J. Arrigo, S. R. Weitsman, A. S. Go, A. Haislip, and I. S. Y. Chen.** 1990. HIV-1 entry into quiescent primary lymphocytes: molecular analysis reveals a labile, latent viral structure. Cell **61:**213-222.

217. **Zack, J. A., A. M. Haislip, P. Krogstad, and I. S. Chen.** 1992. Incompletely reverse-transcribed human immunodeficiency virus type 1 genomes in quiescent cells can function as intermediates in the retroviral life cycle. J. Virol. **66:**1717-25.

218. **Zagury, D., J. Bernard, R. Leonard, R. Cheynier, M. Feldman, P. S. Sarin, and R. C. Gallo.** 1986. Long-term cultures of HTLV-III--infected T cells: a model of cytopathology of T-cell depletion in AIDS. Science **231:**850-3.

219. **Zhang, J. Y., L. N. Martin, E. A. Watson, R. C. Montelaro, M. West, L. Epstein, and M. Murphey-Corb.** 1988. Simian immunodeficiency virus/delta-induced immunodeficiency disease in rhesus monkeys: relation of antibody response and antigenemia. J. Infect. Dis. **158:**1277-86.

220. **Zhuge, W., F. Jia, I. Adany, O. Narayan, and E. B. Stephens.** 1997. Plasmas from lymphocyte- and macrophage-tropic SIVmac-infected macaques have antibodies with a broader spectrum of virus neutralization activity in macrophage versus lymphocyte cultures. Virology **227:**24-33.

221. **Zijenah, L. S., W. E. Hartogensis, D. A. Katzenstein, O. Tobaiwa, J. Mutswangwa, P. R. Mason, and L. G. Louie.** 2002. Association of high HIV-1 RNA levels and homozygosity at HLA class II DRB1 in adults coinfected with Mycobacterium tuberculosis in Harare, Zimbabwe. Hum. Immunol. **63:**1026-32.